1-1-2012

Discovery of small-molecule natural products that target cellular bioenergetics

Sandipan Datta
University of Mississippi

DISCOVERY OF SMALL-MOLECULE NATURAL PRODUCTS THAT TARGET CELLULAR BIOENERGETICS

A Dissertation
presented in partial fulfillment of requirements
for the degree of Doctor of Philosophy
in the Department of Pharmacognosy,
The University of Mississippi

by

SANDIPAN DATTA

December 2012

ABSTRACT

Molecular-targeted antitumor therapy has found favor in antitumor drug discovery programs. Hypoxia (< 5% oxygen) is a common feature of solid tumors and hypoxia-inducible factor-1 (HIF-1) represents an important antitumor target. Bioenergetic homeostasis is typically altered in tumor cells and HIF-1 plays an important role to produce a glycolytic phenotype. Glycolysis inhibitors are an emerging class of potential tumor-selective adjuvant therapeutic agents. Natural product aerobic glycolysis inhibitors may enhance the effectiveness of current therapies. Mitochondrial oxidative phosphorylation inhibitors in botanical dietary supplements (BDS) possess a potential health hazard which should be identified and appropriately regulated.

Chapter one briefly reviews the molecular-targeted natural product antitumor drug discovery process. Descriptions of tumor hypoxia, HIF-1, HIF-1 regulatory pathways and the effect of HIF-1 on tumor cell bioenergetics are presented. Cellular bioenergetic pathways and natural products that inhibit HIF-1 by interfering with cellular bioenergetics are discussed. Mitochondriotoxic small-molecule natural products reported previously are further reviewed.

Chapter two discusses the effect of chromatographic media on molecular-targeted antitumor drug discovery. A panel of crude extracts was eluted through columns of various chromatographic media using a step gradient method. Total recoveries from the various columns and various elution protocols were compared and statistically analyzed. The crude extracts and column eluates were evaluated for HIF-1 inhibitory activity.

Chapter three discusses the development of a bioenergetics-based screening method to screen crude extracts for glycolysis inhibitors. Crude extracts (10,648) were screened and seven

hits (hit rate 0.72%) were identified. Bioassay-guided isolation of *Moronobea coccinea* crude extract resulted in isolation of a protonophoric compound moronone (**1**) (false positive). The structure of **1** was determined by a combination of spectroscopic and spectrometric means. The protonophoric compounds must be rapidly dereplicated for successful discovery of glycolysis inhibitors.

Chapter four discusses the screening of BDS products and pure compounds for mitochondrial uncouplers or electron transport chain inhibitors. The blue cohosh (*Caulophyllum thalictroides*) extract and three saponins cauloside A (**3**), saponin PE (**4**) and cauloside C (**5**) permeabilize the mitochondrial membrane. Sesamin (**6**) and guggulsterol III (**7**) and guggul (*Commiphora wightii*) extract inhibit mitochondrial complex I. These extracts and compounds are cytotoxic in nature.

DEDICATION

This dissertation is dedicated in memory of my grandmother, Parul Datta, who constantly nurtured my early education and inspired me to be a better human being.

LIST OF ABBREVIATIONS

1,3-BPG	1,3-bisphosphoglycerate
17AAG	17-*N*-allylamino-17-demethoxygeldanamycin
2-DG	2-deoxy-D-glucose
2-PG	2-phosphoglycerate
3BrPA	3-bromopyruvate
3-PGA	3-phosphoglycerate
4E-BP	Eukaryotic initiation factor 4E-binding protein
6PP	2'-4'-dihidroxy-5'-(1'''-dimethylallyl)-6-prenylpinocembrin
AcCoA	Acetyl coenzyme A
ADP	Adenosine diphosphate
ALD	Aldolase
ALDA	Aldolase isoform A
ANOVA	Analysis of variance
Apaf	Apoptotic protease activating factor
ARNT	Aryl hydrocarbon receptor nuclear translocator
ATCC	American type culture collection
ATP	Adenosine triphosphate
BCA	Bicinchoninic acid
BDS	Botanical dietary supplement
bHLH	basic Helix-loop-helix

BNIP	Bcl-2/adenovirus E1b 19 kDa protein interacting protein
CBP	CREB binding protein
CDK	Cyclin-dependent kinase
CITED	p300/CBP-interacting transactivator with glutamate (E)/aspartic acid (D)-rich tail
COX	Cytochrome *c* oxidase
CREB	cAMP reactive element binding protein
C-TAD	C-terminal transactivation domain
DCA	Dichloroacetate
DHAP	Dihydroxyacetone phosphate
DISC	Death-inducing signaling complex
DMEM	Dulbecco's modified eagle's medium
DNA	Deoxyribonucleic acid
EGFR	Epidermal growth factor receptor
EGTA	Ethylene glycol *bis*(2-aminoethyl ether)-*N*,*N*,*N'*,*N'*-tetraacetic acid
eIF	Eukaryotic initiation factor
ENO	Enolase
EPO	Erythropoetin
ERK	Extracellular signal-regulated kinases
ETC	Electron transport chain
ETF	Electron transferring flavoprotein

F1,6BP	Fructose-1,6-bisphosphate
F2,6BP	Fructose-2,6-bisphosphate
F6P	Fructose-6-phosphate
FAD	Flavin adenine dinucleotide
FBS	Fetal bovine serum
FCCP	2-[{4-(trifluoromethoxy)phenyl}hydrazinylidene]propanedinitrile
FDA	Food and Drug Administration
FH	Fumarate hydratase
FTase	Farnesyl transferase
G6P	Glucose-6-phosphate
GA3P	Glyceraldehyde-3-phosphate
GAPDH	Glyceraldehyde-3-phosphate dehydrogenase
gCOSY	Gradient ^{1}H-^{1}H chemical shift correlation spectroscopy
GGTase	Geranylgeranyl transferase
gHMBC	Gradient heteronuclear multiple-bond coherence spectroscopy
gHSQC	Gradient heteronuclear single quantum coherence spectroscopy
GLUT	Glucose transporter
gNOESY	Gradient Nuclear Overhauser effect spectroscopy
GSK	Glycogen synthase kinase
HDAC	Histone deacetylase
HEP3B	Human hepatoma cell line

HEPES	[4-(2-hydroxyethyl)-1-piperazineethanesulfonic acid]
HER2	Human epidermal growth factor receptor 2
HIF-1	Hypoxia-inducible factor-1
HK	Hexokinase
HPLC	High performance liquid chromatography
HRE	Hypoxia-response element
HRESIMS	High-resolution electron spray ionization mass spectrometry
Hsp90	90 kDa heat-shock protein
HTS	High-throughput screening
HUR	Human antigen R
IR	Infrared spectroscopy
IRES	Internal ribosome entry site
KA	Koningic acid
LD_{50}	Lethal dose 50% or median lethal dose
LDH	Lactate dehydrogenase
LND	Lonidamine
MAPK	Mitogen-activated protein kinase
MCT	Monocarboxylate transporter
MDA-MB-231	M. D. Anderson-metastatic breast-231 human breast adenocarcinoma cell line

MEK	Mitogen-activated protein kinase kinase/ extracellular signal-regulated kinase
MHz	Megahertz
MiR	MicroRNA
MMP	Matrix metalloproteinase
M-PER	Mammalian protein extraction reagent
MPTP	Mitochondrial membrane permeability transition pore
MTOR	Mammalian target of rapamycin
NADH	Nicotinamide adenine dinucleotide reduced
NADP	Nicotinamide adenine dinucleotide phosphate
NCI	National Cancer Institute
NCNPR	National center for natural products research
NDUFA4L2	NADH dehydrogenase [ubiquinone] **1** alpha subcomplex 4-like 2
NIH	National Institutes of Health
NLS	Nuclear localization signal
NMR	Nuclear magnetic resonance
N-TAD	N-terminal transactivation domain
OD	Optical density
ODDD	Oxygen-dependent degradation domain
OXPHOS	Oxidative phosphorylation
PAS	Period cicardian-aryl hydrocarbon nuclear translocator-single-minded

PBD	Polyprenylated benzophenone derivative
PDK	Pyruvate dehydrogenase kinase
PDP	Pyruvate dehydrogenase phosphatase
PEP	Phosphoenolpyruvate
PER	Period cicardian
PERK	Protein kinase RNA-like endoplasmic reticulum kinase
PFKBF3	6-Phosphofructo-2-kinase/fructose-2,6-biphosphatase-3
PFKL	Phosphofructokinase isoform L
PGAM	Phosphoglycerate mutase
PGI	Phosphoglucoisomerase
PGK	Phosphoglycerate kinase
PHD	Prolyl-4-hydroxylase
PI3K	Phosphatidylinositol-3-kinase
PIP3	Phosphatidylinositol-3,4,5-triphosphate
PK	Pyruvate kinase
PKC	Protein kinase C
PKM2	Pyruvate kinase isoform M2
Plk3	Polo-like kinase 3
PPP	Pentose phosphate pathway
PTB	Polypyrimidine binding protein
PTM	Posttranslational modification

Q	Ubiquinone
QH2	Ubiquinol
qHTS	Quantitative high-throughput screening
RACK	Receptor of activated protein C kinase
RBM	RNA binding protein
Rbx	Ringbox protein
REDD	Regulated in development and DNA damage responses
RHRE	RNA hypoxia-response element
RNA	Ribonucleic acid
ROS	Reactive oxygen species
RP	Reverse phase
SENP	Sentrin/SUMO-specific protease
SIM	Single-minded protein
SIRT	Sirtuin
SSAT	Spermidine/spermine-N^1-acetyltransferase
SUMO	Small ubiquitin-like modifier
T47D	Human breast ductal carcinoma cells
TCA	Tricarboxylic acid
TES	*N*-[tris(hydroxymethyl)methyl]-2-aminoethanesulfonic acid
TK	Thymidine kinase
TLC	Thin-layer chromatography

TMPD	*N*,*N*,*N*′,*N*′-tetramethyl-*p*-phenylenediamine
TMRM	Tetramethylrhodamine methylester
TNF	Tumor necrosis factor
TOF	Time-of-flight
TPI	Triose phosphate isomerase
TRAIL	TNF-related apoptosis-inducing ligand
TRK	Tyrosine kinase
TSC1/2	Tuberous sclerosis
UM	University of Mississippi
UTR	Untranslated region
UV	Ultraviolet
VDAC	Voltage-dependent anion channel
VDU2	pVHL-interacting de-ubiquitinating enzyme
VEGF	Vascular endothelial growth factor
pVHL	von Hippel-Lindau protein

ACKNOWLEDGEMENT

First and foremost I would like to acknowledge and thank my research advisors Dr. Dale G. Nagle and Dr. Yu-Dong Zhou. Without their support, patience, and training this could not have been possible. I am forever indebted to them for their mentoring and their timely suggestions that have helped me a lot to develop my scientific skills, thought process, and logical reasoning abilities. It was a great honor to work with them and I consider myself fortunate that they have given me an opportunity to work with them. I am also thankful to Drs. Nagle and Zhou and the Department of Pharmacognosy for a Student Research Assistantship.

I thank my committee members Dr. Daneel Ferreira and Dr. Mika B. Jekabsons for their timely advice and interest. I would like to specially thank Dr. Mika B. Jekabson for his expert advice on mitochondrial physiology and experimental designs. I am grateful to Dr. Marc Slattery for his assistance with the statistical analysis. I would also like to thank Dr. Ikhlas A. Khan for providing crude botanical dietary supplement samples and purified compounds.

I would also like to express my thanks to our present and past lab members (Ms. Fakhri Mahdi, Dr. Jun Li, Dr. Lin Du, Dr. Yang Liu, Dr. Coothankandaswamy Veena, and Brian Morgan). I would like to specially mention Ms. Fakhri Mahdi from whom I have learnt a lot. I am grateful to all the staff, faculty members and fellow students for being with me and helping me out during my times of stress and anxiety. I would like to express special thanks to Amanda Waters and for her constant help with my writing.

In addition, I would like to thank my friends in Oxford, MS, especially to Ramshankar Basak, Md. Mamun Mian, Surma Mukherjee, Stephen Frye, Tushar Padwal, Krishna Teja Nagalla and Eugene Chin, whose constant support was a big motivation for me. I would like to thank Stephen Frye in particular for spending his valuable time and helping me out with my dissertation writing.

The work described herein was supported by the National Institutes of Health-National Cancer Institute (grant CA-98787) and the National Oceanic and Atmospheric Administration National Institute for Undersea Science and Technology (grant NA16RU1496). The work was conducted in a facility constructed with Research Facilities Improvement Grant C06 RR-14503 from the National Institutes of Health.

Last but not the least, I would like to express my deepest gratitude to my parents, grandparents, family and friends back in India, without whose sacrifice and support I could not have been whom I am today. Above all I thank the almighty for his blessings.

TABLE OF CONTENTS

LIST OF TABLES

LIST OF FIGURES

CHAPTER I

INTRODUCTION

1.1 Molecular-targeted, natural product antitumor drug discovery

1.1.1 Overview of molecular-targeted antitumor drug discovery

Cytotoxic compounds have until recently been the focus for antitumor drug discovery programs. With the completion of the human genome sequence in the1990s, along with a better understanding of the cellular and molecular biology of cancer, the focus of these programs has gradually shifted towards development of molecular-targeted drugs. Prior to the molecular-targeted era, antitumor therapy was based on the premise that cancer cells can be eradicated by damaging cellular DNA or by blocking the cell division machinery. This approach stemmed from the limited concept that cancer cells divide more rapidly than normal cells, and that cancer cells need DNA replication in order to proliferate. Arguably, these cytotoxic drugs are considered the first generation of 'targeted cancer therapy' (Varmus, 2006). However, many of the processes targeted by these drugs were also critical for the survival of normal cells. Hence, low tumor cell specificities and narrow therapeutic windows limited the use of these cytotoxic compounds in the standard chemotherapeutic regimen. Molecular-targeted cancer therapies were recently developed to overcome these limitations. The goal of the contemporary molecular-targeted approach is to eliminate tumor cells in a selective manner without affecting normal cells, which can be achieved by exploiting the pharmacokinetic, biochemical, and molecular biological differences between normal and malignant cells.

Understanding the molecular basis of cancer is the key factor in the development of antitumor molecular-targeted therapies. Elucidation of the genetic causes of cancer began as early as 1911 with the discovery of the first tumor-causing virus (Rous, 1911). However, the first oncogene was not identified until 1970 (Duesberg and Vogt, 1970). This discovery provided the conceptual breakthrough of gene mutation, which is one of the major factors that contribute to

tumorigenesis. To date, mutations of 487 human genes (~1%) have been shown to contribute to the etiology of cancer (Wellcome Trust Sanger Institute, 2012). Gain-of-function mutations for oncogenes and loss-of-function mutations of tumor suppressor genes both lead to tumorigenesis. These mutations are also often accompanied with epigenetic abnormalities, which results in altered gene expressions (Yoo and Jones, 2006). Such alterations in gene expression (pro-oncogenic) are critical for the survival and maintenance of the malignant cancer cell phenotype. Any perturbation of these pro-oncogenic signaling pathways can profoundly impact cancer cell viability. This phenomenon is known as 'oncogene addiction' (Weinstein, 2002). Studies conducted in a mouse xenograft model revealed that brief pharmacological inactivation of the oncogene *Myc* could prolong animal survival and cause tumor regression (Jain *et al.*, 2002). Numerous studies using transgenic mice that bear activated oncogenes have supported this concept (Varmus *et al.*, 2005). These results support the development of molecular-targeted antitumor therapies.

The process of molecular-targeted drug discovery starts with identification of a target. The prospective target can be a receptor [i.e., human epidermal growth factor receptor2 (HER2)] (Shawer *et al.*, 2002), an enzyme (metalloproteinase) (Li and Wu, 2010), or a transcription factor [i.e., hypoxia-inducible factor (HIF)-1] (Patiar and Harris, 2006). The major criteria for the selection of a molecular target are its unique presence in tumor cells and high importance in tumor cell survival, proliferation, and metastasis. In addition to these factors, feasibility for high-throughput screening is also taken into consideration (Sun, 2006). Certain characteristics (e.g., growth factor-independent cellular proliferation, apoptosis resistance, immortality, angiogenesis, invasion, and metastasis) are attributed as inherent to the cancer cells, and are the distinguishing features from normal cells (Hanahan and Weinberg, 2000). In addition, aerobic glycolysis and

disabling immune destruction are considered to be emerging 'hallmarks' of cancer (Hanahan and Wienberg, 2011). These unique properties of cancer cells allow for targeted therapeutic intervention, and can be exploited for the development of tumor-selective molecular-targeted therapies.

Following its selection, a target must be validated (Benson *et al.*, 2006). The goal of target validation is to assess the correlation between target modulation and disease progression. Target validation also helps to identify any undesirable effect(s) of target inhibition or stimulation. In oncology, an ideal target should enhance cellular survival/proliferation, metastasis or confer resistance when upregulated in tumor cells. On the other hand, inhibition or downregulation of the same target should rapidly and selectively eliminate cancer cells, stop the spread of tumor, reverse drug resistance, and/or have any other specific desirable effects determined by the evaluators (Sun, 2006; Collins and Workman, 2006). In addition, proteins with critical functions should be selected as targets, while proteins with redundant functions should not be pursued (Perry and Weitzman, 2005).

For lead generation, thousands of compounds can be screened, directly or indirectly, against a valid target in a high-throughput manner. The compounds used for screening can originate from either natural product or synthetic compound libraries. This screening approach can be either 'forward' (phenotype to target) or 'reverse' (target to phenotype) (Bredel and Jacoby, 2004). The biochemical high-throughput screening (HTS) assays involving isolated targets have been partially successful in lead generation (Wesche *et al.*, 2005; McDonald *et al.*, 2006). However, due to the overdependence on the assays using isolated targets, the global effects of modulating these targets do not always become clear until the later stages of drug development. A thorough investigation and prediction of possible unwanted effects arising from

the modulation of a particular target should be performed at the earlier stages, which would prevent late stage drug attrition and minimize drug development costs. One prominent example of late stage drug attrition is the farnesyltransferase (FTase) inhibitors, which were developed to treat advanced pancreatic, lung, and colon cancers. Ras (H-Ras/K-Ras) prenylation is essential for the plasma membrane association, as well as oncogenic activity. This prenylation is preferentially catalyzed by FTase in cancer cells; but in the event of pharmacologic inhibition of FTase, the enzyme geranylgeranyltransferase (GGTase) can prenylate and activate K-Ras, thus bypassing this inhibition of the Ras signaling pathway (Rowinsky, 2006). Efforts to simultaneously target FTase and GGTase have failed, due to high incidences of toxicity (Lobel *et al.*, 2001).

Phenotypic screening using intact cells, organisms or animals can be employed for screening of natural product-rich extracts and other substances which are incompatible with isolated targets (Mishra *et al.*, 2008). The main advantage of phenotypic screening is that one can monitor whether the targeted pharmacological intervention can produce the desirable effects at the cellular or organismic level. Phenotypic screening systems also allow for the discovery of novel targets or drug candidates with novel mechanisms of action. However, post-screening determination of the mechanisms of action is difficult, and the precise molecular targets often remain elusive.

Some of the established/validated and emerging antitumor molecular targets include: tyrosine kinases (TrK) (Shawer *et al.*, 2002), endothelial growth factor receptors (EGFR) (Ciardiello and Tortora, 2008), histone deacetylases (HDAC) (Jones and Steinkühler, 2008), cyclin-dependent kinases (CDKs) (Malumbres and Barbacid, 2009), mammalian target of rapamycin (mTOR) (Bjornsti and Houghton, 2004), matrix metalloproteinases (MMP) (Overall

and Kleifeld, 2006), HIF-1 (Semenza, 2007), vascular endothelial growth factor (VEGF) (Ferrara, 2005), VEGF-receptors (Schwartz *et al.*, 2010), proteasome (Adams, 2004), Bcl family proteins (Lessene *et al.*, 2008), topoisomerase (Chikamori *et al.*, 2010), tubulin (Cragg and Newman, 2004), kinesin (Cox and Garbaccio, 2010), 90 kDa heat-shock protein (Hsp90) (Neckers, 2006), and protein kinase C (PKC) (Collins and Workman, 2006). High-throughput screening of synthetic and natural product libraries is carried out to identify novel leads that inhibit one or more of these targets. Some of the tumor phenotype-targeted screenings include screening for agents that target tumor angiogenesis (Spannuth *et al.*, 2008), cancer stem cells (Gupta *et al.*, 2009), multidrug efflux (Szakács *et al.*, 2006), and aerobic glycolysis (Kitagawa *et al.* 2011).

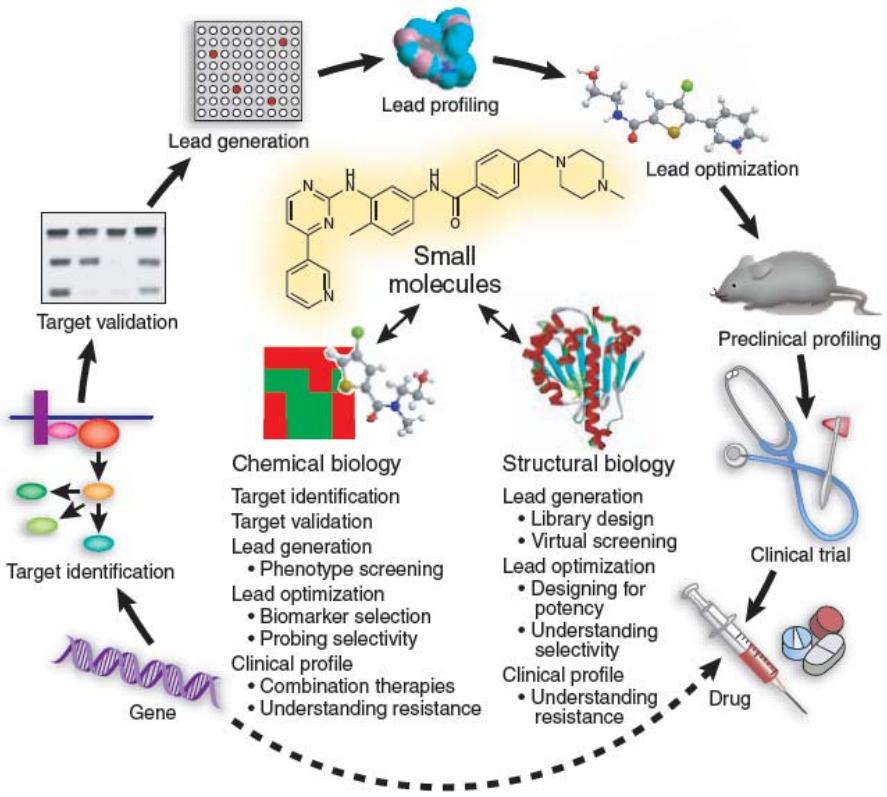

Figure 1.1 The process of molecular-targeted small-molecule drug discovery. The figure was reproduced with appropriate permission from the Nature publishing group (Collins and Workman 2006)

Critics of molecular-targeted antitumor drug discovery suggest that an overemphasis on isolated target-based screening has been the main reason for the lack of productivity in recent drug discovery (Hellerstein, 2008; Sams-Dodd, 2005). Two major problems plaguing the molecular-targeted drug discovery programs are late attrition of drugs due to lack of efficacy and/or toxic off-target effects. It is argued that the difference in functionality of any molecular target in a complex network, as well as the adaptability of cellular signaling pathways, are often overlooked while developing molecular-targeted drugs; these lead to late stage drug attrition (Hellerstein, 2008). Inhibition of drug targets that interconnect several pathways in the physiological setting will affect all the associated pathways, and may produce unwanted off-target effects. Indeed, the immense theoretical potential of the molecular-targeted approach is yet to be fully realized at the clinical level (Broxterman and Georgopapadakou, 2004). However, these pitfalls can be avoided by, (a) employing initial cell-based assays instead of the isolated target-based assays; (b) employing toxicity studies at the earliest feasible stage; (c) careful patient population recruitment in whom the molecular target is overexpressed; and (d) determination of valid molecular target endpoints.

1.1.2 Tumor hypoxia

Mammalian cells undergo oxidative metabolism to produce energy in an efficient manner. Under physiological conditions, most cells need oxygen as the ultimate electron acceptor, to synthesize adenosine triphosphate (ATP) through oxidative phosphorylation (Semenza, 2009). Intracellular O_2 concentrations depend on O_2 diffusion from the vasculature that supplies blood to the tissue. The O_2 diffusion geometry is inversely proportional to the distance of the cells from the vessel walls. A tissue-dependent 24 – 66 mm Hg oxygen partial

pressure [pO_2] (normoxic condition) (Weeks *et al.*, 2010) is usually maintained up to 70 μm from the vessel walls (Vaupel and Harrison, 2004). Apart from the diffusion geometry, the maintenance of tissue-specific normoxic conditions also depends on several factors, such as the O_2 carrying capacity of the blood; morphological and functional normality of the vasculature; perfusion of blood through the vessels, and cellular oxygen demand. Formation of solid tumors is initiated through rapid and uncontrolled cell proliferation. Owing to the sharp increase in oxygen demand caused by rapidly dividing tumor cells, normal tissue vasculature is unable to maintain tissue-specific normoxic conditions (Vaupel *et al.*, 2001). This imbalance in oxygen demand and supply creates 'hypoxia/hypoxic conditions', which can be defined as the oxygen deficiency level (~ 7 mm Hg) that compromises normal cellular functions, and triggers adaptive responses (Semenza, 2009; Goonewardene *et al.*, 2002). One of these adaptive responses to hypoxic conditions is the occurrence of an aberrant and chaotic angiogenesis (formation of new blood vessels) in solid tumors. The new microvasculature, unlike the normal vasculature, is morphologically and functionally deformed, and hence, it is less efficient in supplying nutrients and oxygen to the surrounding tissue (Tredan *et al.*, 2007). The difference between the rate of cell proliferation and the rate of angiogenesis is maintained during the growth of tumors. As a result, a heterogeneous pattern of oxygen partial pressure and chronically hypoxic areas are commonly observed throughout solid tumors.

In the early twentieth century, tumor hypoxia was identified as a major factor in determining tumor sensitivity to ionizing radiation (Mottram, 1936). Since then, the effects of hypoxia on tumor cells have been extensively evaluated. Numerous clinical studies in various solid tumors have shown that tumor hypoxia (2.5 – 22 mm Hg of O_2 partial pressure) is inversely correlated with disease-free and overall survival rates (Hockel and Vaupel, 2001). In an animal

model, several cytotoxic agents, such as doxorubicin, carboplatin, vincristine, etoposide, and cyclophosphamide, have been shown to affect tumors in an oxygen-dependent manner (Teicher *et al.*, 1990). Hypotheses of hypoxic chemoresistance have been formulated, which include decreased cell proliferation, decreased drug penetration to the hypoxic cells, hypoxia-mediated clonal selection, and adaptive modification of the cellular genome and proteome (e.g., induction of multidrug resistance mechanism) (Cosse and Michiels, 2008; Zhu *et al.*, 2005). Currently, tumor hypoxia (< 10 mm Hg of O_2 partial pressure) is an accepted adverse prognostic marker for solid tumor chemo and radiosensitivity to standard antitumor therapeutic regimens.

Measurement of tumor hypoxia had been primarily performed with polarographic needle electrodes. The polarographic needle electrode has been the gold standard in measuring tumor pO_2. Currently, exogenous markers (e.g., pimonidazole and EF5) and endogenous markers (e.g., carbonic anhydrase IX and HIF-1α) of hypoxia are primarily used for clinical tumor hypoxia measurement (Rademakers *et al.*, 2008).

1.1.3 Hypoxia-inducible factor-1α

Adaptive responses to tumor hypoxia are primarily mediated by a group of proteins known as hypoxia-inducible factors (HIF). These proteins are heterodimeric transcription factors that consists of an α and a β subunit protein of basic helix-loop-helix Per-ARNT-Sim (bHLH-PAS) protein superfamily (Wang *et al.*, 1995). Three HIF α subunit isoforms have been discovered, namely HIF-1α, HIF-2α and HIF-3α. The β subunit is also known as aryl hydrocarbon receptor nuclear translocator (ARNT) and is constitutively expressed. Among these three HIF isoforms, HIF-1 is the most prevalent and is ubiquitously expressed in all human tissues examined (Semenza *et al.*, 1997). The HIF-1α subunit is a 120-kDa, 826 amino acid

protein that consists of several distinct functional domains. The major HIF-1α subunit domains that are involved in self-regulation and HIF-1 transcriptional activation are as follows: bHLH domain (amino acid residues 17 – 71, required for heterodimerization and DNA binding); PAS domain (amino acid residues 85 – 298, required for heterodimerization and DNA binding) (Wang *et al.*, 1995); oxygen-dependent degradation domain (ODDD, amino acid residues 401–603, required for oxygen-dependent degradation) (Huang *et al.*, 1998); N-terminal transactivation domain (N-TAD, amino acid residues 531 – 575); and C-terminal transactivation domain (C-TAD, amino acid residues 786 – 826, required for transcriptional coactivator binding) (Jiang *et al.*, 1997). The HIF-1α subunit contains two nuclear localization signal (NLS) domains (amino acid residues 17 – 33 and 718 – 721). The C-terminal NLS is essential for the hypoxia-induced nuclear localization of HIF-1α (Kallio *et al.*, 1998). The HIF-1α protein also contains a nuclear export signal that is responsible for shuttling of HIF-1α between the cytosol and the nucleus (amino acid residues 616 – 658) (Mylonis *et al.*, 2008). Each HIF-1β subunit (91 – 94 kDa, 789 amino acid residues) contains a single transactivation domain. The HIF-1β subunits are devoid of ODDD but contain bHLH and PAS domains (Semenza, 1999).

Under physiological conditions, the limiting factor for HIF-1 activation is the stability of the HIF-1α subunit, which is rapidly degraded in the presence of adequate oxygen (> 5% O_2) (Huang *et al.*, 1996). The lack of ODDD in HIF-1β prevents the oxygen-dependent degradation of HIF-1β and makes the subunit constitutionally active (Semenza, 1999). Hypoxia-inducible factor-1α stabilization allows HIF-1α and β to dimerize. This results in a transcriptionally active HIF-1 that translocates to the nucleus (Wang *et al.*, 1995). Following the transcriptional activation, HIF-1 binds to the cis-acting DNA sequence 5' –(A/G)CGTG– 3' [hypoxia-response element (HRE)] located in the promoter regions of the target genes (Semenza *et al.*, 1996).

Following DNA binding, HIF-1 typically recruits and binds to transcriptional coactivators, such as p300/CBP [CREB (cAMP reactive element binding protein) binding protein] and/or PKM2 (pyruvate kinase isozyme M2) (Luo *et al.*, 2011). However, the direct repression of a target gene by HIF-1 is rare and usually downregulation of genes by HIF-1 is achieved by an indirect mechanism (Semenza, 2011). The HIF-1–p300/CBP interaction is mediated by the first cysteine/histidine-rich region of p300 (p300-C/H1) and HIF-1α-C-TAD, and the HIF-1 coactivator interaction is essential for the HIF-1-induced gene transcription (Bhattacharya *et al.*, 1999; Arany *et al.*, 1996).

1.1.4 Non-mitochondrial HIF-1α regulatory mechanisms

The rapid degradation of HIF-1α under tissue-specific physiological normoxic conditions (>5% O_2) is due to the presence of the ODDD in the subunit structure (amino acid residues 401 – 603). A family of dioxygenases known as prolyl-4-hydroxylases (PHD) is primarily responsible for the oxygen-dependent degradation of the HIF-1α subunit. Three isoforms of PHD are known, namely PHD-1, PHD-2, and PHD-3. All three isoforms can hydroxylate the HIF-1α protein at the proline-402 and proline-564 residues, by using molecular oxygen as a substrate, and iron (Fe^{2+}), 2-oxoglutarate, and ascorbate as cofactors (Figure1.2) (Bruick and McKnight, 2001; Hirota and Semenza, 2005). However, PHD-2 is thought to be the major HIF-1α hydroxylating enzyme in vivo (Berra *et al.*, 2003).

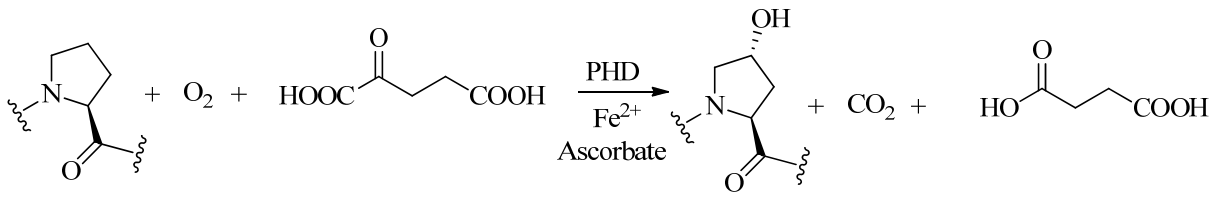

Figure 1.2 Prolyl-4-hydroxylation reaction catalyzed by prolyl-4-hydroxylases (PHDs)

Proline hydroxylation of HIF-1α (residues 402 and 564) allows the recognition of HIF-1α by the von Hippel-Lindau protein (pVHL), and subsequent HIF-1α polyubiquitination by the pVHL-E3 ubiquitin ligase complex [pVHL, elongins B and C, cullin 2, and ringbox protein1 (Rbx1)] (Czyzyk-Krzeska and Meller, 2004; Kamura *et al.*, 1999). Polyubiquitinated HIF-1α is recognized and degraded by the 26S proteasome (Kallio *et al.*, 1999). Any perturbation of this pathway, such as inhibition of the PHDs by small-molecules or transition metals [Co^{2+}, Ni^{2+}, and Mn^{2+}] (Schofield and Ratcliffe, 2004), depletion of any of the cofactors (e.g., depletion of Fe^{2+} by an iron chelator) (Roy *et al.*, 2004), pVHL deficiency (Maxwell *et al.*, 1999), and/or inhibition of 26S proteasome, stabilize HIF-1α under normoxic conditions and cause intracellular accumulation of HIF-1α protein in the absence of hypoxia (Kallio *et al.*, 1999). However, it has been reported that the accumulation of intracellular HIF-1α protein does not necessarily transform into the transcriptionally active HIF-1. In fact, inhibition of the 26S proteasome by bortezomib has been shown to inhibit the transcriptional activity of HIF-1 under both normoxic and hypoxic conditions, but caused significant accumulation of HIF-1α protein under normoxic conditions (Kaluz *et al.*, 2006). The paradoxical response of HIF-1 in response to proteasome inhibitors is suggested to be partially mediated by a protein known as CITED2 [p300/CBP-interacting transactivator with glutamate (E)/aspartic acid (D)-rich tail 2] (Shin *et al.*, 2008). The CITED2 protein is a p300-CH1 domain-binding protein, which inhibits HIF-1 transcriptional response by preventing HIF-1α-p300 interaction (Bhattacharya *et al.*, 1999). Aspargine hydroxylation within the C-TAD at residue 803 by an aspargine hydroxylase (Factor inhibiting HIF-1 [FIH]) prevents the HIF-1-p300/CBP interaction and inhibits subsequent HIF-1 gene transcription (Mahon *et al.*, 2001; Lando *et al.*, 2002).

Other post-translational modifications (PTM) that have been reported to modulate HIF-1α stability, and therefore HIF-1activity, include sumoylation (Bae *et al.*, 2004; Cheng *et al.*, 2007), de-ubiquitination (Li *et al.*, 2005), and phosphorylation of the HIF-1α subunits (Mylonis *et al.*, 2006). In an in vitro study, covalent attachments of a SUMO (small ubiquitin-like modifier protein) at lysine-391 and lysine-471 have been shown to increase HIF-1α stability (Bae *et al.*, 2004). However, a later study using sentrin/SUMO-specific protease-1 (SENP-1)-knockout mice showed that sumoylation promotes HIF-1α degradation through the pVHL-proteasome pathway (Cheng *et al.*, 2007). It has been argued that SUMO overexpression in presence of SENP-1 led to HIF-1 stabilization via sumoylation. A pVHL-interacting de-ubiquitinating enzyme (VDU2) has been identified that mediates the pVHL-dependent HIF-1α de-ubiquitination. De-ubiquitination of HIF-1α leads to intracellular accumulation of HIF-1α and expression of downstream target genes, such as VEGF (Li *et al.*, 2005). Various kinases have been reported to phosphorylate amino acid residues in HIF-1α with opposing effects. Serine-641 and serine-643 phosphorylation by p42/p44 mitogen-activated protein kinase (MAPK) enhances nuclear accumulation and HIF-1 transcriptional activity (Mylonis *et al.*, 2006), whereas serine-551, threonine-555, and serine-589 phosphorylation by glycogen synthase kinase 3 (GSK-3) causes a pVHL and proteasome-dependent HIF-1α destabilization (Flugel *et al.*, 2007). Polo-like kinase 3 (Plk3) has been shown to destabilize HIF-1α by directly phosphorylating serine-576 and serine-657 (Xu *et al.*, 2010).

Apart from post-translational modifications, various cellular signaling pathways can regulate HIF-1α at the translational level. Well-studied cellular signaling pathways that regulate HIF-1α translation include the PI3K (phosphatidylinositol-3-kinase)/Akt (protein kinase B, PKB)/mTOR (mammalian target of rapamycin) pathway and the MAPK pathway (Yee Koh *et al.*, 2008). Growth factors and oncoproteins, such as Ras, upregulate HIF-1α cap-dependent

translation under normoxic conditions in a cell line-dependent manner (Patiar and Harris, 2006). Ras oncoprotein enhances the normoxic HIF-1α translation via Raf-MEK (MAPK kinase)-ERK (extracellular signal-regulated kinases) signaling cascade activation that phosphorylates 4E-BP1 [eukaryotic initiation factor (eIF) 4E-binding protein]. Phosphorylation of 4E-BP1 causes dissociation of 4E-BP1 from eIF-4E and allows the initiation factor to be incorporated into the active eIF-4F, thereby facilitating enhanced HIF-1α translation (Yee Koh *et al.*, 2008; De Benedetti and Graf, 2004). Under normoxic conditions, the PI3K/Akt/mTOR pathway also converges on eIF-4E phosphorylation. Activation of PI3K by the receptor tyrosine kinases (e.g., HER2) enhances the formation of PIP3 (phosphatidylinositol-3,4,5-triphosphate). Subsequently, PIP3 activates the Akt/mTOR signaling cascade that results in 4E-BP and ribosomal S6 kinase hyperphosphorylation (Yee Koh *et al.*, 2008; Ruvinsky *et al.*, 2005; Bronchud, 2007). Under normoxic conditions, this enhances HIF-1α translation.

In an acute response to hypoxia, the phosphorylation of eIF-2α by PERK (protein kinase RNA-like endoplasmic reticulum kinase) prevents the formation of eIF2-GTP-met-tRNA ternary complex and thereby inhibits initiation of protein translation (Koumenis *et al.*, 2002). Additionally, prolonged hypoxic exposure results in a decrease in mTOR activity and 4E-BP hypophosphorylation, which leads to repression of eIF-4F complex activity (Reiling and Sabatini, 2006). The mTOR inhibition is mediated through a hypoxia-inducible protein REDD1 (regulated in development and DNA damage responses 1) and its downstream effector TSC-1/2 (tuberous sclerosis) (DeYoung *et al.*, 2008). However, HIF-1α translation is not compromised under hypoxia. A controversial cap-independent translation mechanism involving an internal ribosome entry site (IRES) has been suggested for hypoxic translation of HIF-1α (Zhou *et al.*, 2004; Lang *et al.*, 2002; Young *et al.*, 2008; Bert *et al.*, 2006). An alternative mechanism that

involves PTB (polypyrimidine binding protein) and HuR (human antigen R) binding to the 3'- and 5'- untranslated regions (UTR) of HIF-1α mRNA, respectively, has also been proposed (Galban *et al.*, 2008; Schepens *et al.*, 2005). A recent study has identified HIF-2α as a translation facilitator under hypoxia. Recognition of an RNA hypoxia-responsive element (rHRE) by RBM4 (RNA binding protein 4) is essential for translation under hypoxic stress in an eIF-4E2 dependent manner (Uniacke *et al.* 2012; Montoya, 2012). Modulation of HIF-1α translation by microRNAs (miRs, "noncanonical RNA species of 18 – 23 nucleotides in length") (Loscalzo, 2010) is observed under both normoxic and hypoxic conditions. MicroRNA-199a inhibited HIF-1α translation under normoxia, but the hypoxic conditions downregulated miR-199a and reversed the HIF-1α inhibition (Rane *et al.*, 2009). Conversely, enhanced miR-130 family levels under hypoxic conditions increased HIF-1α translation in an IRES-dependent manner (Saito *et al.*, 2011).

Another non-mitochondrial HIF-1 regulatory mechanism involves 90kDa heat-shock protein (Hsp90) and RACK1 (receptor of activated protein C kinase). Binding of Hsp90 to the HIF-1α PAS domain promotes HIF-1α nuclear localization and prevents O_2/PHD/VHL-independent degradation (Katschinski *et al.*, 2004; Liu and Semenza, 2007). Conversely, RACK1 binding promotes HIF-1α polyubiquitination and proteasomal degradation by an O_2/PHD/VHL-independent mechanism (Liu *et al.*, 2007). Spermidine/spermine-N^1-acetyltransferase-1 (SSAT1) stabilizes the RACK1-HIF-1α complex and is essential for RACK1-mediated HIF-1 polyubiquitination (Baek *et al.*, 2007). Both Hsp90 and RACK1 compete for the same HIF-1α binding site, and downregulation of HIF-1 by the Hsp90 inhibitors [e.g., 17-(allylamino)-17-demethoxygeldanamycin (17AAG) (**1**)] is mediated by RACK1 (Liu *et al.*, 2007; Isaacs *et al.*, 2002).

1.1.5 Mitochondrial HIF-1α regulatory mechanism

Hypoxia-inducible factor-1α stabilization by reactive oxygen species (ROS) from the hypoxic mitochondrial electron transport chain (ETC) is a well-studied HIF-1 regulatory pathway. Based on the pioneering study by Schumacker and Chandel (Chandel *et al.*, 1998), it was proposed that ROS, generated by the mitochondrial ETC, are responsible for hypoxic (1.5% O_2) HIF-1α stabilization and transactivation. This study demonstrated that molecules that inhibit the electron transport chain complexes (specifically complex I and complex III), such as rotenone (**2**) (complex I inhibitor), diphenylene iodonium chloride (**3**) (complex I inhibitor), and myxothiazol (**4**) (complex III inhibitor), decrease mitochondrial ROS and inhibit hypoxic stabilization of HIF-1α. In addition, mitochondrial DNA depletion (ρ^0 cells) or treatment with antioxidants abolished the ROS generation and transcription of erythropoietin (EPO, a target gene of HIF-1) in cells. In a later study, Chandel and coworkers proposed that ROS generation at the Q_o site of mitochondrial complex III is essential for hypoxic HIF-1α transactivation (Bell *et al.*, 2007).

The electron transfers from complexes I and II to complex III is carried out by ubiquinone (Q), a membrane soluble electron carrier (Trumpower, 1990; Klimova and Chandel, 2008). A ubiquinone molecule accepts two electrons and is subsequently converted to ubiquinol (QH_2). The QH_2 molecule transfers the electron pair to complex III via the Q cycle. In the Q cycle, QH_2 transfers one electron to the Rieske iron-sulfur protein within complex III and is then oxidized to form a reactive semiubiquinone (QH·) radical. The formation of QH· occurs in the Q_o site of mitochondrial complex III. The transport of the electron from the Rieske Fe-S protein to complex IV is performed by cytochrome c_1 (complex III) and cytochrome *c* (electron carrier

from complex III to complex IV). The remaining electron on the ubisemiquinone radical reduces the b_L reaction center of cytochrome *b* which is passed on to the cytochrome b_H and finally to Q_i site of complex III. The now fully oxidized ubiquinone, that is at the center "i" site of complex III again produce the semiquinone. The QH· radical is very reactive and can readily transfer the single electron to available molecular oxygen leading to production of superoxide radicals ($O_2^{\cdot -}$) at the Q_o site (Figure 1.3) (Trumpower, 1990; Klimova and Chandel, 2008). In accordance with the ROS hypothesis, the Q_o site inhibitor stigmatellin (**5**), prevents mitochondrial ROS generation while, the Q_i site inhibitor antimycin A (**6**), had no effect on mitochondrial ROS generation (Guzy *et al.*, 2005; Chandel *et al.*, 1998). The ROS hypothesis is further supported by other independent studies. Using $JunD^{-/-}$ cells, Gerald and coworkers demonstrated that under normoxic conditions, oxidative stress could stabilize HIF-1α by decreasing the Fe^{2+} availability and thus inhibiting PHD activity (Gerald *et al.*, 2004).

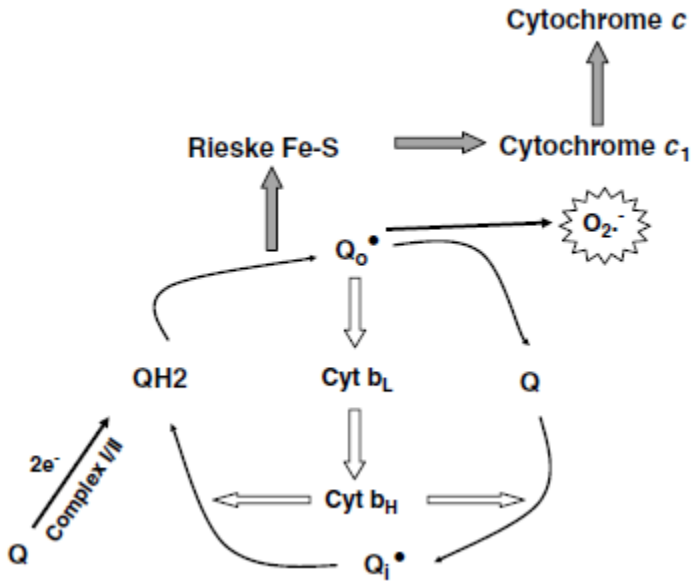

Figure 1.3 Electron transfer and ROS production by the ubiquinone (Q) cycle in mitochondrial complex III at Q_o site. The figure was reproduced with appropriate permissions from the Nature publishing group (Klimova *et al.*, 2008).

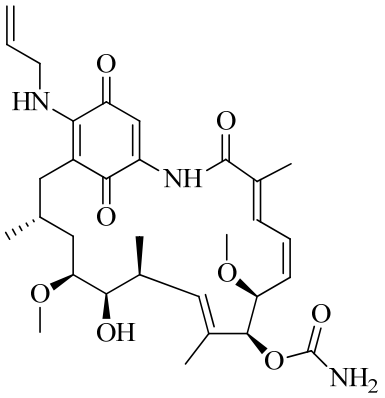

17AAG (**1**)

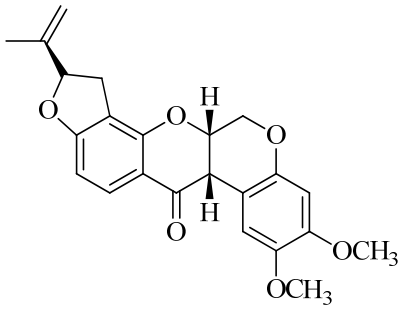

Rotenone (**2**)

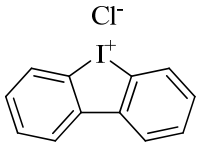

Diphenylene iodonium chloride (**3**)

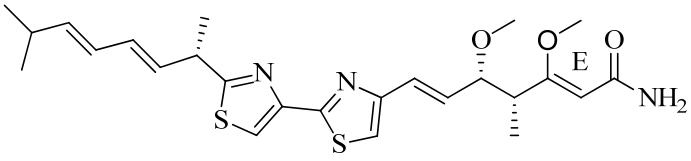

Myxothiazol (**4**)

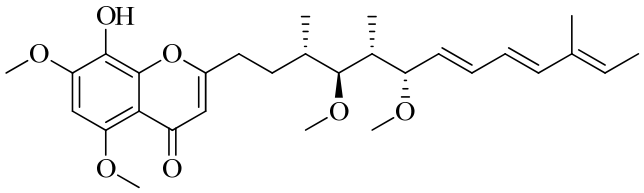

Stigmatellin (**5**)

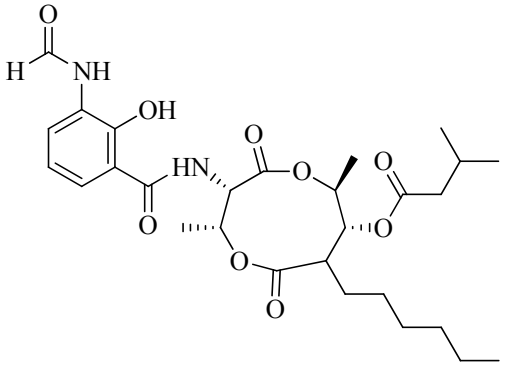

Antimycin A (**6**)

Figure 1.4 Natural products that inhibit Hsp90 [17AAG (**1**)] and mitochondrial respiratory complexes (complexes I and III).

In a separate study, Pan and coworkers used a fusion protein containing HIF-1α ODDD to demonstrate that under hypoxic conditions (1.5% O_2) a loss of PHD activity occurs, which can be restored by the presence of mitochondrial ETC inhibitors, such as rotenone (**2**) and myxothiazol (**4**). In addition, HIF-1α stabilization by exogenous H_2O_2 was also observed. However, this study was unable to determine whether the HIF-1α stabilization was ROS-mediated or due to "oxygen redistribution" (Pan *et al.*, 2007). This evidence indicates that hypoxic conditions enhance ROS generation by mitochondrial ETC and the enhanced ROS levels oxidize Fe^{2+} to Fe^{3+}. Depletion of the intracellular Fe^{2+} pool inhibits the PDH-dependent degradation of HIF-1α, and activates HIF-1. Inhibition of the mitochondrial complexes I and III under hypoxia decrease mitochondrial ROS generation, and thus prevent HIF-1α stabilization.

An "oxygen redistribution" hypothesis was later proposed for hypoxic HIF-1α stabilization. A study by Hagen and coworkers observed that inhibition of normal mitochondrial oxygen consumption under hypoxia by an NO donor increased oxygen concentrations in the cytosol. They further observed that inhibition of PHD activity under hypoxia (1% O_2) could be reversed by the presence of a mitochondrial inhibitor. In addition, antioxidants (ascorbate, glutathione, and *N*-acetylcysteine) did not affect hypoxic HIF-1α stabilization. These observations led to the formulation of the hypothesis that under hypoxic conditions, normal mitochondrial activity inhibits PHD activity by limiting the availability of O_2 for the HIF-1α hydroxylation reaction. On the other hand, mitochondrial ETC inhibitors increase the cytosolic O_2 concentrations and destabilize HIF-1α under hypoxia by restoring PHD activity (Hagen *et al.*, 2003).

The 'oxygen redistribution hypothesis' appears to be inconsistent with the ROS hypothesis. The observation that cells which lack cytochrome *b* showed drastically less oxygen

consumption, yet retained the ability for hypoxia-induced ROS generation and HIF-1α stabilization, contradicts the oxygen redistribution hypothesis (Bell *et al.*, 2007). The observed interexperimental inconsistency in the effects of antioxidants on HIF-1α stabilization (Chandel *et al.*, 1998; Hagen *et al.*, 2003) may be due to the mechanistic nature of antioxidants used in the experiments or the inherent difference in the cell lines used (hepatoma *vs.* embryonic kidney cells). However, under physiological conditions both mitochondrial ROS and oxygen redistribution by mitochondria may act together to stabilize HIF-1α under hypoxic conditions (Taylor, 2008).

Apart from mitochondrial respiration-mediated regulation, HIF-1α is also regulated by tricarboxylic acid (TCA) cycle intermediates, namely succinate and fumarate. Prolyl hydroxylases generate succinate from 2-oxoglutarate in the cytoplasm during hydroxylation of HIF-1α. The succinate is then transported to the mitochondrial matrix, and converted to fumarate by the enzyme succinate dehydrogenase (mitochondrial complex II). Theoretically, increased succinate/fumarate concentrations in the cytoplasm can stabilize HIF-1α by preventing HIF-1α hydroxylation by a negative feedback mechanism. Indeed, dysfunctional succinate dehydrogenase has been demonstrated to increase ROS, tumorigenecity and intracellular HIF-1α protein accumulation (Selak *et al.*, 2005; Guzy *et al.*, 2008). Similarly, accumulation of fumarate can inhibit the forward reaction by PHDs and a number of studies demonstrate that mutations in fumarate hydratase (FH) or FH deficiency can stabilize HIF-1α (Pollard *et al.*, 2005; Isaacs *et al.*, 2005; Sudarshan *et al.*, 2009).

The mitochondrial deacetylase sirtuin-3 (SIRT3) has been shown to negatively regulate HIF-1α in a mitochondrial ROS and PHD-dependent manner (Finley *et al.*, 2011a; Bell *et al.*, 2011). Knockout of SIRT3 imparts a glycolytic phenotype in the mouse embryonic fibroblasts

(MEF), which can be reversed by genetic HIF-1α removal (Finley *et al.*, 2011a). Conversely, overexpression of SIRT3 under hypoxic conditions destabilizes HIF-1α and reduces HIF-1 transcriptional activity. In addition, tumorigenicity in xenografts are reduced in mice that overexpressed SIRT3 (Bell *et al.*, 2011). Sirtuin-3 can also affect HIF-1α stability via succinate dehydrogenase. It has been shown that succinate dehydrogenase is deacetylated by SIRT-3, and SIRT-3 is essential for normal succinate dehydrogenase activity. Loss of SIRT3 reduces succinate dehydrogenase activity, which may contribute to HIF-1α upregulation (Finley *et al.*, 2011b). The cytosolic sirtuins SIRT1 and SIRT6 have also been shown to regulate HIF-1 activity. While SIRT1 decreases HIF-1 transcriptional activity by deacetylating HIF-1α at Lysine-674 (Lim *et al.*, 2010), SIRT6 negatively regulates HIF-1 activity by acting as a transcriptional corepressor of HIF-1 target genes involved in glycolysis. In addition, SIRT6 knockout cells show enhanced HIF-1α translation suggesting that SIRT6 may downregulate HIF-1α protein synthesis under physiological conditions (Zhong *et al.*, 2010).

1.1.6 HIF-1 and tumor cell bioenergetics

Metabolic analysis revealed that cellular ATP utilization regulates approximately 50% of mitochondrial respiration, in contrast to the less than 15% regulation by the actual electron transport (Brown *et al.*, 1990). In this study, nicotinamide adenine dinucleotide (NADH) supply or concentration (15 – 30%) and proton leak (20%) were suggested as the other regulating factors for mitochondrial respiration. Later, a study by Chandel and his coworkers under hypoxic conditions demonstrated a control coefficient for NADH concentration similar to the earlier study (Chandel *et al.*, 1997). Decreasing cellular ATP consumption is an acute adaptive response to hypoxia. Cellular processes that consume ATP, such as Na/K ATPase activity and protein

translation, are immediately shut down in response to decreased oxygen (< 5%) (Tormos and Chandel, 2010). Prolonged exposure to hypoxia has also been shown to decrease mitochondrial oxygen consumption in a time-dependent manner. Hypoxic activation of HIF-1 mediates long-term adaptive responses to hypoxia, and plays a pivotal role in shaping tumor cell bioenergetics.

Hypoxia-inducible factor-1 stabilization shifts cellular bioenergetics towards a glycolytic phenotype by actively downregulating mitochondrial oxidative phosphorylation and simultaneously upregulating glycolytic flux. One of the mechanisms by which HIF-1 downregulates mitochondrial oxidative phosphorylation is by decreasing the availability of pyruvate to the TCA cycle (Kim *et al.*, 2006; Papandreou *et al.*, 2006). The glycolytic end product pyruvate is transported across the mitochondrial inner membrane by the pyruvate transporters and then decarboxylated to acetyl coenzyme A (AcCoA) by the pyruvate dehydrogenase (PDH) complex; the AcCoA then enters into the TCA cycle for further oxidation. The enzymatic activity of PDH is inversely proportional to the concentration of AcCoA, NADH and ATP. In addition, phosphorylation of the E1 subunit of PDH by pyruvate dehydrogenase kinase (PDK) deactivates PDH. Deactivated PDH can be dephosphorylated and subsequently reactivated by pyruvate dehydrogenase phosphatase (PDP) (Papandreou *et al.*, 2006; Sugden *et al.*, 2003). Pyruvate dehydrogenase kinase-1 was identified as a HIF-1 target gene, and it was demonstrated that under hypoxia, the absence of PDK1 in HIF-$1^{-/-}$ lymphoma cells enhanced mitochondrial ROS generation and hypoxia-induced cell death. In an independent study, exposure to prolonged hypoxia demonstrated decreased cellular oxygen consumption in a PDK1-dependent manner (Papandreou *et al.*, 2006). These results indicate that one of the mechanisms of HIF-1 mediated adaptation of cellular bioenergetics is by induction of PDK1.

Activated HIF-1 can reduce the cellular mitochondrial content by inhibiting mitochondrial biogenesis via repression of c-Myc activity and induction of BNIP3-mediated mitophagy. The HIF-induced mitophagy and repression of mitochondrial biogenesis provide a selective advantage to hypoxic cells by preventing the lethal mitochondrial ROS generation under hypoxia (Zhang *et al.*, 2007; Zhang *et al.*, 2008).

Complementary to the effect of hypoxic conditions on PDK1 induction, HIF-1 activates conversion of pyruvate to lactate, in order to shunt pyruvate away from mitochondrial metabolism. Lactate dehydrogenase is an enzyme that converts pyruvate to lactate. Lactate dehydrogenase type 5 (LDH-5 or LDH-A, that consists of four LDH-A subunits) is a HIF-1 target gene (Semenza *et al.*, 1994). Hypoxia-inducible factor-1 also activates the gene MCT4, which encodes a plasma membrane lactate transporter to facilitate lactate efflux from the cell (Ullah *et al.*, 2006).

Apart from the aforementioned modifications to mitochondrial metabolism, HIF-1 is responsible for modifying the mitochondrial respiratory complex structure and function. Under hypoxia, the composition of mitochondrial complex IV changes in a HIF-1-dependent manner. Mitochondrial complex IV (Cytochrome *c* oxidase, COX) consists of 13 subunits, and subunit 4 (COX4) performs a regulatory role by mediating ATP-induced allosteric COX inhibition (Napiwotzki and Kadenbach, 1998). Under hypoxic conditions, HIF-1 mediates the substitution of COX4 isoform 1 (COX4-1) by COX4 isoform 2 (COX4-2) in vitro. The COX4-1 isoform substitution enhances COX oxygen utilization efficiency, and represents an adaptive response to hypoxia (Fukuda *et al.*, 2007). Complex I inhibition by HIF-1 was observed in an in vitro model. Hypoxia induces NADH dehydrogenase [ubiquinone] **1** alpha subcomplex 4-like 2 (NDUFA4L2), a HIF-1 target protein, which shares a 65% homology with NDUFA4, a subunit

of complex I. Under hypoxia (1% O_2), silencing of NDUFA4L2 prevents a decrease in mitochondrial complex I activity, causes an increase in mitochondrial oxygen consumption, and decreases the cell viability. The exact mechanism by which NDUFA4L2 inhibits complex I activity is not clear. However, within 24 h of hypoxia, a decrease in NDUFA4 and an increase in NDUFA4L2 levels were observed. It was proposed that these proteins may be independently regulated (Tello *et al.*, 2007).

Chan and coworkers showed that mitochondrial oxidative metabolism could be suppressed by a HIF-1-induced microRNA miR-210. Induction of miR-210 prevents the assembly of iron-sulfur cluster assembly proteins ISCU1 and ISCU2 (Chan *et al.*, 2009). Iron sulfur cluster assembly proteins 1 and 2 are responsible for the assembly of prosthetic groups that facilitate electron transfer and redox reactions at the respiratory complexes. However, in this study the relatively low oxygen concentration of 0.2% was used.

While mitochondrial oxidative metabolism is downregulated, glycolytic flux is upregulated by HIF-1 via an increase in glucose catabolising enzymes (Semenza *et al.*, 1994). Tumor cells show enhanced glucose uptake and an increased expression of specific glucose transporter isoforms, namely glucose transporter type 1 (GLUT1) and glucose transporter type 3 (GLUT3) (Macheda *et al.*, 2005). The enhanced expression of glucose transporters (GLUT1 and GLUT3) is mediated by HIF-1 (Macheda *et al.*, 2005). Activation of HIF-1 enhances tumor-specific expression of glycolytic enzyme isoforms, such as hexokinase I and II (HKI and HKII), phosphofructokinase L (PFKL), aldolase A (ALDA), enolase 1 (ENO1), phosphoglycerate kinase 1 (PGK1), glyceraldehyde-3-phosphate dehydrogenase (GAPDH), pyruvate kinase muscle isozyme (PKM2), and LDH-A (Semenza *et al.*, 1994; Semenza, 2012; Higashimura *et al.*, 2011). Apart from these glycolytic enzymes, HIF-1 also regulates the glycolysis-associated

enzyme 6-phosphofructo-2-kinase/fructose-2,6-biphosphatase-3 (PFKBF3). This bifunctional enzyme is responsible for fructose-2,6-bisphosphate (F2,6BP) synthesis; F2,6BP acts as a potent PFK1 activator. Because PFK1 catalyzes the first control of flux reaction in the glycolysis pathway, activation of PFK1 results in increased glycolytic flux. In addition, PFKBF3 also diverts fructose-6-phosphate (F6P) to the pentose phosphate pathway (PPP) for synthesis of 5-phosphoribosyl-1-pyrophosphate (precursor for nucleic acid biosynthesis). The enzyme PFKBF3 is reported to be constitutively active in human cancer cell lines and serves as one of the contributors to the aerobic glycolysis (Warburg effect) (Minchenko *et al.*, 2002). In addition, HIF-1 mediates the PPP enzyme transketolase upregulation (Zhao *et al.*, 2010). Luo and coworkers recently discovered a novel role for PKM2 in metabolic reprogramming (Luo *et al.*, 2011). Independent of its enzymatic activity, PKM2 acts as a HIF-1 coactivator, and enhances the expression of HIF-1 downstream targets, such as VEGF. Prolyl hydroxylation enhances the coactivator activity of PKM2. Because PKM2 is a HIF-1 target gene, PKM2 can create a positive feedback response that alters tumor cell bioenergetics (Luo *et al.*, 2011). Taken together HIF-1 alters tumor cell bioenergetics, and imparts a highly glycolytic tumor cell phenotype which is crucial for cellular survival and proliferation under hypoxic conditions.

1.1.7 Downregulation of HIF-1α by natural product small-molecules that inhibits cellular bioenergetic pathways

Inhibition of HIF-1 activation is a valid and attractive antitumor molecular target (Nagle and Zhou, 2011). Efforts to discover clinically useful natural product or synthetic small-molecules that target HIF-1 or its downstream effectors (e.g., PDK1, LDH-A, and HK) have been undertaken by several antitumor drug discovery groups (Narita *et al.*, 2009; Lin *et al.*,

2008; Bobkova *et al.*, 2010; Xu *et al.*, 2009; Kalusmeyer *et al.*, 2007; Ward *et al.*, 2012; Vander Heiden *et al.*, 2010). Natural product-derived small-molecules that have been shown to inhibit the cellular bioenergetic pathways (glycolysis and mitochondrial ETC) and affect HIF-1 activity, will be briefly discussed. In an effort to discover chemically and mechanistically novel HIF-1 inhibitors, the molecular-targeted antitumor drug discovery group at the University of Mississippi has screened more than 60,000 natural product-rich extracts from plants and marine invertebrates (NCI Open Repository Program) in a T47D human breast tumor cell-based reporter assay system. A number of the HIF-1α inhibitors recently identified by this group are molecules that interfere with mitochondrial complex I or uncouple oxidative phosphorylation (Mohammed *et al.*, 2004; Liu *et al.*, 2009a; Mao *et al.*, 2009; Liu *et al.*, 2009b; Coothankandaswamy *et al.*, 2010; Morgan *et al.*, 2010; Du *et al.*, 2010; Du *et al.*, 2011; Mahdi *et al.*, 2011, Li *et al.*, 2011). The first compound that was identified to inhibit mitochondrial respiration by this group was laurenditerpenol (**7**) (Mohammed *et al.*, 2004). This algal-derived diterpene-type compound potently (IC_{50} 0.4 μM) inhibited hypoxic (1% O_2) HIF-1 activation in a human breast tumor T47D cell-based luciferase reporter assay system. Laurenditerpenol inhibits mitochondrial complex I in isolated mouse liver mitochondria (Mohammed *et al.*, 2004). Subsequently, the marine sponge-derived compound furospongolide (**8**) inhibited hypoxia-induced HIF-1 (IC_{50} 2.9 μM, T47D) activation by suppressing cellular respiration at mitochondrial complex I (Liu *et al.*, 2008). The plant metabolite 4'-*O*-methylalpinumisoflavone (**9**) was the first mitochondrial inhibitor identified by this group from *Lonchocarpus glabrescens* Benth. (Fabaceae), and was reported to inhibit hypoxic HIF-1 activation (IC_{50} 0.6 μM) by simultaneous inhibition of mitochondrial complex I and mammalian protein translation (Liu *et al.*, 2009a). Numerous other natural product small-molecules that inhibited mitochondrial complex I in cell-based assays were

identified by the Nagle/Zhou group. These mitochondriotoxic compounds from plants and marine invertebrates preferentially abolished HIF-1 activation under hypoxic conditions. These include mycalenitrile-6 (**10**) (Mao *et al.*, 2009), mycalenitrile-7 (**11**) (Mao *et al.*, 2009), caulerpin (**12**) (Liu *et al.*, 2009b), manassantin A (**13**) (Hossain *et al.*, 2005), manassantin B (**14**) (Hodges *et al.*, 2004), 4-*O*-methylsaucerneol (**15**) (Hossain *et al.*, 2005), thyrsiferol (**16**) (Mahdi *et al.*, 2011), mycothiazole (**17**) (Morgan *et al.*, 2010), 10-hydroxyglaucanetin (**18**) (Coothankandaswamy *et al.*, 2010), annonacin (**19**) (Coothankandaswamy *et al.*, 2010), annonacin A (**20**) (Coothankandaswamy *et al.*, 2010), skimmiarepin A (**21**) (Li *et al.*, 2011) and skimmiarepin C (**22**) (Li *et al.*, 2011) (Figures 1.4 – 1.5). Among these, **13** and **14** were the most potent complex I inhibitors (IC_{50} 0.003 μM) discovered by this group. Skimmiarepin A (**21**) inhibits the initiation and elongation steps of protein translation in T47D and MDA-MB-231 breast cancer cells by eIF2α and eEF2 hyperphosphorylation in a mitochondrial complex I inhibition-dependent manner (Li *et al.*, 2011). Hypoxia-induced and iron chelator-induced HIF-1 activation is inhibited by protonophoric compounds or uncouplers of oxidative phosphorylation. Fifteen isoprenylated dihydroxycoumarins that inhibit HIF-1 by this mechanism were identified (Du *et al.*, 2011). Among these, mammea E/BB [IC_{50} 0.96 μM, 1% O_2, 16 h, T47D] (**23**), mammea F/BA [IC_{50} 1.72 μM, 1% O_2, 16 h, T47D] (**24**), and mammea F/BB_1 [IC_{50} 2.23 μM, 1% O_2, 16 h, T47D] (**25**) were the most potent ones (Du *et al.*, 2011) (Figure 1.7). The mechanisms for HIF-1 inhibition by uncouplers are not clearly understood.

Apart from mitochondrial inhibitors, glycolysis inhibitors, such as 2-deoxy-D-glucose [2DG] (**26**) and sodium iodoacetate (**27**) (Figure 1.7), inhibit HIF-1α protein accumulation in response to hypoxia (0.1% O_2) in HT-1080 human fibrosarcoma cells (Staab *et al.*, 2007).

Glycolysis inhibitors also produced a dose-dependent decrease of HIF-1α accumulation in hypoxic (< 0.1% O_2) HEK293 cells (Zhou *et al.*, 2007).

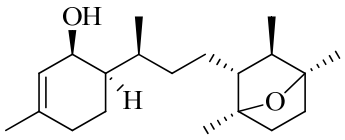

Laurenditerpenol (**7**)

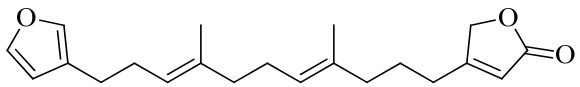

Furospongolide (**8**)

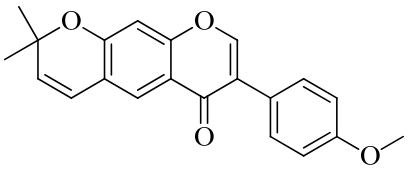

4'-*O*-methylalpinumisoflavone (**9**)

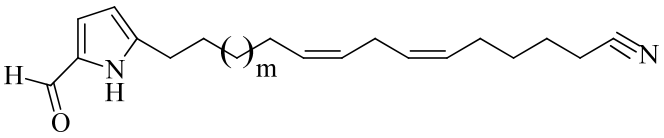

Mycalenitrile-6 (**10**) m=9
Mycalenitrile-7 (**11**) m=11

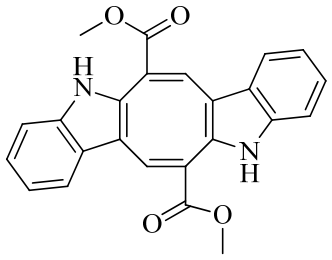

Caulerpin (**12**)

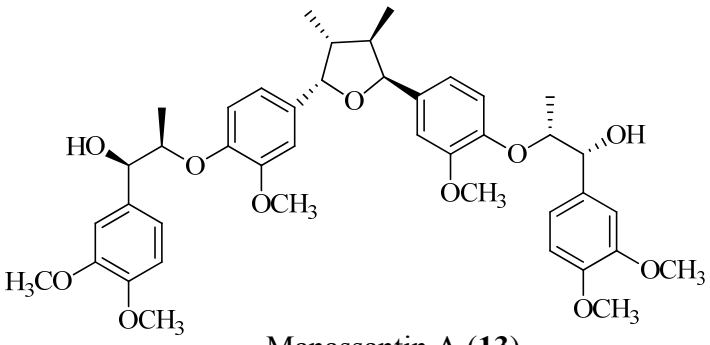

Manassantin A (**13**)

Figure 1.5 Natural products that inhibit mitochondrial complex I and thereby inhibit HIF-1 activation.

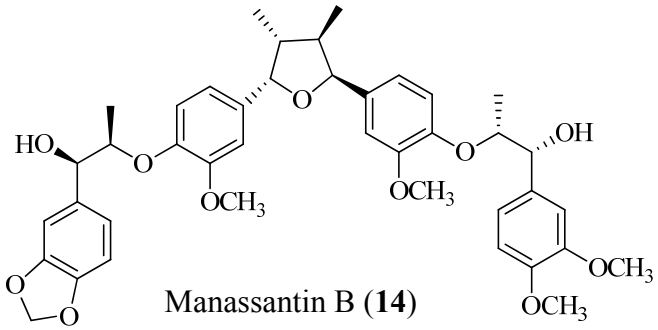

Manassantin B (**14**)

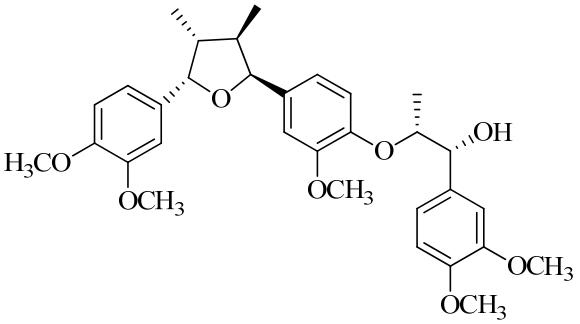

4-*O*-methylsaucerneol (**15**)

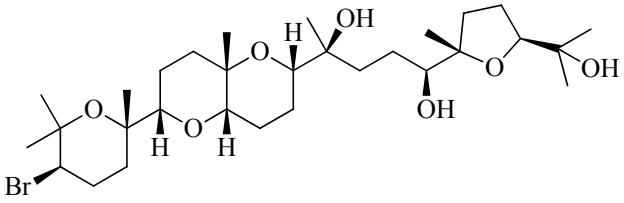

Thyrsiferol (**16**)

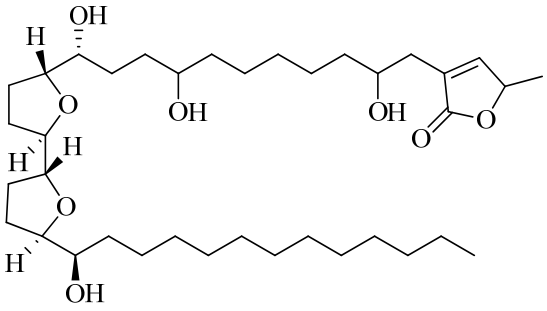

10-hydroxyglaucanetin (**18**)

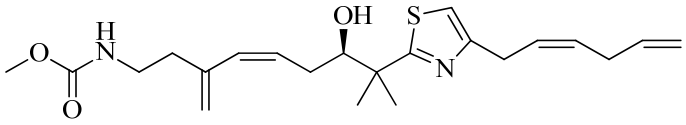

Mycothazole (**17**)

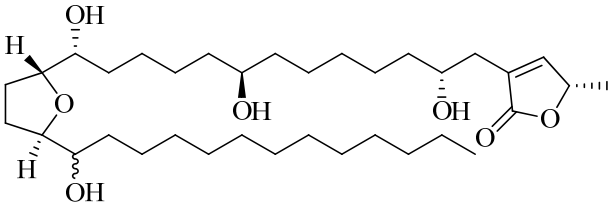

Annonacin (**19**)
Annonacin A (**20**)

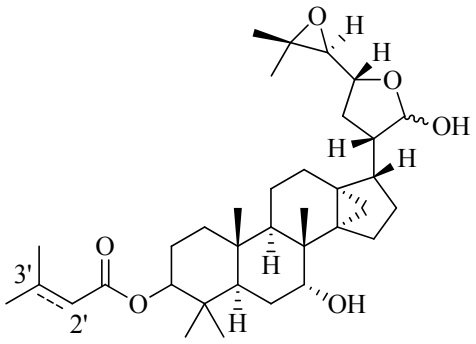

Skimmiarepin A (**21**)
Skimmiarepin C (**22**) 2' – 3' unsaturated

Figure 1.6 Natural products that inhibit mitochondrial complex I and thereby inhibit HIF-1 activation.

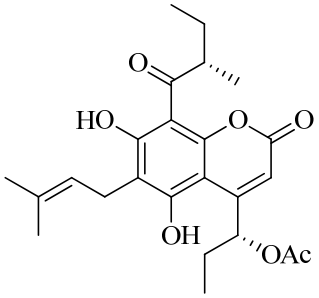

Mammea E/BB (**23**)

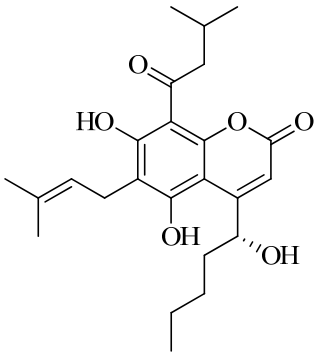

Mammea F/BA (**24**)

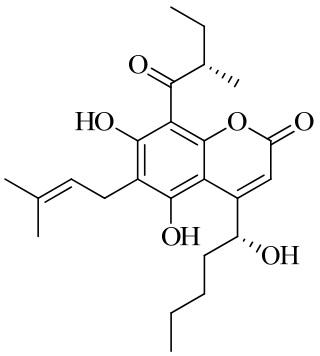

Mammea F/BB$_1$ (**25**)

Figure 1.7 Natural products that uncouple oxidative phosphorylation and thereby inhibit HIF-1 activation.

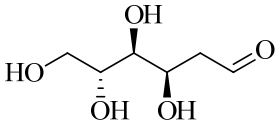

2-deoxy-D-glucose (**26**)

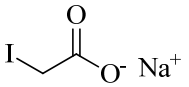

Sodium iodoacetate (**27**)

Figure 1.8 Small-molecules that inhibit HIF-1 via inhibition of glycolysis.

1.2 Cellular bioenergetic pathways

1.2.1 Glycolysis

Mammalian cells generate energy required for cellular reactions by catabolizing glucose (Lehninger *et al.*, 2005). This process known as glycolysis occurs by a cascade of enzymatic reactions. Because glucose is a highly hydrophilic molecule, specialized glucose transporters (GLUTs) are required for cellular glucose uptake. The glycolytic reactions can be grouped into two phases: (a) the reactions that use ATP or the preparatory phase and (b) the reactions that generate ATP or the payoff phase. The preparatory phase consists of five reactions that convert one hexose molecule (glucose) into two triose molecules (glyceraldehyde-3-phosphate and dihydroxyacetone phosphate). Together, these reactions consume two molecules of ATP. Each glyceraldehyde-3-phosphate molecule is then converted to pyruvate by another series of reactions, generating two ATP molecules (Lehninger *et al.*, 2005) (Figure 1.9).

The first step towards glucose oxidation is entrapment of the glucose molecule by phosphorylation (Lehninger *et al.*, 2005; Munoz-Pinedo *et al.*, 2012). The enzyme hexokinase catalyzes the conversion of glucose to glucose-6-phosphate. Glucose-6-phosphate is then converted by hexosephosphate isomerase to F6P. Fructose-6-phosphate can subsequently be phosphorylated either at position-1 or position-2, generating either F1,6BP or F2,6BP. The conversion of F6P to F1,6BP is the first committed step in glycolysis. The F2,6BP molecule generated in this step is not further processed by the glycolytic pathway. Rather, F2,6BP is used by PPP to generate nucleic acid precursors. However, F2,6BP plays a critical role in glycolysis regulation, by potently activating PFK. The enzyme PFK catalyzes the conversion of F6P to F1,6BP. Thus, increased F2,6BP levels can maintain a high cellular glycolysis rate. The F1,6BP is cleaved by aldolase to generate one molecule of glyceraldehyde-3-phosphate and one molecule

of dihydroxyacetone phosphate. Subsequently, the dihydroxyacetone phosphate molecule is converted to glyceraldehyde-3-phosphate by triosephosphate isomerase. Glyceraldehyde-3-phosphate dehydrogenase (GAPDH) converts glyceraldehyde-3-phosphate to 1,3-bisphosphoglycerate with generation of NADH from NAD^+. Pyruvate is generated from 1,3-bisphosphoglycerate in four steps, generating two ATP molecules. Depending on the oxygen availability and/or pathological state of the cell, the pyruvate is either transported to the mitochondria where it enters the TCA cycle (after conversion to acetyl-CoA); or it can be converted into lactate (Figure 1.9) (Lehninger *et al.*, 2005; Munoz-Pinedo *et al.*, 2012).

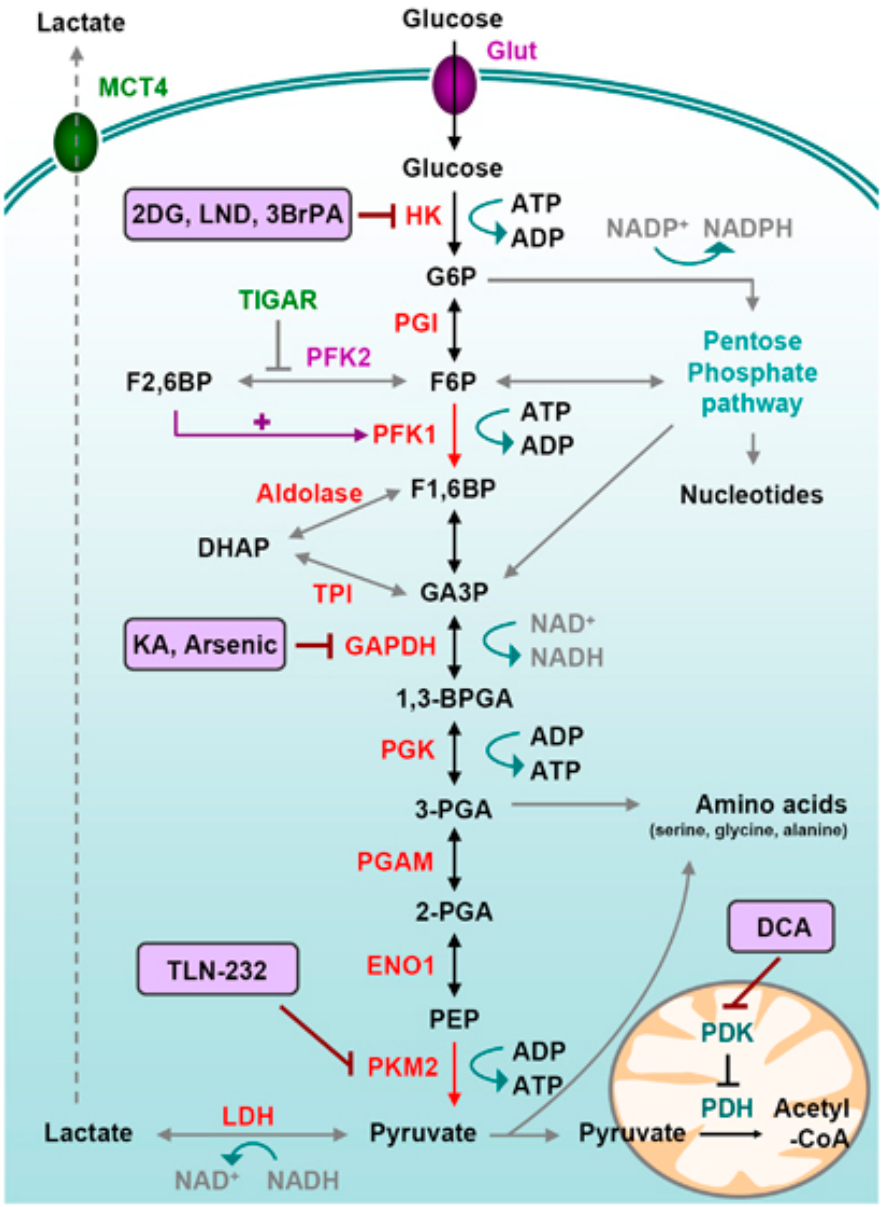

Figure 1.9 The glycolysis pathway and its inhibitors. (Munoz-Pinedo, C. *et al. Cell Death Dis.* **2012**, *3*, e248.) Glut: Glucose transporter; MCT: monocarboxylate transporter; G6P: Glucose-6-phosphate; F6P: fructose-6-phosphate; F1,6BP: fructose-1,6-bisphosphate; F2,6BP: fructose-2,6-bisphosphate; DHAP: dihydroxyacetone phosphate; GA3P: Glyceraldehyde-3-phosphate; 1,3-BPG: 1,3-bisphosphoglycerate; 3-PGA: 3-phosphoglycerate; 2-PG: 2-phosphoglycerate; PEP: phosphoenolpyruvate; HK: hexokinase; PGI: phosphoglucoisomerase; PFK: phosphofructokinase; TPI: triose phosphate isomerase; GAPDH: glyceraldehyde 3-phosphate dehydrogenase; PGK: phosphoglycerate kinase; PGAM: phosphoglycerate mutase; ENO1: enolase 1; PK: pyruvate kinase; LDH: lactate dehydrogenase; 2-DG: 2-deoxy-D-Glucose; LND: lonidamine; 3BrPA: 3-bromopyruvate, KA: koningic Acid; TLN-232 is a synthetic cyclic heptapeptide which targets PK; DCA: dichloroacetate

1.2.2 Oxidative phosphorylation

Transfer of an electron pair to either complex I or complex II of the respiratory chain initiate the process of oxidative phosphorylation. Complex I (NADH:ubiquinone oxidoreductase or NADH dehydrogenase) is one of the entry points into the electron transport chain (Lehninger *et al.*, 2005; Nicholls and Ferguson, 2002; Suski *et al.*, 2011). Complex I is a large 'L' shaped, membrane bound enzyme complex that contains 45 subunits eight of which are iron-sulfur proteins. Complex I is comprised of a peripheral portion that extends to the mitochondrial matrix (cytoplasm in case of bacteria) and a membrane-embedded component (Lehninger *et al.*, 2005; Nicholls and Ferguson, 2002). The NADH molecules generated during glycolysis or from the TCA cycle interact with the peripheral arm of complex I and transfers electrons to the subunit that possesses flavin mononucleotide as a prosthetic group. Subsequently, the electrons are transferred through eight iron-sulfur proteins and ultimately delivered to ubiquinone (Q) by the N2 iron-sulfur cluster. Complete reduction of ubiquinone is mediated through formation of an ubisemiquinone molecule, since the N2 iron-sulfur cluster delivers the electron pair in two steps. During this process of electron movement, four protons are extruded in the intramembrane space, resulting in a proton pumping stoichiometry of $4H^+/2e^-$. The ubiquinol molecule shuttles the electrons to complex III (ubiquinone:cytochrome *c* oxidoreductase or cytochrome bc_1 complex) by diffusion through the mitochondrial inner membrane lipid bilayer. Mitochondrial complex I inhibitors like rotenone (**2**) and piericidin A (**28**) (Figure 1.11) inhibit the transfer of electrons from the iron-sulfur proteins to ubiquinone.

Three other enzymes may reduce ubiquinone and initiate oxidative phosphorylation (Lehninger *et al.*, 2005; Nicholls and Ferguson, 2002). Mitochondrial complex II (succinate dehydrogenase) oxidizes succinate to fumarate and transfers two electrons to ubiquinone.

Electrons from succinate are rapidly transferred through flavin adenine dinucleotide (FAD) and three iron-sulfur proteins, before they are accepted by ubiquinone. No proton translocation takes place during mitochondrial complex II electron movement.

Apart from complexes I and II, electrons can be donated to ubiquinone by electron-transferring flavoproteins (ETF): ubiquinone oxidoreductase and *s,n*-glycerophosphate dehydrogenase (Lehninger *et al.*, 2005; Nicholls and Ferguson, 2002). Both of these contain one FAD and one iron-sulfur cluster, and are attached to the inner mitochondrial membrane. However, the former is attached to the matrix side of the mitochondria, while the latter is attached to the cytosolic side. The ubiquinol molecules generated in complexes I and II or in either of these proteins, translocate to complex III.

The cytochrome bc_1 complex known as complex III (ubiquinol:cytochrome *c* oxidoreductase) oxidizes the reduced ubiquinol through the Q cycle (previously described, Figure 1.3) (Lehninger *et al.*, 2005; Nicholls and Ferguson, 2002). Complex III structural features involved in the electron transfer process include cytochrome b, cytochrome *c*1, and the Rieske protein (iron-sulfur protein). The final electron acceptor in this step is the single-electron carrier cytochrome *c*, which shuttles the electrons to complex IV (cytochrome *c* oxidase). During the electron transfer process, two protons per electron (or $4H^+$ per $2e^-$) are extruded into the intermembrane space.

Mitochondrial complex IV carries out oxygen reduction, the final step of the electron transport process (Lehninger *et al.*, 2005; Nicholls and Ferguson, 2002). Cytochrome *c* initially transfers an electron to one of the copper centers (Cu_A); the electron is subsequently transferred through cytochrome *a*, cytochrome a_3, and a second copper center (Cu_B), in that order, before it

is accepted by the molecular oxygen. Translocation of one proton to the intermembrane space occurs for each electron transported through complex IV.

The protonmotive force generated by extrusion of protons into the intermembrane space is utilized by the mammalian F_0F_1-ATP synthase enzyme to generate ATP (Lehninger *et al.*, 2005; Nicholls and Ferguson, 2002; Suski *et al.*, 2011). This enzyme channels the passive reentry of protons into the mitochondrial matrix and couples the process of energy generation with the electron transport. For every three protons reentering the mitochondrial matrix, one ATP molecule is generated and released into the matrix. In the absence of sufficient protonmotive force, F_0F_1-ATP synthase enzyme acts as an ATPase and pumps protons into the intermembrane space in order to maintain the protonmotive force. Since the phosphorylation of ADP is coupled to oxygen reduction, this process is known as oxidative phosphorylation (Figure 1.10).

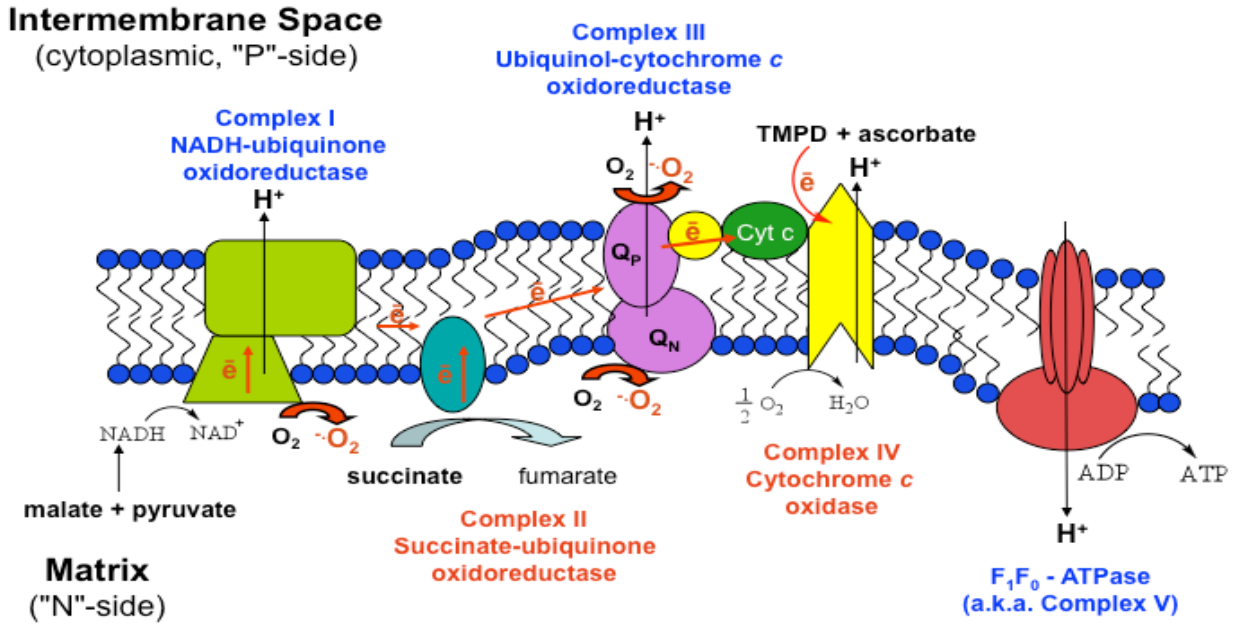

Figure 1.10 Mitochondrial electron transport chain and oxidative phosphorylation. Reproduced with permission from Dr. Dale G. Nagle (Nagle and Zhou, 2010).

1.3 Natural product mitochondriotoxic small molecules

Though mitochondrial inhibitors are valuable antitumor leads, exposure to mitochondriotoxic agents may lead to idiosyncratic toxicity. Over the past decade, it has become increasingly apparent that some of the FDA approved drugs have unexpected toxicity because of their effects on the mitochondria. The role of mitochondrial impairment in drug toxicity has gained considerable attention (Dykens and Will, 2007). Aerobically poised tissues with a high mitochondrial dependence, and tissues exposed to high drug concentrations (e.g., liver) are commonly affected by drug-induced mitochondrial dysfunction (Wallace, 2008; Labbe *et al.*, 2008). The most common manifestation of drug-induced mitochondrial impairment is hepatotoxicity (Sanchez *et al.*, 2006). Other major symptoms include cardiotoxicity, nephrotoxicity, neuropathy, skeletal myopathy, retinopathy, ototoxicity, hepatic steatosis, and hematotoxicity (Haller and Benowitz, 2000; Gabardi *et al.*, 2007; Palmer *et al.*, 2003). Typically, chronic use of these drugs leads to mitochondria-mediated toxicity, because a threshold level of cellular mitochondrial dysfunction is required to trigger cell collapse and tissue injury (Scatena *et al.*, 2007). However, high doses of certain drugs [e.g., acetaminophen] are capable of inflicting acute liver injury and hepatic failure (Chun *et al.*, 2009).

Every year, numerous new drug applications are denied, and a small percentage (2 – 3%) of clinically approved drugs is withdrawn from the market due to adverse effects. Most drugs with FDA Black Box Warnings for hepatotoxicity and cardiotoxicity are known mitochondrial poisons (Dykens and Will, 2007).

Apart from the clinically approved drugs, many small-molecule natural products have been reported to cause mitochondrial dysfunction in experimental settings (Nagle and Zhou, 2012). The most common mechanisms for mitochondrial dysfunction following an exposure to

drugs or natural phytohemicals/environmental toxins are: (a) inhibition of oxidative phosphorylation and (b) uncoupling of oxidative phosphorylation (Scatena *et al*. 2007).

Inhibition of oxidative phosphorylation may occur at any of the electron transport chain (ETC) protein complexes (complexes I to IV) or at the F_0F_1-ATP synthase (*aka* complex V). Mitochondrial ETC complex I (NADH-ubiquinone oxidoreductase) is the most common target of small-molecule inhibitors (Degli Esposti, 1998). The simplistic structural feature for complex I inhibition is a cyclic head and a hydrophobic tail (Degli Esposti, 1998; Wallace, 2008). More than 60 classes of compounds have demonstrated complex I inhibitory activity (Wallace, 2008). The previously discussed group of natural products **2** and **7** – **22**, inhibit mitochondrial complex I and subsequently inhibit HIF-1 activation. Natural products that inhibit complex I can be broadly categorized into six groups; (a) rotenoids, (b) piericidins, (c) annonaceous acetogenins, (d) antibiotics, (e) vanilloids, and (f) miscellaneous plant products (Degli Esposti, 1998). This classification is somewhat arbitrary, and according to this classification most of the earlier mentioned complex I inhibitors fall into the rotenoid, acetogenin, and miscellaneous categories.

Among the natural products, rotenone (**2**) was isolated from a variety of plants from the Fabaceae family (Jiang *et al.*, 2012; Kamal and Mathur, 2010; Liu *et al.*, 2009a; Mai *et al.*, 2010; Cao *et al.*, 2004). Rotenone is a well-studied complex I inhibitor that is the prototype for the rotenoid class of mitochondrial inhibitors. Rotenone is used as a natural insecticide, fish toxin and it is routinely used as a pharmacological/molecular probe in mitochondrial mechanistic studies (Radad *et al.*, 2006; Liu *et al.*, 2009a). Deguelin (**29**) (Figure 1.11) is another rotenoid that is produced by the African terrestrial plant *Mundulea sericea* (Willd.) A. Chev. (Leguminosae). Deguelin is a potent complex I inhibitor that is used as a pesticide (Clark, 1931).

Piericidin A (**28**) is a *Streptomyces sp.*-derived antibiotic that inhibits mammalian and bacterial NADH:ubiquinone oxidoreductase (Tamura *et al.*, 1963). It is believed to inhibit ubiquinone reduction by preventing access of ubiquinone to the ubiquinone-binding site (Friedrich *et al.*, 1994).

Annonaceous acetogenins are a group of natural product small-molecules, which are isolated from plants belonging to the family Annonaceae. The complex I inhibitory properties of acetogenins have been widely studied (McLaughlin, 2008). They have been shown to inhibit complex I at nanomolar concentrations, in various experimental models that include bovine heart mitochondria, bovine submitochondrial particles, and human cell lines. More than 350 anonaceous acetogenins from 37 species have been identified from 1982 to 1998 (Alali *et al.*, 1999). Some of the representative compounds from this group include bullatacin (**30**), uvaricin (**31**), diepomuricanin B (**32**), and muconin (**33**) (McLaughlin, 2008; Alali *et al.*, 1999).

Structurally diverse compounds from higher plants have also been shown to inhibit mitochondrial complex I. Many plant alkaloids are known mitochondrial toxins. The plant alkaloid berberine (**34**), inhibits complex I in rat skeletal muscle cells (IC_{50} 15 μM) (Turner *et al.*, 2008). The opium alkaloid papaverine (**35**) inhibits state 3 respiration at complex I in isolated mouse-brain mitochondria (IC_{50} 6.45 μM) (Morikawa *et al.*, 1996). Another group of phytochemicals which has shown to interfere with mitochondrial complex I activity are the flavonoids. Some of the flavonoids that inhibit complex I enzymatic activity include quercetin (**36**), kaempferol (**37**), and apigenin (**38**) (Lagoa *et al.*, 2011).

Several antibiotics specifically inhibit mitochondrial complex I, these include phenoxan (**39**), thiangazole (**40**), aureothin (**41**), and cochlioquinone B (**42**) (Friedrich *et al.*, 1994; *Lim et al.*, 1996). Cinnamaldehyde (**43**) (Usta *et al.*, 2002), acrolein (**44**) (Sun *et al.*, 2006), eugenol (**45**)

(Usta *et al.*, 2002; Cotmore *et al.*, 1979), 2',4'-dihidroxy-5'-(1'"-dimethylallyl)-6-prenylpinocembrin (6PP, **46**) (Elingold *et al.*, 2008), and 4,20-dideoxyphorbol-12,13-*bis*(isobutyrate) (**47**) disrupt complex I activity (Betancur-Galvis *et al.*, 2003). Apart from complex I inhibition, **44** and **45** inhibit complex II and uncouple oxidative phosphorylation, respectively (Sun *et al.*, 2006; Cotmore *et al.*, 1979).

Specific complex II (succinate dehydrogenase) inhibition by xenobiotics is uncommon relative to the inhibition of other complexes. Chloramphenicol succinate (**48**) (Ambekar *et al.*, 2004), surangin B (**49**) (Deng and Nicholson, 2005), siccanin (**50**) (Mogi *et al.*, 2009), and doxorubicin (**51**) (Marcillat, 1989) inhibit complex II activity. Acrolein and surangin B have been shown to inhibit other respiratory complexes too (Sun *et al.*, 2006; Deng and Nicholson, 2005).

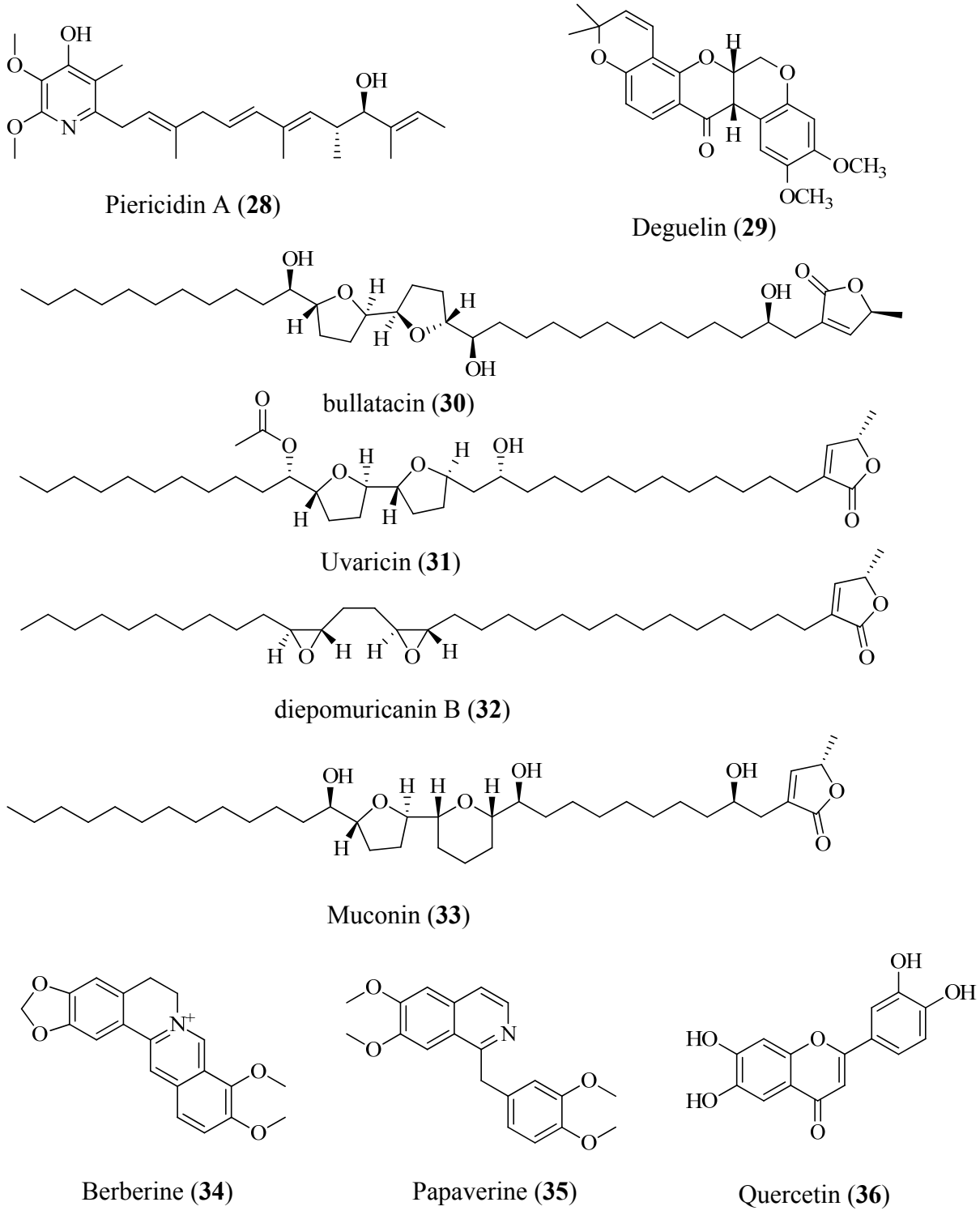

Figure 1.11 Natural products that inhibit mitochondrial complex I (NADH:ubiquinone oxidoreductase).

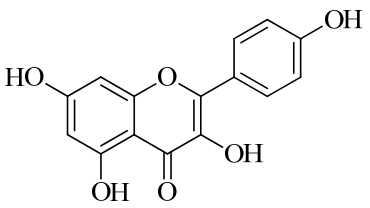

Kaempferol (**37**)

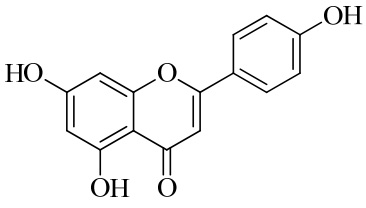

Apigenin (**38**)

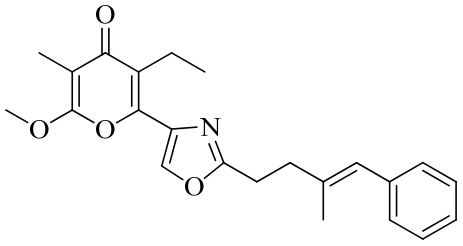

Phenoxan (**39**)

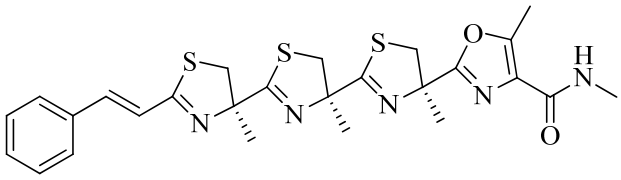

Thiangazole (**40**)

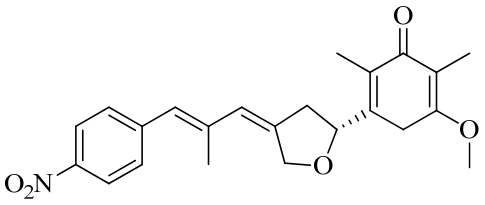

Aureothin (**41**)

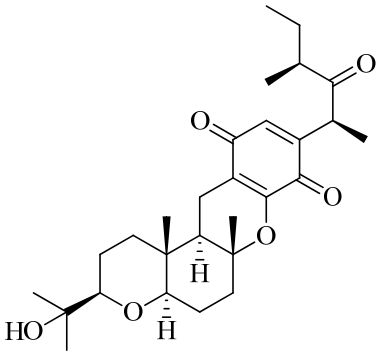

Cochlioquinone B (**42**)

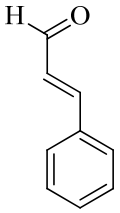

Cinnamaldehyde (**43**)

Acrolein (**44**)

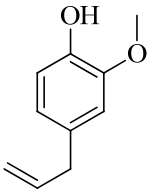

Eugenol (**45**)

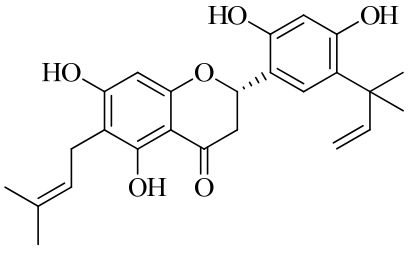

2',4'-dihidroxy-5'-(1'"-dimethylallyl)-6-prenylpinocembrin (**46**)

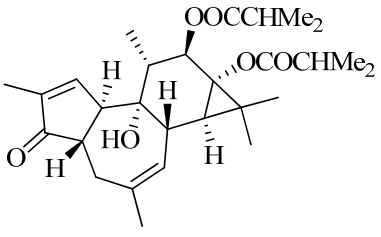

4,20-dideoxyphorbol-12,13-*bis*(isobutyrate) (**47**)

Figure 1.12 Natural products that inhibit mitochondrial complex I (NADH:ubiquinone oxidoreductase).

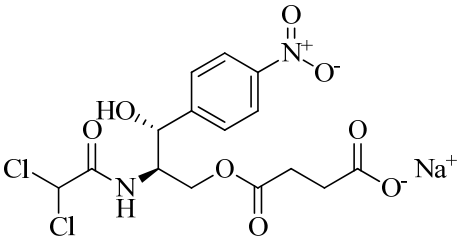

Chloramphenicol succinate (**48**)

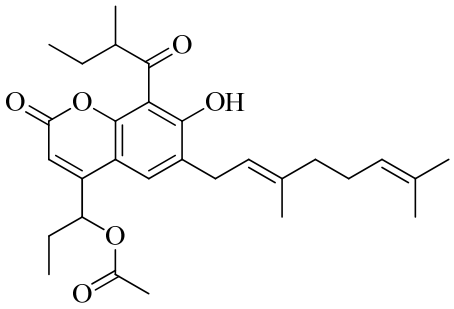

Surangin B (**49**)

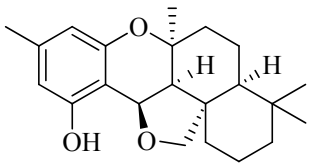

Siccanin (**50**)

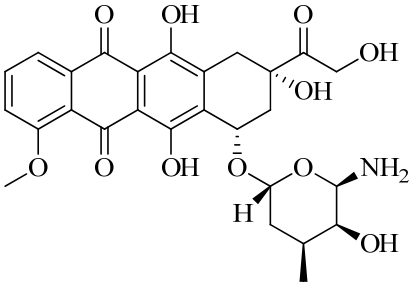

Doxorubicin (**51**)

Figure 1.13 Natural products that inhibit mitochondrial complex II (succinate dehydrogenase).

Mitochondrial complex III (cytochrome bc_1-complex, ubiquinol:cytochrome *c* oxidoreductase) is a major site for inhibition by small-molecules (Thierbach and Reichenbach, 1981; Von Jagow *et al.*, 1986; Bell *et al.*, 2007; Brandt *et al.*, 1988). Inhibition of complex III often produces significant toxicity. Hence, molecules that inhibit complex III are devoid of clinical utility. Natural product-derived quinol antagonists, such as myxothiazol (**4**) (Thierbach and Reichenbach, 1981), strobilurin A (**52**) (Von Jagow *et al.*, 1986), stigmatellin (**5**) (Bell *et al.*, 2007), and oudemansin (**53**) (Brandt *et al.*, 1988), inhibit complex III at the Q_o site by blocking the oxidation of ubiquinol to ubiquinone. Compounds that contain a 6-hydroxyquinone moiety inhibit the transfer of electron between the Rieske protein and cytochrome *c*1 (Von Jagow and Link 1986).

The complex III inhibitor, antimycin A (**6**), blocks electron transfer at the Q_i center (Chandel *et al.*, 1998). Together with funiculosin (**54**), the Q_i center inhibitors comprise a third group of the complex III inhibitors (Von Jagow and Link, 1986). However, certain complex III inhibitors, such as myxothiazol (**4**) and stigmatellin (**5**) also inhibit complex I at higher concentrations (Degli Esposti *et al.*, 1993). Sorgoleone (**55**), a benzoquinone derivative, inhibits plant mitochondria at complex III (Rasmussen *et al.*, 1992). Rubratoxin B (**56**) (Hayes, 1976), lamellarin D (**57**) (Ballot *et al.*, 2010), and polyalthidin (**58**) (Zafra-Polo *et al.*, 1996) also inhibit complex III.

Natural product complex IV inhibitors are rare. The xanthone α-mangostin (**59**) inhibits mitochondrial complex IV and reduces oxygen consumption rates under state 3 respiration conditions. However, **59** increases state 4 respiration most likely by uncoupling oxidative phosphorylation (Martinez-Abundis *et al.*, 2010). Cyanides or azides are used to inhibit complex IV in mitochondrial mechanistic studies.

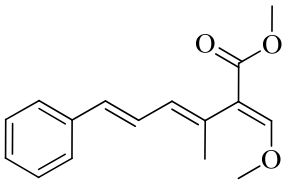

Strobilurin (**52**)

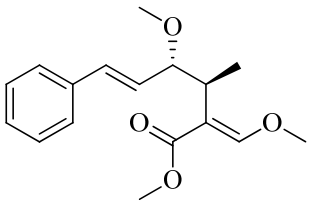

Oudemansin (**53**)

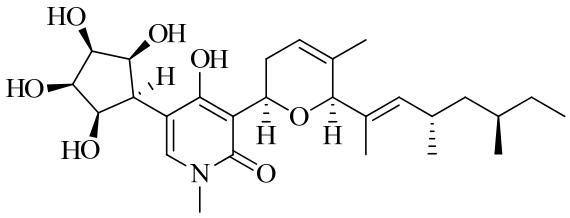

Funiculosin (**54**)

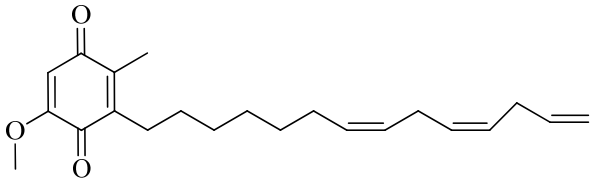

Sorgoleone (**55**)

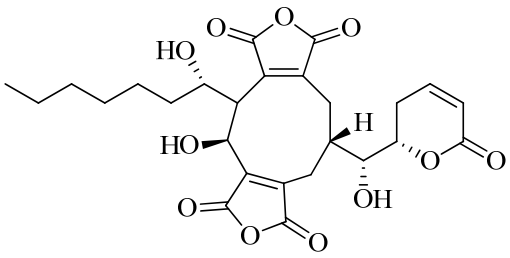

Rubratoxin B (**56**)

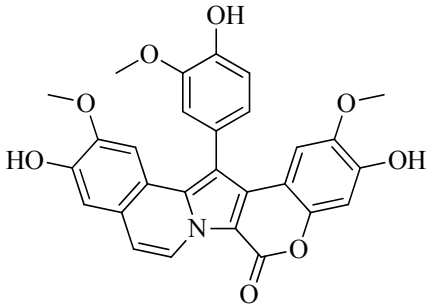

Lamellarin D (**57**)

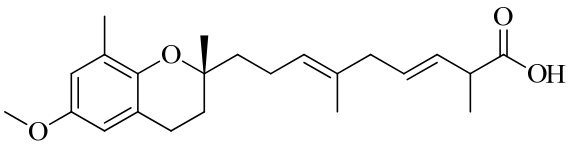

Polyalthidin (**58**)

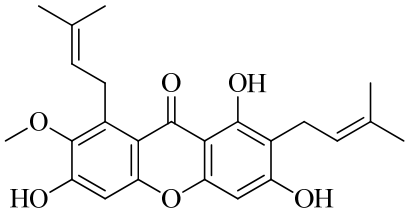

α-mangostin (**59**)

Figure 1.14 Natural products that inhibit mitochondrial complex III (coenzyme Q:cytochrome *c* oxidoreductase) (**52** – **58**) and complex IV (cytochrome *c* oxidase) (**59**).

The F_0F_1-ATP synthase generates ATP in the mitochondria and is also known as complex V. Several antibiotics potently inhibit this enzyme. Some of the macrolide natural products that inhibit F_0F_1-ATP synthase are apoptolidin (**60**) (Salomon *et al.*, 2001), the oligomycins (oligomycin A, **61**) (Linnett and Beechey, 1979), aurovertin B (**62**) (Gledhill and Walker, 2006), venturicidin A (**63**) (Matsuno-Yagi and Hatefi, 1993), ossamycin (**64**), and cytovaricin (**65**) (Salomon *et al.*, 2000). Polyphenols bind to and inhibit mammalian F_0F_1-ATP synthase. Notable polyphenols that inhibit the enzymatic activity are resveratrol (**66**), piceatannol (**67**), quercetin (**36**), and epigallocatechin gallate (**68**) (Gledhill *et al.*, 2007). Cruentaren A (**69**), a benzolactone, has been reported to inhibit F_0F_1-ATP synthase at low nanomolar concentrations by binding to the catalytic F_1-subunit of the enzyme (Kunze *et al.*, 2007).

Protonophores uncouple oxidative phosphorylation by shuttling protons directly across the mitochondrial inner membrane to the mitochondrial matrix, and dissipate the mitochondrial membrane potential (Kessler *et al.*, 1977). Thereby, uncouplers disrupt ATP synthesis by preventing proton channeling through the F_0F_1-ATP synthase. In order to maintain the mitochondrial membrane potential, the F_0F_1-ATP synthase starts hydrolyzing ATP and pumping protons into the intermembrane space, which can leads to cellular ATP depletion, and subsequent cytotoxicity (Das, 1998).

Usnic acid (**70**) is a popular lichen-derived dietary weight-loss supplement in the US (Sanchez *et al.*, 2006). Usnic acid and the other lichen metabolite, vulpinic acid (**71**), potently uncouple isolated mice-liver mitochondria (Abo-Khatwa *et al.*, 1996). Steviobiosides are natural product small-molecules from *Stevia rebaudiana* (Bertoni) (Asteraceae) that are used as natural sweeteners (Goyal *et al.*, 2010). Isosteviol (**72**), obtained by stevioside acid hydrolysis, potently uncouples oxidative phosphorylation (Kelmer Bracht *et al.*, 1985). Natural products, such as

rottlerin (**73**) (Soltoff, 2001), juglone (**74**) (Sailing *et al.*, 2011), Δ^9-tetrahydrocannabinol (**75**) (Sarafian *et al.*, 2003), ferulenol (**76**) (Nadia *et al.*, 2009), desaspidin (**77**) (Runeberg, 1962), and ochratoxin (**78**) (Wei *et al.*, 1985), uncouple mitochondrial oxidative phosphorylation. Recently the three isocoumarins paepalantine (**79**), paepalantine-8,8'-dimer (**80**), and vioxanthin (**81**) that are produced by *Paepalanthus bromelioides* (Silveira) (Eriocaulaceae) have been identified as mitochondrial uncouplers (Calgaro-Helena *et al.*, 2006).

Apart from purified compounds with well-defined mechanisms of action, several plant-derived extracts and dietary supplement products disrupt mitochondrial electron transport or uncouple oxidative phosphorylation. The extract of *Phyllanthus urinaria* Linn. (Euphorbaceae) has been shown to exert a biphasic effect on isolated rat-liver mitochondria. *Phyllanthus urinaria* extract was reported to stimulate state 4 respiration but inhibits state 3 respiration at 500 μg/mL (Chudapongse *et al.*, 2010). An extract of *Cynara scolymus* Linn. (Asteraceae) was reported to inhibit more than one mitochondrial respiratory complex (Juzyszyn *et al.*, 2010). Interestingly, a mixture of β-carotene cleavage products inhibited mitochondrial respiration (Siems *et al.*, 2002). It was proposed that the inhibition of adenine nucleotide transporter was responsible for this effect.

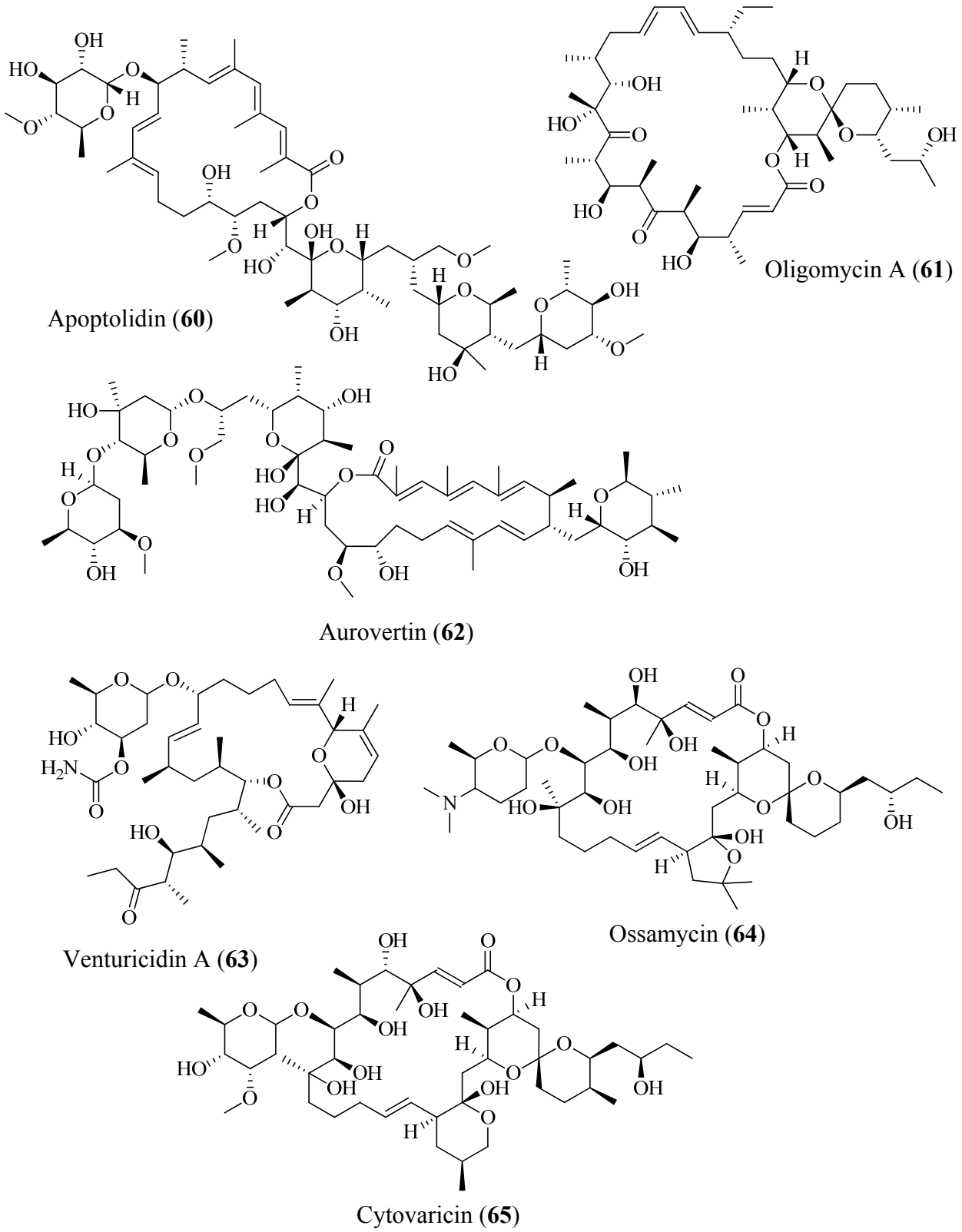

Figure 1.15 Natural product small-molecules that inhibit mitochondrial F_0F_1-ATP synthase.

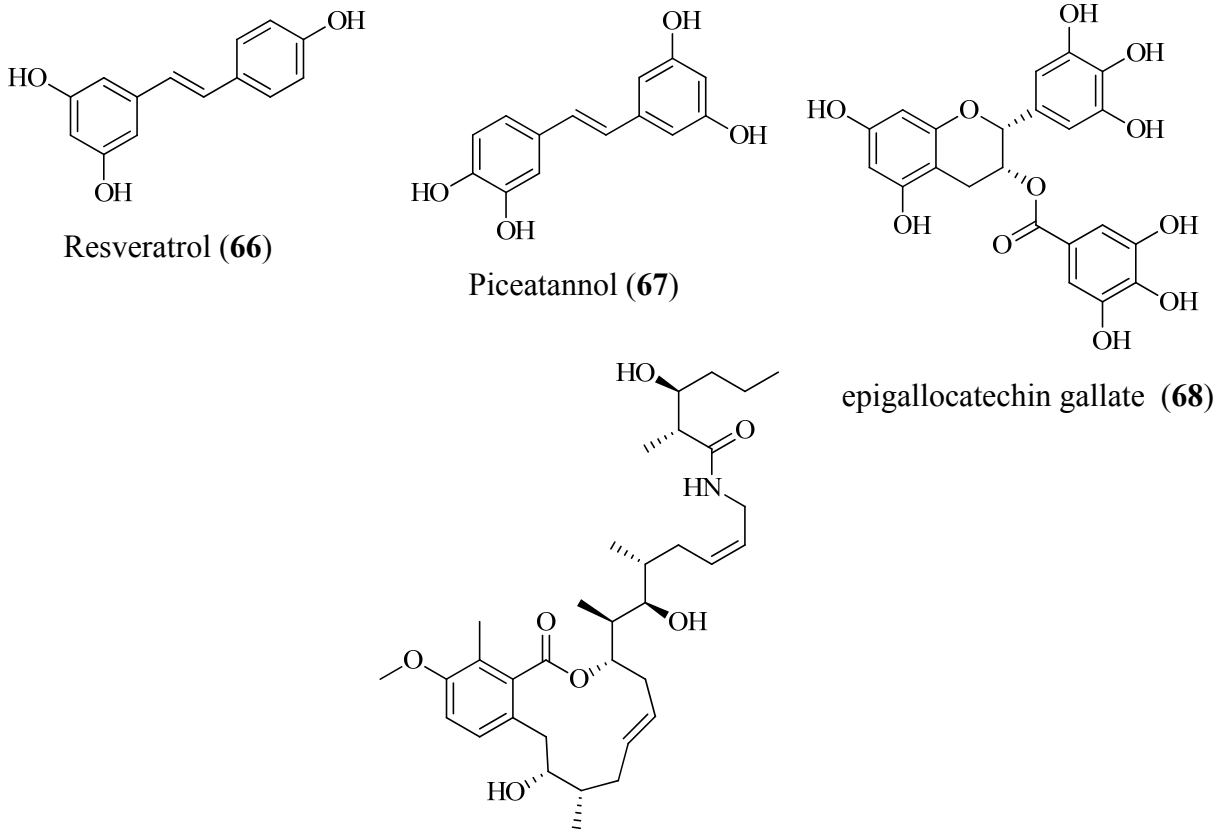

Resveratrol (**66**)

Piceatannol (**67**)

epigallocatechin gallate (**68**)

Cruentaren A (**69**)

Figure 1.16 Natural product small-molecules that inhibit mitochondrial F_0F_1-ATP synthase.

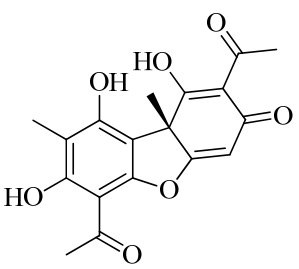

Usnic acid (**70**)

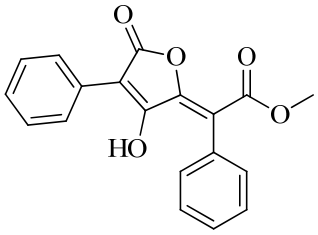

Vulpinic acid (**71**)

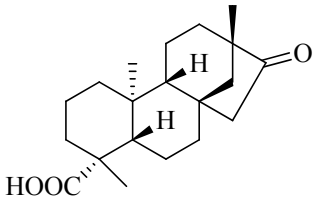

Isosteviol (**72**)

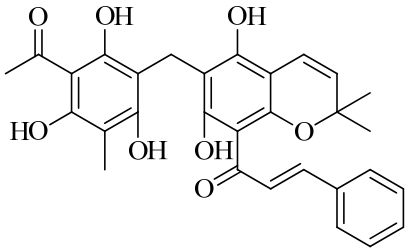

Rottlerin (**73**)

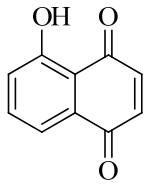

Juglone (**74**)

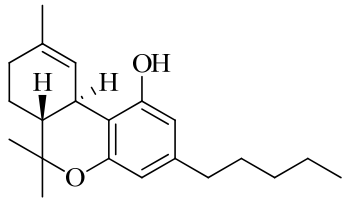

Δ^9-tetrahydrocannabinol (**75**)

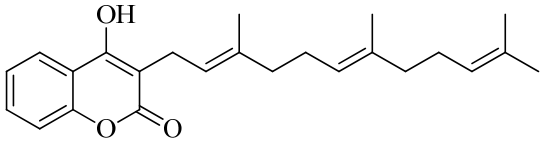

Ferulenol (**76**)

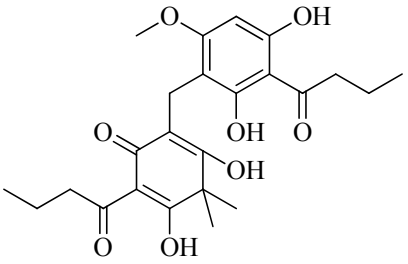

Desaspidin (**77**)

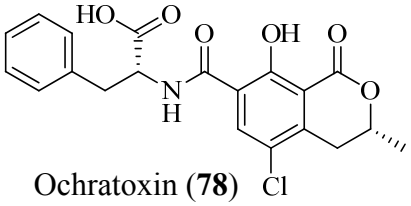

Ochratoxin (**78**)

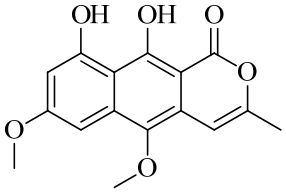

Paepalantin (**79**)

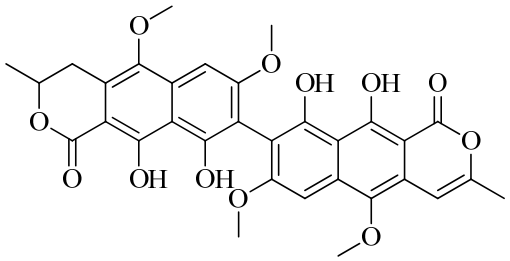

Paepalantin dimer (**80**)

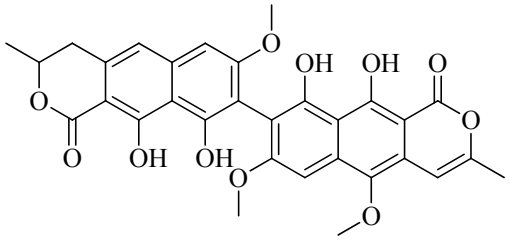

Vioxanthin (**81**)

Figure 1.17 Natural product small-molecules that uncouple oxidative phosphorylation.

1.4 Conclusions

The contemporary oncology drug discovery process is increasingly focusing toward molecular-targeted approaches. Identification of molecular targets and HTS lead generation are at the core of this process. Molecular-targeted drug discovery approach has found only limited success in the generation of new therapeutic agents (e.g., tamoxifen, Gleevec®, and Velcade®). In order to increase the success rate of molecular-targeted antitumor drug discovery, the selection of a valid molecular target, a robust assay system and an appropriate endpoint are essential. Hypoxia-inducible factor-1 is a valid antitumor target in oncology research. Agents that inhibit HIF-1 are currently in clinical trials (e.g., topotecan, EZN-2968, and dutasteride). Natural products are extensively used in current antitumor therapies. Efforts to develop clinically useful HIF-1 inhibitors from natural products are underway (Onnis *et al.*, 2009).

As a transcription factor, HIF-1 controls expression of genes that modulate cellular metabolism and bioenergetics. It has been hypothesized that HIF-1 induces aerobic glycolysis by actively downregulating mitochondrial oxidative metabolism and upregulating glycolytic enzyme activities. Tumor cell metabolism, especially glycolysis, is an emerging target for antitumor therapy. In addition, mitochondria-targeted agents are also being evaluated as possible antitumor leads. Indeed, disruption of cellular bioenergetics by mitochondrial ETC inhibitors, uncouplers, and glycolysis inhibitors suppress HIF-1 activation. The inhibition of HIF-1 makes tumor cells more susceptible to the existing chemotherapy (Song *et al.*, 2006; Chang *et al.*, 2006; Moeller *et al.*, 2005; Schwartz *et al.*, 2009). In spite of the association between enhanced glycolytic metabolism and poor prognosis/advanced disease stage, there has only been limited effort to discover glycolysis inhibitors.

Mitochondrial inhibitors can be valuable antitumor leads, but toxic effects from off-target mitochondrial ETC inhibition may be observed in healthy individuals. This is exemplified by the fact that several clinically approved drugs (e.g., troglitazone and cerivastatin) (Dykens and Will, 2007) have been withdrawn from the market due to their off-target mitochondrial effects. The possibility of idiosyncratic adverse effects from botanical dietary supplements may be underestimated relative to synthetic drugs, especially because natural products are becoming more recognized as a major source of mitochondrial toxins. Identification of mitochondrial toxins from botanical dietary supplements can facilitate better understanding the mechanisms responsible for the adverse effects associated with botanical dietary supplement (BDS) products and the possible withdrawal of potentially toxic supplements from the market.

CHAPTER II

COMPARATIVE EVALUATION OF CHROMATOGRAPHIC MEDIA IN MOLECULAR-TARGETED ANTITUMOR DRUG DISCOVERY

CONTRIBUTION OF AUTHORS

The work described in this chapter is a collaborative effort between Drs. Dale G. Nagle, Yu-Dong Zhou, and myself. Drs. Nagle and Zhou conceived the idea, designed the experiments, supervised the project, and helped to interpret the data. Dr. Nagle served as my major advisor, while Dr. Zhou provided additional advice regarding the biological experiments. I performed the experiments, analyzed, and interpreted the data. Dr. Marc Slattery helped with statistical analysis.

2.1 Overview

2.1.1 Introduction

Natural products and natural product-rich extracts have been extensively used for medicinal purposes in traditional medicinal systems worldwide (Harvey, 2008). Numerous natural product-based drugs have become available in the clinic for disease treatment and management over the past 30 years (Newman and Cragg, 2012). Most preliminary drug discovery efforts screen natural product-rich extracts or purified compounds for specific bioactivities in vitro. Once an extract is identified as an 'active' or a hit in the molecular-targeted bioassay, the extract is subjected to chromatographic separation to isolate the molecules responsible for the bioactivity. Chromatographic separation can be chemistry-guided or bioassay-guided. In the chemistry-guided approach, compounds are isolated in a bioactivity-blind manner. In the bioassay-guided isolation approach, the fractions are generated and evaluated in the molecular-targeted bioassay and only the active fractions are subjected for further purification. In both cases, suitable normal or reversed-phase chromatographic media or size-exclusion resins (Si gel, diol, C_8, C_{18}, Sephadex®LH-20) are used to fractionate the bioactive chemical constituents to pure form. The synthetic polymer-based medium Diaion™ HP20SS (cross-linked polystyrenic matrix) is an alternative to Si gel or more expensive bonded-phase media and size-exclusion resins. A common problem in the natural products drug discovery process is poor sample recovery or/and the loss of bioactivity of fraction(s) subsequent to the chromatographic separation process. Hence, selection of appropriate chromatographic media for each fractionation or purification step is critical for the successful isolation of bioactive compounds. However, no report is available that directly evaluates and compares these various chromatographic media used for natural product drug discovery.

Hypoxia-inducible factor-1 (HIF-1) has emerged as an important molecular target for antitumor drug discovery (Semenza, 2008). A cell-based reporter assay was used to examine a library of extracts from the NCI's Open Repository. Bioassay-guided isolation had been hampered by the prevalence of biologically active, yet chromatographically unstable, extract components. For a comparative evaluation of the chromatographic media, an array of chemically diverse extracts was selected as a representative test panel. Diaion® HP20SS was evaluated side-by-side with normal-phase media for the loss of recovery due to irreversible binding. Additional recovery by EtOAc and other non-polar solvents added to a typical HP20SS elution system was examined. Various solvent fractions from a single column were pooled and subjected for TLC to observe any major chemical alterations. Chemical profiles of the individual solvent fractions including the final EtOAc elute from HP20SS were examined by TLC. The HIF-1 inhibitory activities of the recombined extracts were compared side-by-side with the activities of the original extracts to assess the impact of various chromatographic media on the HIF-1 inhibitory activity of natural product-rich extracts.

2.1.2 Evaluation of natural products for drug discovery

The success of natural products as a source of chemically and mechanistically novel drug leads has been unparalleled. In the last three decades, 34% of small-molecules approved by the FDA to be used therapeutically were either natural products or were directly derived from them (Newman and Cragg, 2012). However, with the invention of high-throughput screening (HTS) technologies, the pharmaceutical industry has lost interest in natural products in a shift toward the screening of synthetic pure compound libraries as a primary source of new drug leads (McChesney *et al.*, 2007). This decline in interest in natural products stems from the much more

resource and time intensive nature of traditional extract testing and isolation efforts when compared to the rapid HTS and identification of the 'hits' from the synthetic pure compound libraries. Dereplication of nuisance, ubiquitously active, or previously known compounds present in the extracts and potential new molecule structure elucidation problems present major challenges with natural product-based drug discovery efforts. Moreover, varying active principle potency and abundance in the extracts can add another level of complexity that leads to false positives or negatives (Koehn, 2008). Technological advances have helped to promote the development of new approaches to overcome some of these challenges. Recent improvements in the NMR spectroscopic and mass spectrometric methods have simplified minute sample natural product structural elucidation. Advances in screening technologies, such as the quantitative high-throughput screening (qHTS) approach, is currently used to minimize the generation of false positives and negatives (Inglese *et al.*, 2006). However, the generation of chemically diverse drug-like screening libraries still remains a limiting step for the success of many drug discovery programs (Koehn, 2008). To improve natural product screening library acceptability, prefractionated, semipurified and purified natural product libraries are slowly replacing the traditional extract-based sample libraries (Bugni *et al.*, 2008a). Both pure compound libraries and extract-based libraries are being generated by the National Institutes of Health (NIH) at the National Cancer Institute (NCI), but the pharmaceutical industry has shifted away from the use of the extracts to focus only on the purified compounds (NIH Molecular Libraries Program: pathways to discovery, website accessed on 03/11/2012; Newman and Nagle, personal communication, 2008).

The University of Mississippi (UM), Department of Pharmacognosy's Molecular-Targeted Antitumor Discovery Group runs a HIF-targeted drug discovery program. Hypoxia-

inducible factor-1 has been identified as an important potential molecular target in treatment of solid tumors (Semenza, 2008). Solid tumors often outgrow the blood vessels that supply them with essential oxygen and nutrients. This creates a low oxygen or 'hypoxic' environment within the tumor mass. Tumor-hypoxia causes activation of an oxygen-sensitive heterodimeric transcription factor HIF-1 constituted by an α and a β subunit. Though HIF-1α protein is constitutively expressed in the cytosolic compartment of cells, it is rapidly degraded by the 26S proteosome with a short half-life (approximately 5 min) under the normoxic conditions (Ke and Costa, 2006). However, hypoxic conditions prevent the oxygen-dependent degradation of HIF-1α and cause HIF-1α stabilization. Stabilized HIF-1α subunit translocates into the nucleus, forms a complex with HIF-1β and transcriptionally regulates more than 100 genes that produce an overall effect that helps the tumor cells to adapt and survive under hypoxic stress (Sememza and Wang, 1992; Semenza, 2008). Activated HIF-1 has been associated with increased aggressiveness and resistance to both chemotherapeutic agents and radiation therapy (Tatum *et al.*, 2006). To date, there is no approved therapeutic agent that specifically target HIF-1 for treatment of cancer. Considerable efforts are underway to discover clinically useful HIF-1 inhibitors (Onnis *et al.*, 2009). In our laboratory, over 60,000 extracts from the NCI Open repository of marine invertebrates and higher plants were evaluated for their abilities to inhibit hypoxia-induced HIF-1 activation in a cell-based reporter assay (a molecular-targeted assay for antitumor drug discovery). The hits were prioritized and then subjected to confirmatory assays and a dereplication process before subjecting them to bioassay-guided isolation.

2.1.3 Selection of chromatographic media for bioassay-guided isolation and natural products stability studies

Traditionally a chemistry-based phytochemical approach was used to fractionate, isolate and purify the bioactive compounds from natural sources. However, bioassay-guided fractionation has found favor as laboratories shifted to an emphasis on the modern molecular-targeted drug discovery. Following biological evaluation, active extracts are initially fractionated into 5-10 fractions which have distinctly different chemical compositions as determined by TLC. These fractions are dried and dissolved in an assay-compatible solvent and evaluated in the original bioassay system. The steps are repeated until purified compounds are identified that are responsible for the observed bioactivity. The bioassay-guided approach has the advantage of ignoring the inactive fractions or compound, in favor of active constituents. Appropriate assay design can differentiate the cytotoxic compounds from the 'active' compounds and increase the hit rate with reduced effort. The selection of chromatographic media is a critical step for a successful bioassay-guided isolation of active compounds. Exposure to inappropriate chromatographic media can cause catalytic degradation or irreversible binding of the compounds to the solid phase. This can lead to a loss of bioactivity or the production of artifactual compounds. In a bioassay-guided isolation process, inappropriate medium selection in any one of the fractionation steps can result in partial or complete loss of bioactivity in the subsequent fractions. Routinely used chromatographic media can be broadly classified into normal-phased or bonded normal-phased (Si gel, diol), styrene-divinylbenzene polymers and bonded reversed-phases (C_8, C_{18}, phenyl-hexyl). Inexpensive Si gel is often used for initial fractionation of extracts by normal-phase separation (Linington *et al.*, 2007). However, Si gel irreversibly binds certain natural products and promotes the acid-catalyzed rearrangement or degradation of others.

To overcome this problem, Si gel is often substituted with C_8, C_{18}, phenyl-hexyl or diol bonded-phase media. Among these, C_8, C_{18}, and phenyl-hexyl are used for reversed-phase separation and provide versatility in the separation process. Diol bonded-phase media is used as a chemically less reactive alternative for normal-phase separations where Si gel-like elution properties are required. However, large scale usage of these bonded-phase media is often limited by their relatively high cost. Diaion HP20SS is a synthetic styrene-divinylbenzene polymer used for reversed-phase like separation. It is less reactive, reusable and has emerged as a possible substitute for Si gel for mass use (Bugni *et al.*, 2008b). Though HP20SS is more expensive than Si gel, it is much more economical than the bonded-phase materials and suitable for repeated use. Diaion HP20SS provides an aromatic surface on which aromatic molecules are adsorbed by Van der Waal's forces (Shimizu, 2005). Sephadex® LH-20 is another chromatographic medium which is often used in natural product isolation. It is a hydroxypropylated dextran and works through gel permeation mechanisms (Seidel, 2005). Our HIF-1 bioassay-guided natural product isolation efforts were found to be severely hampered by the loss of bioactivity following routine fractionation protocols with Si gel. A variety of chromatographic media are used in the field of natural product drug discovery. However, these media have not been subjected to side-by-side comparison studies for their advantages/disadvantages in natural product based drug discovery efforts. Our objective of this study was to (a) characterize the elution profile of HP20SS; (b) compare the potential of various chromatographic media for irreversible binding of natural products present in plant extracts; and (c) examine the potential of these alternative media to reduce the loss of bioactivity in a typical reporter-based molecular-targeted (HIF-1) bioassay.

2.2 Materials and methods

2.2.1 General Experimental Procedures

The TLCs were performed using Merck $Si_{60}F_{254}$ or $Si_{60}RP_{18}F_{254}$ plates, visualized under UV at 254 nm and heated after spraying with a 10% H_2SO_4 solution in EtOH. The solvents were purchased from Fisher Scientific unless otherwise specified. The Si gel (32-63 μM) was purchased from Selecto Scientific and HP20SS ((Diaion 75 -100 μM, Supelco), Diol (50 μM, Discovery® Supelco) and Sephadex LH-20 was purchased from Sigma.

2.2.2 Preparation of columns

Miniature columns of Si gel, HP20SS, Diol, and Sephadex LH-20, were prepared by packing the pasture pipettes (Corning) with each respective chromatographic medium. Each column was 7.5 cm long with 0.55 cm internal diameter. The Si gel and diol were activated before elution by heating at 110°C for 30 min and then cooling to room temperature immediately before packing the columns. The HP20SS columns were washed with EtOAc and then with MeOH prior to the elution of the extracts.

2.2.3 Preparation and elution of extracts

Punica granatum L. (Puniaceae) freeze-dried juice, *Vaccinium macrocarpon* A. (Ericaceae) spray-dried juice, *P. granatum*, *Aspalathus linearis* (Burm. F) Dahlg. (Fabaceae), and *Cyclopia intermedia* L. (Fabaceae) extracts were kindly provided by Dr. Daneel Ferreira, (University of Mississippi, Department of Pharmacognosy). *Curcuma longa* L. (Zingiberaceae) powder (McCormik) was purchased from local store and extracted with several volumes of EtOH (500 mL) at 24 hour intervals by maceration at room temperature until the supernatant was

almost colorless. *Podophyllum peltatum* L. (Berberidaceae) root materials were collected from Oxford, Mississippi in the US and stored at -80°C and air dried at 40°C. Dried roots and rhizomes of *P. peltatum* were crushed in a mortar and pestle and extracted with EtOH (500 mL) at room temperature by several macerations at 24 hour intervals until the extract was almost colorless. *Saururus cernuus sec*-butanol/water partitionate was prepared previously by Dr. Chowdhury Faiz Hossain (Hossain *et al.*, 2005). Briefly, *S. cernuus* underground parts were extracted with CH_2Cl_2 and MeOH and combined. The combined extract was dissolved in $CHCl_3$ and partitioned with water. Then the water residue was partitioned with *sec*-butanol to obtain the *sec*-butanol/water partitionate. Commercially available *Asimina triloba* dietary supplement capsules (Nature's Sunshine) were purchased and the capsule contents were extracted with several volumes of 500 mL CH_2Cl_2 at room temperature by maceration till the supernatant was colorless. The solvent was replaced every 24 hours and the extract was used for the subsequent experiments. *Citrus reticulata* B. (Rutaceae) fruits were purchased from local store and the peels were air dried. The dried fruit peels were extracted with several volumes of EtOH until the supernatant was almost colorless. The *C.* reticulata EtOH-extract was used for subsequent experiments. All the extracts were dried and stored at -20 °C freezer.

The dried extracts were first weighed accurately to one-tenth of a milligram in small vials and dissolved in EtOH at a concentration of 200 mg/mL. Because not all the extracts were completely soluble in EtOH, the partially soluble extracts were first dissolved in a small amount of a water-EtOH (50:50) mixture and then diluted with EtOH to get the target concentration. The columns were loaded with the stock solution (30 mg, 150 µL). As controls, identical volumes (150 µL) of the stock solutions were placed directly in pre-weighed vials and were dried (n = 3). These served as controls for the losses in recovery due to sample handling and in the TLC

analysis. For the Sephadex LH-20 columns, *C. longa* and *C. reticulata* extracts were dissolved in MeOH, filtered, and no significant extract residues remained on the filter papers. The columns were loaded with the MeOH soluble portions (150 μL). The extracts were allowed to sit on top of the columns for 30-45 min, and overnight for the diol columns. The Si gel columns were eluted successively with hexanes (2 mL), EtOAc (5 mL), MeOH (5 mL) and water (2 mL), while the HP20SS columns were eluted successively with 50% MeOH-water (2 mL), MeOH (5 mL), EtOAc (5 mL) and hexanes (2 mL). Step gradients (100:0, 75:25, 50:50, 25:75, 0:100; 6 mL each) of water in isopropanol were applied for the elution of *C. longa*, *C. reticulata* and *S. cernuus* extracts. The combined dry weights of these fractions were used to calculate the total extract recoveries. Because solvent systems were unable to completely elute *C. reticulata* and *C. longa* from the columns (apparent yellow color on the columns, but the sample recovery loss was not statistically significant), we repeated the elution using a water-acetone step gradient in identical manner as the water-isopropanol system. Step gradients of hexanes-dichloromethane (9:1; 6 mL), dichloromethane-EtOAc (20:1; 6 mL), EtOAc (6 mL), EtOAc-MeOH (5:1; 6 mL) and MeOH (6 mL) were used to elute diol columns. Sephadex LH-20 columns were eluted with MeOH.

2.2.4 Tumor cell culture and cell-based HIF-1 reporter assay

Human breast tumor T47D cells were purchased from ATCC and were maintained in Dulbecco's Modified Eagle's Mediun (DMEM) and Ham's F-12 (1:1) media containing 2.5 mM L-glutamine (Mediatech). The medium was supplemented with fetal bovine serum (FBS, 10% v/v final concentration, Hyclone), penicillin (50 units/mL) and streptomycin (50 μg/mL) (pen/strep) (BioWhittaker). Exponentially grown T47D cells were transfected with the pTK-

HRE3-luc reporter by electroporation using an ECM830 square wave electroporation system (BTX Inc) at 140 V for 70 ms (1 pulse). The transfected cells were plated at 3 x 10^4 cells per well into 96-well plates in a volume of 100 µL of DMEM/F12 medium supplemented with 10% FBS and antibiotics. After 24 h, the test compounds were diluted (2x final concentration) in DMEM/F12 medium with antibiotics, added in a volume of 100 µL per well, and the incubation continued for another 30 min at 37 °C. The cells were exposed to hypoxic (1% O_2, 5% CO_2, 94% N_2) or normoxic (5% CO_2, 95% air) conditions or hypoxia mimetic (1,10-phenanthroline, 10 µM, Sigma) at 37 °C for 16 h. Hypoxic conditions were achieved by incubationg the cells in a humidified chamber (Billups-Rothenberg) that was purged with a hypoxic gas mixture (1% O_2, 5% CO_2, 94% N_2). The cells were then lysed using a lysis buffer (1%Triton X-100, 1 mM $CaCl_2$, and 1 mM $MgCl_2$ in 1 x phosphate buffered saline pH7.4) and luciferase activities determined following manufacturer's instructions (Promega) using a microplate reader (Biotek). The following formula was used to calculate the % inhibition data:

$$\% \text{ inhibition} = (1 - \text{luminescence}_{\text{treated}}/\text{luminescence}_{\text{induced}}) \times 100$$

Extracts for bioassay were prepared as stock solutions in DMSO and the final concentration of solvent was less than 0.5% (v/v) in all assays.

2.2.5 Statistical Analysis

Data was compared using the Student's *t* test, one-way ANOVA and Bonferroni post hoc analyses (GraphPad Prism 5.0). Differences were considered significant when $p < 0.05$.

2.3 Results and discussion

2.3.1 Effects of chromatographic media and elution protocols on extract recovery

Ten natural product-rich extract samples from terrestrial plants, with chemically different HIF-1 inhibitory constituents were selected for evaluating the effects of chromatographic media on natural product metabolite recovery and HIF-1 inhibitory activity (Table 2.1).

Natural product-rich mixtures	Active constituents
Pomegranate - *Punica granatum*(Punicaceae) extract	Flavonoids, anthocyanins, tannins (Seeram *et. al.*, 2006)
Pomegranate juice - *P.granatum* juice	Flavonoids, anthocyanins (Seeram *et. al.*, 2006)
Cranberry – *Vaccinium macrocarpon* (Ericaceae) freeze-dried juice	Polyphenols (Neto, 2007)
Rooibos - *Aspalathus linearis* (Fabaceae) extract	Flavonoids (Bramati *et al.*, 2002)
Honeybush - *Cyclopia intermedia* (Fabaceae) extract	Flavonoid glycosides (Kamara *et al.*, 2003)
Tangerine - *Citrus reticulata* (Rutaceae) extract	Flavonoid glycosides (Khan *et al.*, 2010)
Turmeric - *Curcuma longa* (Zingiberaceae) extract	Curcuminoids (Roth *et al.*, 1998)
Lizard's tail - *Saururus cernuus* (Saururaceae) *sec*-butanol partitionate	Sesquineolignans, dineolignans (Rao and Rao, 1990)
Paw paw - *Asimina triloba* (Annonaceae) extract	Annonaceous acetogenins (Coothankandaswamy *et al.*, 2010)
Mayapple - *Podophyllum peltatum* (Berberidaceae)	Lignans (Moraes *et al.*, 2002)

Table 2.1 Selected extracts for comparative evaluation of chromatographic media

Among the ten extract samples examined, *V. macrocarpon* juice and extracts of *A. triloba*, and *P. granatum* showed a significant level of irreversible sample loss on Si gel columns when eluted with typically used solvent systems [hexanes, EtOAc, MeOH, and water for Si gel and MeOH-water (1:1), MeOH, EtOAc and hexanes for HP20ss] (Figure 2.1).

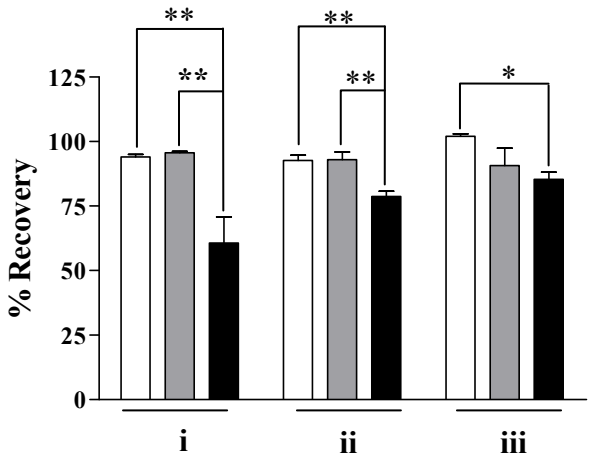

Figure 2.1 Recovery of extracts (30 mg; 150 µL stock solution) from various columns (▒ HP20SS, ■ Si Gel) after elution with water-MeOH, MeOH, EtOAC and hexanes; (**i**) *V. macrocarpon*; (**ii**) *A. triloba*; (**iii**) *P. granatum*. Stock solutions (150 µL) was directly placed in a vial and dried ($n = 3$). The dried material served as sample recovery controls (□). Data shown are average + standard deviation from three separate columns ($n = 3$). One-way ANOVA with Bonferroni post hoc test were applied to analyze the data using GraphPad Prism 5.0; Differences between data sets were considered statistically significant when $p < 0.05$ (* $p < 0.05$, ** $p < 0.01$).

Drastic losses in the masses of *C. longa*, *C. reticulata* and *S. cernuus* extracts were observed (approx 50%, data not shown) on both HP20SS and Si gel. Rather than irreversible binding, this suggested that these columns were insufficiently eluted by the initial solvent systems. Hence a water-isopropanol step gradient system was used to completely elute the *C. longa*, *C. reticulata* and *S. cernuus* extracts from the HP20SS columns. The weights of the combined water-isopropanol gradient fractions were used to calculate total recovery. This is particularly noteworthy that the use of the water-isopropanol gradient alone was unable to completely elute the *C. longa* and *C. reticulata* extracts from the HP20SS columns. A non-polar solvent such as EtOAc was required for significantly improve column recovery. The water-isopropanol gradient system has been reported for natural product library production by the Ireland group (Bugni *et al.*, 2008a; Bugni *et al.*, 2008b) at the University of Utah and the Orjala group at the University of Illinois at Chicago to elute cyanobacterial extracts from HP20SS

columns (Sturdy *et al.*, 2010). In the case of *C. longa* the total sample recovery was significantly increased ($p = 0.0015$) when a final EtOAc elution step was added to the typically used MeOH solvent system; while when compared with water-isopropanol gradient system alone, the increase in the total recovery with a final EtOAc elution step was marginally significant ($p = 0.0527$). The recovery of *A. triloba*, and *C. reticulata* extracts also showed significant improvement following final elution with EtOAc (Figure 2.2). Previously reported water-acetone gradients (Boonlarppradab and Faulkner, 2007) completely eluted of *C. longa* extract from the HP20SS columns.

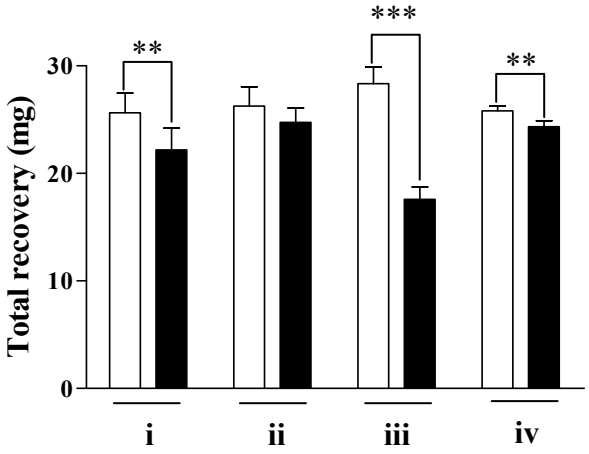

Figure 2.2 Eluting HP20SS column with non-polar solvent such as EtOAc can increase extract recovery. (**i**) *Curcuma longa* extract recovery using a water-MeOH system inclusive (□) or exclusive (■) of EtOAc elution ($p = 0.0015$); (**ii**) *Curcuma longa* extract recovery using a water-IPA system inclusive or exclusive of EtOAc elution ($p = 0.0527$); (**iii**) *Asimina triloba* extract recovery using a water-MeOH system inclusive or exclusive of EtOAc elution ($p = 0.0009$); (**iv**) *Citrus reticulata* extract recovery using a water-MeOH system inclusive or exclusive EtOAc elution ($p = 0.0036$). Data shown are average + standard deviation from three separate columns ($n = 3$). Student's paired *t*-test (two-tailed) was used to compare the data using GraphPad Prism 5.0; Differences between data sets were considered statistically significant when $p < 0.05$ (** $p < 0.01$, *** $p < 0.001$).

The Si gel elute of the *P. peltatum* extract showed a noticeable change in its chemical composition as observed by analysis of its TLC profile (Figure 2.3A). The *C. reticulata* (Figure 2.3B) and *C. longa* (Figure 2.3C) extract TLC profiles indicated that considerable loss on the HP20SS columns can occur unless the media is subjected to further elution with a non-polar solvent such as EtOAc.

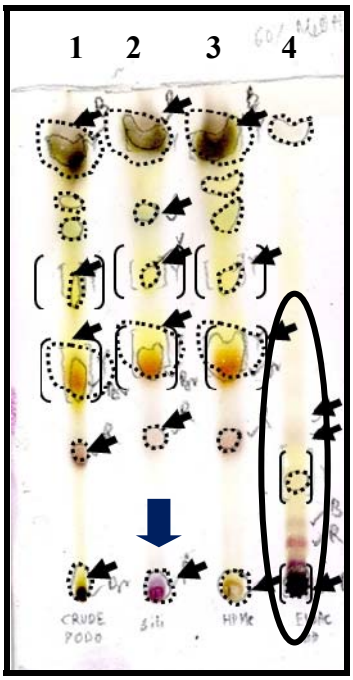

Figure 2.3A TLC analysis of the *Podophyllum peltatum* extract exposed to elution with various chromatographic media. Notable chemical alterations in (Blue arrow) and active phytochemicals retained in EtOAc eluent (solid circle); **1** – *Podophyllum* extract, **2** – Combined *Podophyllum* fractions from a Si gel column, **3** – Combined water-MeOH fractions of *Podophyllum* from a HP20SS column and **4** – EtOAc wash of *Podophyllum* from a HP20SS columns after water-MeOH elution. C_{18} reversed-phase TLC eluted with 60% MeOH in water; Pigments = "bracketed" spots, UV_{254}-absorbing compounds = "dotted circles" and 10% ethanolic sulphuric acid-charred compounds = "arrows".

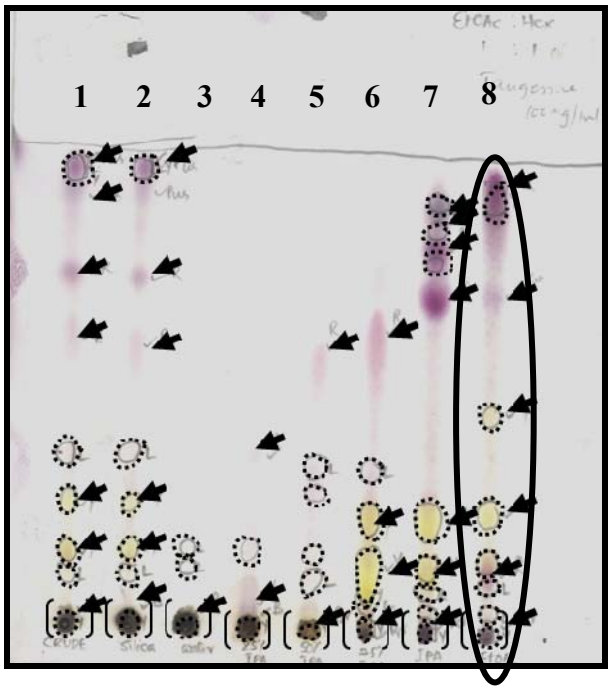

Figure 2.3B TLC analysis of the *Citrus reticulata* extract and fractions exposed to elution with various chromatographic media. **1** – *C. reticulata* extract, **2** – Combined *C. reticulata* fractions from a Si gel column, **3** – Water fraction of *C. reticulata* extract from a HP20SS column, **4** – Isopropanol-water (1:3) fraction of *C. reticulata* extract from a HP20SS column, **5** – Isopropanol-water (1:1) fraction of *C. reticulata* extract from a HP20SS column, **6** – Ipropanol-water fraction (3:1) of *C. reticulata* extract from a HP20SS column, **7** – Isopropanol fraction of *C. reticulata* extract from a HP20SS column and **8** – EtOAc wash after isopropanol-water elution of *C. reticulata* extract from a HP20SS column; active phytochemicals retained in EtOAc eluent (solid circle); Si gel normal phase TLC eluted with hexanes:EtOAc (1:1). Pigments = "bracketed" spots, UV_{254}-absorbing compounds = "dotted circles" and 10% ethanolic sulphuric acid-charred compounds = "arrows".

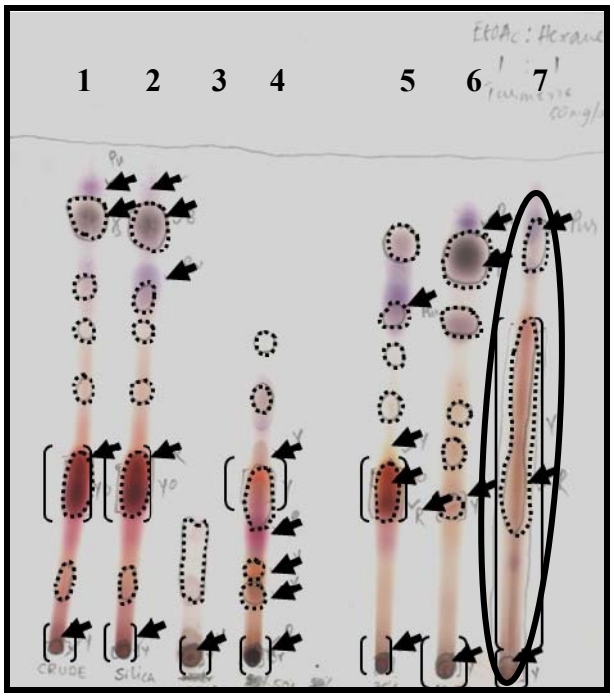

Figure 2.3C TLC analysis of the *Curcuma longa* extract and fractions exposed to elution with various chromatographic media. **1** – *C. longa* extract, **2** – Combined *C. longa* fractions from a Si gel column, **3** – Isopropanol-water(1:3) fraction of *C. longa* extract from a HP20SS column, **4** – Isopropanol-water (1:1) fraction of *C. longa* extract from a HP20SS column, **5** – Isopropanol-water (3:1) fraction of *C. longa* extract from a HP20SS column, **6** – Isopropanol fraction of *C. longa* extract and **7** – EtOAc wash of *C. longa* extract from a HP20SS column after isopropanol-water elution; active phytochemicals retained in EtOAc eluent (solid circle); Si gel normal-phased TLC eluted with hexanes:EtOAc (1:1). Pigments = "bracketed" spots, UV_{254}-absorbing compounds = "dotted circles" and 10% ethanolic sulphuric acid-charred compounds = "arrows".

The extracts of *C. longa, C. reticulata* and *S. cernuus* were subjected to elution on diol, a chromatographic medium used by Dr. Gustafson (National Cancer Institute) for generating natural product libraries, to evaluate its elution properties (Gustafson and Nagle, personal communication, 2008). Of the three extracts, *C. reticulata* showed a significant loss of recovery on diol. The elution profiles of *C. longa* and *C. reticulata* extract MeOH soluble portions were evaluated on Sephadex LH-20. *Citrus reticulata* extract also showed a significant loss of recovery from Sephadex LH-20 (Figure 2.4).

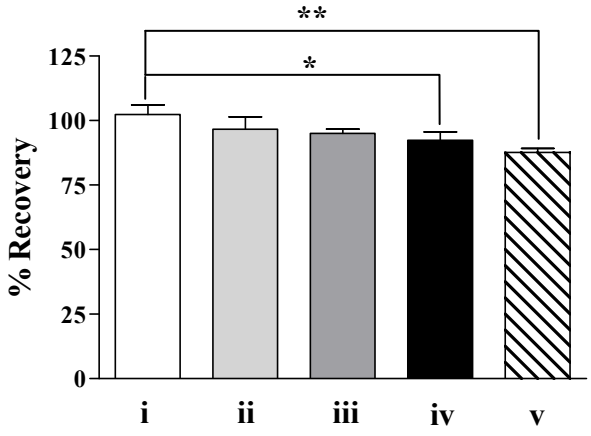

Figure 2.4 Total recovery of *C. reticulata* extract from various chromatographic columns. (**i** – Control, **ii** – HP20SS, **iii** – Si Gel, **iv** – Diol, **v** – Sephadex LH-20) Data shown are average + standard deviation ($n = 3$) and was analyzed by one-way ANOVA with Bonferroni post hoc test; using GraphPad Prism 5.0; Differences between data sets were considered statistically significant when $p < 0.05$ (* $p < 0.05$, ** $p < 0.01$).

These results clearly indicate the potential of Si gel, relative to other chromatographic media, to cause an irreversible binding or chemical alteration of the plant extract chemical constituents. Use of Si gel as a chromatographic medium for fractionation of extracts obtained from terrestrial or marine organisms with an unknown chemical profile can result in a loss of potential chemical diversity, sample quantity or produce corresponding experimental artifacts. Although the alternative media evaluated such as diol-bonded phase and Sephadex LH-20 also caused observable losses in sample recovery that were elution protocol dependant, Si gel caused the greatest sample recovery loss. The water-isopropanol solvent systems used for the elution of HP20SS columns appear to be insufficient for the complete elution of extracts, especially for extracts with lipophilic constituents. Elution of HP20SS with non-polar solvents, such as EtOAc, prevents the loss of the intermediate to highly non-polar compounds. While certain drug discovery programs may choose to exclude these constituents because they may not serve as promising drug candidates due to their high lipophilicity, but they may serve as valuable

molecular probes or as potential 'template' molecules from which to construct potential drug candidates. Such considerations are of special importance in the generation of natural product-rich extracts/fraction libraries. Another observation worth noting is that the use of non-polar solvents, such as EtOAc, cause elution of fine HP20SS particles during the separation process. However, this is preventable by first washing the HP20SS columns with EtOAc and then washing the column with MeOH.

2.3.2 Effects of chromatographic media on extract HIF-1 inhibitory activity

We examined whether exposure of the extracts to these chromatographic media affects extract bioactivities. The HIF-1 inhibitory activity of the extracts was evaluated using a 96-well plate-based method. Of the 10 extracts, *A. triloba* (0.5 µg/mL), *C. reticulata* (50 µg/mL), *P. peltatum* (50 µg/mL), *S. cernuus* (50 µg/mL), and *C. longa* (25 µg/mL) extracts inhibited HIF-1 activity by > 50% (Figure 2.5) in the T47D cell-based HIF-1 reporter assay. Other extracts were inactive. However, the *P. peltatum* extract was excluded from further evaluation because it was highly unstable and decomposed during storage. The HIF-1 inhibitory activity of these extracts was not secondary to cytotoxic effects (cytotoxicity < 25%). In addition, a review of literature indicated that some of these extracts contain known HIF-1 inhibitors and it is unlikely that these extracts interfere with the luciferase assay system (Coothankandaswamy *et al.*, 2010; Hodges *et al.*, 2004; Choi *et al.*, 2006).

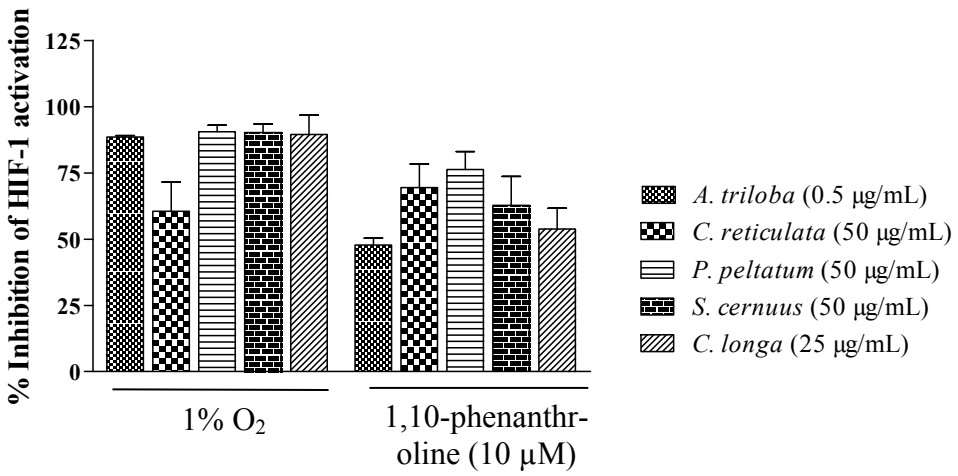

Figure 2.5 Inhibiton of physiological hypoxia (1% O_2) and 1,10-phenanthroline-induced HIF-1 activation by active extracts. Data shown are average + standard deviation from single experiment assayed in triplicate.

When *C. reticulata* and *C. longa* extracts were eluted through HP20SS medium, considerable active materials remained on the column until ultimately eluted with EtOAc. The EtOAc eluted material inhibited both hypoxia-induced (1% O_2) and 1,10-phenanthroline (10 μM)-induced HIF-1 activation at 50 μg/mL (suppression of cell viability $< 25\%$, data not shown) (Figure 2.6).

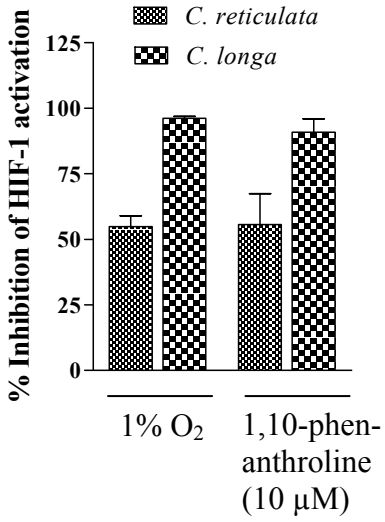

Figure 2.6 Inhibition of HIF-1 activity under physiological hypoxia (1% O_2) and 1,10-phenanthroline-induced HIF-1 activation by *Citrus reticulata* and *Curcuma longa* EtOAc eluates (50 μg/mL) from HP20SS columns. Data shown are average + standard deviation from one representative experiment in triplicate.

All fractions obtained from each extract/column combination were recombined and evaluated for HIF-1 inhibitory activity to assess the impact of each media exposure on the extracts' total bioactivity. Under physiological hypoxic conditions (1% O_2), reconstituted *C. longa* extract samples from the HP20SS, Si gel, and diol columns were significantly less active relative to the original extract (Figure 2.7A). Under chemical hypoxia (1,10-phenanthroline, 10 μM), reconstituted *C. longa* extract samples from both Si gel and HP20SS columns exhibited significantly lower activities (Figure 2.7B). For the reconstituted extract samples eluted from the Sephadex LH-20 and diol columns, there was no difference in activity when compared with the original extract. The inhibitory activity towards 1,10-phenanthroline-induced HIF-1 activation by the Si gel eluted *C. reticulata* pooled material was markedly reduced (Figure 2.7C). In all cases suppression of cell viability was ≤ 25% (data not shown).

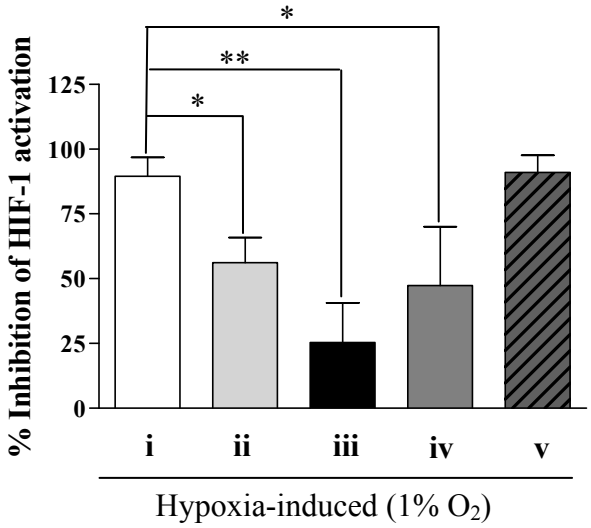

Figure 2.7A Inhibition of physiological hypoxia-induced HIF-1 activation by recombined *Curcuma longa* eluates (25 µg/mL) [**i** – Control, **ii** – HP20SS, **iii** – Si Gel, **iv** – Diol, **v** – Sephadex LH-20]. The stock solution used to load the columns were placed in dried vials in identical volumes ($n = 3$). The HIF-1 inhibitory activity of the dried material served as control. Data represent average + standard deviation from one representative experiment in triplicate. Data was analyzed by one-way ANOVA with Bonferroni post hoc test; Differences between data sets were considered statistically significant when $p < 0.05$. (* $p < 0.05$, ** $p < 0.01$).

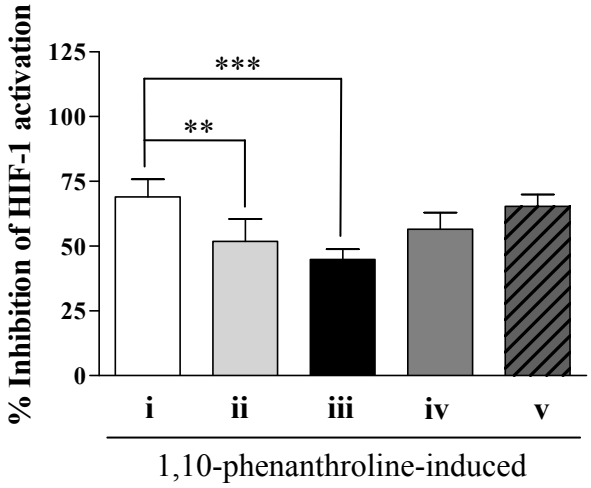

Figure 2.7B Inhibition of 1,10-phenanthroline-induced HIF-1 activation by recombined *Curcuma longa* eluates (25 µg/mL) [**i** – Control, **ii** – HP20SS, **iii** – Si Gel, **iv** – Diol, **v** – Sephadex LH-20]. The stock solution used to load the columns were placed in dried vials in identical volumes ($n = 3$). The HIF-1 inhibitory activity of the dried material served as control. Data represent average + standard deviation from one representative experiment in triplicate. Data was analyzed by one-way ANOVA with Bonferroni post hoc test; Differences between data sets were considered statistically significant when $p < 0.05$. (** $p < 0.01$, *** $p < 0.001$).

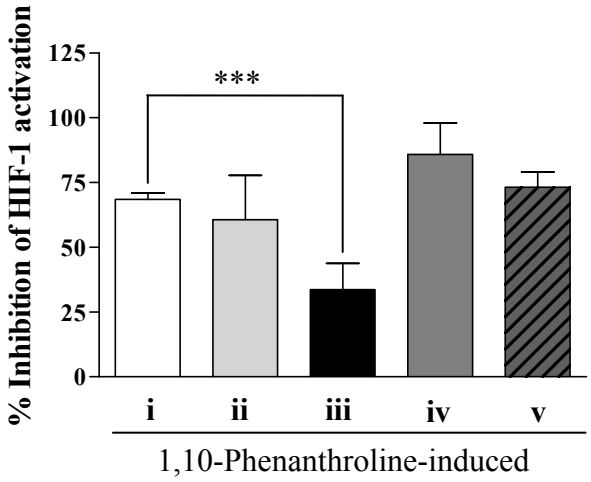

Figure 2.7C Inhibition of 1,10-phenanthroline-induced HIF-1 activation by recombined *Citrus reticulata* eluates (50 µg/mL) [**1** – Control, **2** – HP20SS, **3** – Si Gel, **4** – Diol, **5** – Sephadex LH-20]. The stock solution used to load the columns were placed in dried vials in identical volumes ($n = 3$). The HIF-1 inhibitory activity of the dried material served as control. Data represent average + standard deviation from one representative experiment in triplicate. Data was analyzed by one-way ANOVA with Bonferroni post hoc test; Differences between data sets were considered statistically significant when $p < 0.05$. (*** $p < 0.001$).

Both the original and reconstituted *S. cernuus* and *A. triloba* extracts selectively inhibit hypoxia-induced HIF-1 activation (1% O_2). The *S. cernuus* extract lost activity upon Si gel elution. Similar loss was not observed upon HP20SS elution. The reconstituted *A. triloba* extract lost considerable HIF-1 inhibitory activity when eluted through HP20SS but retained its activity when eluted through Si gel (Figure 2.8A and 2.8B). The suppression of cell viability by *S. cernuus* and *A. triloba* column eluates was ≤ 20% in all cases (data not shown).

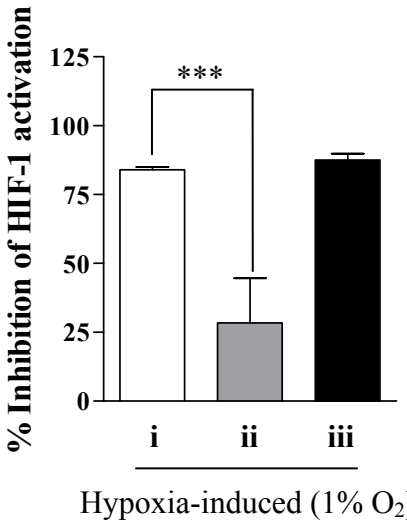

Figure 2.8A Inhibition of physiological hypoxia-induced HIF-1 activation by recombined *Asimina triloba* eluates (0.05 µg/mL) [**i** – Control, **ii** – HP20SS, **iii** – Si Gel]. The stock solution used to load the columns were placed in dried vials in identical volumes ($n = 3$). The HIF-1 inhibitory activity of the dried material served as control. Data represent average + standard deviation from one representative experiment in triplicate. Data was analyzed by one-way ANOVA with Bonferroni post hoc test; Differences between data sets were considered statistically significant when $p < 0.05$. (*** $p < 0.001$).

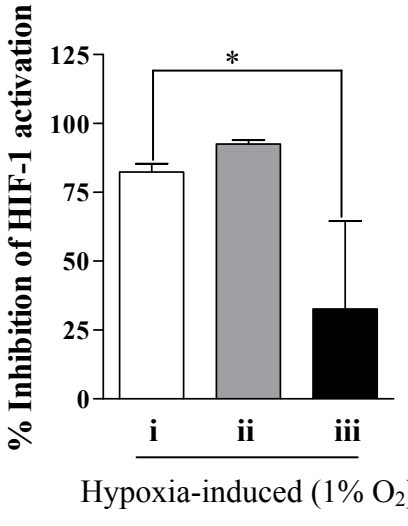

Figure 2.8B Inhibition of physiological hypoxia-induced HIF-1 activation by recombined *Saururus cernuus* eluates (3.125 µg/mL) [**i** – Control, **ii** – HP20SS, **iii** – Si Gel]. The stock solution used to load the columns were placed in dried vials in identical volumes ($n = 3$). The HIF-1 inhibitory activity of the dried material served as control. Data represent average + standard deviation from one representative experiment in triplicate. Data was analyzed by one-way ANOVA with Bonferroni post hoc test; Differences between data sets were considered statistically significant when $p < 0.05$ (* $p < 0.05$).

Many laboratories identify molecular-targeted antitumor natural products through the use of bio-assay guided isolation approach. Because bioassay-guided fractionation relies on the bioactivity of extracts and subsequent fractions, loss of activity due to inappropriate chromatographic media selection, can significantly impact the drug discovery outcome. Three of the four extracts that inhibited HIF-1 activation, exhibited a significant loss of bioactivity when subjected to Si gel-based chromatographic methods. For *C. longa* extract, no loss in sample mass recovery was detected upon HP20SS or Diol elution, while considerable loss in bioactivity was observed. Only the extracts of *A. triloba* and *C. longa* lost significant HIF-1 inhibitory activity upon HP20SS elution relative to the original extracts. Moreover, neither extract showed significant mass loss upon HP20SS elution but *A. triloba* lost mass upon Si gel elution. Because *A. triloba* extract contains unsaturated, lipophilic active acetogenin constituents, it is possible that its active constituents bind to the aromatic skeleton of HP20SS by π-bonding. Because these extremely potent acetogenins are relatively minor extract components, the overall loss of sample mass was not statistically significant. Such sample losses can be prevented by eluting HP20SS with a highly non-polar solvent such as CH_2Cl_2 or hexanes. Although the loss of bioactivity upon elution through Si gel was apparent for some extracts, HP20SS elution may also cause significant losses in bioactivity. Hence, chromatographic media selection should prioritize alternatives to Si gel when possible, but the specific elution protocol when the HP20SS medium is selected should be carefully considered. Unless the aim of the separation is to include a "defattening" step to remove lipophilic compounds, HP20SS elution protocols must include a final non-polar wash with EtOAc, CH_2Cl_2 or other lipophilic solvent to ensure a more complete elution of sample than that may be obtained with commonly used aqueous-MeOH or aqueous-isopropanol gradients. However, HP20SS columns must be prewashed with EtOAc and

equilibrated with MeOH to avoid elution of small HP20SS particles when the elution protocol involves a final non-polar solvent wash.

CHAPTER III

DEVELOPMENT OF A BIOENERGETICS-BASED SCREEN FOR IDENTIFICATION OF SMALL-MOLECULE GLYCOLYSIS INHIBITORS

CONTRIBUTION OF AUTHORS

The work described in this chapter is a collaborative effort between Drs. Dale G. Nagle, Yu-Dong Zhou, Jun Li and myself. Drs. Nagle and Zhou conceived the idea, helped to design the experiments, supervised the project, and helped to interpret the data. Dr. Nagle served as my major advisor, while Dr. Zhou provided additional advice regarding the biological experiments. I performed the experiments, analyzed, and interpreted the data. Drs. Nagle and Li helped me to solve the structure of moronone (**1**). Dr. Li helped in writing the structure elucidation portion. Ms. Mahdi edited the images for membrane potential experiments.

3.1 Overview

3.1.1 Introduction

Tumor cells produce lactate as an end product of glucose catabolism in the presence of adequate oxygen. This phenomenon is known as 'aerobic glycolysis' (Gatenby and Gillies, 2004). Tumor cells with a high rate of aerobic glycolysis are usually associated with poor prognosis, malignant aggressiveness, and resistance to standard therapeutic regimens (Mason *et al.*, 2010; Wolf *et al.*, 2011; Zhou *et al.*, 2010; Pitroda *et al.*, 2009; Klawitter *et al.*, 2009). Aerobic glycolysis is less efficient in producing adenosine triphosphate (ATP) compared to oxidative phosphorylation (OxPhos). However, it is hypothesized that generating energy through the glycolytic pathway constitutes an advantageous metabolic environment for unrestricted cell proliferation and tumor growth (Vander Heiden *et al.*, 2009; Kroemer and Pouyssegur, 2008; Brand and Hermfisse, 1997). Metabolic targeting of tumors has been in the limelight for several decades (Papandreou *et al.*, 2011). Inhibitors of the enzymes required for aerobic glycolysis are currently being explored for their therapeutic potential (Scatena *et al.*, 2008). Small-molecules that target aerobic glycolysis, such as 2-deoxy-D-glucose (**2**) and lonidamine (**3**) (Figure 3.1B), have undergone clinical evaluation for the treatment of refractory tumors (ClinicalTrials.gov, website accessed on 04/03/2012; Di Cosimo *et al.*, 2003).

Natural products from plants and marine organisms have been widely investigated as a potential source of new anticancer agents (Newman and Cragg, 2012). Natural products that target the mitochondria have been explored as a class of potential antitumor therapeutic agents (Wolvetang *et al.*, 1994) and screening methods have been developed to identify mitochondrial inhibitors (Lin *et al.*, 2008). However, there have been limited efforts to discover small-molecule inhibitors of aerobic glycolysis from natural sources (Kitagawa *et al.*, 2011).

More than 10,000 lipid extracts from the National Cancer Institute's (NCI) Open Repository of higher plants and marine invertebrates were examined to identifyr inhibitors of aerobic glycolysis (glycolysis inhibitors) from natural sources (hit rate 0.72%). The extract of *Moronobea coccinea* Aubl. (Clusiaceae) was 'active' in our screening assay. Polyprenylated benzophenone derivatives (PBDs), which had been previously isolated from the plant, were initially hypothesized to be responsible for its glycolysis inhibitory activity (Marti *et al.*, 2009). A wide spectrum of activities including cytotoxic, antimicrobial, antioxidant, and anti-inflammatory activities have been attributed to prenylated benzophenones isolated from the plants belonging to the family Clusiaceae (Acuna *et al.*, 2009). Bioassay-guided isolation and structure elucidation led us to the discovery of moronone (**1**), a PBD with a new carbon skeleton. In this report, we describe the development of an assay system to screen for glycolysis inhibitors and the discovery of a protonophoric benzophenone derivative. The well studied protonophore 2-[{4-(trifluoromethoxy)phenyl}hydrazinylidene]propanedinitrile (**4**)[FCCP] was also found to be active in our assay system. It was concluded that the protonophoric compounds or extracts containing protonophoric components are possible nuiscance compounds and needs to be dereplicated in order to successfully discover the glycolysis inhibitors.

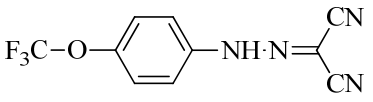

FCCP (**4**)

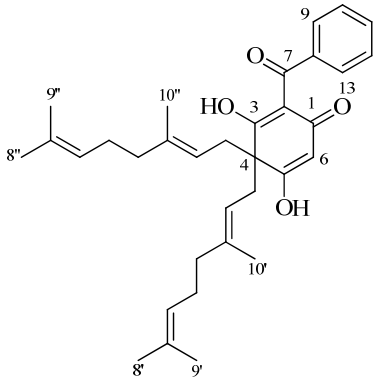

Moronone (**1**)

Figure 3.1A Structure of FCCP (**4**) and proposed structure of moronone (**1**)

3.1.2 Cancer cell metabolism and bioenergetics

Normal mammalian cells generate ATP by metabolizing glucose through two complementary cellular pathways, i.e., glycolysis and OxPhos. Under aerobic conditions, the cellular glycolytic flux is limited. However, under anaerobic conditions, the lack of oxygen inhibits mitochondrial OxPhos, and pyruvate generated in the glycolytic pathway is converted to lactate in the cytosol (Kim and Dang, 2006). Hence, for non-malignant cells under anaerobic conditions, glycolysis is the major supplier of cellular ATP, while under aerobic conditions the ATP demands of the same cells are mainly met by ATP synthesized by OxPhos.

This bioenergetic homeostasis is altered in tumors. In tumor cells, the glycolytic flux is high, even in the presence of adequate oxygen. Increased glucose uptake, increased production of lactate from pyruvate and lower OxPhos by tumor cells, even under aerobic conditions, are collectively considered to be one of the hallmarks of cancer (Yeung *et al.*, 2008). This phenomenon was first reported in the early twentieth century by Otto Warburg (Warburg, 1956), and is currently termed as the 'Warbug effect' or aerobic glycolysis. A previous study estimated that 40-75% of cellular ATP production is generated by aerobic glycolysis (Mathupala *et al.*, 2010). However, a newer study has challenged the paradigm that aerobic glycolysis is the universally predominant ATP supplier for tumor cells (Zu and Guppy, 2004). This study indicates that the extent of ATP contribution by aerobic glycolysis can be cell line and tumor type-dependent. In some tumor cell lines, mitochondrial OxPhos has been known to contribute 50-97% of cellular ATP generation (Moreno-Sanchez *et al.*, 2009). Although aerobic glycolysis may not be the predominant energy generating pathway in all tumor cells, enhanced cellular glycolytic metabolism is often associated with poor prognosis, aggressiveness, and chemotherapy resistance (Mason *et al.*, 2010; Wolf *et al.*, 2011; Zhou *et al.*, 2010; Pitroda *et al.*,

2009; Klawitter *et al.*, 2009). Hypoxic conditions in tumor masses are hypothesized to be a key mediator of cellular dependence on glycolysis. Hypoxic conditions activate HIF-1 and induce more than 100 HIF-1-regulated genes in tumor cells, including multiple glycolytic enzymes (Ke and Costa, 2006). Specific isoforms of several glycolytic enzymes induced by HIF-1 (hexokinase II, phosphofructokinase-1 and lactate dehydrogenase isoform A) contribute to the glycolytic tumor cell phenotype. A major redistribution of hexokinase II (HKII), one of the four isoforms of the enzyme hexokinase, from the cytosol to the outer mitochondrial membrane occurs in tumor cells (Nakashima *et al.*, 1986). The binding of HKII to the voltage-dependent anion channels (VDAC) on the mitochondrial outer membrane is believed to give the glycolytic enzyme preferential access to mitochondrial ATP. This preferential access to ATP enhances the catalytic activity of the enzyme (Arora and Pedersen, 1988). This binding of HKII to VDAC also may disable the activation of the mitochondria-mediated apoptotic pathway via Bax, a pro-apoptotic Bcl-2 family protein (Pastorino *et al.*, 2002). Aerobic glycolysis is inefficient from the bioenergetics perspective, since the net ATP gain/mole of glucose in this process is 17–18 fold less than that of OxPhos. However, the predominantly glycolytic metabolism is hypothesized to create a pro-proliferation and pro-survival environment for tumor cells. Rapidly dividing cells in living tissues undergo similar metabolic rearrangements (Vander Haiden *et al.*, 2009; Wang *et al.*, 1976; Almeida *et al.*, 2010; Herrero-Mendez *et al.*, 2009; Colombo *et al.*, 2010). As the cells rapidly multiply, they require biosynthetic building blocks such as amino acids, nucleic acids and lipids. Certain glycolytic intermediates, such as glucose-6-phosphate, can be utilized by pentose phosphate pathway to generate some of the components required for continuous cell division (Barger and Plas, 2010). In addition, evidence suggests that lactate is used as a substrate for

OxPhos, and a possible symbiotic relationship exists between the hypoxic and oxygenated cells in solid tumors (Sonveaux *et al.*, 2008).

3.1.3 The glycolytic pathway as an antitumor target

Selective tumor cell targeting is the single most important objective in antitumor drug discovery. Cancer researchers aim to identify the genetic, biochemical and structural differences between malignant cell and non-malignant cells. Enhanced tumor cell glucose consumption and increased dependence on the glycolytic pathway for ATP synthesis can be exploited to selectively target tumor cells. Indeed, inhibition of aerobic glycolysis has emerged as one of the potential adjuvant therapies to treat various solid tumors (Rodriguez-Enriquez *et al.*, 2009; Cheng *et al.*, 2012). Targeting glycolysis in tumor cells can potentially interfere with the intracellular signaling that stimulate uncontrolled proliferation, as well as enhance the efficacy of the conventional antitumor regimens (Scatena *et al.*, 2008; Cheng *et al.*, 2012). In addition, ATP depletion due to the inhibition of glycolysis can lead to the circumvention of multidrug resistance mechanisms (Nakano *et al.*, 2011). Because tumore cells are more dependent on glycolysis for their energy needs, proliferation and survival, a comparatively small perturbation of the glycolytic pathway is expected to have higher impact on tumor cells relative to normal cells and thus result in a selective tumor cell targeting.

The enzyme hexokinase catalyzes the first step of glycolysis, i.e., phosphorylation of glucose. To date, this enzyme has been the most common target for the discovery of agents that inhibit aerobic glycolysis. Compounds that result in a decrease in hexokinase enzymatic activity, such as 2-deoxy-D-glucose (**2**) [2-DG] and lonidamine (**3**) (Figure 3.1B), have undergone clinical evaluation for the treatment of advanced malignancies, both as monotherapies and in

combination with other chemotherapeutic agents (ClinicalTrials.gov, website accessed on 04/03/2012; Di Cosimo *et al.*, 2003). The phase II clinical trial of 2-DG for advanced prostate cancer was terminated due to slow patient accrual (ClinicalTrials.gov, website accessed on 07/03/2012). However, a phase I clinical trial found that administering 2-DG in combination with taxol is feasible and safe (Raez *et al.*, 2005). In preclinical studies, 3-bromopyruvate (**5**) [another HKII inhibitor] has shown promising results against hepatocellular carcinoma (Ko and Pedersen, 2001; Ko *et al.*, 2004). However, 3-bromopyruvate (**5**) is reported to inhibit mitochondrial respiration and to have non-selective thiol-alkylating effects (Shoshan, 2012). Inhibition of HKII by 3-bromopyruvate (**5**) might be non-specific and only partly responsible for its demonstrated activity. Gossypol [AT-101] (**6**), a promiscuous inhibitor of glycolytic enzymes including glyceraldehyde-3-phosphate dehydrogenase (GAPDH) (Scatena *et al.*, 2008) and lactate dehydrogenase (LDH) (Granchi *et al.*, 2011), is currently being evaluated in multiple clinical trials as a treatment option for aggressive tumor phenotypes, such as glioblastoma multiforme (ClinicalTrials.gov, website accessed on 07/06/2012). Pyruvate kinase, the enzyme that converts phosphoenolpyruvate to pyruvate, has been identified as another plausible molecular target in the glycolysis pathway. Cancer cells overexpress the specific pyruvate kinase isoform PKM2, which is usually detected in early fetal tissues (Christofk *et al.*, 2008). A seven amino acid peptide known as CAP-232/TLN-232 (**7**) targets PKM2, and recently underwent a phase II clinical trial for the treatment of metastatic renal cell carcinoma (ClinicalTrials.gov, website accessed on 07/07/2012). Lactate dehydrogenase isoform A (LDH-A) is another glycolytic enzyme that is overexpressed in tumor cells. It catalyzes the conversion of pyruvate to lactate. Tumor cell-specific LDH-A upregulation suggests that LDH-A may be a potential target to suppress aerobic glycolysis (Granchi *et al.*, 2011). Inhibitors for almost all the enzymes

involved in the glycolytic process have been reported (Scatena *et al.*, 2008). However, a clinically useful aerobic glycolysis inhibitor is yet to be discovered. Inhibitors of parasitic glycolysis have been evaluated for their therapeutic (anti-infetive) potential (Coley *et al.*, 2011; Rosenthal, 2003; Sharlow *et al.*, 2010), but drug discovery efforts to identify inhibitors of aerobic glycolysis have been limited. Only one study that describe glycolysis inhibitor screening using a cell-based assay has recently been published (Kitagawa *et al.*, 2011).

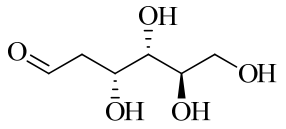

2-deoxy-D-glucose (**2**)

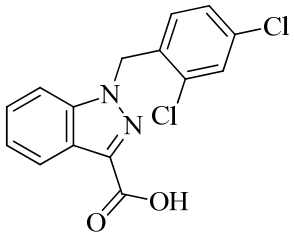

Lonidamine (**3**)

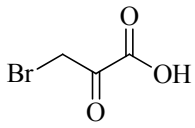

3-bromopyruvate (**5**)

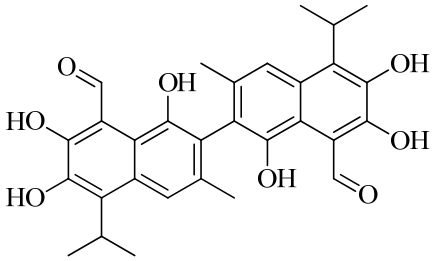

Gossypol (**6**)

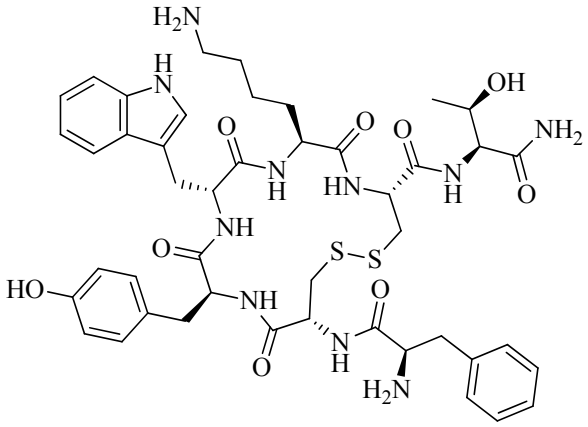

CAP-232/TLN-232 (**7**)

Figure 3.1B Small-molecule glycolysis inhibitors.

3.1.4 Benzophenones as bioactive natural products

Small-molecule natural products have been the single most successful source for antitumor drug discovery (Newman and Cragg, 2012). Apart from the clinically successful natural product-derived drugs, natural product-derived small-molecules that exhibit interesting bioactivities are widely used as both pharmacological and molecular probes. Benzophenones are a class of compounds that have demonstrated a broad spectrum of bioactivities (Acuna *et al.*, 2009). Approximately 150 known benzophenones from 13 different families have been isolated. More than 50% of these compounds are found in members of the *Clusia*, *Garcinia* and *Hypericum* genera from the family Clusiaceae. The core of a benzophenone type molecule is composed of a 13-carbon skeleton (Figure 3.2) which is later modified with substituent additions and subsequent cyclizations. Benzophenones are thought to be biosynthetically derived from the shikimate and mevalonate pathways. Benzophenones can be broadly classified into two categories: a) basic benzophenones and b) polyprenylated benzophenone derivatives (PBDs).

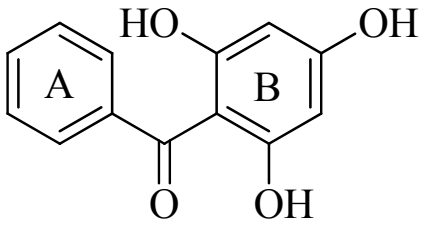

Figure 3.2 Core structure of benzophenones.

Prenylation of benzophenones occurs mainly on the B ring, and the prenyl units often undergo cyclization leading to bi-, tri- and tetracyclic molecules. Only four compounds have been reported with prenylation on the A ring (cudraphenones A–D, **8**–**11**) (Baggett *et al.*, 2005).

Cytotoxic, antimicrobial, antiviral and antioxidant activities have been attributed to benzophenones (Cuesta-Rubio *et al.*, 2005). Guttiferones A–F (**12**–**17**) prevented the cytopathic

effects of HIV infection in human T-lymphoblastoid CEM-SS cells in vitro (EC_{50} 1–23 μg/ mL), but were also toxic to the host cells (IC_{50} 50–82 μg/ mL) (Gustafson *et al.*, 1992; Fuller *et al.*, 1999a). Other known anti-HIV benzophenones include laxifloranone (**18**) (Bokesch *et al.*, 1999), vismiaphenone D (**19**) (Fuller *et al.*, 1999b), and garciosaphenone A (**20**) (Rukachaisirikul *et al.*, 2003).

Numerous benzophenones have shown broad spectrum antibacterial, antifungal and antiprotozoal activities. Some prominent antibacterial benzophenones include: 7-epiclusianone (**21**), garcinol (**22**), guttiferone I (**23**), isogarcinol (**24**), microsphaerins A-D (**25–28**), nemorosone (**29**), isoxanthochymol (**30**) and xanthochymol (**31**). Among these, isoxanthochymol (**30)**, isogarcinol (**24**), xanthochymol (**31**), microsphaerins A-D (**25–28**) and garcinol (**22**) are active against MRSA. Antiplasmodial activity was observed with coccinones A-E (**32**–**36**), 7-epigarcinol (**37**), 7-epiisogarcinol (**38**), garcinol (**22**), isogarcinol (**24**), while 3-geranyl-2, 4, 6-trihydroxybenzophenone (**39**), and pestalachlorides A–C (**40–42**) demonstrateded antifungal activity. Trypanosidal and leishmanicidal activities were also reported for a number of benzophenone compounds (Acuna *et al.*, 2009).

In addition to the antiviral and antimicrobial activities, guttiferones A (**12**), E (**16**), G, (**43**), H (**44**), I (**23**), J (**45**), K (**46**), L (**47**), curdaphenones A–D (**8–11**), garcinol (**22**), isogarcinol (**24**), hyperibone K (**48**) and L (**49**), xanthochymol (**31**), isoxanthochymol (**30)** and nemorosone (**29**) showed broad spectrum cytotoxic effects against numerous cell lines derived from colon, breast, ovarian, oral, cervical, lung, prostate and hepatocellular carcinomas (Acuna *et al.*, 2009). These PBDs have been shown to (a) induce cell cycle arrest and apoptosis; (b) bind and inhibit tubulin disassembly during cell division; (c) activate caspase-3; and (d) inhibit enzymatic activity of histone acetyl transferase, proteases and kinases (Acuna *et al.*, 2009). However, this type of

broad spectrum inhibition may be indicative of nonspecific suppression of cell viability or the targeting of a central pathway that affects many cellular reactions.

The keto-enol equilibria within PBD structures are essential for their bioactivity, and the compounds devoid of this functional group are drastically less active. Guttiferones A-F (**12**–**17**) have been shown to be active in HIV-inhibitory assay in vitro. However, isoxanthochymol (**30**), a cyclized derivative of guttiferone E (**16**), which was missing the enol functionality, was inactive (Gustafson *et al.*, 1992).

A recent study showed that nemorosone (**29**), a strong antiplasmodial and cytotoxic benzophenone, potently uncoupled mitochondria and depleted intracellular ATP levels in HepG2 cells. The keto-enol tautomerism had been shown to be responsible for the protonophoric activity of nemorosone (**29**) (Pardo-Andreu *et al.*, 2011). Uncoupling of oxidative phosphorylation owing to the enolic functionality present in the benzophenone compounds can explain the broad spectrum of the antimicrobial and cytotoxic activity of this class of compounds.

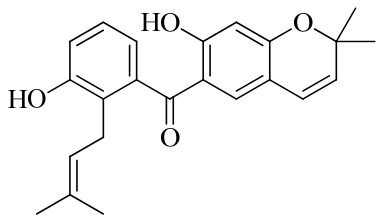

Cudraphenone A (**8**)

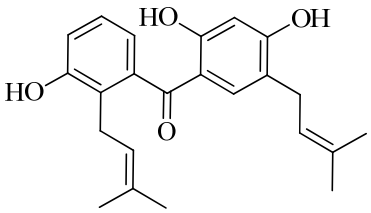

Cudraphenone B (**9**)

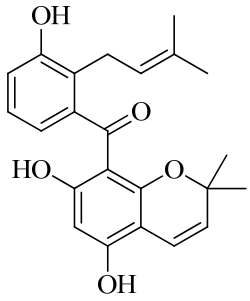

Cudraphenone C (**10**)

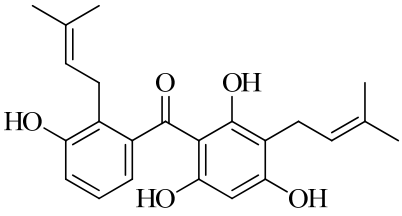

Cudraphenone D (**11**)

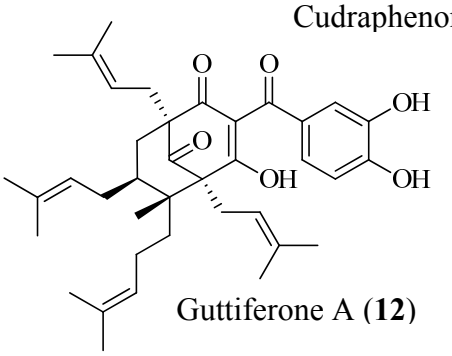

Guttiferone A (**12**)

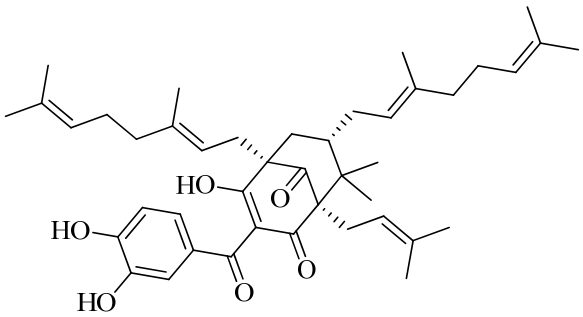

Guttiferone B (**13**)

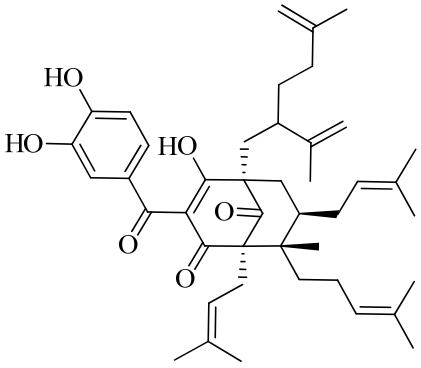

Guttiferone C (**14**)

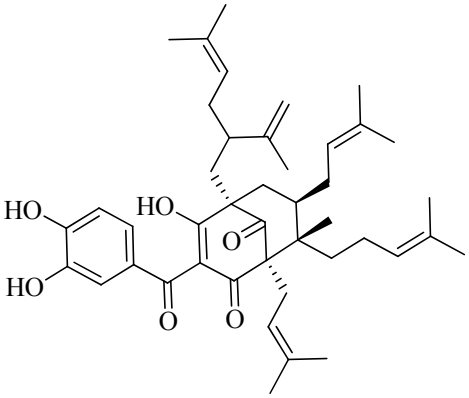

Guttiferone D (**15**)

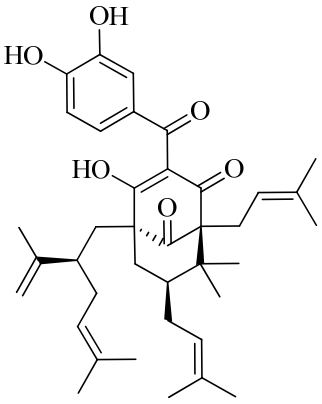

Guttiferone E (**16**)

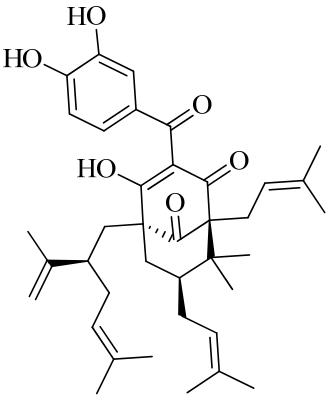

Guttiferone F (**17**)

Figure 3.3 Bioactive polyprenylated benzophenone derivatives (PBDs).

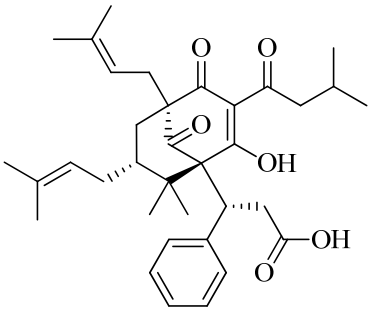

Laxifloranone (**18**)

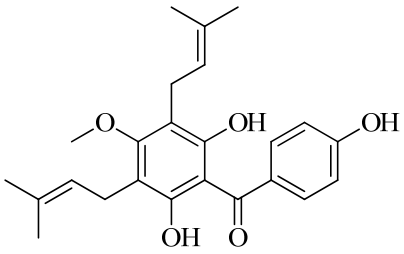

Vismiaphenone D (**19**)

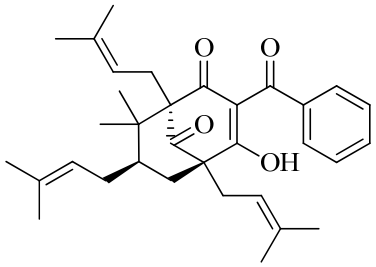

7-epiclusianone (**21**)

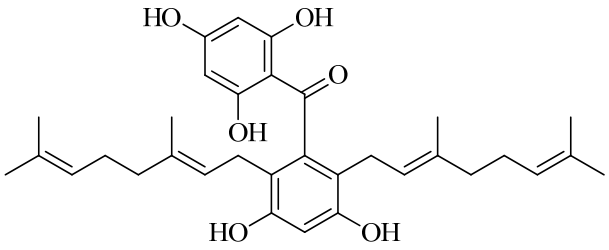

Garciosaphenone A (**20**)

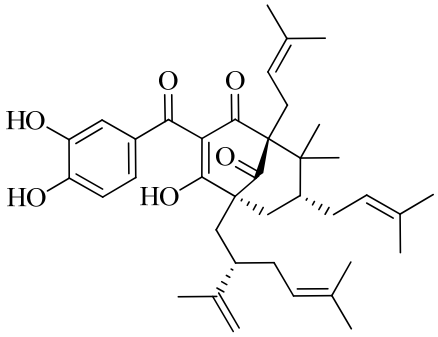

Garcinol (**22**)

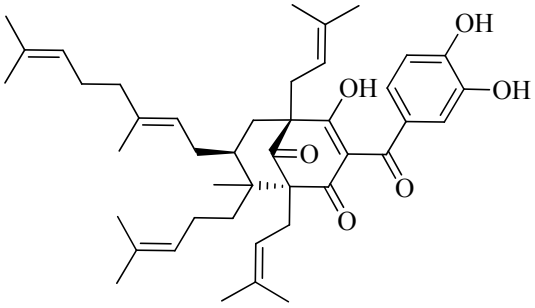

Guttiferone I (**23**)

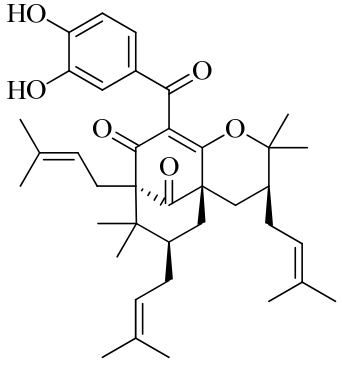

Isogarcinol (**24**)

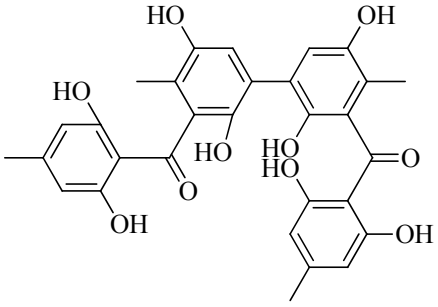

Microsphaerin A (**25**)

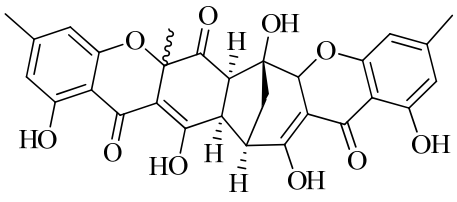

Microsphaerin B (**26**)
Microsphaerin C (**27**)

Figure 3.4 Bioactive polyprenylated benzophenone derivatives (PBDs).

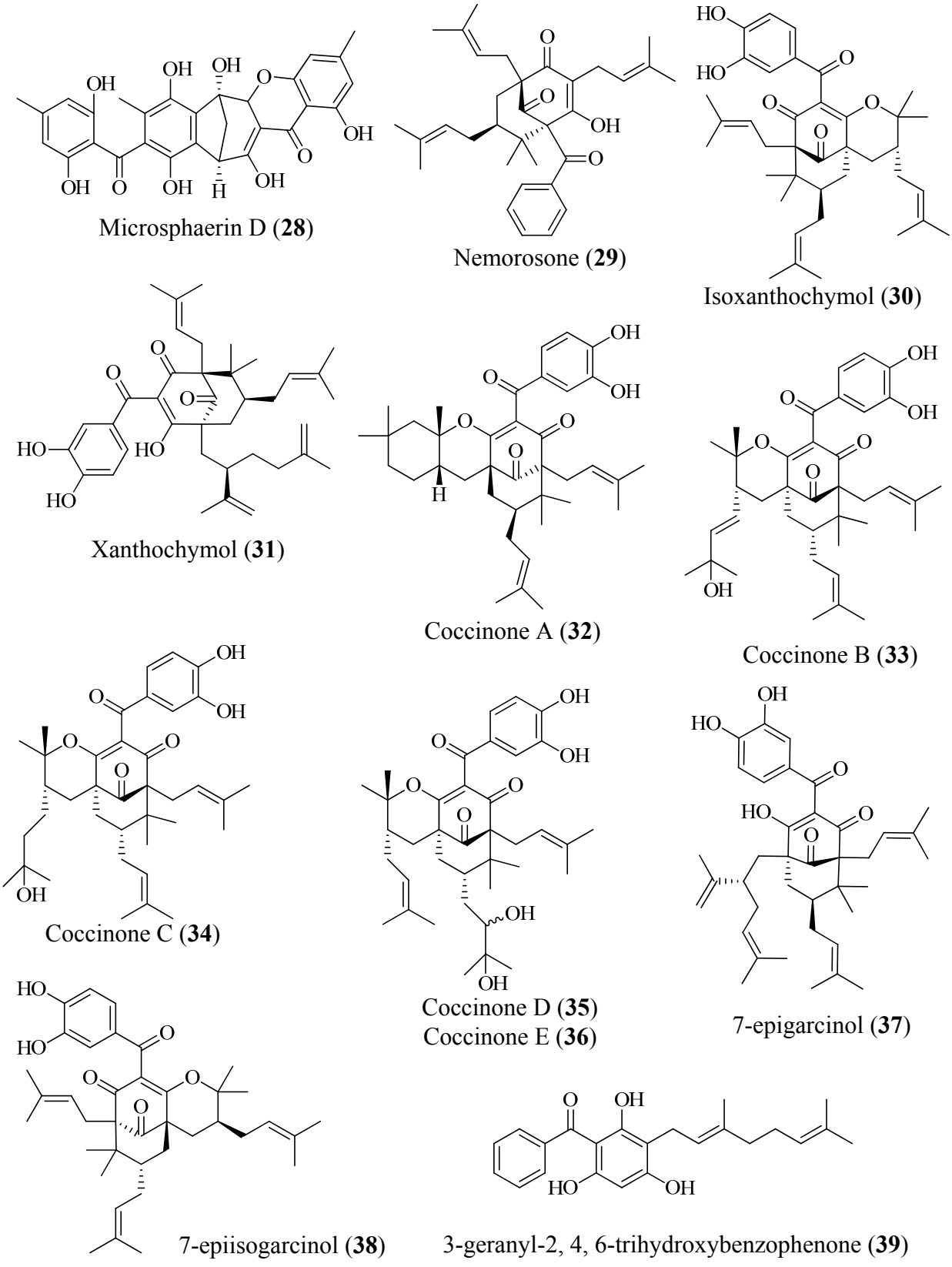

Figure 3.5 Bioactive polyprenylated benzophenone derivatives (PBDs).

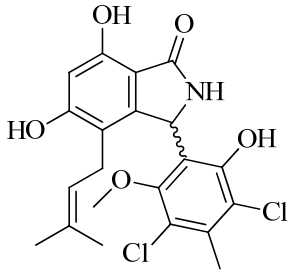

Pestalachloride A (**40**)

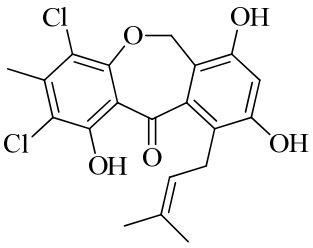

Pestalachloride B (**41**)

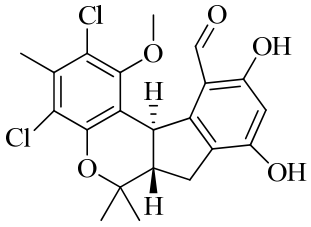

Pestalachloride (**42**)

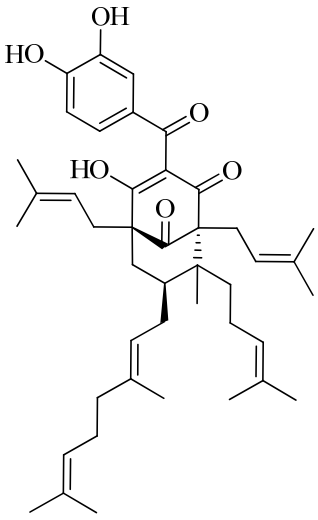

Guttiferone G (**43**)

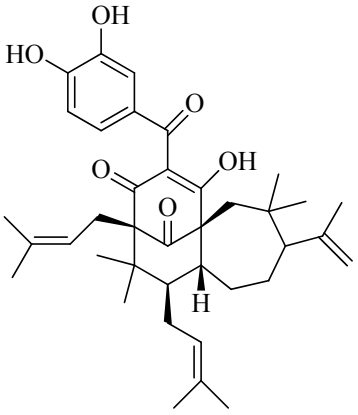

Guttiferone H (**44**)

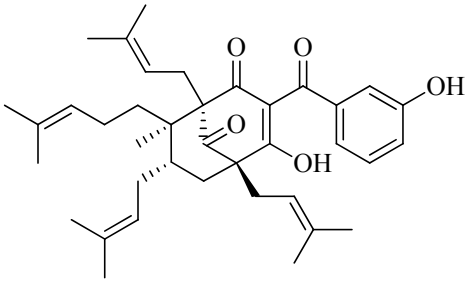

Guttiferone J (**45**)

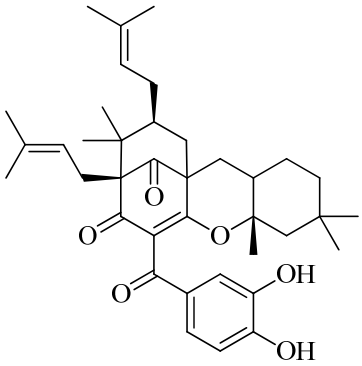

Guttiferone K (**46**)

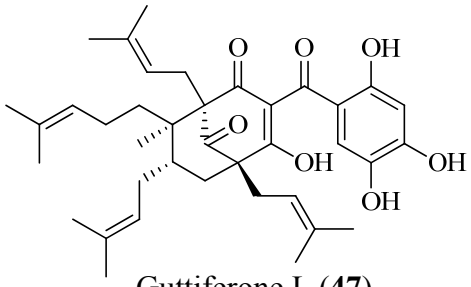

Guttiferone L (**47**)

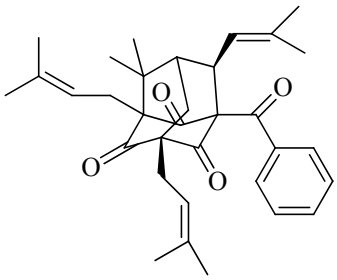

Hyperibone K (**48**)

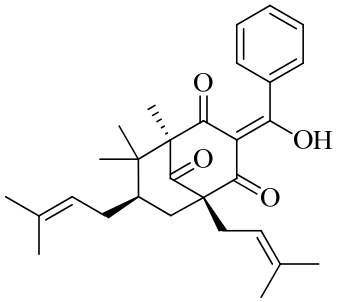

Hyperibone L (**49**)

Figure 3.6 Bioactive polyprenylated benzophenone derivatives (PBDs).

3.2 Materials and methods

3.2.1 General experimental procedures

A Varian 50 Bio spectrophotometer was used to record UV spectrum and IR spectrum was obtained by a Bruker Tensor 27 Genesis Series FTIR. Bruker AMX-NMR spectrophotometers operating at 400 MHz for ^{1}H and 100 MHz for ^{13}C were used to record the NMR spectra. Moronone (**1**) was dissolved in pyridine-d_5 (Sigma) to record the NMR spectra, and solvent resonances were used as internal references [8.74 (s) for ^{1}H and 150.35 (t) for ^{13}C]. A Bruker Daltonic micro TOF fitted with an Agilent 1100 series HPLC and an electrospray ionization source was used to obtain the HRESIMS. Merck $Si_{60}F_{254}$ or $Si_{60}RP_{18}F_{254}$ (Sorbent Technologies) were used to obtain TLC. Ethanolic sulfuric acid (10% H_2SO_4 in EtOH) was used as visualizing agent. The TLC plates were first observed under UV at 254 nm, and sprayed with the visualizing agent, followed by heating. HPLC was performed on a Waters system equipped with a 600 controller and a 2998 photodiode array detector. Semi-preparative HPLC column (Phenomenex Luna RP-18, 5 μm, 250 × 10.00 mm) was employed for isolation. Solvents and formic acid for HPLC were purchased from Fisher unless specified otherwise. The purity of the compound was judged on the percentage of the integrated signal at UV 220 nm. The compound submitted for bioassay was at least 95% pure as judged by this method.

3.2.2. Plant material

Moronobea coccinea Aubl. (Clusiaceae) stem woods were collected from British Guyana (October 21, 1991) and identified by Dr. S. Tiwari (New York Botanical Gardens, Bronx, NY). A voucher specimen was deposited at the Smithsonian Institution National Museum of Natural History, Washington, DC, and a collection number 0CKF0401 was assigned to the sample.

3.2.3 Extraction and isolation

The plant material was extracted with CH_2Cl_2-MeOH (1:1). The extract was vacuum-dried and stored at -20 °C in the NCI repository at the Frederick Cancer Research and Development Center (Frederick, Maryland). An NCI Open Repository Sample number, N063783, was assigned to the extract. The extract (3.0 g) showed enhanced suppression of cell viability in a MDA-MB-231 cell-based viability assay under a glycolysis-dependent condition compared to regular culture conditions. The extract was eluted through Sephadex LH-20 to prepare preliminary fractions. Seven fractions were obtained using step gradients of CH_2Cl_2-MeOH (1:1), CH_2Cl_2-MeOH (1:2), and MeOH. The second fraction (373.1 mg), eluted with CH_2Cl_2-MeOH (1:1) at 1 column volume, was active in the glycolysis inhibitor screening assay. The active fraction was subjected to Si gel column chromatography using step gradients of hexanes-EtOAc (6:1, 4:1, 2:1, 1:1, 0:1). The column was washed with MeOH. Eight sub-fractions were obtained; the second fraction (112.2 mg), eluted with hexanes-EtOAc (6:1), being active in the glycolysis inhibitor screening assay. TLC of the active fraction showed a UV-active yellow char, indicating that it might be similar to the PBDs previously isolated from this plant (Marti *et al.*, 2011). The active fraction was dissolved in MeOH and centrifuged. Subsequently, the supernatant was filtered and subjected to semi-preparative isolation (Phenomenex Luna RP-18, 5 μm, 250 × 10 mm) using acetonitrile : formic acid (0.1%) [87:13]. This reversed-phase separation produced the pure compound moronone (83.5 mg, 2.78% yield). The purity of the compound was determined by the percentage of the integrated signal at UV 220 nm and the compound was at least 95% pure as judged by this method.

3.2.4 Moronone (1)

Dark brown oil; optically inactive; UV (MeOH) λ_{max} (log ε) 237 (4.29), 281 (4.04), 351 (4.39) nm; IR (NaCl block) ν_{max} 3510, 2968, 2918, 1642, 1566, 1504, 1446, 1384, 1316, 1220, 1105, 1066 cm^{-1}; ^{1}H NMR and ^{13}C NMR data, see Table 1; HRESIMS *m*/*z* 525.2997 $[M+Na]^{+}$ (calcd. for $C_{33}H_{42}O_4Na$, 525.2981).

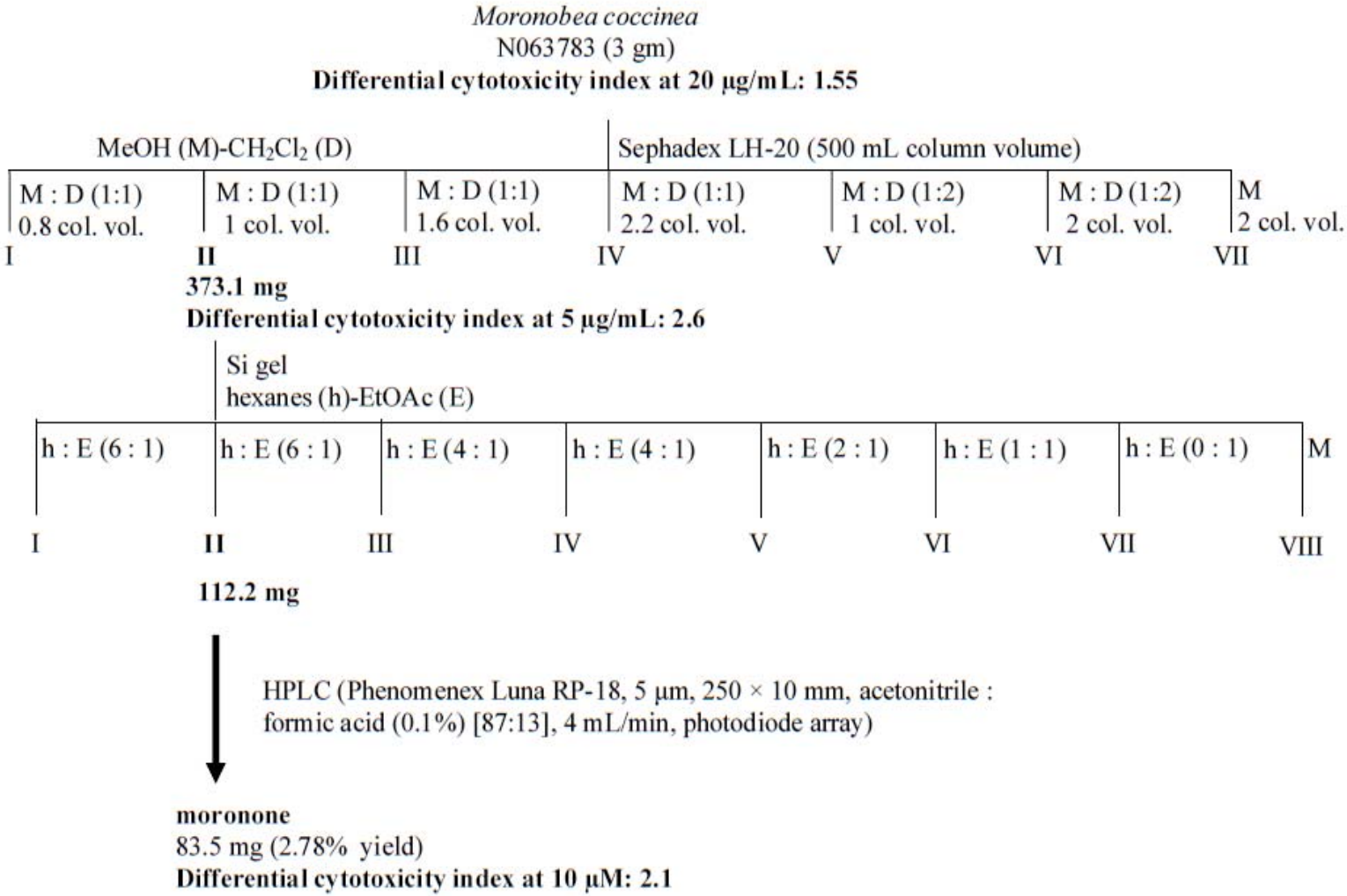

Figure 3.7 Isolation scheme for moronone (**1**).

3.2.5 Tumor cell culture

Human breast tumor T47D and MDA-MB-231 cells were purchased from American type culture collection (ATCC). These cells were maintained in the Roswell Park Memorial Insitute 1640 medium containing 2 mM L-glutamine (Mediatech). The medium was supplemented with fetal bovine serum [FBS, 10% v/v final concentration, Hyclone] and a mixture of penicillin (50 units/mL final concentration) and streptomycin (50 µg/mL final concentration) (pen/strep) (Lonza).

3.2.6 Glycolysis inhibitor screening assay

MDA-MB-231 cells were plated at 3 x 10^4 cells per well into 96-well plates in a volume of 100 µL RPMI 1640 medium supplemented with FBS and penicillin/streptomycin (pen/strep) as described in the previous section. After 24 h, extracts or test compounds were diluted with the serum free RPMI 1640 medium with pen/strep (2x final concentration) and added in a volume of 100 µL per well. The final concentration of each extract was 20 µg/mL. The cells were treated with extracts in the presence or absence of rotenone (0.1 µM) and incubated at 37 °C under normoxic conditions (95% air, 5% CO_2) for 48 h. At the end of the specified incubation period, cell viability was measured using the sulforhodamine B method (Skehan *et al.*, 1990). The cell viability was measured for each extract Extracts with a differential cytotoxicity index of ≥ 1.5 that exerted ≥ 45% cytotoxicity in the presence of rotenone (0.1 µM), were considered 'active'. The differential cytotoxicity index was calculated using the following formula:

$$\text{Differential cytotoxicity index} = \frac{\text{cytotoxicity in the presence of rotenone (0.1 µM)}}{\text{cytotoxicity in the absence of rotenone}}$$

The Z-factor for each plate was calculated by the following formula:

$$\text{Z-factor} = 1 - \frac{3 \times \text{standard deviation [2-DG or (2-DG + rotenone)]} - 3 \times \text{standard deviation media}}{\text{Mean [2-DG or (2-DG + rotenone)]} - \text{Mean media control}}$$

3.2.7 Cell viability assay by the sulforhodamine B method

MDA-MB-231 cells were plated at 3 x 10^4 cells per well into 96-well plates in a volume of 100 µL of RPMI1640 medium supplemented with FBS (10% v/v final concentration) and pen/strep. After 24 h, each test compound was diluted with the serum free DMEM/F12 medium with pen/strep (2x final concentration) and added in a volume of 100 µL per well, and the incubation continued for another 2 days or 6 days at 37 °C (95% air, 5% CO_2). For the 6-day exposure study, the conditioned media were replaced after 3 days with fresh culture media that contained test compounds. Following a 2- or 6-day incubation period, the cells were fixed by replacing 100 µL of conditioned medium with 100 µL trichloroacetic acid solution (20% w/v in 1x PBS, pH 7.4) per well. Following incubation at 4 °C for 1 h, the supernatant was removed, and the cells were washed with tap water (4x) and air dried. A sulforhodamine B solution (0.4% w/v, in 1% actetic acid) was added in a volume of 100 µL per well and incubated at room temperature for 10 min. The stained cells were washed with 1% acetic acid (4x) and air dried. The dye was eluted by adding 200 µL of Trizma® base (10 mM) per well and incubating for 10 min at room temperature. The plates were gently shaken for 2–3 min, and absorbance was measured at 490 nm and background absorbance at 630 nm, on a BioTek Synergy plate reader. The ΔOD values were used for subsequent data analysis and were calculated by subtracting the background absorbance from the absorbance at 490 nm. The following formula was used to calculate the percentage inhibition data:

$$\% \text{ inhibition} = (1 - \Delta OD_{treated}/\Delta OD_{control}) \times 100$$

3.2.8 Cellular respiration assay

The effects of compound on MDA-MB-231 or T47D cellular oxygen consumption were measured by a Clarke-type electrode system (Oxytherm, Hansatech). To determine the effect of **1** on cellular respiration, 5×10^6 T47D or MDA-MB-231 cells were added to the chamber of an Oxytherm Clark-type electrode system (Hansatech), containing 1 mL of DMEM/F-12 medium (JRH) (equilibrated to 37 °C) free of serum and antibiotics. Glucose (17.5 mM) in the DMEM/F-12 medium served as the major metabolic substrate. Once the base-line respiration had been established (for a 12 min interval), **1** dissolved in DMSO was injected into the chamber 1–2 min after the establishment of steady-state respiration, using a 10-μL syringe (Hamilton). The data were presented as "Respiration rate relative to untreated control" and was calculated using the following formula:

$$\text{Respiration rate relative to untreated control} = 100 \times \frac{\text{oxygen consumption rate}_{\text{compound}}}{\text{oxygen consumption rate}_{\text{control}}}$$

The mitochondrial uncoupler FCCP (Sigma) was used as a positive control. For mechanistic studies, state 4 respiration was initiated by the addition of oligomycin (1 μM, Sigma). Following subsequent addition of either FCCP or **1**, the effects of each compound on state 4 respiration were determined by monitoring the rates of cellular oxygen consumption.

3.2.9 Mitochondrial membrane potential assay

MDA-MB-231 and T47D cells were plated into four-well Lab-Tek II coverglass chambers (Nunc) at a density of 1×10^5 cells per well and incubated at 37 °C. Following overnight incubation, the conditioned media were replaced with a buffer which contained TES (20 mM), pH 7.3, NaCl (150 mM), KCl (5 mM), $CaCl_2$ (1.3 mM), $MgCl_2$ (1.3 mM), glucose (5

mM), Na_2SO_4 (1.2 mM), KH_2PO_4 (0.4 mM), BSA (0.3% w/v), and tetramethylrhodamine methylester ($TMRM^+$) (2 nM). The cells were incubated with the membrane potential-dependent dye $TMRM^+$ [Molecular Probe] at 37 °C for 2 h, for equilibration of the dye across the membrane. At the end of incubation, test compounds were added, and incubation continued for another 30 min. Live cell imaging was performed with an Axiovert 200M epifluorescence microscope (Zeiss).

3.2.10 Glucose uptake and lactate secretion assays

MDA-MB-231 cells were plated at 3 x 10^4 cells per well into 96-well plates in a volume of 100 µL RPMI 1640 medium supplemented with FBS and pen/strep as described in the previous section. After 24 h, test compounds were diluted with serum free RPMI 1640 medium with pen/strep (2x final concentration) and added in a volume of 100 µL per well. The cells were incubated at 37 °C under normoxic conditions (95% air 5% CO_2) for 24, 48 or 72 h. The levels of glucose and lactate in the conditioned media samples were measured spectrophotometrically using enzymatic assays. To determine glucose level in the conditioned media samples, 6 µL of the conditioned media were added to 194 µL of reaction buffer that contained triethanolamine (100 mM, pH 7.3), $MgCl_2$ (7 mM), ATP (2 mM), nicotinamide adenine dinucleotide phosphate ($NADP^+$, 2 mM), hexokinase (1 unit/mL) and glucose-6-phosphate dehydrogenase (1 unit/mL). After an 8 min incubation at the room temperature, the absorbance was measured at 340 nm on a BioTek Synergy plate reader. Distilled deionized (dd) water and the glucose free RPMI 1640 medium were used as the blanks. The average reading from the media wells (used as the blank reading) was subtracted from the sample readings. The average reading from the water wells (used as the blank reading) was subtracted from the standard wells. A glucose stock solution of

30 mM in dd water was diluted with dd water to achieve the final concentration of 1.25, 2.5, 5, 6, 10, 15, 20 and 30 mM. This set of glucose standards was used to generate the standard curve. Glucose concentrations of the conditioned media samples were determined from the standard curve.

To determine lactate concentration in the conditioned media, 8 μL of conditioned media was added to 192 μL of reaction buffer composed of glycylglycine (100 mM, pH 8.0), glutamate (100 mM), nicotinamide adenine dinucleotide (NAD^+, 1mM), lactate dehydrogenase (LDH, 1 unit/mL), and glutamate/pyruvate transaminase (1 unit/mL). After 1 h incubation at room temperature, fluorescence was measured at an excitation wavelength of 340 nm and an emission wavelength of 460 nm, on a BioTek Synergy plate reader. Distilled deionized water and the RPMI 1640 medium supplemented with FBS and pen/strep were used as the blanks. The average reading from the media wells (used as the blank reading) was subtracted from the sample readings. The average reading from the water wells (used as the blank reading) was subtracted from the standard wells. A lactate stock solution of 20 mM in dd water was diluted with dd water to achieve the final concentration of 2.5, 5, 7.5, 10, 12.5, 15, 17.5, 20 mM. This set of lactate standards was used to generate the standard curve. Lactate concentrations in the conditioned media samples were determined from the standard curve. Enzymes, NAD^+ and $NADP^+$ were purchased from Calzyme, and other reagentss were purchased from Sigma. The test compounds may produce cytotoxic effects and affect the net glucose uptake or lactate production. Hence the net glucose uptake or lactate production was normalized to protein concentrations. Following extraction of the cellular proteins with M-PER (Pierce), in presence of protease inhibitor cocktail (Sigma; 1:10 dilution), the protein concentrations were determined using a Micro BCA assay kit (Pierce, manufacturer's instructions).

3.2.11 Statistical analysis

The cytotoxicity data for FCCP and **1** were analyzed using two-way ANOVA, followed by Bonferroni post hoc analyses (GraphPad Prism 5). The glucose and lactate concentration data was analyzed using one-way ANOVA, followed by Dunnett's post hoc analysis for each time point. Differences between the data sets were considered significant when $p < 0.05$.

3.3 Results and discussion

3.3.1 Development of the bioenergetics-based screening system for the identification of glycolysis inhibitors

For the identification of the inhibitors of aerobic glycolysis, MDA-MB-231, a well characterized triple negative human breast cancer cell line was used as the in vitro experimental model. This cell line was selected for its glycolytic, aggressive, and hormone refractory phenotype that resembles tumor tissues in advanced state of malignancy (Robey *et al.*, 2008). At the concentration of 0.1 μM rotenone exerts maximal mitochondrial complex I inhibition (Liu *et al.*, 2009) but exhibits only marginal cell proliferation/viability suppression in MDA-MB-231 cells. In breast and colon tumor cells, the simultaneous inhibition of glycolysis and OxPhos displays enhanced cytotoxicity than either of them alone (Cheng *et al.*, 2012; Fath *et al.*, 2009). Hence, it was hypothesized that the potential glycolysis inhibitors can be identified by enhanced suppression of MDA-MB-231 cell viability in the presence of OxPhos inhibitors. Rotenone (**50**, Figure 3.8A) and 2-deoxy-D-glucose (2-DG, **2**) were selected as prototypical OxPhos and glycolysis inhibitors, respectively. We evaluated the concentration-dependent effects of 2-DG (1 to 30 mM, in half log increments) and rotenone (0.001 to 0.1 μM, in half-log increments) on MDA-MB-231 cell viability. Cell viability was measured by the sulforhodamine B method after

48 h of compound treatment at 37 °C (Skehan *et al.*, 1990). Combinations of rotenone and 2-DG at different concentrations were also evaluated. Rotenone enhanced the cytotoxic effects of 2-DG at lower concentrations (1 and 3 mM). A the concentrations of 10 and 30 mM, 2-DG was cytotoxic and rotenone did not further enhance the cytotoxicity of 2-DG (Figure 3.8B).

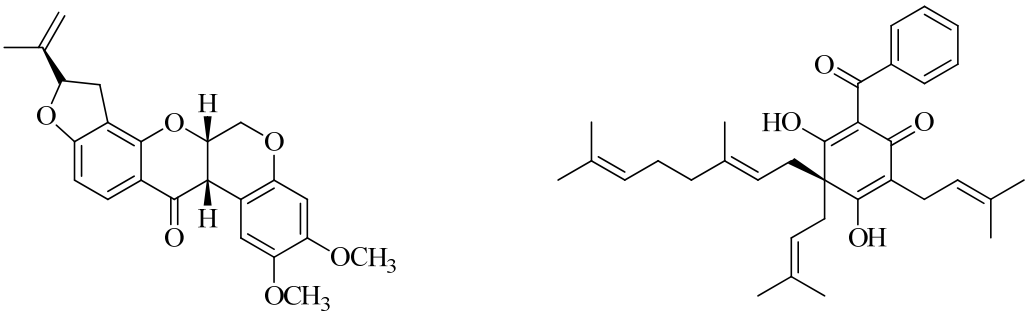

Rotenone (**50**) Kolanone (**51**)

Figure 3.8A Structure of rotenone (**50**) and kolanone (**51**)

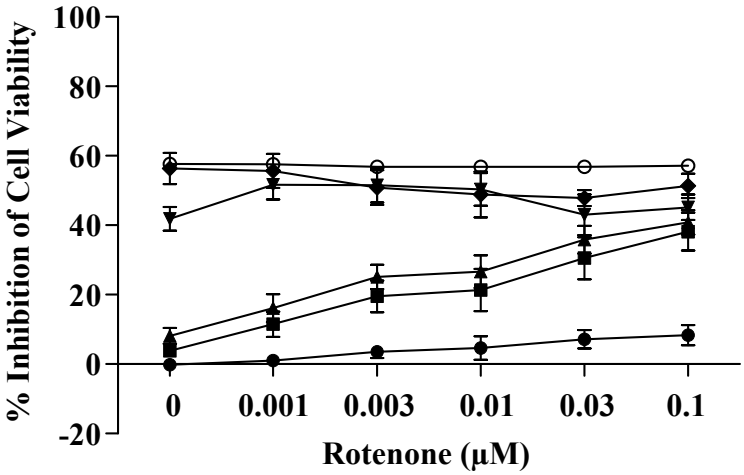

Figure 3.8B Effects of rotenone and 2-DG combinations on MDA-MB-231 cell viability. MDA-MB-231 cells were treated with 2-DG [(■) 1 mM, (▲) 3 mM, (▼) 10 mM, (◆) 30 mM], and cycloheximide [(○) 100 µM], in the presence or absence of rotenone [(●) 0.0, 0.001, 0.003, 0.01, 0.03, and 0.1 µM] for 48 h under normoxia (37 °C, 95% air, 5% CO_2). Cell viability was measured by the sulforhodamine B method. Data shown are average ± standard deviation from three independent experiments performed in duplicate.

Concentration of MDA-MB-231 cells with rotenone (0.1 μM) and 2-DG (3 mM) exerted a ~2.5-fold increase in cytotoxicity, in comparison to the additive effects of rotenone and 2-DG (Figure 3.9A). The mitochondrial respiration inhibitor antimycin (1 μM) and an F_1F_0-ATPase inhibitor oligomycin (1 μM) were also evaluated in combination with 2-DG for their effects on the MDA_MB-231 cells. These agents produced results similar to those observed with rotenone (data not shown). To confirm that the cytotoxicity-enhancing effect of rotenone is specific to the glycolysis inhibitor 2-DG, we also evaluated a protein synthesis inhibitor, cycloheximide (100 μM). There was no additive or synergistic effects of rotenone on the suppression of MDA-MB-231 cell viability by cycloheximide (Figure 3.9A).

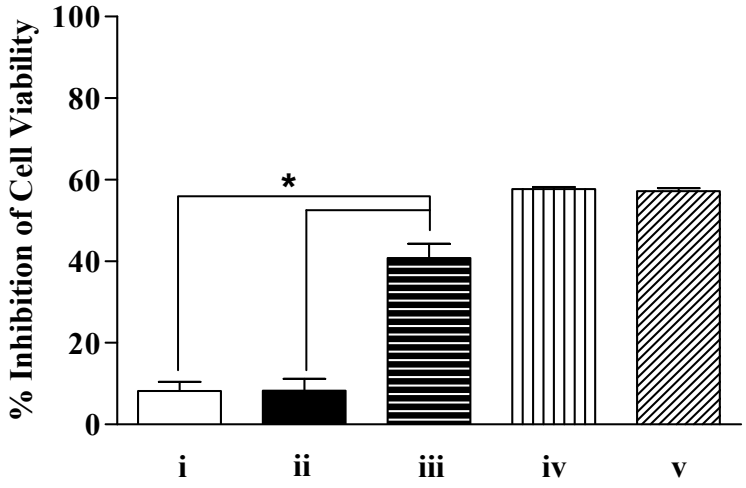

Figure 3.9A Effect of rotenone on 2-deoxy-D-glucose (2-DG) cytotoxicity. MDA-MB-231 cells were treated with 2-DG (3 mM) and cycloheximide (100 μM) in the presence (or absence) of rotenone (0.1 μM) and incubated for 48 h under normoxic conditions (37 °C, 95% air, 5% CO_2). Cell viability was measured by the sulforhodamine B method. Data shown are average + standard deviation from three independent experiments performed in duplicate ($n = 6$). [**i** (2-DG), **ii** (rotenone), **iii** (2-DG + rotenone), **iv** (cycloheximide), **v** (cycloheximide + rotenone)] The "*" denotes statistical significance ($p < 0.05$) when compared with cytotoxicity of either 2-DG or rotenone.

At the concentration of 0.1 μM, rotenone exerted maximal inhibition of complex I of the respiratory chain (with the minimal suppression of cell viability) and exhibited maximal

enhancement of the cytotoxicity of 2-DG (3 mM). This rotenone concentration was used to force the cells to survive under glycolysis-dependent conditions. The combination of a mitochondrial inhibitor and a glycolysis inhibitor was significantly more cytotoxic than either one alone. For this reason, we used the aforementioned system as the primary screening assay for the discovery of natural product-based inhibitors of glycolysis. We evaluated the NCI's Open Repository of higher plant and marine invertebrate extracts for aerobic glycolysis inhibitory activities. A total of 10,648 samples (121 plates, 88 samples/plate) were evaluated in this bioenergetics-based cytotoxicity assay, and cell viability was measured 48 h post sample treatment (20 μg/mL) in the presence (plate #1) or absence (plate #2) of rotenone (0.1 μM), using the sulforhodamine B method (Figure 3.9B). For plate #1, media and 2-DG (3 mM) in the presence of rotenone (0.1 μM) were used as the negative and positive control, respectively, while for plate #2, media and 2-DG (3 mM) were used as the negative and positive control, respectively. The controls were plated in triplicate (n = 3) in each plate. The 'Z-factor' was calculated for individual plates. While the mean Z-factor from 121 screened plates for media control relative to the 2-DG + rotenone combination was 0.856 (Figure 3.9C), the Z-factors for media control vs. 2-DG alone (plate #2) were highly variable. This variation may be due to the low cytotoxic effect of 2-DG (3 mM). The extracts (20 μg/mL) with a differential cytotoxicity index of ≥ 1.5 [cytotoxicity in the presence of rotenone (0.1 μM)/cytotoxicity in absence of rotenone (0.1 μM)], that showed ≥ 45% inhibition of cell viability in the presence of rotenone (0.1 μM), were selected for further evaluation (highly potent glycolysis inhibitors may not be selected in this assay system as they may completely block the glycolytic pathway, prevent the substrate availability to the mitochondria, and produce toxicity irrespective of the presence of rotenone). The 77 hits identified in the primary assay (0.72% hit rate) were prioritized according to their potency and

differential cytotoxicity index, and the top 23 extracts were subjected to reconfirmation. The active extracts (20 μg/mL) were reevaluated in triplicate using the primary assay system. Seven of the 23 extracts were active in the confirmatory assay.

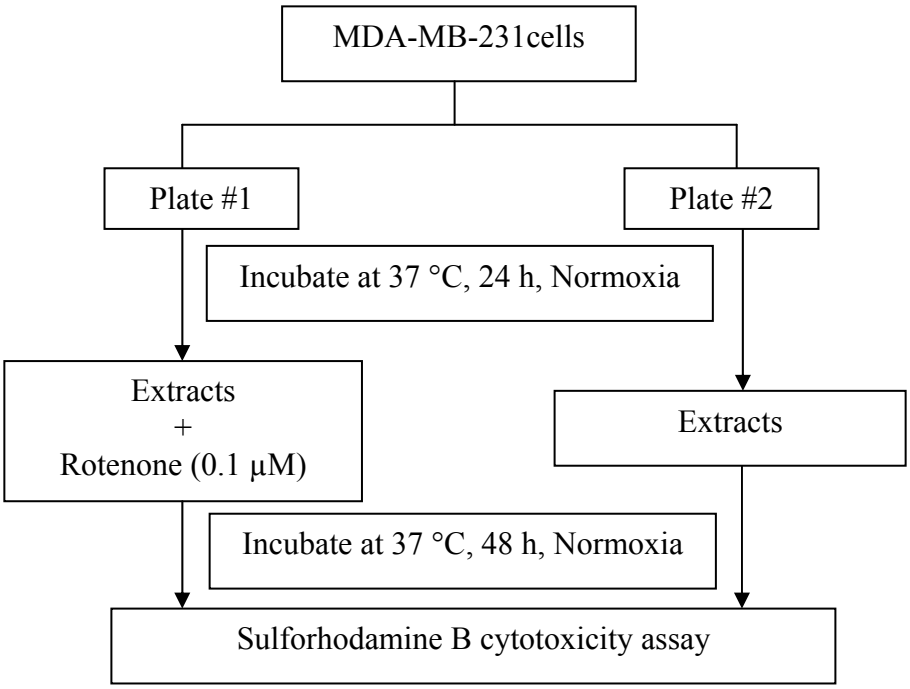

Figure 3.9B A schematic diagram of the assay system for the identification of glycolysis inhibitors.

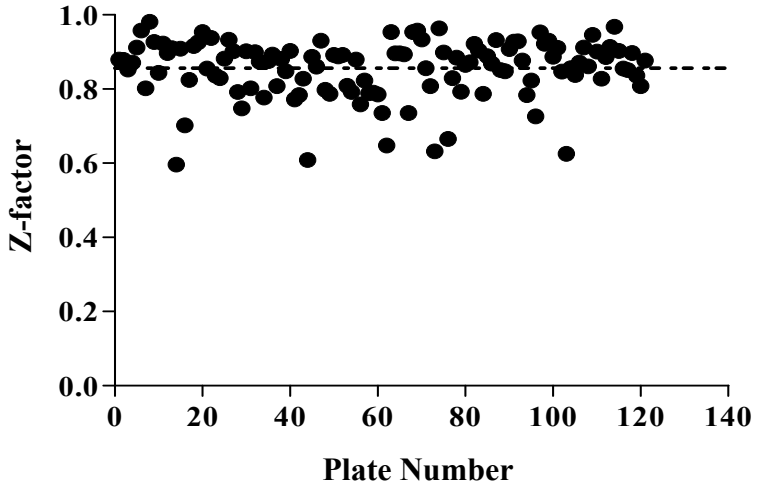

Figure 3.9C Frequency distribution of calculated Z-factors between media control and 2-DG (3 mM) + rotenone (0.1 μM). The dotted line indicates the average Z-factor (0.856) from all the plates screened.

3.3.2. Moronone (1) structural elucidation

Species identification of the active extracts and additional extract material for chemical studies were obtained from the NCI repository. Bioassay-guided isolation of a *Moronobea coccinea* plant extract resulted in the identification of a new, active compound that was named moronone (**1**) (Figure 3.10). The HREISMS data of **1** showed a pseudomolecular ion (*m/z*) at 525.2997 $[M + Na]^+$, suggesting a molecular formula of $C_{33}H_{42}O_4$. This formula indicated that the structure contained 13 hydrogen deficiency indices. The UV spectrum showed absorptions at 237, 281, and 351 nm indicating the presence of a conjugated benzophenone chromophore (1,3-dicarbonyl system) (Hussain *et al.*, 1982). The IR spectrum supported the presence of an α, β-conjugated carbonyl group (1642 cm^{-1}) and a hydroxy group (3510 cm^{-1}) in **1**. NMR spectra of **1** (Figure 3.11–3.12) contained resonances for a benzophenone group [δ_H 7.84 (2H, d, J = 7.2 Hz, H-9, 13), 7.46 (3H, overlapped, H-10, 11, 12); δ_C 198.0 (C-7), 142.0 (C-8), 132.1 (C-11), 130.0

(C-9, 13), 129.1 (C-10, 12)] and two geranyl moieties [δ_H 5.51 (2H, t, J = 7.2 Hz, H-2', 2"), 5.17 (2H, t, J = 6.4 Hz, H-6', 6"), 3.02 (4H, overlapped, H_2-1', 1"), 2.15 (4H, overlapped, H_2-5', 5"), 2.07 (4H, overlapped, H_2-4', 4"), 1.79 (6H, s, H_3-10',10"), 1.66 (6H, s, H_3-8',8"), 1.56 (6H, s, H_3-9', 9"); δ_C 139.5 (C-3', 3"), 132.6 (C-7', 7"), 125.9 (C-6', 6"), 120.8 (C-2', 2"), 41.4 (C-4', 4"), 39.3 (1', 1"), 28.2 (C-5', 5"), 27.0 (C-8', 8"), 19.0 (C-9', 9"), 17.9 (C-10', 10"], which were assigned on the basis of HSQC (Figure 3.13) and HMBC experiments (Figure 3.14). In addition, one carbonyl (δ_C 190.2), one quaternary carbon (δ_C 60.2) and four olefinic (δ_C 196.3, 109.9, 184.6, 100.4) resonances were observed in the ^{13}C NMR spectrum of **1**. According to the hydrogen deficiency indices, the structure was deduced to contain an additional ring. Accordingly, six additional carbons were attributed to an α, β-conjugated cyclohexenone moiety as proposed in Figure 3.10 (partial structure C_1–C_6). The NMR data of partial structure C_1–C_{13} was comparable to that of kolanone (**51**) (Hussain *et al.*, 1982) (Figure 3.8A), except that an additional proton singlet (δ_H 6.15) was present in the ^{1}H NMR spectra of **1**. The position of this singlet proton was located at C-6, as confirmed by the HMBC correlations between H-6 (δ_H 6.15) and C-1 (δ_C 190.2), C-5 (184.6), C-2 (109.5), C-4 (60.2). The connection of two geranyl groups to C-4 in the partial structure C_1–C_{13} was established on the basis of HMBC correlations between H-1' and C-3, C-4, C-5, C-1", and between H-1" and C-3, C-4, C-5, C-1'. The observation of NOESY correlation (Figure 3.16) between H-2'/2" (δ_H 5.51) and H-4'/4" (δ_H 2.07) suggested *E*-configurations of the $\Delta^{2',3'}$ and $\Delta^{2",3"}$ double bonds. Therefore, the structure of moronone was determined to be **1** (Figure 3.10).

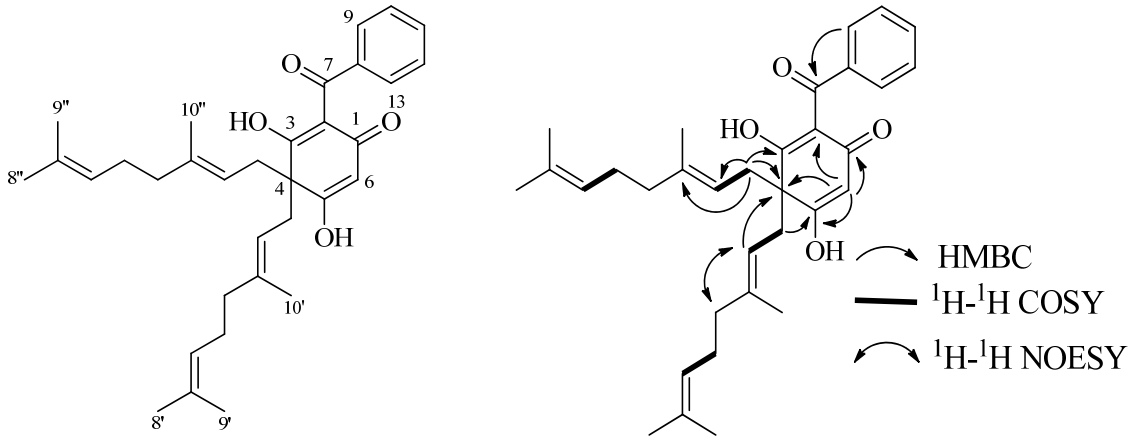

Moronone (**1**)

Figure 3.10 Structure and selected HMBC, ^{1}H-^{1}H COSY, and NOESY of moronone (**1**).

Position	δ_C, type	δ_H (J in Hz)	HMBC
1	190.2, C		
2	109.5, C		
3	196.3, C		
4	60.2, C		
5	184.6, C		
6	100.4, CH	6.15, s	1, 2, 4, 5
7	198.0, C		
8	142.0, C		
9	130.0, CH	7.84, d (7.2)	7, 8, 10, 11, 13
10	129.1, CH	7.47, overlapped	8, 9, 11, 12
11	132.1, CH	7.47, overlapped	9, 10, 12, 13
12	129.1, CH	7.47, overlapped	8, 10, 11, 13
13	130.0, CH	7.84, d (7.2)	7, 8, 9, 11, 12
1'	39.3, CH_2	3.02, overlapped	3, 4, 5, 2', 3', 1"
2'	120.8, CH	5.51, t (7.2)	4, 3', 4', 10'
3'	139.5, C		
4'	41.4, CH_2	2.07, overlapped	2', 3', 5', 6', 10'
5'	28.2, CH_2	2.15, overlapped	3', 4', 6', 7'
6'	125.9, CH	5.17, t (6.4)	4', 5', 8', 9'
7'	132.6, C		
8'	27.0, CH_3	1.66, s	6', 7', 9'
9'	19.0, CH_3	1.56, s	6', 7', 8'
10'	17.9, CH_3	1.79, s	2', 3', 4'
1"	39.3, CH_2	3.02, overlapped	3, 4, 5, 2", 3", 1'
2"	120.8, CH	5.51, t (7.2)	4, 3", 4", 10"
3"	139.5, C		
4"	41.4, CH_2	2.07, overlapped	2", 3", 5", 6", 10"
5"	28.2, CH_2	2.15, overlapped	3", 4", 6", 7"
6"	125.9, CH	5.17, t (6.4)	4", 5", 8", 9"
7"	132.6, C		
8"	27.0, CH_3	1.66, s	6", 7", 9"
9"	19.0, CH_3	1.56, s	6", 7", 8"
10"	17.9, CH_3	1.79, s	2", 3", 4"
OH		8.85, br s	

Table 3.1 NMR spectroscopic data for **1** at 400 MHz (^{1}H) and 100 MHz (^{13}C) in pyridine-d_5. Carbon (^{13}C) assignments were assigned from HSQC data.

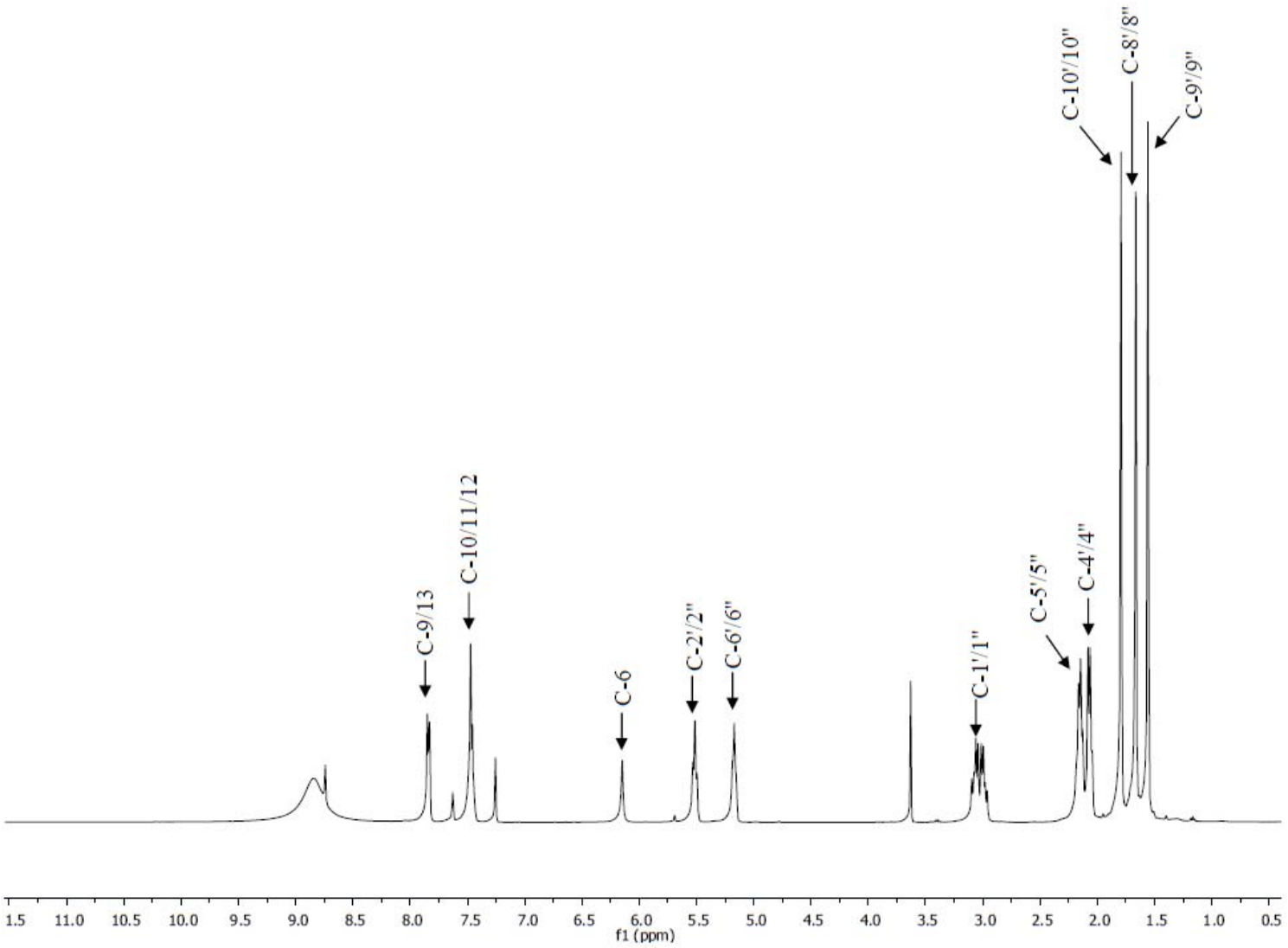

Figure 3.11 ^{1}H NMR spectrum of moronone (**1**) in pyridine-d_5. Corresponding carbons for the proton resonances are indicated.

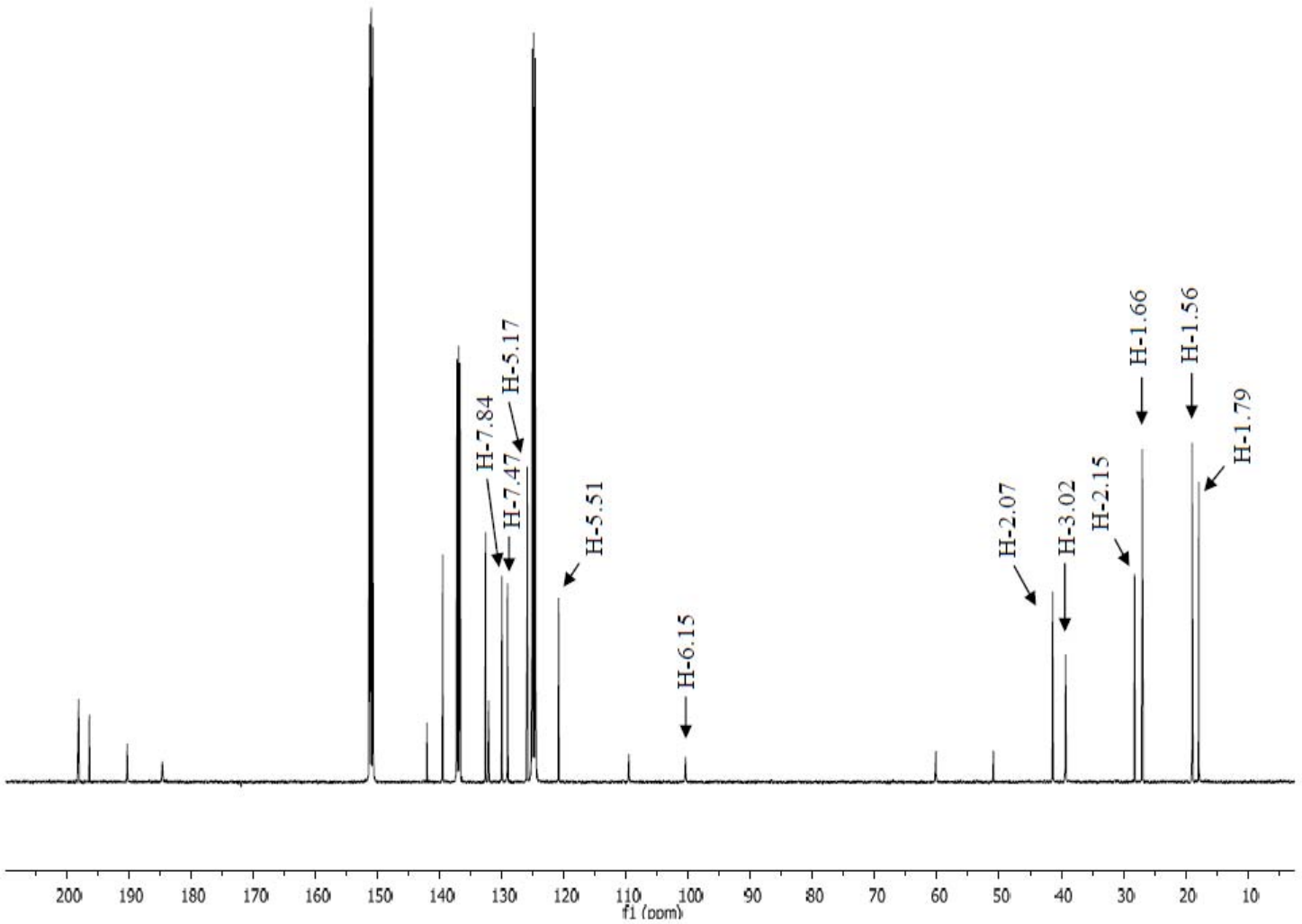

Figure 3.12 ^{13}C NMR spectrum of moronone (**1**) in pyridine-d_5. Corresponding protons for the carbon resonances are indicated.

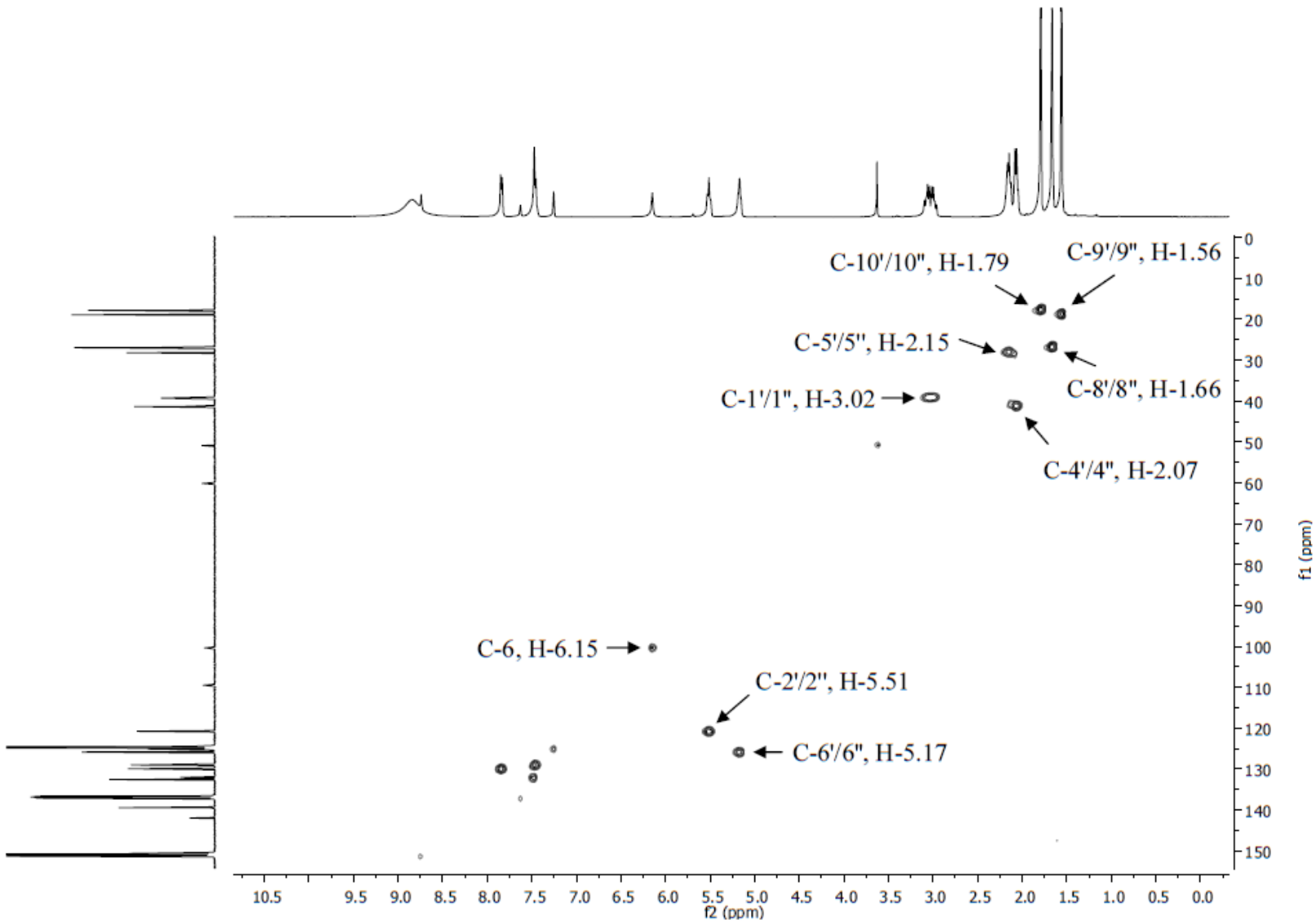

Figure 3.13 gHSQC spectrum of moronone (**1**) in pyridine-d_5.

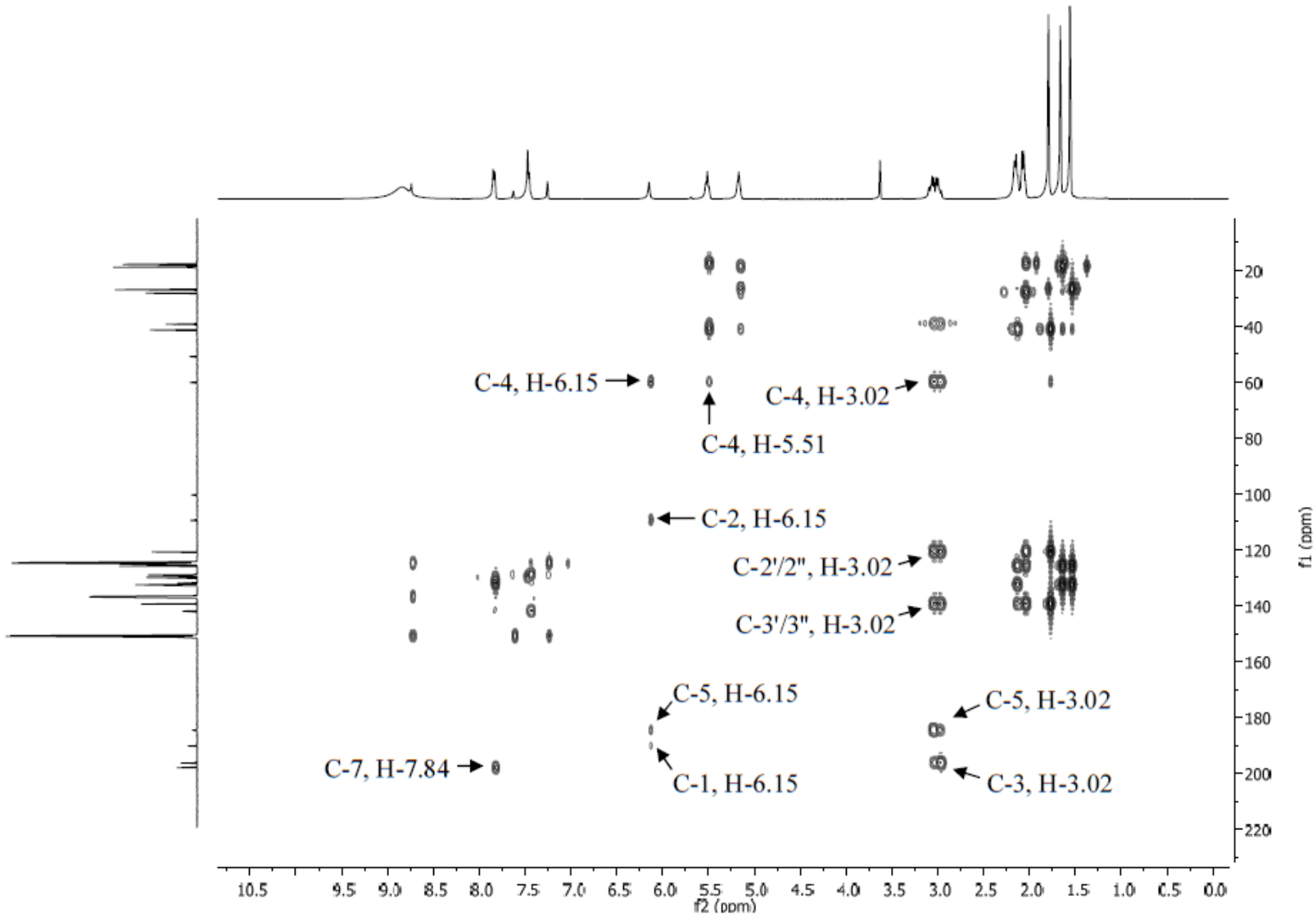

Figure 3.14 gHMBC spectrum of moronone (**1**) in pyridine-d_5.

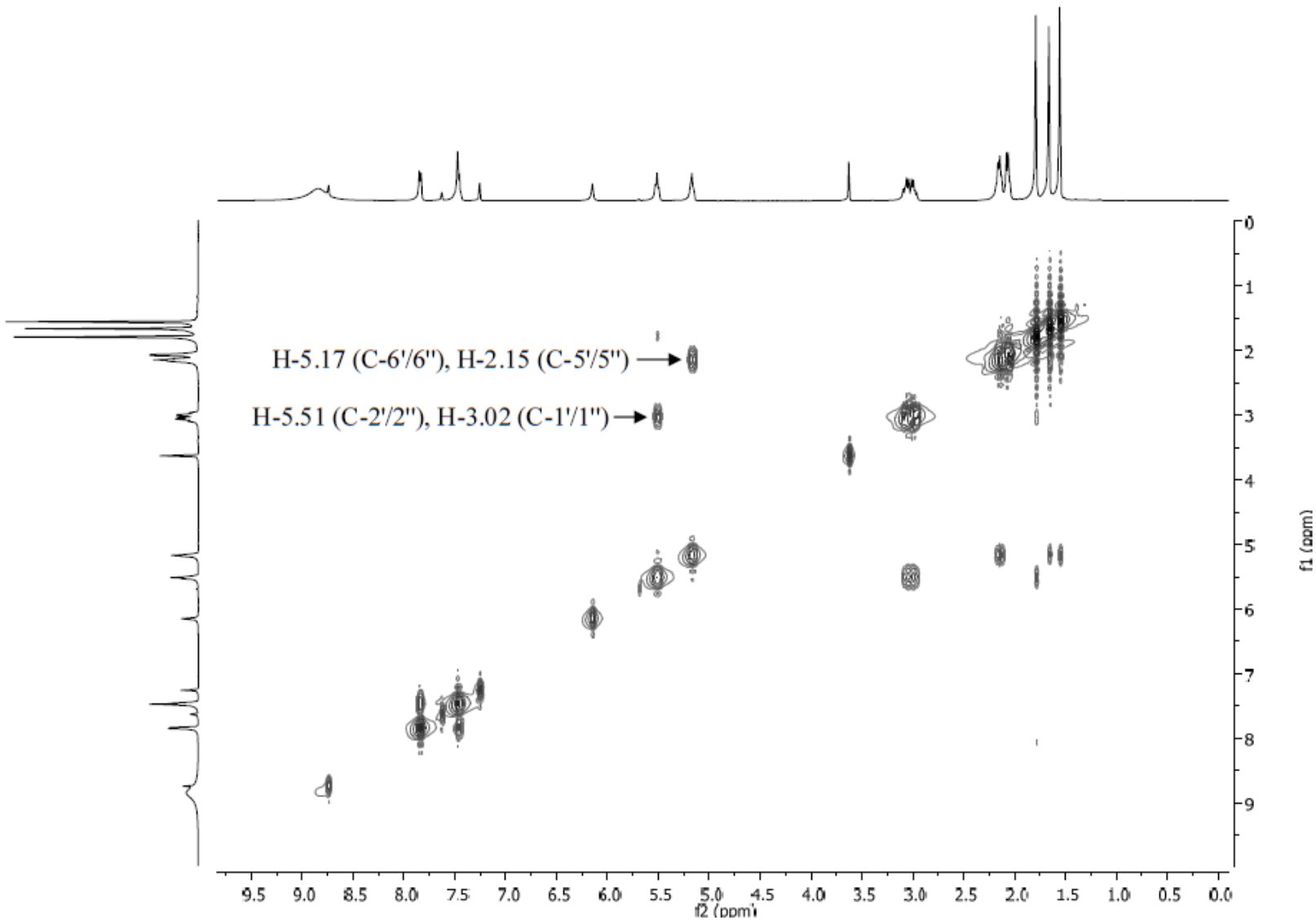

Figure 3.15 gCOSY spectrum of moronone (**1**) in pyridine-d_5.

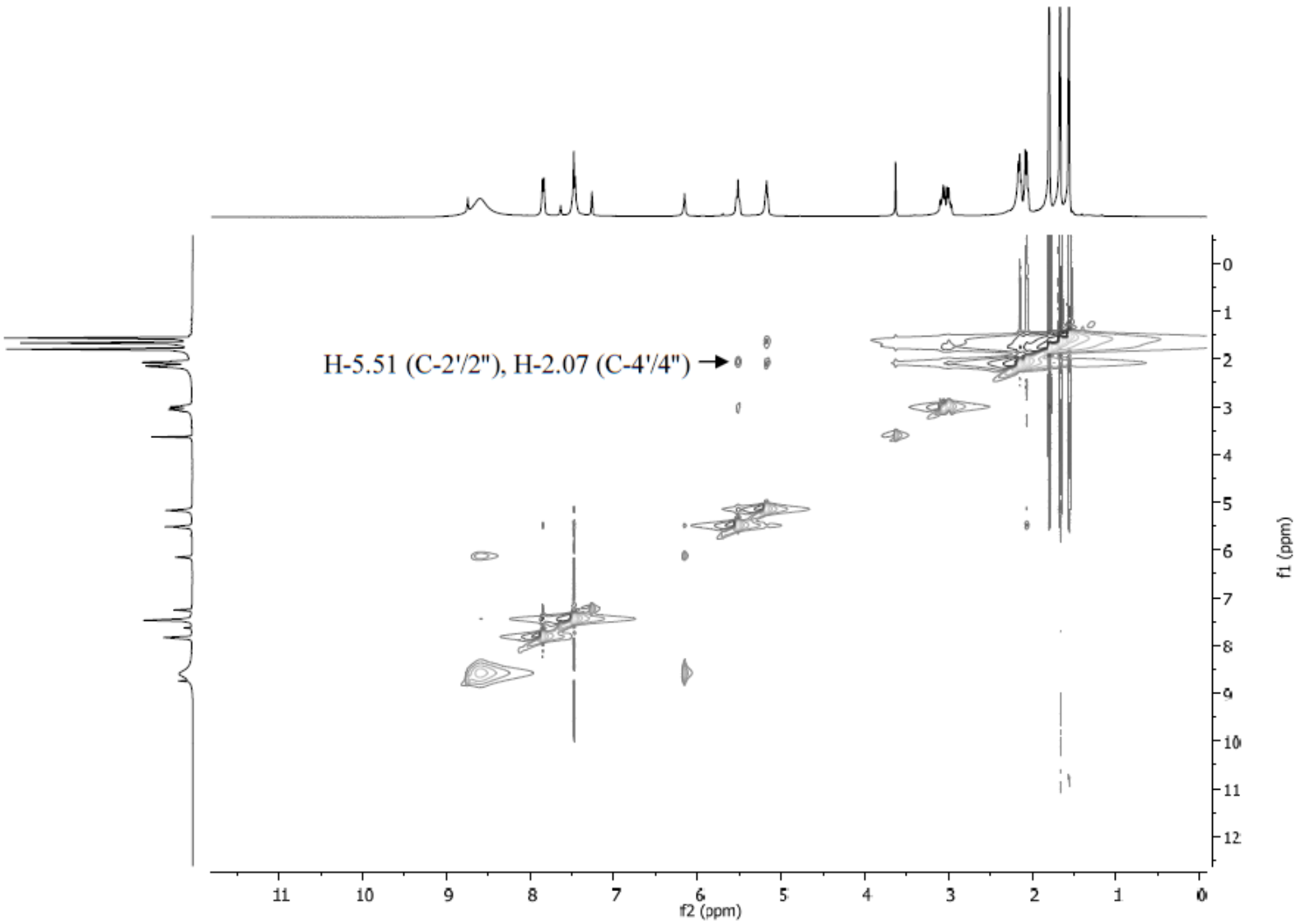

Figure 3.16 gNOESY spectrum of moronone (**1**) in pyridine-d_5.

3.3.3 Bioactivity of moronone (1)

In order to confirm the glycolysis inhibitory effect of **1,** glucose uptake and lactate production by MDA-MB-231 cells were measured in the presence of **1** (1, 3, 10 and 30 μM) after 24, 48 and 72 h. Moronone (**1**) significantly increased cellular glucose uptake at the concentrations of 10 and 30 μM, at all the time points, with a corresponding increase in lactate production (Table 3.2). This was suggestive of a stimulatory effect on the glycolytic pathway instead of a glycolysis inhibitory effect. When cells were treated with a well-known mitochondrial uncoupler FCCP (0.1, 0.3, 1 and 3 μM), similar changes to cellular glucose uptake and lactate production was observed at the concentrations of 1 and 3 μM. Rotenone (0.1 μM) enhanced the cellular glucose uptake and lactate production at all the time points. The observation that FCCP stimulate glycolysis is consistent with an earlier report of glycolysis stimulation in mammalian tumor cells by uncouplers (Sturdik *et al.*, 1986).

		Glucose consumed (nmol/μg cellular protein)			Lactate produced (nmol/μg cellular protein)		
		24 hrs	48 hrs	72 hrs	24 hrs	48 hrs	72 hrs
Untreated Cells		17.2 ± 2.0	43.0 ± 8.4	10.3 ± 6.1	23.6 ± 2.0	40.5 ± 6.0	125.3 ± 31.6
Rotenone (0.1 μM)		37.5 ± 7.7*	177.6 ± 20.1*	135.9 ± 23.8*	75.7 ± 21.8*	190.4 ± 5.6*	297.5 ± 57.7*
2-DG (3 mM)		22.5 ± 2.2	50.2 ± 18.8	8.5 ± 7.4	26.3 ± 5.1	52.8 ± 6.2	103.6 ± 31.6
Rotenone (0.1 μM) + 2-DG (3 mM)		35.9 ± 3.2*	138.7 ± 30.2*	63.0 ± 29.5*	71.3 ± 12.3*	155.0 ± 12.3*	267.8 ± 71.7*
Moronone (1)	1 μM	26.7 ± 3.8	44.7 ± 12.9	23.3 ± 3.1	21.9 ± 4.2	49.3 ± 11.5	99.6 ± 8.7
	3 μM	25.9 ± 5.3	73.4 ± 5.4	33.3 ± 6.9	25.4 ± 3.6	67.3 ± 16.0*	129.2 ± 3.8
	10 μM	45.8 ± 3.0*	168.4 ± 6.5*	198.1 ± 17.2*	59.5 ± 6.4*	168.5 ± 22.2*	364.8 ± 14.6*
	30 μM	40.9 ± 5.9*	129.2 ± 45.8*	62.7 ± 10.4*	53.4 ± 5.6*	128.1 ± 18.9*	226.9 ± 9.4*
FCCP	0.1 μM	20.9 ± 2.2	49.8 ± 12.6	25.4 ± 3.8	20.1 ± 2.7	47.1 ± 7.7	100.8 ± 7.2
	0.3 μM	25.8 ± 4.4	64.0 ± 23.0	29.6 ± 3.3	25.2 ± 2.9	55.1 ± 7.1	103.2 ± 8.5
	1 μM	32.9 ± 11.1*	95.0 ± 13.4*	50.5 ± 5.1*	45.4 ± 12.6*	94.3 ± 14.2*	151.7 ± 13.5
	3 μM	46.3 ± 8.2*	164.4 ± 33.6*	136.9 ± 5.3*	60.6 ± 9.5*	151.1 ± 8.5*	315.8 ± 11.2*

Table 3.2 Effect of **1** and FCCP on cellular glucose uptake and lactate secretion. MDA-MB-231 cells were treated with the test compounds as specified for 24, 48 or 72 h. Glucose and lactate concentrations in the conditioned media was measured spectrophotometrically by an enzymatic assay. Cellular protein concentrations were measured by Micro BCA assay kit. Glucose consumption was determined by subtracting the residual glucose concentrations in the conditioned media from glucose concentration of non-conditioned RPMI 1640 medium (determined from the standard curve). The data was presented as average ± standard deviation from single experiment assayed in triplicate. Data were compared using one-way ANOVA and Dunnett's post hoc analyses (GraphPad Prism 5). The "*" denotes statistical significance ($p < 0.05$) when compared with untreated cells.

Based on the observations that **1** contains two geranyl moieties and keto-enolic functionalities in the structure, and stimulate cellular glucose uptake and lactate production, it was hypothesized that **1** might penetrate the mitochondrial membrane and act as a protonophore. Hence, we evaluated **1** in MDA-MB-231 and T47D cell-based mitochondrial respiration assays (Liu *et al.* 2009). Moronone (**1**) exerted a biphasic effect on cellular oxygen consumption in both MDA-MB-231 and T47D cells. At lower concentrations (0.1, 0.3, and 1 μM), **1** increased cellular oxygen consumption. A decline in the respiration rate was observed at a higher concentration (3 μM) (Figure 3.17A). When the prototypical uncoupler FCCP was added to both cell lines at increasing concentrations (0.03, 0.1 0.3 and 1 μM), a similar change was observed on cellular oxygen consumption. The magnitude of the enhancement of the relative respiration rate was higher in MDA-MB-231, compared to that of T47D. This phenomenon might be explained by a lower baseline oxygen consumption rate in MDA-MB-231 cells compared to that of T47D cells (Li *et al.*, 2011). In order to eliminate possible effects of **1** on ATP turnover, and determine if **1** acts as a protonophore (increases cellular oxygen consumption), we evaluated the effect of **1** on cellular respiration in the presence of an F_0F_1-ATPase inhibitor oligomycin. Inhibition of F_0F_1-ATPase by oligomycin increases the mitochondrial membrane potential by preventing proton re-entry into the mitochondrial matrix, which in turn inhibits electron transfer through the respiratory chain. Protonophores, such as FCCP, release the inhibition of respiration by translocating protons to the mitochondrial matrix through the inner mitochondrial membrane. Moronone (**1**) and FCCP each overcame oligomycin exerted inhibition on cellular oxygen consumption in MDA-MB-231 (Figure 3.17B, 3.17C) and T47D cells (data not shown), and accelerated oligomycin-induced state 4 respiration.

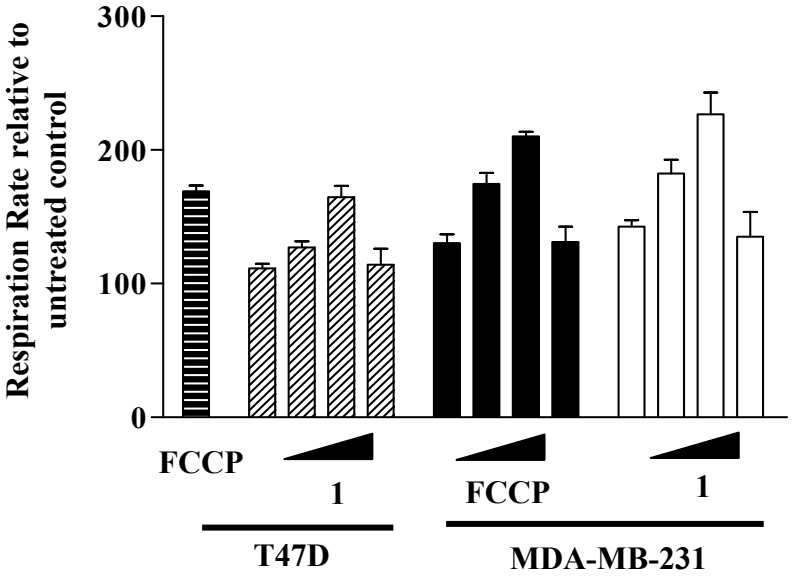

Figure 3.17A Concentration-response effects of **1** and FCCP on cellular respiration in T47D and MDA-MB-231 cells. Moronone was tested at 0.1, 0.3, 1 and 3 μM, while FCCP was tested at 0.3 μM in T47D cells and at 0.03, 0.1, 0.3 and 1 μM in MDA-MB-231 cells. Oxygen consumption rates were recorded before and after treatments and the data were presented as relative respiration rates. Data shown are average + standard deviation from three independent experiments (n = 3).

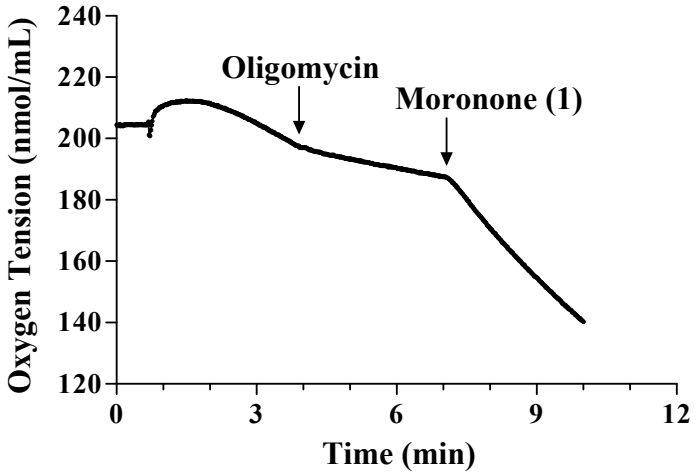

Figure 3.17B Accelaration of state 4 respiration initiated by oligomycin (1 μM) in MDA-MB-231 cells by moronone (1 μM)

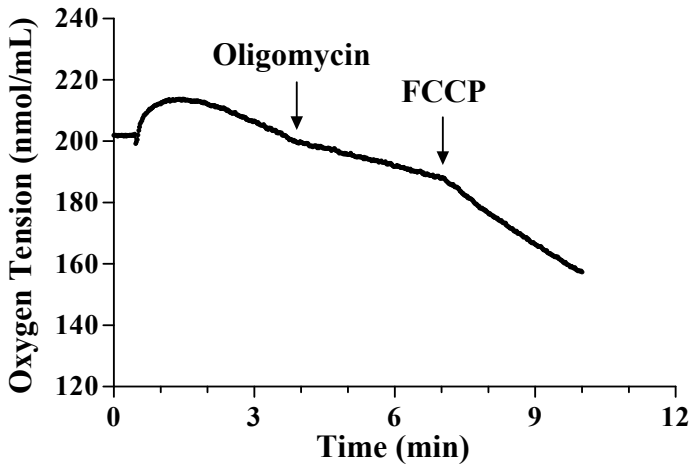

Figure 3.17C Accelaration of state 4 respiration initiated by oligomycin (1 μM) in MDA-MB-231 cells by FCCP (0.3 μM).

In order to confirm the protonophoric activity of **1** and to exclude enhanced substrate oxidation as the cause of an increase in the relative respiration rate, we evaluated the effect of **1** on mitochondrial membrane potential in MDA-MB-231 and T47D cells. A cationic, fluorescent dye, $TMRM^+$, was used to assess mitochondrial membrane potential. Owing to its cationic charge, $TMRM^+$ accumulates into the mitochondrial matrix under the normal mitochondrial membrane potential, and stains the mitochondria. Protonophores, such as FCCP, dissipate mitochondrial membrane potential and cause diffusion of the $TMRM^+$ dye, which results in reduction of the fluorescent dye intensity. Moronone (**1**) decreased mitochondrial membrane potential significantly in MDA-MB-231, which supported the protonophoric nature of this compound (Figure 3.18).

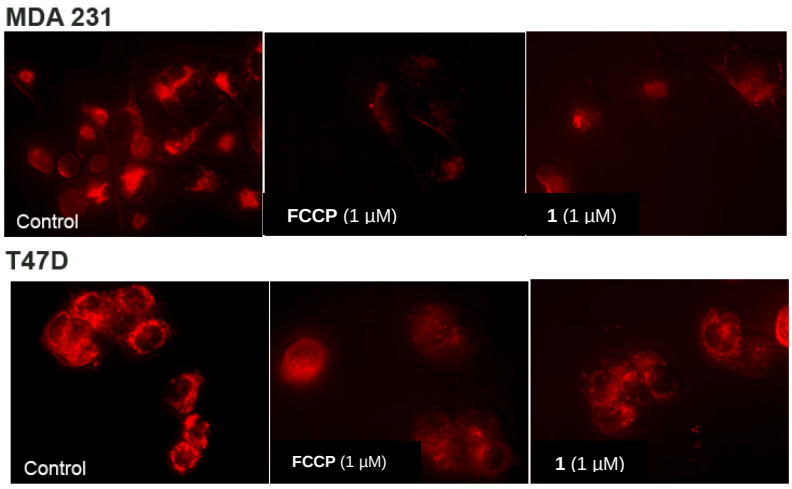

Figure 3.18 Dissipation of mitochondrial membrane potential by **1** and FCCP. MDA-MB-231 (upper panel) and T47D (lower panel) cells were incubated with 2 nM $TMRM^+$ for 2 h. The cells were treated with either **1** (1 µM) or FCCP (1 µM) for 30 min, and the cells were imaged with an Axiovert 200 M epifluorescent microscope. Images representative of each condition are shown above.

Since bioassay-guided fractionation of the active extract led us to the isolation of **1** that acts as a protonophore, we decided to evaluate the effect of the uncoupler standard FCCP in our assay system. MDA-MB-231 cells were treated with either FCCP or **1**, in the presence (or absence) of a mitochondrial inhibitor, such as rotenone. Rotenone (0.1 µM) significantly enhanced the cytotoxic effect of both FCCP and **1** on the normoxic MDA-MB-231 cells under normoxia (Figure 3.19).

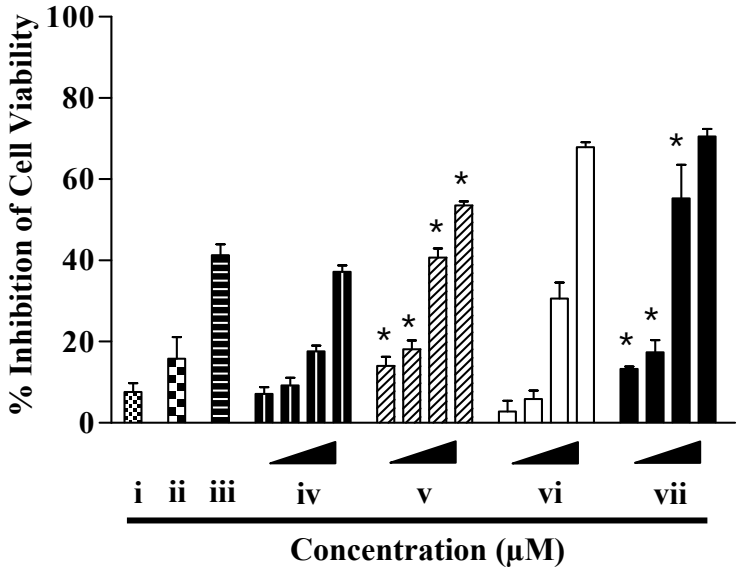

Figure 3.19 Differential suppression of MDA-MB-231cell viability by moronone and FCCP in the presence (or absence) of rotenone. MDA-MB-231 cells were treated with moronone [1, 3, 10, and 30 μM] or FCCP [0.1, 0.3, 1 and 3 μM], with (or without) rotenone and incubated for 48 h under normoxic conditions (37 °C, 95% air, 5% CO_2). Data shown are average + standard deviation from two independent experiments assayed in triplicate [**i** (rotenone), **ii** (2-DG), **iii** (2-DG + Rotenone), **iv** (FCCP), **v** (FCCP + Rotenone), **vi** (moronone), **vii** (moronone + rotenone)]. The "*" denotes statistical significance ($p < 0.05$) when compared with cytotoxicity in the absence of rotenone.

The results indicate that, mitochondrial respiration inhibitors enhance the cytostatic/cytotoxic effects of mitochondrial uncouplers, similar to those reported for glycolysis inhibitors. The concentration that produced optimum uncoupling in the cell-based respiration assay was lower than the concentration at which FCCP (1 μM) and moronone (10 μM) produced optimum differential cytotoxicity [≥45% cytotoxicity in the presence of rotenone (0.1 μM) with a differential index of ≥ 1.5].

The glucose analog 2-DG inhibits glycolysis by indirectly decreasing enzymatic hexokinase (an enzyme that catalyzes the intracellular glucose phosphorylation) activity. Clinical 2-DG monotherapy phase I trials was successful; however, the phase II clinical trial was

terminated due to slow patient enrollment (ClinicalTrials.gov, website accessed on 04/03/2012). Inhibition of aerobic glycolysis by small molecules is a promising approach to treat advanced stages of cancer (Scatena *et al.*, 2008); hence, the discovery of natural product-derived small-molecules that inhibit aerobic glycolysis more potently than 2-DG is a critical step towards finding an effective agent for cancer therapy. The stem wood extract of *Moronobea coccinea* showed a differential cytotoxicity index of 1.5 ($\geq$ 45% cytotoxicity in the presence of rotenone) in the initial screening assay. Bioassay-guided fractionation of *Moronobea coccinea* led to the isolation of polyprenylated benzophenone derivative moronone (**1**). Rotenone, FCCP, and **1** stimulated cellular glucose uptake and enhanced lactate secretion, in a concentration and time-dependent manner. Moronone uncoupled mitochondrial respiratory chain in both the cellular respiration assay and the mitochondrial membrane potential assay. When evaluated in the primary screening system, an increased cytotoxicity was observed for both FCCP and **1** in the presence of rotenone. The observed differential suppression of cell viability under glycolysis-dependent conditions by either FCCP or **1** might be due to glucose deprivation and subsequent ATP depletion. Further investigations are needed to reveal the actual mechanism. It has been reported that the combination of a mitochondrial respiratory chain inhibitor and a mitochondrial uncoupler stimulate cellular sugar uptake, depletion of cellular ATP levels (due to ATP hydrolysis by the F_1F_0-ATPase), and suppression of cell viability in mammalian cells. Oligomycin, an F_1F_0-ATPase inhibitor, protected the cells from the cytotoxic effect (Nieminen *et al.*, 1994). Alternatively, one school of thought contends that, under normoxic conditions, the presence of an uncoupler with a mitochondrial complex I inhibitor lead to enhanced superoxide production, which cause enhanced cytotoxicity (Cadenas and Han, 2007). The protonophoric nature of some polyprenylated benzophenone analogs may possibly explain general

antimicrobial, cytotoxic and some other activities exhibited by these analogs. In this bioassay system, the mitochondrial uncouplers tend to mimic the effect of glycolysis inhibitors on MDA-MB-231 cell viability under glycolysis-dependent conditions. In order to discover inhibitors of aerobic glycolysis by using this system, one must rapidly dereplicate the mitochondrial uncouplers from specific glycolysis inhibitors. A tumor cell-based respiration assay may be employed to dereplicate extracts with protonophoric properties, after primary screening and identification of the hits. Alternatively, rotenone may be substituted with oligomycin in order to prevent experimental artifact resulting from ATP hydrolysis by F_0F_1-ATPase.

CHAPTER IV

MITOCHONDRIAL TOXINS FROM BOTANICAL DIETARY SUPPLEMENTS

CONTRIBUTION OF AUTHORS

The work described in this chapter is a collaborative effort between Drs. Dale G. Nagle, Yu-Dong Zhou, Ms. Fakhri Mahdi and myself. Drs. Nagle and Zhou conceived the idea, helped to design the experiments, supervised the project and helped to interpret the data. Dr. Nagle served as my major advisor, while Dr. Zhou provided additional advice regarding the biological experiments. I performed the experiments, analyzed and interpreted the data. Ms. Mahdi performed the preliminary screening and confirmatory assays of the herbal extracts for the presence of mitochondrial inhibitors.

4.1 Overview

4.1.1 Introduction

Only recently has the potential for drug-induced mitochondrial dysfunction become recognized to significantly limit pharmaceutical development, and has forced the withdrawal of major drugs used to treat diabetes [troglitazone (**1**)] and hyperlipidemia [cerivastatin (**2**)]. Nearly half of the drugs with hepatoxicity and cardiovacular toxicity-associated FDA Black Box Warnings are known to interfere with mitochondrial function (Dykens and Will, 2007). These safety issues highlight the critical importance of employing measures to assess the potential mitochondrial toxicity of new drug leads early in the drug development process. While the pharmaceutical industry has only recently begun to recognize and test for the potential mitochondrial liability of new therapeutic agents, similar efforts have not been applied to the plethora of phytochemicals in botanical dietary supplement (BDS) products. As an initial exploratory study, extracts from more than 350 species of plants and other organisms used in traditional Chinese, Ayurvedic, and Western Herbal Medicine were evaluated for their ability to disrupt mitochondrial function.

Extracts from 24 different plant species suppressed mitochondrial respiration in mammalian cells. The extracts from five species uncoupled oxidative phosphorylation. Several species that were identified in our assays [i.e., *Glycyrrhiza glabra* L. (Fabaceae), *Chenopodium botrys* L. (Amaranthaceae), *Larrea tridentata* (Sessé & Moc. ex DC.) Coville (Zygophyllaceae), and *Tripterygium wilfordii* Hook.f. (Celastraceae)], contain compounds that interfere with mitochondrial function (Pardini *et al.*, 1973; Monzote *et al.*, 2009; Su *et al.*, 2007). Extracts of *Caulophyllum thalictroides* (L.) Michx. (Berberidaceae) and *Commiphora wightii* (Arn.) Bhandari (Burseraceae) contain components that can disrupt mitochondrial function and

potentially produce idiosyncratic mitochondria-mediated toxicities. The three blue cohosh (*C. thalictroides*) saponins, cauloside A (**3**), saponin PE (**4**), and cauloside C (**5**) were preliminarily identified as potential mitochondriotoxic components using a cell-based HIF-1 reporter gene assay. In addition to permeabilizing the plasma membrane, these saponins disrupt mitochondrial function in the Clarke-type electrode-based cellular respiration assay by permeabilizing mitochondrial membranes. Sesamin (**6**) and guggulsterol III (**7**) from guggul (*C. wightii*) extract preferentially inhibited hypoxia-induced HIF-1 activation, and disrupted mitochondrial complex I. Further investigation of guggul compounds is required because the extract was more active than the samples of pure compounds evaluated. Our results indicate the presence of mitochondriotoxic substances in popular dietary supplements and the need for systematic investigation of BDS products to identify the components that disrupt mitochondrial function.

4.1.2 General mechanisms of mitochondria-mediated toxicity

The term 'toxicity' means the harm caused to a living being by chemical, physical or biological agents (Society of Toxicology, accessed on 05/04/2012). Toxicity is often the end result of a cascade of events initiated by the initial exposure of an organism to toxic agents. Toxins elicit a wide variety of toxic effects ranging from nonlethal biochemical dysfunction to massive tissue/organ injury and even death of the organism (Society of Toxicology, accessed on 05/04/2012). Based on the pathological effects induced by the toxins, toxicity can be broadly categorized into the following: (a) cell death/tissue injury; (b) altered phenotype/function; (c) immunological hypersensitivity; and (d) cancer (Liebler and Guengerich, 2005). Among these, the most prevalent toxic response is the cell death/tissue injury.

Mitochondria are double membrane-bound cellular organelles which synthesize ATP via oxidative phosphorylation to provide energy for cellular reactions. Apart from meeting the cellular energy demand, mitochondria also regulate a number of pathways critical for cellular homeostasis and specialized metabolic processes such as fatty acid β-oxidation and the Kreb's cycle (Eaton *et al.*, 1996; Alberts *et al.*, 2002). Certain biosynthetic processes, such as heme and urea syntheses, partially occur in the mitochondrial matrix (Fontenay *et al.*, 2006; Mori *et al.*, 1983). Additionally, mitochondria play a key role in resulting cellular injury or cell death (Green and Kroemer, 2004). Mitochondrial content may vary widely depending on cell type. Cells with high ATP turnover contain more mitochondria than cells with low ATP turnover. It is hypothesized that cells have some functional mitochondrial reserve capacity; and when mitochondrial damage exceeds a certain threshold, cells initiate the process of either apoptotic or necrotic cell death (Jones *et al.*, 2010). When cellular injury or cell death is widespread in a particular tissue or organ, it results in tissue or organ toxicity, such as cardiotoxicity, neurotoxicity, nephrotoxicity and hepatotoxicity.

Cell death pathways can be broadly categorized into the following, based on the molecular mechanisms: (a) apoptosis; (b) necrosis; (c) autophagy; and (d) mitotic catastrophe (Kroemer *et al.*, 2007). Mitochondria are involved in effecting cell death through all four pathways. However, we will mainly focus on apoptosis and necrosis, as these are the most relevant pathways in drug/chemical-induced toxicity.

Apoptotic or programmed cell death is mediated by either of the two major pathways: (a) the extrinsic or death receptor pathway and (b) the intrinsic or mitochondrial pathway. Both pathways can be further divided into initiation, integration, and execution stages (Kroemer *et al.*, 2007; Jin and El-Deiry, 2005). Extracellular ligands bind to the cell surface death receptors

[tumor necrosis factor (TNF) receptor-1, Fas, and TRAIL receptors-1 and -2] to initiate the extrinsic apoptotic pathway. Following ligation, the death receptors undergo oligomerization, forming a death-inducing signaling complex (DISC). The DISC contains Fas-associated death domain (FADD) and an initiator caspase (i.e., caspase-8). Caspase-8 in the DISC undergoes autoactivation, leading to the activation of executioner caspases (i.e., caspase-3, -6 and -7) (Ashkenazi and Dixit, 1998). Activated caspase-8 cleaves and activates Bid, a proapoptotic Bcl-2 family protein, which results in mitochondrial membrane permeabilization. Activated executioner caspases (caspase-3, -6 and -7) cleave specific cellular substrates, resulting in apoptotic cell death (Kroemer *et al.*, 2007).

The intrinsic apoptotic pathway is the predominant apoptotic pathway in mammalian cells (Green and Kroemer, 2004). This pathway is initiated by diverse intracellular signals, such as damaged cellular organelles or DNA, and/or toxic substances. Permeabilization of the mitochondrial outer membrane occurs in response to intracellular apoptotic stimuli, and cytochrome *c* is released from the mitochondrial intermembrane space to cytosol (Kroemer *et al.*, 2007). The presence of cytochrome *c* in cytosol activates caspase-9 via formation of the apoptosome [a multiprotein complex that consists oligomerized apoptotic protease activating factor-1 (Apaf-1)] (Cain *et al.*, 2002). Following activation, caspase-9 cleaves, and activates procaspase-3, -6, and -7, resulting in apoptotic cell death. Irrespective of the pathway involved, apoptotic cell death is characterized by cell shrinkage, nuclear pyknosis, karyorhexis and phosphatidylserine exposure to the extracellular environment. During apoptosis, apoptotic bodies are formed and cleared phagocytically without producing an inflammatory reaction (Elmore, 2007).

Necrosis, on the other hand, usually results from a highly intense toxicological insult. Necrosis is typically accompanied with oncosis, including mitochondrial swelling and eventual mitochondrial and cell membrane rupture. Spillage of cytosolic content into the extracellular space results in inflammatory responses (Kroemer *et al.*, 2007; Robertson and Orrenius, 2002).

Mitochondria also play an important role in cell death via necrosis. Opening of a mitochondrial membrane permeability transition pore (mPTP) is often associated with necrosis. Opening of mPTP dissipates the mitochondrial membrane potential ($\Delta\Psi m$), disrupts the intracellular electrochemical and pH gradients, and results in mitochondrial and cellular swelling. Eventually, cellular and mitochondrial lyses occur due to increased osmotic pressure (Gregus, 2008). Some of the key factors that determine whether a cell will undergo necrosis or apoptosis in response to a toxicant include the toxin concentration, exposure time, and intracellular ATP concentration. High toxin concentrations, prolonged exposure period and intracellular ATP depletion usually lead to necrotic cell death (Kroemer *et al.*, 1998). In spite of the differences in the molecular mechanisms, mitochondrial dysfunction is often the final common step that leads to cellular death.

4.1.3 Drug or small-molecule-induced mitochondrial toxicity

From the discussion in the introduction section, it is obvious that both clinically approved drugs and natural products, may potentially cause mitochondrial dysfunction. However, natural products are commonly thought to be free of adverse effects, compared to clinically approved drugs. Hence, the rigorous scrutiny that is mandatory for clinically approved drugs are not applied for over-the-counter (OTC) natural products. Several drugs, such as troglitazone (**1**) and cerivastatin (**2**) (Figure 4.1), have been withdrawn from the market for their mitochondrial

liabilities. Similarly, the mitochondrial toxins in natural product dietary supplements should be identified and a regulatory standard comparable to clinically approved drugs should be set for OTC natural products with mitochondrial toxins.

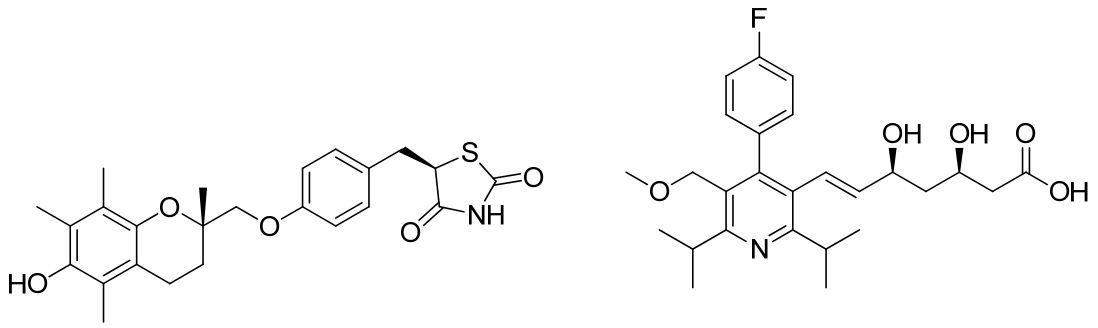

(**1**) (**2**)

Figure 4.1 Examples of clinically approved drugs withdrawn from the market due to mitochondrial toxicity.

4.1.4 Saponin glycoside toxicity

Saponins are ubiquitous plant secondary metabolites with surfactant properties (Sparg *et al.*, 2004). Multiple dietary supplements containing saponin glycosides for various indications are currently marketed in the US (Avula *et al.*, 2011; Kozlova et al., 2011; Yeh *et al.*, 2003). A number of biological properties have been attributed to this class of compounds, with hemolytic or membrane permeabilizing activity being the most prominent (Francis *et al.*, 2002). Based on the sapogenin (aglycone) structure, saponins are categorized into two broad classes: (a) steroidal saponins [e.g., diosgenin (**8**)] and (b) triterpenoid saponins [e.g., oleanolic acid (**9**)]. Owing to their surfactant properties, saponins interact with the lipid bilayers of cellular membranes and alter their permeability by irreversibly forming pores. Mechanistically, they are hypothesized to sequester cholesterol from membranes (Melzig *et al.*, 2001). Alternatively, saponins are proposed to interact with the aquaporins on the cell surface, resulting in unregulated water

transport inside cells and subsequent hemolysis (Gauthier *et al.*, 2009). Following parenteral administration, saponins show high levels of toxicity in animals. Holothurin A (**10**), a sea cucumber-derived saponin, had an LD_{50} of 0.75 mg/kg in mice upon intravenous administration. Due to their poor oral bioavailability, saponins are significantly less toxic upon oral ingestion (LD_{50} 50-1000 mg/kg). Aberrant salivation, vomiting, diarrhea, loss of appetite and paralysis have been reported after saponin intoxication (Hostettmann *et al.*, 1995). Lethal doses of saponins have been shown to cause liver necrosis, as well as bleeding in alveoli and other vessel walls (Hostettmann *et al.*, 1995). However, conflicting results were reported in regard to the correlation of the hemolytic/surfactant activity and saponin toxicity profiles (Wang *et al.*, 2007a; Böttger *et al.*, 2012). Saponins permeabilize respiratory membranes of cold-blooded animals and have been reported to be highly toxic to frogs, fish, and mollusks. Saponins exert cytotoxic effects on a variety of human tumor cell lines (Hostettmann *et al.*, 1995). It has been proposed that cellular internalization is required for steroidal saponin glycoside cytotoxicity (Wang *et al.*, 2007b). Release of cytochrome *c* from mitochondria was observed while investigating the mechanism of cytotoxic activity by avicins, a group of plant saponins. The cytochrome *c* release by avicins resulted from direct mitochondrial membrane permeabilization (Haridas *et al.*, 2001; Lemeshko *et al.*, 2006). Another plant saponin OSW-1 (**11**) has been reported to permeabilize mitochondrial membrane and activate calcium-dependent apoptosis in both leukemia and pancreatic cancer cells (Zhou *et al.*, 2005). Numerous saponins have been reported to affect a number of cellular pathways that result in cytotoxicity (Man *et al.*, 2010; Podolak *et al.*, 2010). However, it is unclear whether the effect observed on the cellular signaling is secondary to a toxic mitochondrial insult. In addition, most cytotoxicity studies do not report whether the effect of the saponins are selective to tumor cell lines, relative to their effects on normal cells. The

potential for saponin selectivity toward tumor cells and a possible correlation between mitochondrial membrane permeabilization and general saponin cytotoxicity warrants further investigation.

The potential of mitochondrial toxicity from BDS has not been well characterized. One of the major challenges for identification of BDS-induced mitochondrial toxicity is that these dietary supplements are often consumed in conjunction with clinically approved drugs, which have off-target effects on the mitochondria. In addition, consumption of BDS is perceived as safe and often goes unreported. From the earlier discussions, it is apparent that natural products are a rich source for mitochondrial toxins and they impair mitochondrial functioning in the same way as synthetic compounds or clinically approved drugs. The presence of mitochondriotoxic substances in BDS may pose a potential health hazard and the characterization of these molecules is necessary to better understand, and potentially prevent, idiosyncratic adverse reactions.

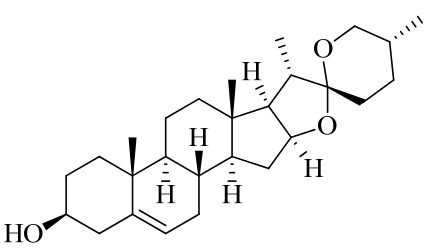

Diosgenin (**8**)

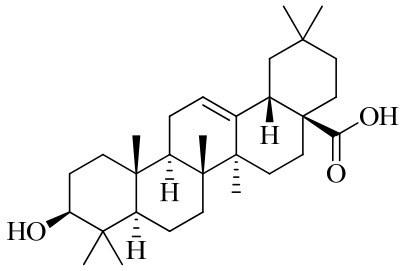

Oleanolic acid (**9**)

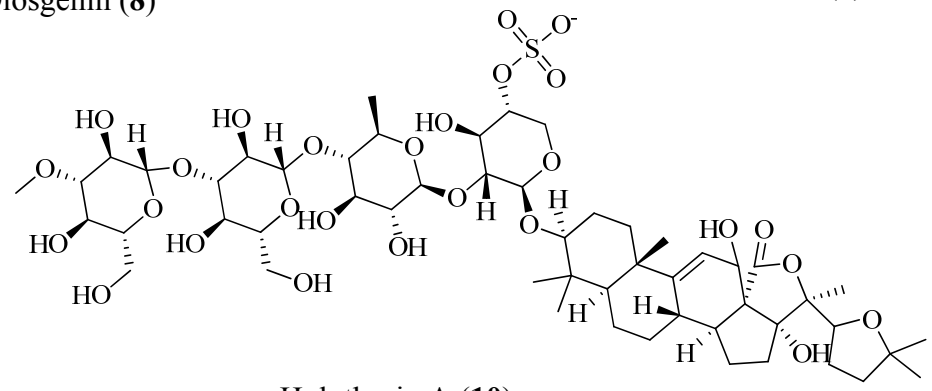

Holothurin A (**10**)

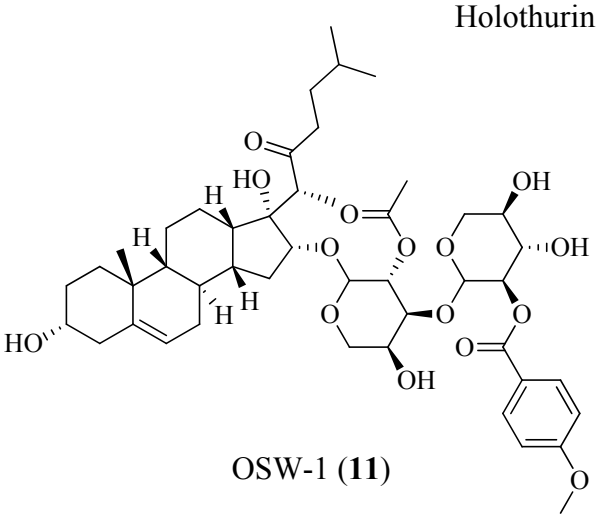

OSW-1 (**11**)

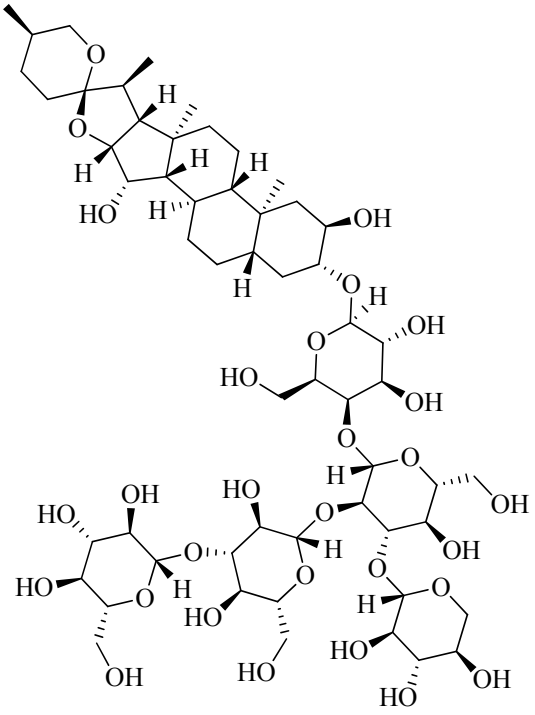

Digitonin (**27**)

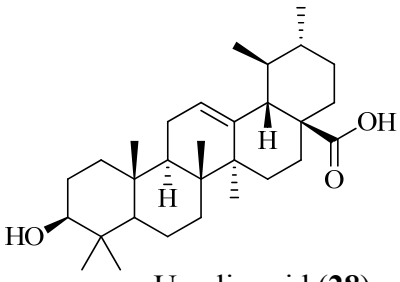

Ursolic acid (**28**)

Figure 4.2 Examples of sapogenins and saponins.

4.2 Materials and methods

4.2.1 Acqusition of extracts and pure compounds

Among 46 active extracts blue cohosh and guggul extracts and the purified compounds from blue cohosh [*N*-methylcytisine (**12**), cauloside H (**13**), cauloside D (**14**), cauloside B (**15**), cauloside G (**16**), leonticin D (**17**), cauloside A (**3**), saponin PE (**4**), cauloside C (**5**), and ciwujianoside A_1 (**18**) (Figures 4.3 – 4.4)] and guggul [(13*E*,17*E*,21*E*)-8-hydroxypolypodo-13,17,21-trien-3-one (**19**), (13*E*,17*E*,21*E*)-polypodo-13,17,21-trien-3,8-diol (**20**), sesamin (**6**), *Z*-guggulsterone (**21**), *E*-guggulsterone (**22**), guggulsterol III (**7**), and (20*S*)-20-acetoxy-4-pregnene-3,16-dione (**23**) (Figures 4.5A)] were further investigated. These extracts and compounds were kindly provided by Dr. Ikhlas A. Khan (National Center for Natural Products Research, University of Mississippi). The extracts and purified compounds were dissolved in either DMSO or isopropanol and 10 mM stock solutions of each were prepared.

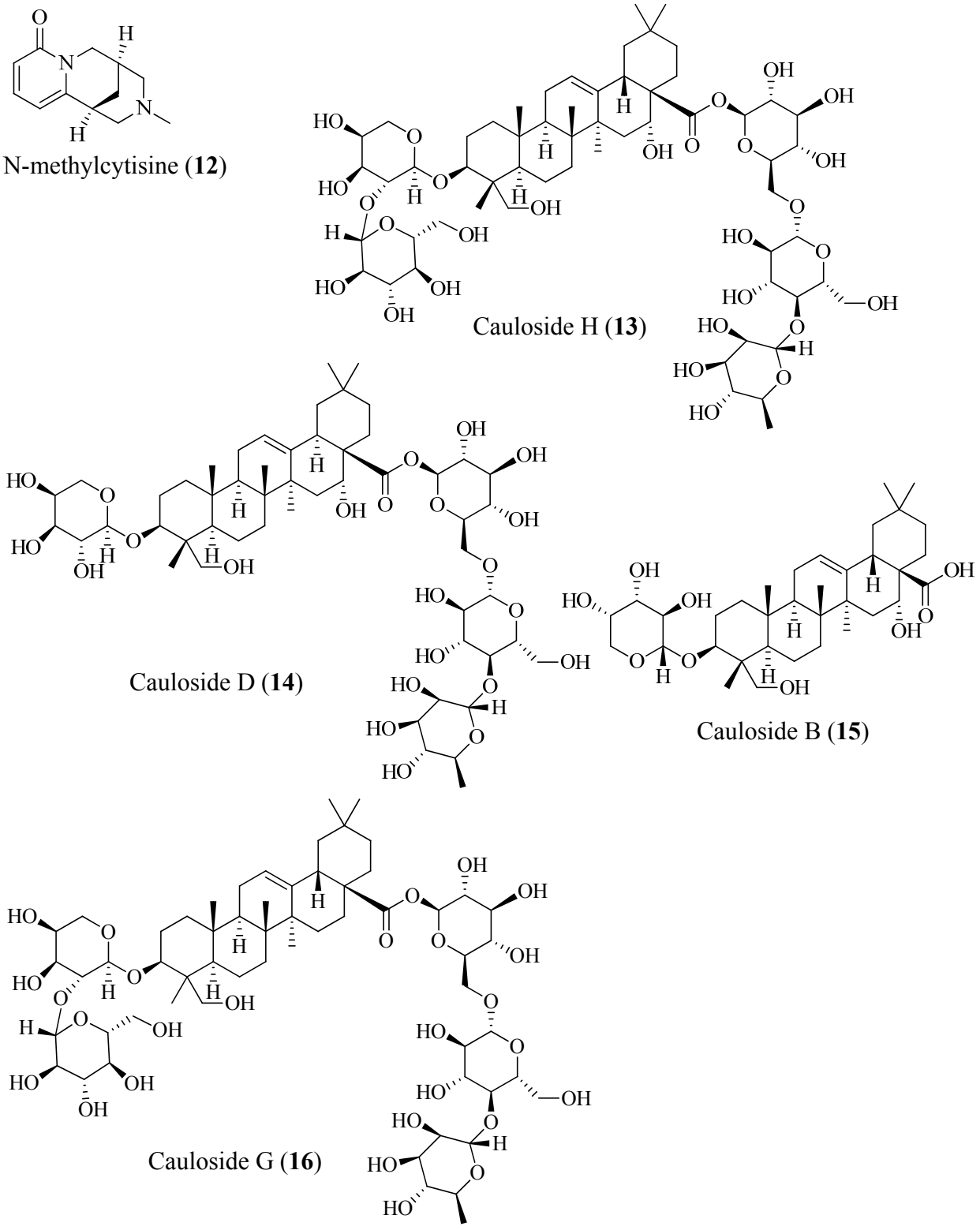

Figure 4.3 Purified blue cohosh compounds that were evaluated for mitochondrial toxicity.

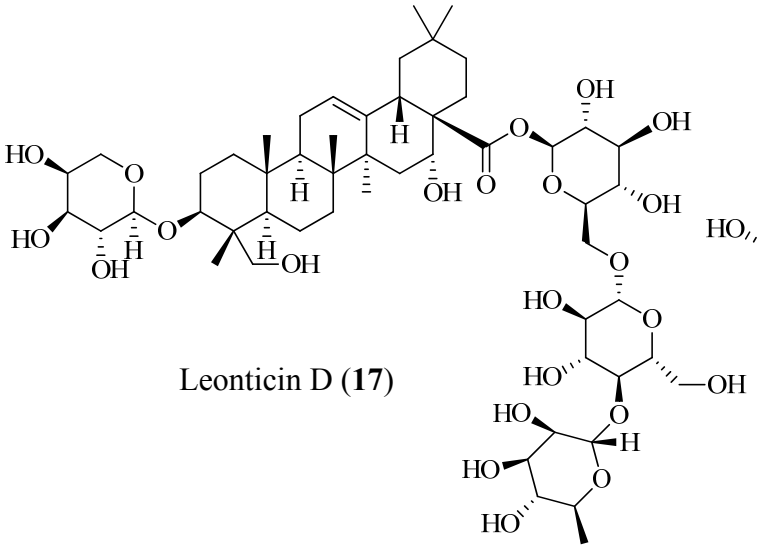

Leonticin D (**17**)

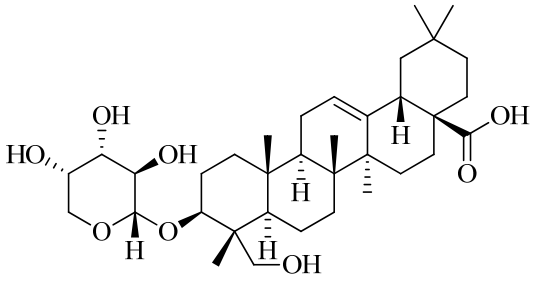

Cauloside A (**3**)

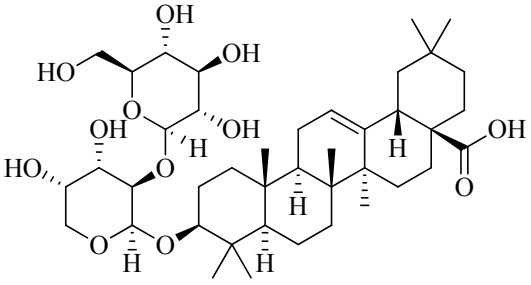

Saponin PE (**4**)

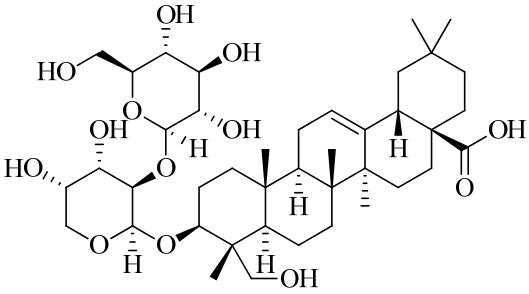

Cauloside C

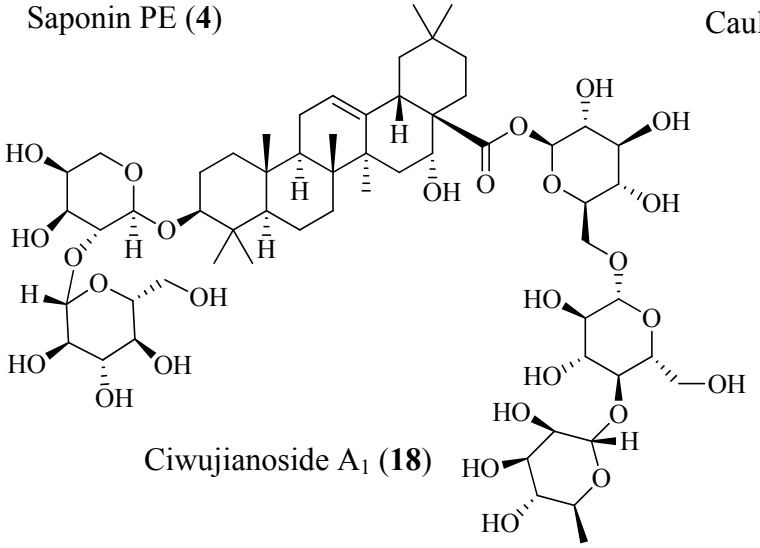

Ciwujianoside A_1 (**18**)

Figure 4.4 Purified blue cohosh compounds that were evaluated for mitochondrial toxicity.

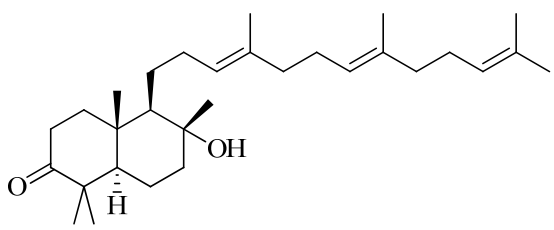

(13*E*,17*E*,21*E*)-8-hydroxypolypodo-13,17,21-trien-3-one (**19**)

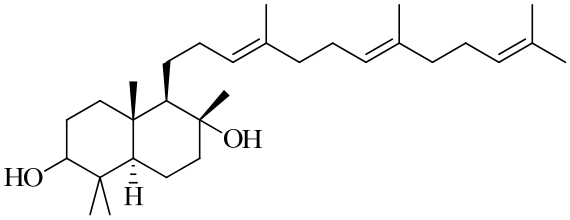

(13*E*,17*E*,21*E*)-polypodo-13,17,21-trien-3,8-diol (**20**)

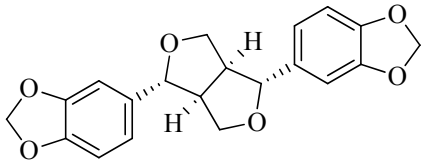

Sesamin (**6**)

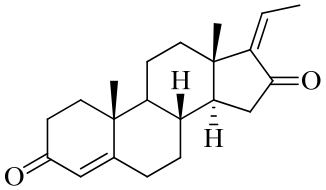

Z-guggulsterone (**21**)

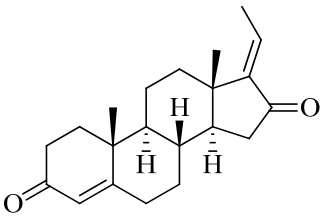

E-guggulsterone (**22**)

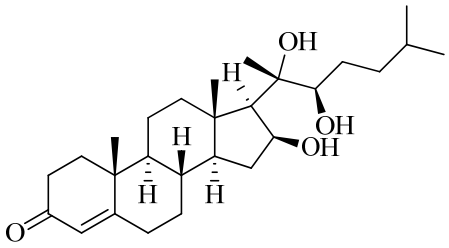

guggulsterol III (**7**)

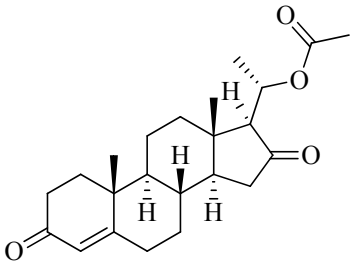

(20*S*)-20-acetoxy-4-pregnene-3,16-dione (**23**)

Figure 4.5A Purified guggul compounds that were evaluated for mitochondrial toxicity.

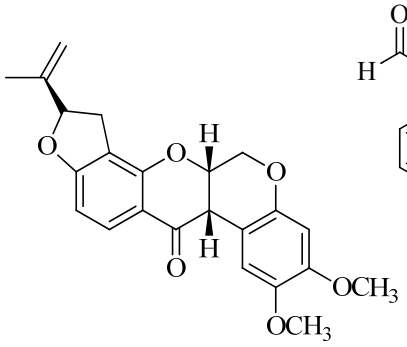

Rotenone (**24**)

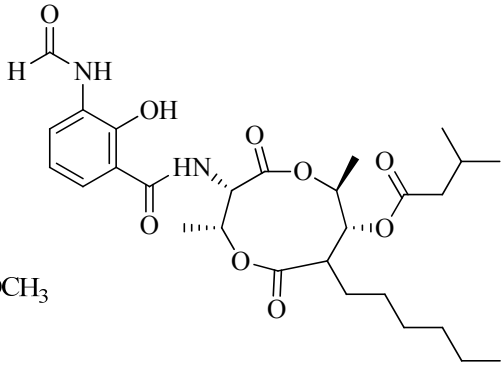

Antimycin A (**25**)

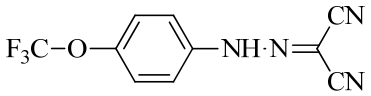

FCCP (**26**)

Figure 4.5B Prototypical mitochondrial inhibitors and uncoupler.

4.2.2 Tumor cell culture and HIF-1 reporter assay

Human breast tumor T47D cells (ATCC) were maintained in Dulbecco's Modified Eagle's Medium (DMEM) and Ham's F-12 (1:1) media with 2.5 mM L-gultamine (Mediatech), supplemented with fetal bovine serum (10% v/v final concentration, Hyclone) and penicillin (50 units/mL) and streptomycin (50 μg/mL) (pen/strep, BioWhittaker). Exponentially grown T47D cells were transfected with the pTK-HRE3-luc reporter by electroporation using an ECM830 square wave electroporation system (BTX Inc) at 140 V for 70 ms (1 pulse). The transfected cells were plated at 3 x 10^4 cells per well in a volume of 100 μL of FBS (10% v/v final concentration) and antibiotics supplemented DMEM/F12 medium, into 96-well plates, and was incubated under normoxic conditions (5% CO_2, 95% air, 37 °C) for overnight. After 24 h, each test compound was diluted (2x final concentration) in serum free DMEM/F12 medium with antibiotics and added in a volume of 100 μL per well. Following the addition of the test compounds, the incubation continued at 37 °C for an additional 30 min. Subsequently, the cells were exposed to hypoxic (1% O_2, 5% CO_2, 94% N_2) or normoxic (5% CO_2, 95% air) or iron chelator-induced hypoxia-mimetic conditions (10 μM 1,10-phenanthroline, Sigma, 5% CO_2, 95% air) at 37 °C for 16 h. The cells were then lysed, and luciferase activities were determined according to manufacturer's instructions (Promega) using a microplate reader (Biotek). The following formula was used to calculate the percentage inhibition data:

$$\% \text{ inhibition} = (1 - \text{luminescence}_{\text{treated}}/\text{luminescence}_{\text{induced}}) \times 100$$

Extracts and compounds for bioassay were prepared as stock solutions in DMSO (or isopropanol) and the final concentration of solvent was less than 0.5% (v/v) in all HIF-1 reporter assays.

4.2.3 Cellular respiration assay

Human T47D or Hep3B cells (5×10^6) suspended in 100 μL of 1x phosphate-buffered saline (PBS), pH 7.4 (Fisher Scientific) were added to the chamber of an Oxytherm Clark electrode system (Hansatech) containing 900 μL of DMEM/F-12 medium (JRH) free of serum and antibiotics (equilibrated to 30 °C). Glucose (17.5 mM) in the DMEM/F-12 media served as the metabolic substrate. Steady state base-line respiration was established (for a 10-min interval) by recording the oxygen consumption of untreated cells. Subsequently, compounds dissolved in DMSO (or isopropanol) were injected into the chamber using a 10-μL syringe (Hamilton). For the compounds that initially stimulated cellular oxygen consumption, the average oxygen consumption rates were measured for a one-minute window 30, 115 and 295 seconds after each addition. For the compounds that inhibited oxygen consumption, the average rate was recorded for a one-minute window 2 min after each addition. For mechanistic studies, the cells were suspended in a buffer that contained 20 mM HEPES, pH 7.3, 120 mM KCl, 2 mM KH_2PO_4, 2 mM $MgCl_2$ and 1 mM EGTA [ethylene glycol *bis*(2-aminoethyl ether)-*N,N,N',N'*-tetraacetic acid], in place of the DMEM/F-12 medium. Plasma membranes were selectively permeabilized with digitonin (4 μM) so that the substrates available to the mitochondria could be manipulated. The buffer was supplemented with the following substrates that provide electrons to different complexes within the mitochondrial respiratory chain: 5 mM sodium pyruvate and 5 mM sodium malate (complex I), 5 mM sodium succinate dibasic hexahydrate (complex II), and 5 mM L-ascorbic acid plus 0.2 mM TMPD (*N,N,N′,N′*-tetramethyl-*p*-phenylenediamine) (complex IV). The prototypical complex I and III inhibitors rotenone (**24**) and antimycin A (**25**) (Figure 4.5B), respectively, were added from EtOH stock solutions to a final concentrations of 1 μM where indicated. All the chemicals were from Sigma, and the final concentration of solvent used in

assays was maintained at less than 0.1% (v/v). The data were presented as percentage inhibitions or relative respiration rates wherever appropriate and were calculated by the following formulas:

$$\% \text{ Inhibition} = 1 - \frac{\text{oxygen consumption rate}_{\text{compound}}}{\text{oxygen consumption rate}_{\text{control}}} \times 100$$

$$\text{Respiration rate relative to untreated control} = 100 \times \frac{\text{oxygen consumption rate}_{\text{compound}}}{\text{oxygen consumption rate}_{\text{control}}}$$

4.2.4 Sulforhodamine B cell viability assay

Exponentially grown T47D or Hep3B cells were plated at 3 x 10^4 cells per well into 96-well plates in a volume of 100 µL of DMEM/F12 medium supplemented with FBS (10% v/v final concentration) and antibiotics. After 24 h, each test compound was diluted (2x final concentration) in the serum free DMEM/F12 medium with antibiotics, added in a volume of 100 µL per well, and incubated for an additional 2-day (or 6-day) period at 37 °C (95% air, 5% CO_2). For the 6-day exposure study, the conditioned media were replaced after 3 days by fresh culture media that contained test compounds. Following a 2-day (or 6-day) incubation period, the cells were fixed by replacing 100 µL of culture medium with 100 µL trichloroacetic acid solution (20% w/v in 1x PBS, pH 7.4) per well. Following incubation at 4 °C for 1 h, the supernatant was removed, and the cells were washed with tap water (4x) and air-dried. A sulforhodamine B solution (0.4% w/v, in 1% actetic acid) was added in a volume of 100 µL per well and incubated at room temperature for 10 min. The stained cells were washed with 1% acetic acid (4x) and air-dried. The dye was eluted by using 200 µL of Trizma® base (10 mM) per well and incubating for 10 min at room temperature. The plates were gently shaken for 2 – 3 min, and absorbance was measured at 490 nm and background absorbance at 630 nm on a BioTek Synergy plate reader. The ΔOD values were used for subsequent data analysis and were calculated by subtracting the

background absorbance from the absorbance at 490 nm. The following formula was used to calculate the percentage inhibition:

$$\% \text{ inhibition} = (1 - \Delta OD_{treated}/\Delta OD_{control}) \times 100$$

4.3 Results and discussion

4.3.1 HIF-1 inhibitory activity of herbal dietary supplements due to suppression of mitochondrial electron transport chain

The evaluation of 352 extracts of botanical dietary supplement products was performed by Ms. Mahdi in the previously described T47D cell-based HIF-1 reporter assay. Transfected T47D cells (pTK-HRE3-Luc) were treated with the extracts (5 µg/mL) and then exposed to either hypoxic conditions (1% O_2) or the iron chelator 1,10-phenanthroline (10 µM) to induce HIF-1 reporter activity. In this assay, mitochondrial ETC inhibitors typically more potently inhibit hypoxia-induced HIF-1 relative to their effect on iron chelator-induced HIF-1 activation (Coothankandaswamy *et al.*, 2010). Protonophores demonstrate nonspecific inhibition of HIF-1 induction irrespective of the inducing conditions (Du *et al.*, 2010). Forty six extracts that displayed an activity profile similar to either a mitochondrial inhibitor or an uncoupler were reconfirmed in a cell-based respiration assay by Ms. Mahdi. Sixteen extracts strongly (> 50%) inhibited cellular respiration, while six extracts only weakly (25 – 50%) inhibited respiration. Five extracts increased cellular oxygen consumption, indicating that they may uncouple oxidative phosphorylation. Active extracts were reconfirmed and subjected for further phytochemical identification and dereplication studies. Among the active extracts, blue cohosh and guggul extracts were identified for further investigations.

4.3.2 Effects of herbal dietary supplement compounds on cellular respiration

4.3.2.1 Blue Cohosh (*Caulophyllum thalictroides*)

The extract of blue cohosh [*Caulophyllum thalictroides* (L.) Michx. (Berberidaceae)] inhibited HIF-1 activity and its effects on cell respiration were reconfirmed in the oxygen consumption assay. Ten purified compounds from blue cohosh were obtained from Dr. Khan's pure compound repository for further evaluation (Figures 4.3 – 4.4).

The compounds were evaluated in the HIF-1 assay at multiple concentrations (1, 10 and 30 μM) (Figures 4.6A – B). These concentrations were within the concentration range that was reported to be present in the commercial dietary supplements (Avula *et al.* 2011)

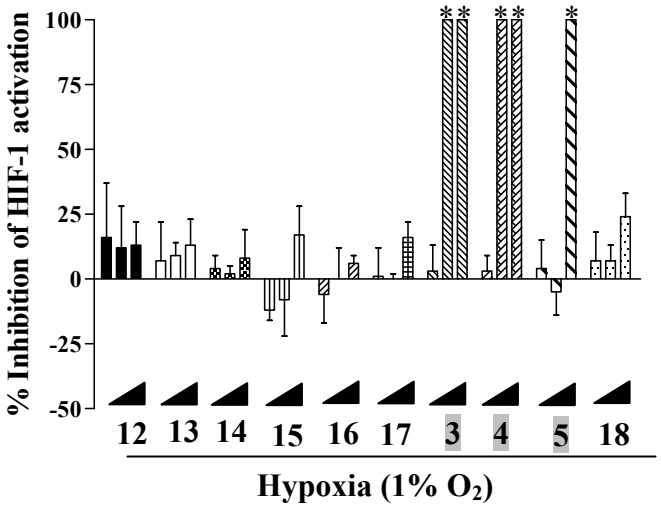

Figure 4.6A Inhibition of hypoxia-induced HIF-1 by blue cohosh pure compounds. Transfected (pTK-HRE3-luc) T47D cells were treated with compounds (1, 10 and 30 μM) and exposed to hypoxic (1% O_2) conditions for 16 h. Data shown are average + standard deviation from single representative experiment performed in triplicate. Absence of error bars due to identical readings for any data point is denoted by '*'.

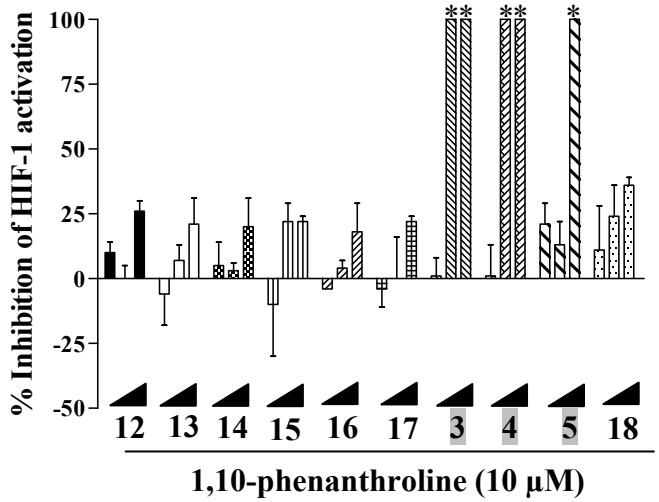

Figure 4.6B Inhibition of 1,10-phenanthroline-induced HIF-1 by blue cohosh compounds. Transfected (pTK-HRE3-luc) T47D cells were treated with compounds (1, 10 and 30 μM) and exposed to 1,10-phenanthroline (10 μM) for 16 h. Data shown are average + standard deviation from single representative experiment performed in triplicate. Absence of error bars due to identical readings for any data point is denoted by '*'.

Among the 10 compounds tested, cauloside A (**3**), Saponin PE (**4**), and cauloside C (**5**) demonstrated inhibition of both hypoxia, and 1,10-phenanthroline-induced HIF-1 activation. Because the HIF-1 activity profiles of **3**, **4** and **5** were similar to mitochondrial protonophores, these compounds were further evaluated for their effects on cell respiration. The compounds exhibited a time and concentration-dependent biphasic effect on T47D (intact) cell oxygen consumption in the respiration assay (Figures 4.7A – C). The blue cohosh extract also showed similar a concentration-response effect on T47D cell respiration (Figure 4.7D). Saponin PE (**4**) most potently perturbed mitochondrial respiration. The solvent being DMSO (a well-characterized solvent), possibility of any solvent effect was ruled out.

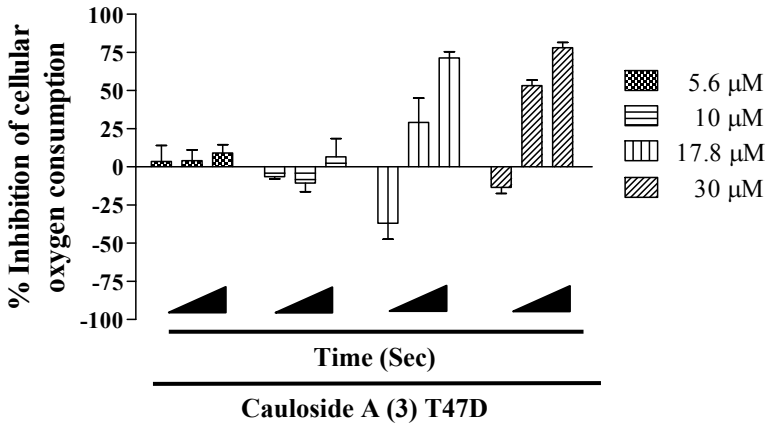

Figure 4.7A Concentration-response effect of cauloside A (**3**) on T47D respiration. Cauloside A (**3**) was tested at 5.6, 10.0, 17.8 and 30.0 µM. Oxygen consumption rates were recorded 30, 115 and 295 seconds after each treatment and the data were presented as percentage inhibition of oxygen consumption rate compared to the average oxygen consumption rate of untreated T47D cells. Negative values indicate a relative stimulation of oxygen consumption. Data shown are average + deviation from the mean for the 5.6 µM data point from two independent experiments (n = 2) and average + standard deviation for the rest of the data points from three independent experiments (n = 3).

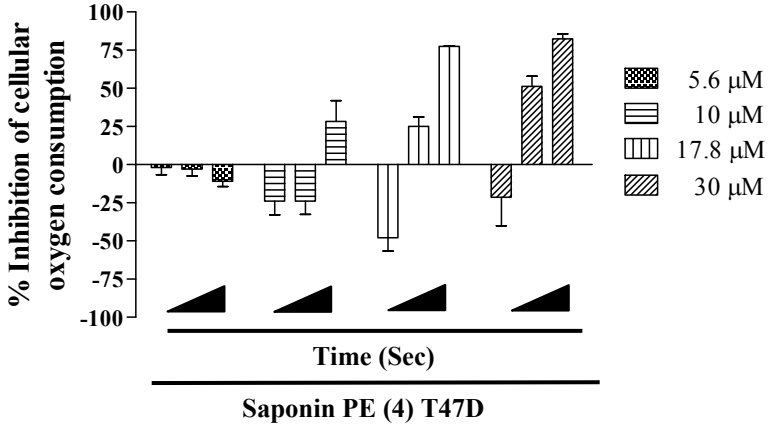

Figure 4.7B Concentration-response effect of saponin PE (**4**) on T47D cell respiration. Saponin PE (**4**) was tested at 5.6, 10.0, 17.8 and 30.0 µM. Oxygen consumption rates were recorded 30, 115 and 295 seconds after each treatment and the data were presented as percentage inhibition of oxygen consumption rate compared to the average oxygen consumption rate of untreated T47D cells. Negative values indicate a relative stimulation of oxygen consumption. Data shown are average + standard deviation from three independent experiments (n = 3).

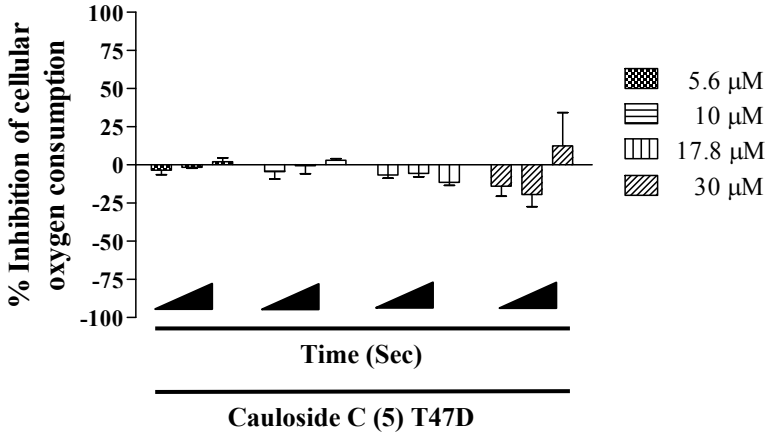

Figure 4.7C Concentration-response effect of cauloside C (**5**) on T47D cell respiration. Cauloside C (**5**) was tested at 5.6, 10.0, 17.8 and 30 µM. Oxygen consumption rates were recorded 30, 115 and 295 seconds after each treatment and the data were presented as percentage inhibition of oxygen consumption rate compared to the average oxygen consumption rate of untreated T47D cells. Negative values indicate a relative stimulation of oxygen consumption. Data shown are average + standard deviation from three independent experiments (*n* = 3).

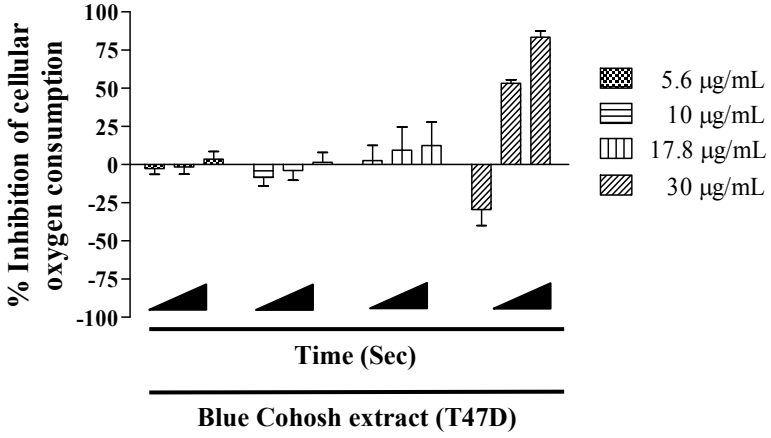

Figure 4.7D Concentration-response effect of blue cohosh extract on T47D cell respiration. Blue cohosh extract was tested at 5.6, 10.0, 17.8 and 30.0 µg/mL. Oxygen consumption rates were recorded 30, 115 and 295 seconds after each treatment and the data were presented as percentage inhibition of oxygen consumption rate compared to the average oxygen consumption rate of untreated T47D cells. Negative values indicate a relative stimulation of oxygen consumption. Data shown are average + standard deviation from three independent experiments (*n* = 3).

Hepatocyte mitochondrial impairment is one of the major reasons for drug-induced hepatotoxicity. The potential of **3**, **4**, **5** and the original extract to disrupt the hepatic mitochondrial respiration was evaluated in Hep3B (a human hepatocellular carcinoma cell line)

cell-based respiration assay, using intact Hep3B cells. Compounds **3** – **5** exerted time- and concentration-dependent biphasic effects on the Hep3B cell oxygen consumption similar to their effects on T47D cell respiration. However, Hep3B cells were more sensitive to the effects of the compounds, compared to the T47D cells (Figures 4.8A – D). Since Hep3B cells are of neoplasmic origin, these compounds needs to be further evaluated against primary hepatocytes or purified mammalian liver mitochondria to eliminate the possibility of tumor cell-selective toxicity. The magnitude of toxicity toward primary hepatocytes or purified mitochondria by these compounds will be indicative of the potential adverse effects in the healthy population.

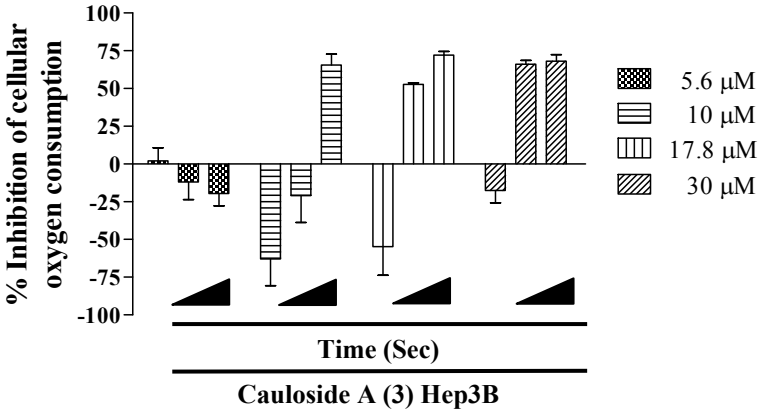

Figure 4.8A Concentration-response effect of cauloside A (**3**) on Hep3B cell respiration. Cauloside A (**3**) was tested at 5.6, 10.0, 17.8 and 30.0 µM. Oxygen consumption rates were recorded 30, 115 and 295 seconds after each treatment and the data were presented as percentage inhibition of oxygen consumption rate compared to the average oxygen consumption rate of untreated T47D cells. Negative values indicate a relative stimulation of oxygen consumption. Data shown are average + standard deviation from three independent experiments (n = 3).

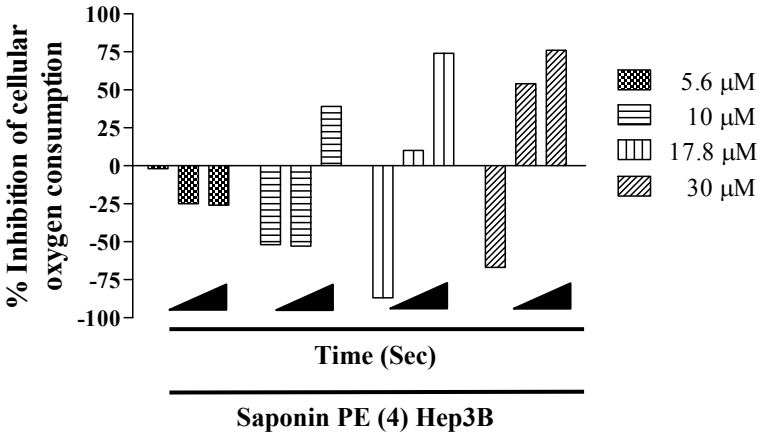

Figure 4.8B Concentration-response effect of saponin PE (**4**) on Hep3B cell respiration. Saponin PE (**4**) was tested at 5.6, 10.0, 17.8 and 30.0 µM. Oxygen consumption rates were recorded 30, 115 and 295 seconds after each treatment and the data were presented as percentage inhibition of oxygen consumption rate compared to the average oxygen consumption rate of untreated T47D cells. Negative values indicate a relative stimulation of oxygen consumption. Data shown are values obtained from a representative experiment (n = 1).

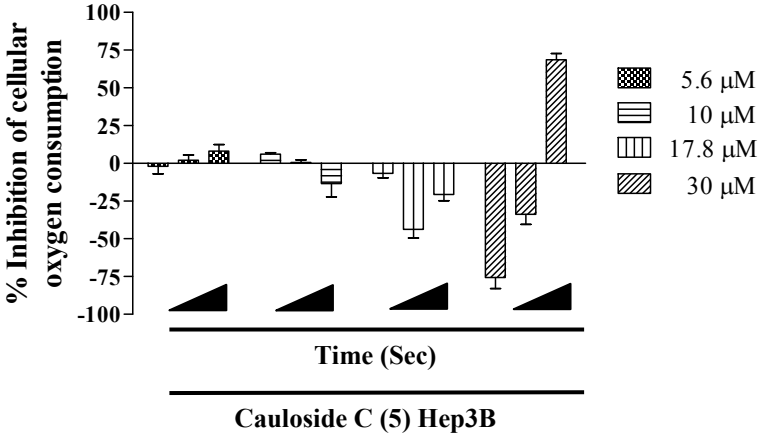

Figure 4.8C Concentration-response effect of cauloside C (**5**) on Hep3B cell respiration. Cauloside C (**5**) was tested at 5.6, 10.0, 17.8 and 30.0 µM. Oxygen consumption rates were recorded 30, 115 and 295 seconds after each treatment and the data were presented as percentage inhibition of oxygen consumption rate compared to the average oxygen consumption rate of untreated T47D cells. Negative values indicate a relative stimulation of oxygen consumption. Data shown are average + standard deviation from three independent experiments (n = 3).

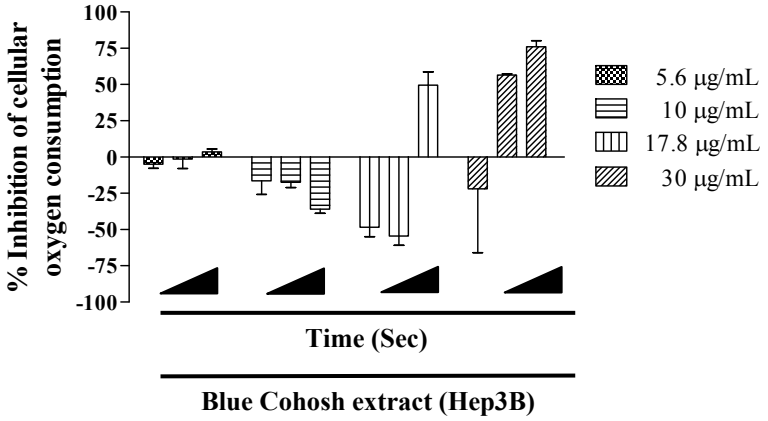

Figure 4.8D Concentration-response effect of blue cohosh extract on Hep3B cell respiration. Blue cohosh extract was tested at 5.6, 10.0, 17.8 and 30.0 µg/mL. Oxygen consumption rates were recorded 30, 115 and 295 seconds after each treatment and the data were presented as percentage inhibition of oxygen consumption rate compared to the average oxygen consumption rate of untreated T47D cells. Negative values indicate a relative stimulation of oxygen consumption. Data shown are average + deviation from the mean from two independent experiments ($n = 2$).

The protonophore control 2-[{4-(trifluoromethoxy)phenyl}hydrazinylidene]propanedinitrile (FCCP, **26**, Figure 4.5B) [0.3 µM] stimulated oxygen consumption in both T47D and Hep3B cells; although the effect was greater in Hep3B cells, relative to the effect on T47D cells. However, **26** (0.3 µM) did not show a time-dependent biphasic effect on cell respiration (Figure 4.9).

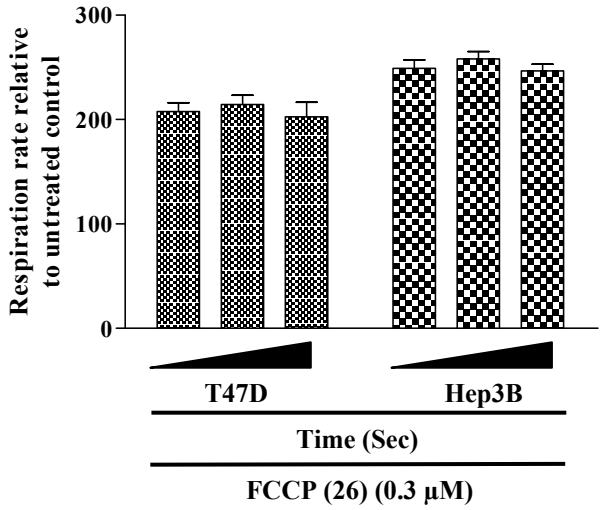

Figure 4.9 Effect of FCCP (**26**) on T47D and Hep3B cell respiration. Compound **26** was tested at 0.3 μM in both the cell lines. Oxygen consumption rates were recorded 30, 115 and 295 seconds after each treatment and the data were presented as relative respiration rates. Positive values indicate a relative stimulation of oxygen consumption. Data shown are average + standard deviation from three independent experiments (n = 3).

Since **26** did not show a time-dependent biphasic response on cell respiration, it is unlikely that simple protonophoric activity is responsible for the observed effects of **3** – **5** on mitochondrial respiration. Structurally, these compounds are plant saponins and plant saponins are reported to interact with, and solubilize cell membranes (Wassler *et al.*, 1987). Hence, we hypothesized that blue cohosh saponins disregulate cell respiration by permeabilizing the plasma and mitochondrial membranes. We further hypothesized that digitonin (**27**, Figure 4.2), a plant saponin commonly used in mechanistic mitochondrial studies, would exert similar a similar effect on cellular respiration. To selectively permeabilize the plasma membrane, we used a relatively low concentration of **27** (4 μM). Addition of **27** (4 μM) to intact cells did not alter oxygen consumption rates of the cells and did not permeabilize the mitochondrial membrane (data not shown). However, at elevated concentrations, **27** (17.8 and 30 μM) produced a time-

dependant biphasic effect on the cellular oxygen consumption similar to the effect observed with the blue cohosh saponins (Figure 4.10).

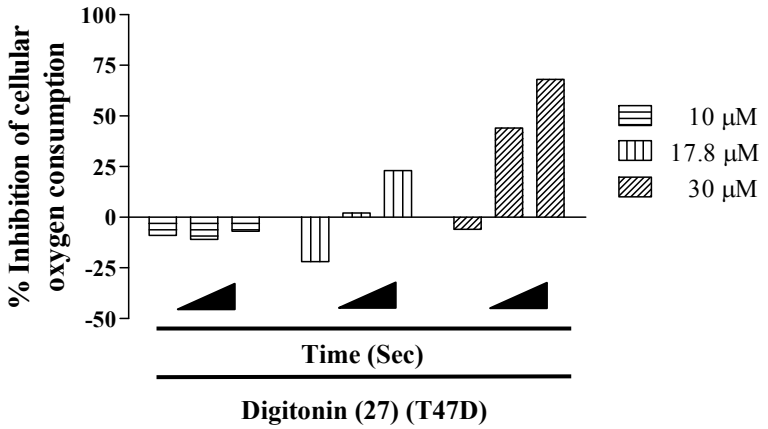

Figure 4.10 Concentration-response effect of digitonin (**27**) on T47D cell respiration. Digitonin (**27**) was tested at 10.0, 17.8 and 30.0 μM. Oxygen consumption rates were recorded 30, 115 and 295 seconds after each treatment and the data were presented as percentage inhibition of oxygen consumption rate compared to the average oxygen consumption rate of untreated T47D cells. Negative values indicate a relative stimulation of oxygen consumption. Data shown are recording from a single experiment.

Dicarboxylic acids, and succinic acids, are Kreb's cycle intermediates that serve as substrates for mitochondrial oxidation at mitochondrial and complex II. However, because succinate forms anion in solution, it cannot penetrate the plasma membrane. The mitochondrial inner membrane contains specialized transporters that transport succinate into the mitochondrial matrix. When added externally, succinate acts as a substrate for complex II and overcome mitochondrial complex I inhibitor-induced inhibition of cell respiration only when the plasma membrane is permeabilized. Digitonin (**27**) [4 μM] is routinely used to selectively permeabilize the plasma membrane. Selective plasma membrane permeabilization with **27** is performed in whole cell-based mitochondrial mechanistic studies to manipulate substrates at specific mitochondrial complexes. To assess whether blue cohosh saponins permeabilize the cellular

membranes, we examined cauloside A (**3**) as a representative compound. In the presence of **3** (10 μM), externally supplemented succinate (5 mM) restored T47D cell oxygen consumption in the presence of the complex I inhibitor rotenone (1 μM). However, at a reduced concentration, **3** (5.6 μM) did not produce an observable membrane permeabilization effect (Figures 4.11A – C). These observations correlate with the previously observed effects of **3** on cell respiration.

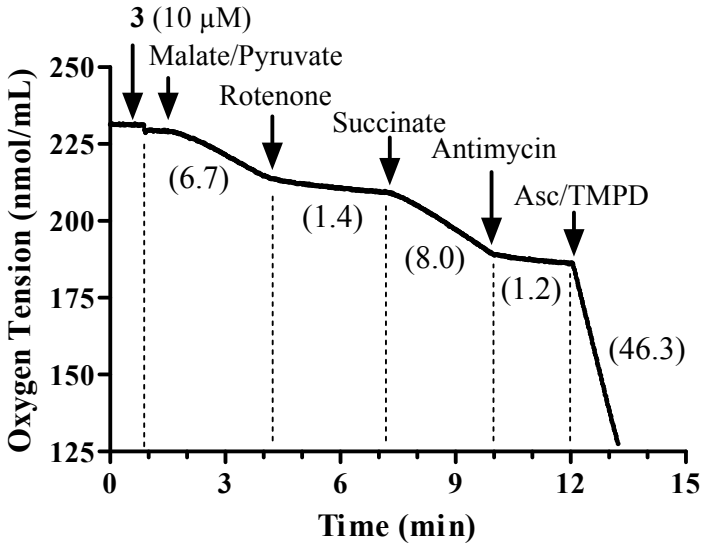

Figure 4.11A Effect of cauloside A (**3**) membrane permeabilization on T47D cell respiration. Cauloside A (**3**) was tested at 10 μM. Oxygen consumption rates were recorded after each treatment and the average oxygen consumption rate for each section are given in the parentheses. Data shown are recordings from a representative experiment (n = 1).

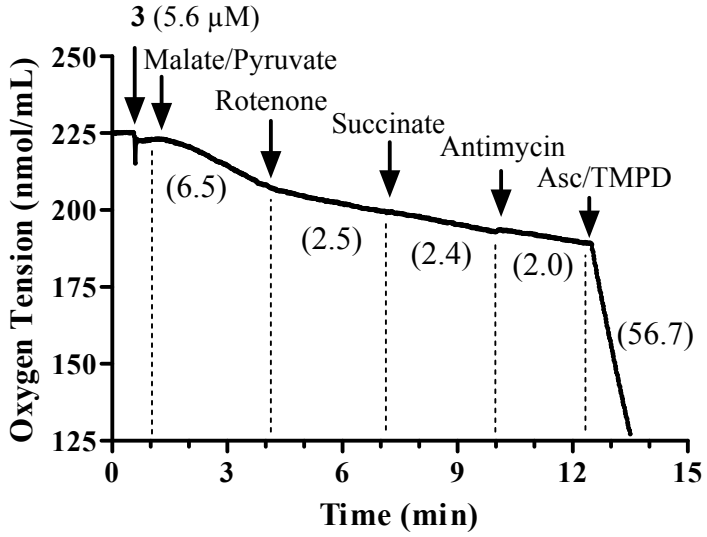

Figure 4.11B Effect of cauloside A (**3**) membrane permeabilization on T47D cell respiration. Cauloside A (**3**) was tested at 5.6 μM. Oxygen consumption rates were recorded after each treatment and the average oxygen consumption rate for each section are given in the parentheses. Data shown are recordings from a representative experiment (n = 1).

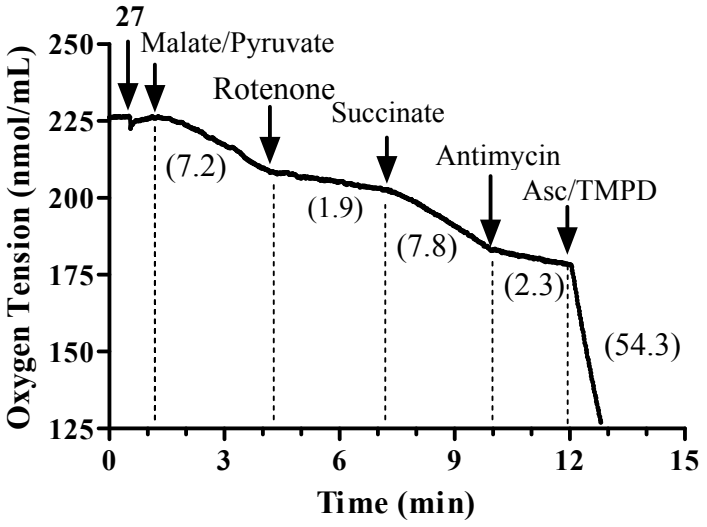

Figure 4.11C Effect of digitonin (**27**) membrane permeabilization on T47D cell respiration. Digitonin (**27**) was tested at 4 μM. Oxygen consumption rate was recorded after each treatment and the average oxygen consumption rate for each section are given in the parentheses. Data shown are recording from a representative experiment (n = 1).

The results observed in Figures 4.11A – C support our hypothesis that **3** – **5** exert their effects on cellular oxygen consumption indirectly by permeabilizing cell membranes. The initial stimulation of cellular respiration is possibly due to the saponins disrupting the lipid packing of mitochondrial inner membrane leading to proton leak into the matrix. Exposure of mitochondrial inner membrane to the saponins for longer period of time possibly result in complete solubilization of the membrane causing complete disruption of oxidative phosphorylation and thus leads to time-dependent biphasic effects. These compounds are not selective mitochondrial inhibitors. However, when present in sufficient concentrations, they cause mitochondrial dysfunction due to their detergent-like properties.

4.3.2.2 Ursolic and oleanolic acids

Lipophilic weak organic acids such as ursolic acid (**28)** have been previously reported to uncouple oxidative phosphorylation in isolated rat heart mitochondria (Liobikas *et al.*, 2011). Oleanolic acid (**9**), a weak organic acid, is a regioisomer of ursolic acid. The oleanane-type saponins found in blue cohosh contain oleanolic acid or a modified oleanolic acid moiety as their core sapogenin. To rule out the potential for mitochondrial uncoupling caused by the free carboxylic group in the aglycone moiety, the effects of **9** on cell respiration was investigated. Oleanolic acid (up to 30 μM) did not exert any observable effects on cell respiration using intact T47D and Hep3B cells (data not shown). When **28** (0.03 – 30 μM) was examined at the concentrations within the range that was previously reported to uncouple oxidative phosphorylation, **28** did not affect respiration in either intact or digitonin-permeabilized T47D cells. Similarly, **28** (0.03 – 30 μM) treatment did not affect Hep3B (intact) respiration (Figure 4.12). These results contradict a previous report that **28** uncouples mitochondria (Liobikas *et al.*,

2011). Our results suggest that the inability of **28** to uncouple mitochondrial respiration may result from differences in the experimental models (intact/permeabilized cells *vs.* isolated mitochondria or the use of heart mitochondria *vs.* breast/liver cancer cells).

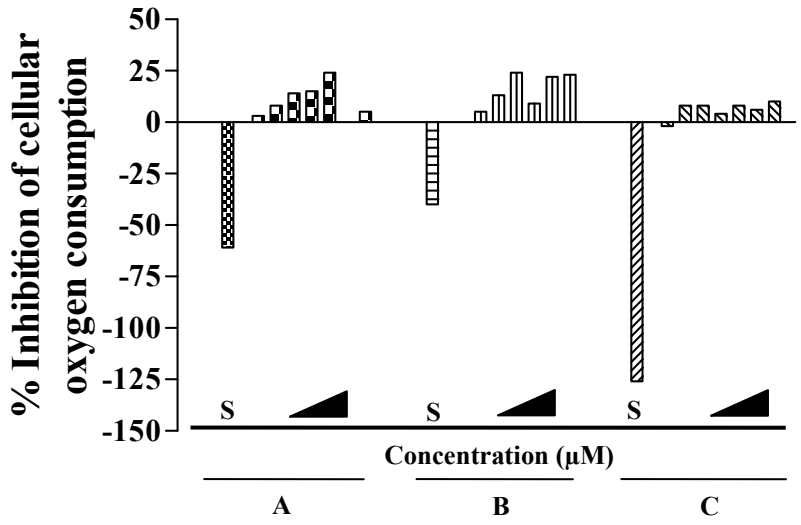

Figure 4.12 Concentration-response effects of ursolic acid (**28**) on intact (**A**) and digitonin-permeabilized (**B**) T47D and intact Hep3B (**C**) cell respiration. Compound **28** was tested at 0.03 – 30 μM in both the cell lines in half-log increments and FCCP (**26**) [0.3 μM] was used as a standard (**S**). Oxygen consumption rates were recorded after each treatment and the data were presented as percentage inhibition of oxygen consumption rates compared to the average oxygen consumption rate of untreated intact T47D and Hep3B cells. For the digitonin-permeabilized T47D cells digitonin (4 μM) was used to selectively permeabilize the plasma membrane and the percentage inhibition of oxygen consumption was calculated by comparing with the initial (untreated) oxygen consumption rates of the cells. Data are from a single representative experiment (n = 1).

4.3.2.3 Guggul (*Commiphora wightii*)

The extract of guggul [*Commiphora wightii* (Arn.) Bhandari (Burseraceae)] was identified as a possible mitochondriotoxic herbal dietary supplement. Seven pure compounds from guggul gum resin were obtained from Dr. Khan's pure compound repository (Figure 4.5A) and examined in the T47D cell-based HIF-1 reporter assay (Figures 4.13A – B).

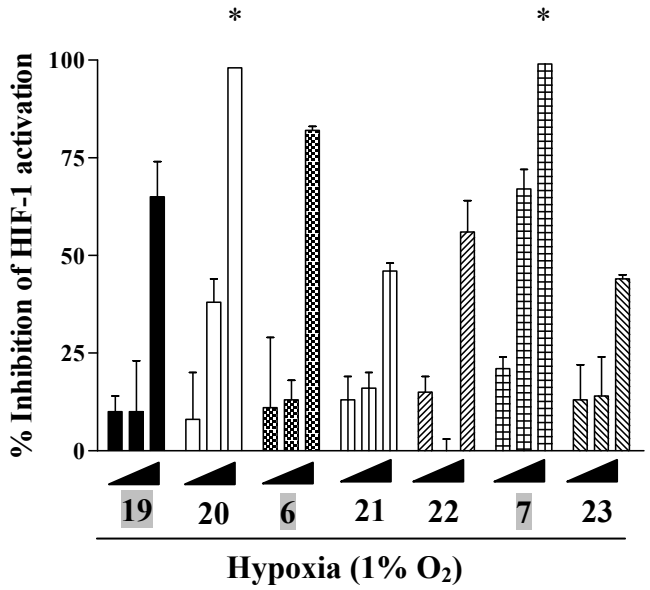

Figure 4.13A Inhibition of hypoxia-induced HIF-1 by guggul compounds. Transfected (pTK-HRE3-luc) T47D cells were treated with compounds (1, 10 and 30 μM) and exposed to hypoxia (1% O_2) for 16 h. Data shown are average + standard deviation from a representative experiment performed in triplicate. Absence of error bars due to identical readings for any data point is denoted by '*'.

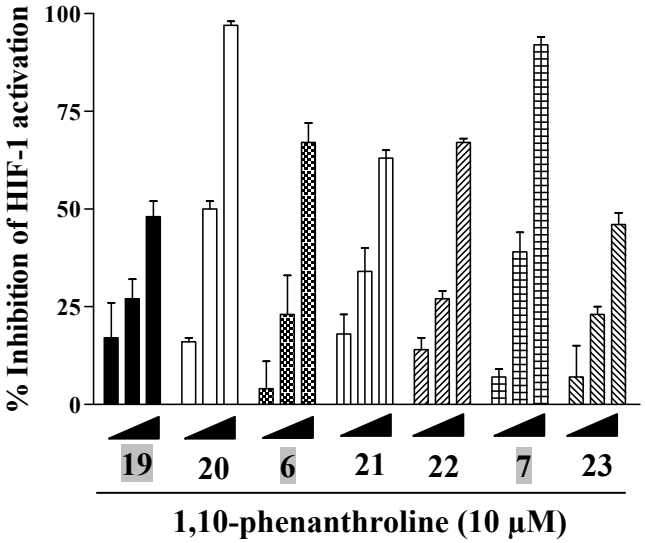

Figure 4.13B Inhibition of 1,10-phenanthroline-induced HIF-1 by guggul compounds. Transfected (pTK-HRE3-luc) T47D cells were treated with compounds (1, 10 and 30 μM) and exposed to 1,10-phenanthroline (10 μM) for 16 h. Data shown are average + standard deviation from a representative experiment performed in triplicate.

Of the seven compound tested, compounds (13*E*,17*E*,21*E*)-8-hydroxypolypodo-13,17,21-trien-3-one (**19**), sesamin (**6**), and guggulsterol III (**7**) showed increased potency against hypoxia-induced HIF-1 activity relative to iron chelator-induced HIF-1, which suggested that they may inhibit mitochondrial respiration. These compounds were further evaluated in a T47D cell-based respiration assay. The concentration-response effects of these three compounds and the guggul extract (**G**) were determined. Among the three compounds **6** (30 μM) and **7** (10 μM) strongly suppressed cellular respiration while **19** was inactive (Figure 4.14). Compound **20** and **21** were weak (< 30% inhibition at 30 μM) suppressors of mitochondrial respiration (data not shown).

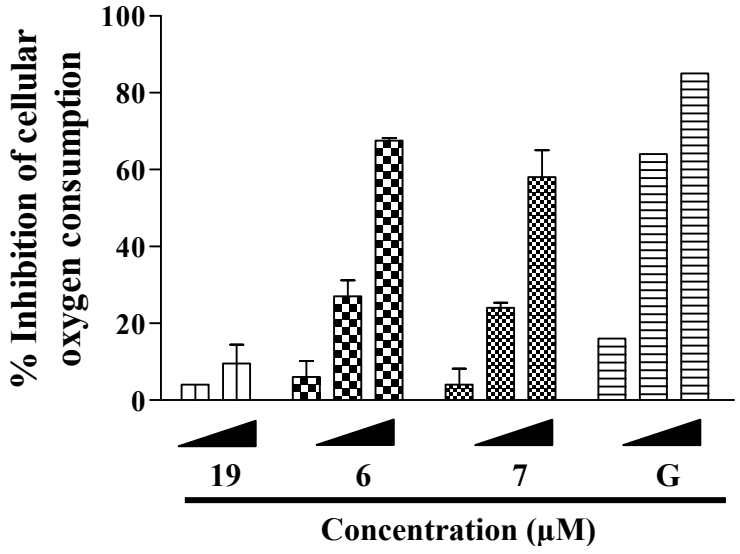

Figure 4.14 Concentration-response effects of **19**, **6**, **7** and guggul extract (**G**) on the T47D cell respiration. Compound **19** was tested at 10 and 30 μM. Compound **6** was tested at 3, 10 and 30 μM. Compound **7** was tested at 1, 3, and 10 μM. Guggul extract (**G**) was tested at 10, 30 and 100 μg/mL. Oxygen consumption rates were recorded after each treatment and the data were presented as percentage inhibition of oxygen consumption rates compared to the average oxygen consumption rate of untreated T47D cells. Data are average + deviation from the mean for **19**, **6**, and **7** from two independent experiments ($n = 2$), while for **G** data are from a single representative experiment ($n = 1$).

Mechanistic studies were performed to identify the mitochondrial complex(es) targeted by the guggul compounds. In digitonin-permebilized cells, addition of exogenous succinate (5 mM) restored cell respiration that had been inhibited by sesamin (**6**) and guggulsterol III (**7**). This indicates that these compounds selectively inhibit mitochondrial complex I (Figures 4.15A – B).

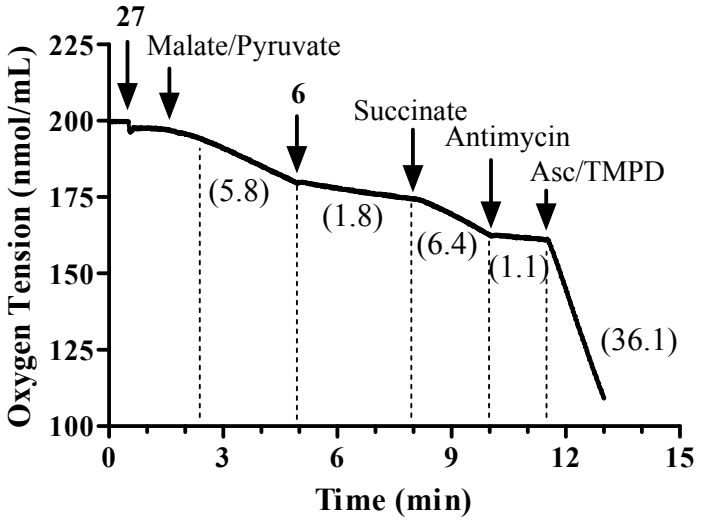

Figure 4.15A Sesamin (**6**) [30 μM] inhibits mitochondrial respiration by selectively targeting mitochondrial complex I. Exponentially cultured T47D cells (5 x 10^6) were permeabilized with digitonin (4 μM) and respiratory complex substrates and **6** (30 μM) were added sequentially as specified. Sesamin (**6**) [30 μM] did not affect complex II, III or IV. Data are from a representative experiment.

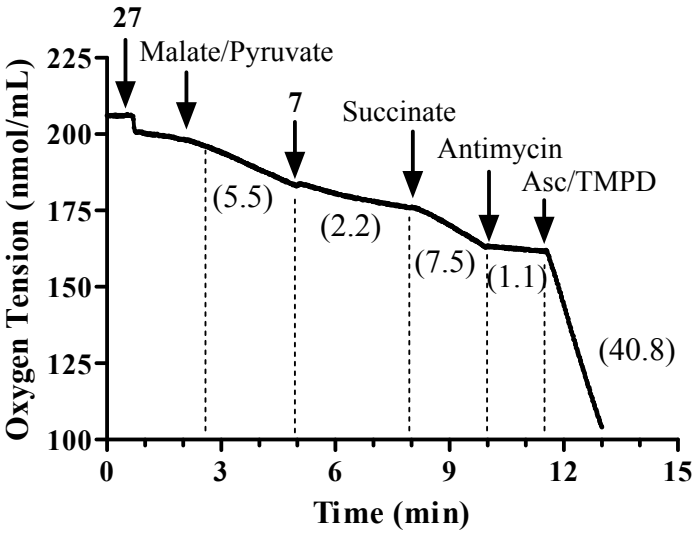

Figure 4.15B Guggulsterol III (**7**) [10 μM] inhibits mitochondrial respiration by targeting complex I. Exponentially cultured T47D cells (5 x 10^6) were permeabilized with digitonin (4 μM) and respiratory complex substrates and **7** (10 μM) were added sequentially as specified. Guggulsterol III (**7**) [10 μM, did not affect complex II, III or IV. Data are from a representative experiment.

4.3.3 Cytotoxicity of herbal dietary supplement compounds

4.3.3.1 Blue Cohosh (*Caulophyllum thalictroides*)

The cytotoxic potential of cauloside A (**3**), saponin PE (**4**), cauloside C (**5**), cauloside B (**15**), and blue cohosh extract were evaluated in both 2-day and 6-day cell viability assays using the sulforhodamine B method. Both human breast tumor (T47D) and hepatocarcinoma (Hep3B) cells were used as experimental models. The purified blue cohosh saponins and the extract demonstrated potent cytotoxic activity in both cell lines (Figures 4.16A – E). The saponins and the extract were more toxic to Hep3B cells. This preferential cytotoxicity was consistent with the results obtained in respiration studies. The cytotoxicity also increased with extended cell exposure, as the IC_{50} values were significantly lower in the 6-day cell viability assay, relative to

the 2-day cell viability assay (Tables 4.1 and 4.2). We have observed this kind of activity profile with the compounds that interfere with mitochondrial function. The maximum solvent present in the assay was 1.1% v/v. The effect of solvent alone on cell viability was minimal (< 10%) even after 6 days of incubation.

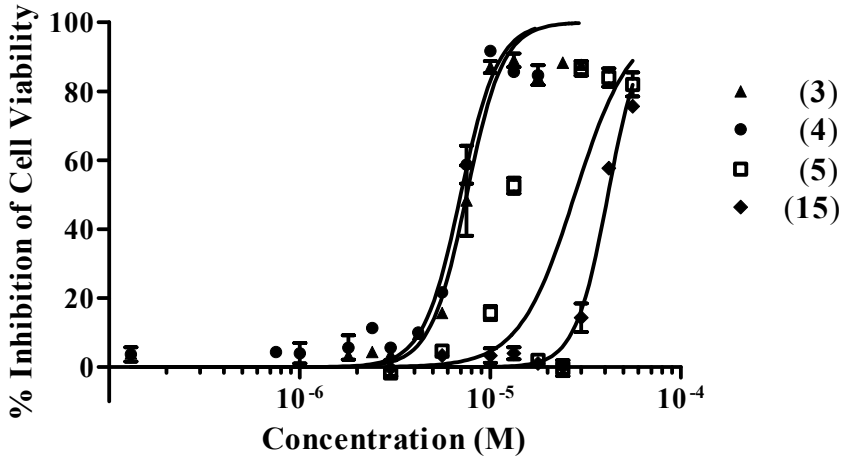

Figure 4.16A Effect of blue cohosh compounds on Hep3B cell viability following short-term (48 h) incubation. Exponentially cultured Hep3B cells were incubated for 48 h with the test compounds (**3**, **4**, **5** and **15**) and cell viability was measured using the sulforhodamine B method. Data shown here are average ± standard deviation from a representative experiment performed in triplicate.

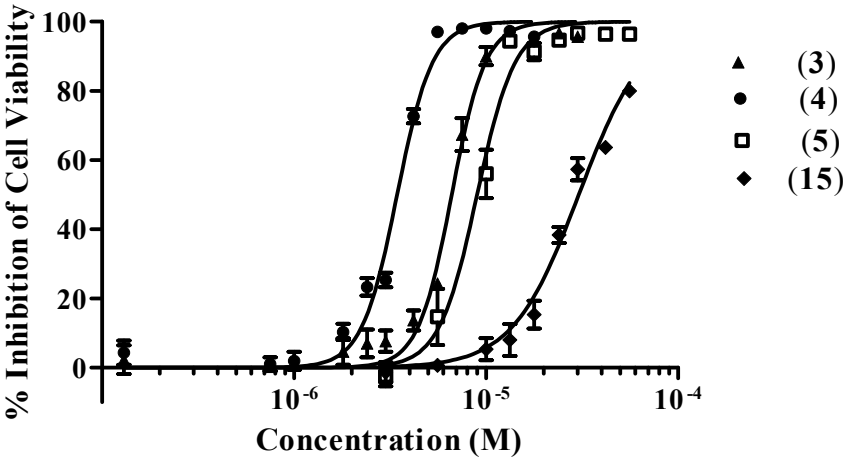

Figure 4.16B Effect of blue cohosh compounds on Hep3B cell viability following prolonged (6-day) incubation. Exponentially cultured Hep3B cells were incubated for 6 days with the test compounds (**3**, **4**, **5** and **15**) and cell viability was measured using the sulforhodamine B method. Data shown here are average ± standard deviation from a representative experiment performed in triplicate.

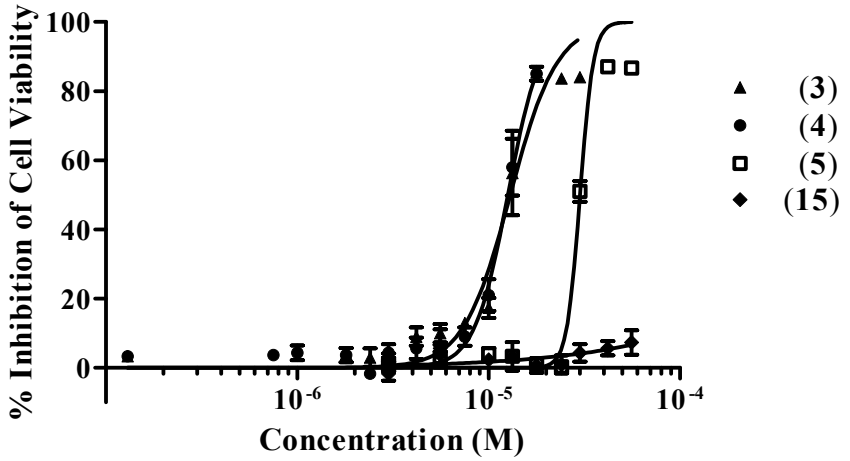

Figure 4.16C Effect of blue cohosh compounds on T47D cell viability following short-term (48 h) incubation. Exponentially cultured T47D cells were incubated for 48 h with the test compounds (**3**, **4**, **5** and **15**) and cell viability was measured using the sulforhodamine B method. Data shown here are average ± standard deviation from a representative experiment performed in triplicate.

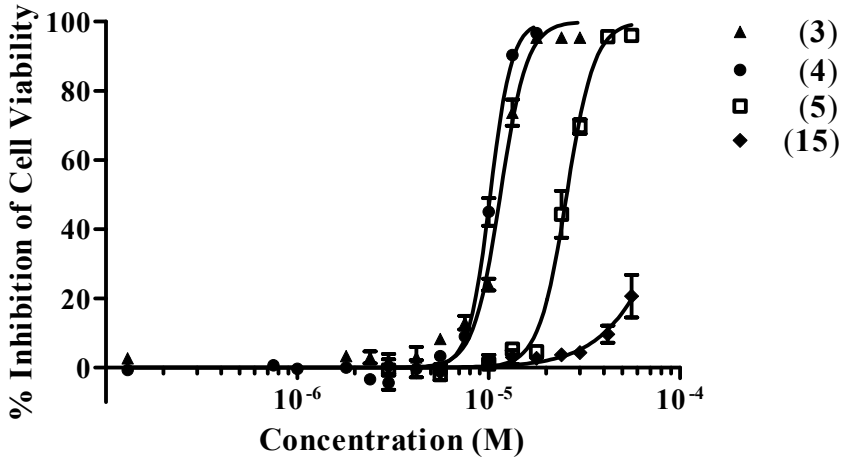

Figure 4.16D Effect of pure blue cohosh compounds on T47D cell viability following prolonged (6-day) incubation. Exponentially cultured T47D cells were incubated for 6 days with the test compounds (**3**, **4**, **5** and **15**) and cell viability was measured using the sulforhodamine B method. Data shown here are average ± standard deviation from a representative experiment performed in triplicate.

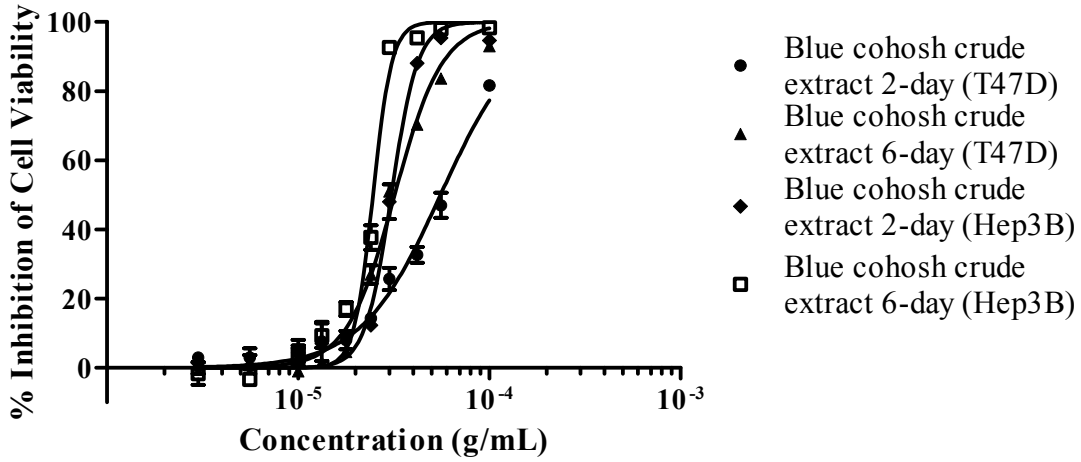

Figure 4.16E Effect of the blue cohosh extract on T47D and Hep3B cell viability following 2-day and 6-day incubation periods. Exponentially grown T47D and Hep3B cells were incubated for 48 h or 6 days with blue cohosh extract and cell viability was measured using the sulforhodamine B method. Data shown here are average ± standard deviation from a representative experiment performed in triplicate.

Compound/ Extract	**IC_{50} (95% CI) µM (or µg/mL*)**	
	T47D	
	48 h	6 days
3	12.98 (12.21 - 13.80)	11.52 (11.21 – 11.85)
4	12.60 (12.23 - 12.99)	10.21 (10.08 – 10.35)
5	30.07 (29.30 - 30.86)	25.60 (25.03 – 26.18)
15	> 56	>56
*Blue cohosh extract	55.61 (52.69 – 58.68)	32.03 (30.92 – 33.19)

Table 4.1 IC_{50} values of **3**, **4**, **5**, **15** and the blue cohosh extract on T47D cell proliferation/viability in a concentration-response study (2-day and 6-day). Data shown are from a representative experiment performed in triplicate.

Compound/ Extract	**IC_{50} (95% CI) µM (or µg/mL*)**	
	Hep3B	
	48 h	6 days
3	7.53 (7.11 – 7.98)	6.63 (6.41 – 6.87)
4	7.00 (6.63 – 7.39)	3.45 (3.32 – 3.58)
5	27.83 (22.31 – 34.72)	8.99 (8.46 – 9.56)
15	41.49 (40.13 – 42.89)	30.44 (28.95 – 32.00)
*Blue cohosh extract	30.77 (29.93 – 31.64)	24.66 (23.91 – 25.43)

Table 4.2 IC_{50} values of **3**, **4**, **5**, **15** and the blue cohosh extract in Hep3B cell proliferation/viability in a concentration-response study (2-day and 6-day). Data shown are from a representative experiment performed in triplicate.

Oleanolic acid (**9**) was examined for its cytotoxic effect on T47D cells. Compound **9** (30 µM) was mildly cytotoxic only in 6-day cell proliferation/viability assay (< 30% inhibition of cell viability at 30 µM).

4.3.3.2 Guggul (*Commiphora wightii*)

Six pure compounds isolated from guggul were evaluated in the T47D cell proliferation/viability assay. The compounds and the guggul extract showed time- and concentration-dependent suppression of the T47D cell proliferation/viability (Figures 4.17A – C). Guggulsterol III (**7**) was the most potent among the compounds tested (IC_{50} values 13.8 µM and 3.38 µM, in 2-day and 6-day cell viability assays, respectively (Table 4.3). The guggul extract was more cytotoxic upon extended exposure, suggesting mitochondrial disruption may be responsible for the observed cytotoxicity.

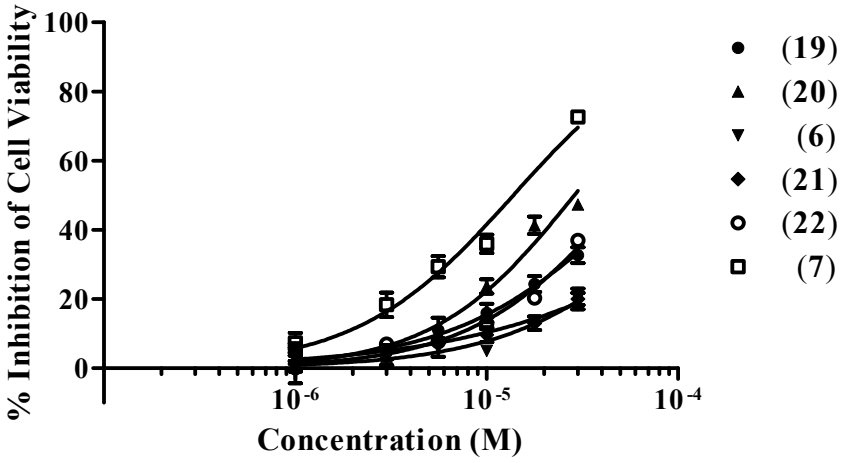

Figure 4.17A Effect of guggul compounds on T47D cell viability following short-term (48 h) incubation. Exponentially cultured T47D cells were incubated for 48 h with the test compounds and cell viability was measured using the sulforhodamine B method. Data are average ± standard deviation from a representative experiment performed in triplicate.

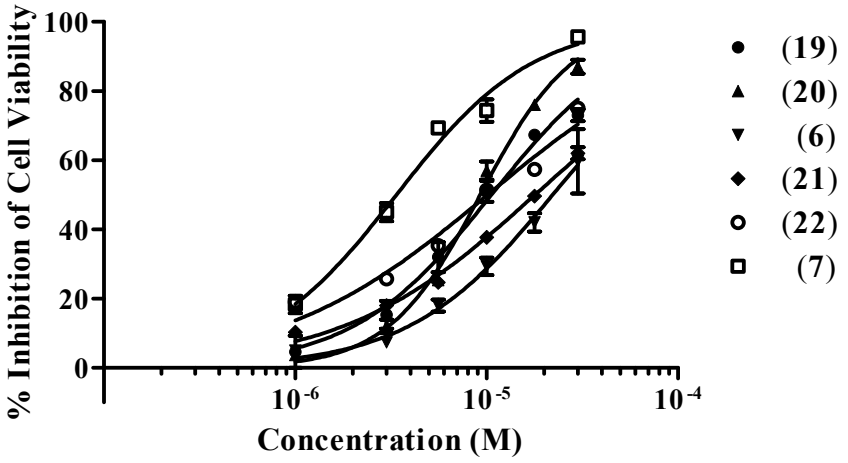

Figure 4.17B Effect of guggul compounds on T47D cell viability following long-term (6-day) incubation. Exponentially cultured T47D cells were incubated for 6 days with the test compounds and cell viability was measured using the sulforhodamine B method. Data here are average ± standard deviation from a representative experiment performed in triplicate.

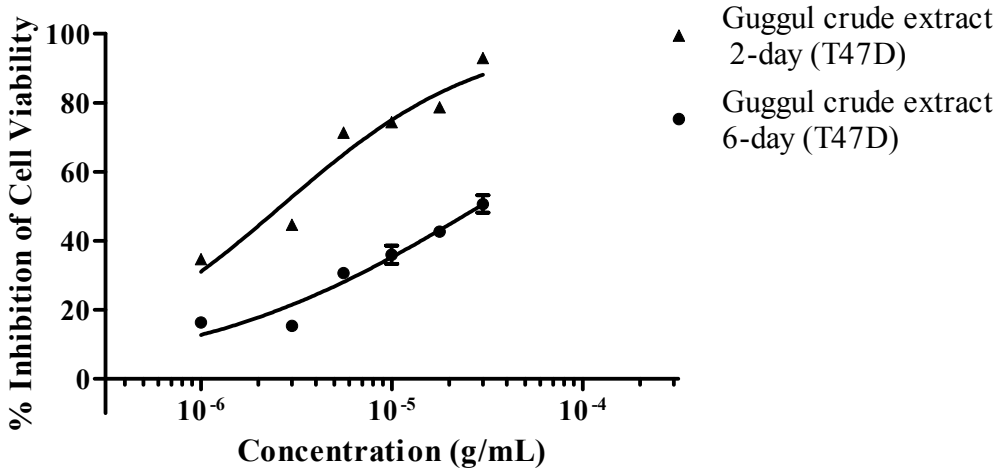

Figure 4.17C Effect of guggul extract on T47D cell viability following 2-day and 6-day incubation periods. Exponentially cultured T47D cells were incubated for either 48 h or 6 days with the guggul extract and cell viability was measured using the sulforhodamine B method. Data are average ± standard deviation from a representative experiment performed in triplicate .

Compound/ Extract	**IC_{50} (95% CI) µM (µg/mL*)**	
	T47D	
	48 h	6 days
19	> 30	10.60 (9.69 – 11.61)
20	28.75 (25.26 – 32.72)	9.28 (8.82 – 9.76)
6	>30	22.15 (19.78 – 24.81)
21	> 30	17.90 (16.88 – 18.99)
22	> 30	10.12 (9.01 – 11.38)
7	13.80 (12.13 – 15.70)	3.38 (3.06 – 3.73)
*Guggul extract	49.33 (40.72 – 59.78)	5.75 (5.03 – 6.58)

Table 4.3 Human breast cancer T47D cell proliferation/viability study. The IC_{50} values of **6**, **7**, **19**, **20**, **21**, **22** and the guggul extract on in a 2-day and 6-day exposure concentration-response study. Data are from a representative experiment performed in triplicate.

Mitochondria are important cellular organelles, mediating cell death (Green and Kroemer, 2004). Drug-induced toxicity is often mediated through the induction of mitochondrial

dysfunction and resulting cell death (Begriche *et al.*, 2011). Botanical dietary supplements and herbal remedies are widely consumed for a variety of health conditions. They are often perceived as safe and devoid of adverse effects or toxicity due to their natural origin. However, toxicities due to botanical dietary supplement consumption have been reported (Stickel *et al.*, 2011). The toxicities are often similar in nature to the toxicities observed with compounds that target the mitochondria (Frazier and Krueger, 2009). Mitochondriotoxic substances are common in nature and, while chemically undefined, botanical dietary supplements and other herbal remedies are likely to have a similar potential to induce mitochondrial dysfunction as clinically approved drugs or other synthetic molecules. Currently the data on the presence of possible mitochondriotoxic substances in the dietary supplements and their daily consumption, percentage yield, bioavailability, metabolism, and pharmacokinetics are unavailable. Hence, it is difficult to predict whether or not these compounds are in high enough concentrations to cause toxicity in vivo. Mitochondria play an important regulatory role in hypoxia-induced HIF-1 activation (Agani *et al.*, 2000). Inhibition of the mitochondrial ETC strongly prevents activation and stabilization of hypoxia-induced HIF-1 relative to iron chelator-induced HIF-1 (Coothankandaswamy *et al.*, 2010). Uncoupling of oxidative phosphorylation abolishes HIF-1 activation, regardless of the nature of the inducing stimulus (Du *et al.*, 2010). Even though the class of mitochondrial inhibitors can be a valuable tool in antitumor therapy, these compounds can produce serious adverse effects in healthy individuals.

A T47D cell-based HIF-1 reporter gene assay, in conjunction with an intact cell-based respiration assay, was used to preliminarily identify mitochondriotoxic extracts from plants used in botanical dietary supplement products. Over 350 botanical dietary supplement plant extracts from the National Center for Natural Products Research (NCNPR) repository were evaluated in a

human breast cancer T47D cell-based HIF-1 reporter gene assay. The extracts that preferentially inhibited hypoxia-induced HIF-1 activation were selected and reconfirmed in a T47D cell-based cell respiration assay. Blue cohosh and guggul extracts were identified as hits in the screening and confirmatory assays. Pure compounds previously isolated from blue cohosh and guggul were obtained from Dr. Ikhlas A. Khan's pure compound repository. The saponin glycosides from blue cohosh [cauloside A (**3**), saponin PE (**4**), and cauloside C (**5**)] disrupted both hypoxia-induced and 1,10-phenanthroline-induced HIF-1 activation. Saponins are amphiphylic in nature and are known to form pores in the lipid bilayer of cellular membranes. Further investigation revealed that HIF-1 inhibition and the biphasic effect on cellular oxygen consumption by these compounds and blue cohosh extract were due to the membrane disrupting properties of the saponins. Oleanolic acid (**9**), which is structurally similar to the aglycone part of the saponin glycosides, was inactive in the mitochondrial respiration assay. The presence of an additional hydroxy group on the aglycone core reduced the bioactivity of the saponins. The hepatocellular carcinoma cell line Hep3B was more sensitive to the saponins **3** – **5** relative to its effect on the breast cancer T47D cell line. This difference in sensitivity may result from differences in their membrane lipid composition, a concept that may warrant further study. The cytotoxicity of saponins in various tumor cell lines has been reported previously (Podolak *et al.*, 2010). The blue cohosh extract and the blue cohosh pure compounds were cytotoxic to both T47D and Hep3B cells, with higher potency in Hep3B cells. It is particularly noteworthy that oleanolic acid (**9**) was inactive in the T47D-cell based cellular respiration and the viability assays indicate that the sugar moieties are essential for the activities. Since the overall tumor cell selectivity profile of these compounds are yet to be established, it is possible that mammalian hepatocytes could be similarly susceptible to the membrane disrupting activity of blue cohosh saponins and blue

cohosh extract. In that case, the potential for hepatotoxicity from consuming herbal remedies that contain blue cohosh is greater than previously estimated. Blue cohosh (*Caulophyllum thalictroides*) is a plant indigenous to North America that has a history of traditional use. As a dietary supplement it is used as an antispasmodic, emenagogue (menstrual flow stimulator), parturifacient (labor inducer) and abortifacient (Dugoua *et al.*, 2008). In 1999, it was estimated that 64% of midwives in the US used blue cohosh as a labor-inducer (McFarlin *et al.*, 1999). However, the safety profile and adverse effects of blue cohosh in pregnant women and neonates are unknown. Perinatal stroke, acute myocardial infarction, congestive heart failure, multiple organ injury and shock in neonates have been associated with consumption of blue cohosh tincture/dietary supplements (Dugoua *et al.*, 2008). Such idiosyncratic toxicities may be explained by the plasma and mitochondrial membrane permeabilizing effects of saponin glycosides. Further monitoring and reporting of adverse effects due to blue cohosh consumption is required to better understand the toxic potential of this over-the-counter dietary supplement.

Guggul gum resin is a popular dietary supplement used for its hypolipidemic and anti-inflammatory effects (Shishodia *et al.*, 2008). Sporadic cases of guggul-associated hepatotoxicity had been reported (Yellapu *et al.*, 2011; Grieco *et al.*, 2009). However, this work is the first to report that guggul extract and purified guggul gum resin compounds act as mitochondrial ETC inhibitors. Sesamin (**6**) and **7** both inhibit mitochondrial complex I in cellular respiration assays in a concentration-dependent manner. Guggulsterol III (**7**) was more potent than **6**. Compound **19** was inactive in the mitochondrial respiration assay although it preferentially suppressed hypoxia-induced HIF-1 activation. Other compounds (i.e, **20** and **21**) were weak inhibitors (< 30% inhibition at 20 μM, data not shown) of T47D cell respiration. The potency of guggul extract to suppress mitochondrial respiration cannot be fully explained by the activity of these

two compounds. It is possible that other known or unreported, compounds present in the guggul extract contribute towards the enhanced mitochondrial suppression observed with guggul extract. Irrespective of their activity profile in the mitochondrial respiration assay, six out of seven guggul compounds strongly suppressed T47D cell viability (IC_{50} values 3.38 – 22.15 μM, 6-day assay). However, these guggul compounds were only weakly cytotoxic in 2-day cell viability studies. Direct mitochondrial ETC targeting does not seem to be the main cytotoxic mechanism for some of these compounds and it is possible that these substances exert their effects through non-mitochondrial mechanism. Alternatively, weak mitochondrial inhibition for a prolonged period or metabolic activation of the compounds may produce the observed suppression of cell proliferation/viability. It must be noted that while the guggul extract, *E*- and *Z*-guggulsterone, and other isolated guggul compounds are cytotoxic to T47D cells; their selectivity profile has not been established. Further investigations to characterize the toxicity and selectivity profile of the guggul extract and isolated guggul compounds are required. Until the toxicity profiles and mechanisms for toxicity are completely defined, caution should be exercised with the use of botanical dietary supplements/herbal remedies that contain guggul.

Another notable observation during this investigation was the inability of ursolic acid (**28**) (0.03 – 30 μM) to uncouple oxidative phosphorylation in both intact and permeabilized T47D and Hep3B cells. This contradicts a previous report that demonstrated the mitochondrial uncoupling effect of **28** in isolated rat heart mitochondria (Liobikas *et al.*, 2011). However, the selection of the experimental model to evaluate the mitochondrial function during screening and respiration studies of mitochondriotoxic agents is critical. Intact or permeabilized cells are more complex systems than isolated mitochondria. The difference in plasma membrane permeability and/or protein binding between intact and permeabilized cells might affect the activity observed

in either system. While it can be argued that respiration in cell-based systems may be influenced by non-mitochondrial factors, intact cells may be more physiologically relevant as models for the study of chemical toxins with unknown membrane permeability profiles. Further, the loss of intracellular communication between organelles and the loss of mitochondrial network structure might also produce artifactual results in studies that evaluate potential mitochonriotoxic agents in isolated mitochondria (Brand and Nicholls, 2011).

SUMMARY

Small-molecules that target cellular bioenergetics are an emerging class of antitumor agents. Successful discovery of natural product small-molecules that inhibit glycolysis and/or oxidative phosphorylation depends on proper identification and valiadation of a target; a robust screening system; bioassay-guided fractionation; structure elucidation; biological characterization, and multiple other factors. Selection of chromatographic media for bioassay-guided isolation is one of the many critical steps in the drug discovery process. Hypoxia-inducible factor-1 (HIF-1) is an important antitumor target that regulates cellular bioenergetics. One of the major functions of HIF-1 is regulation of cellular bioenergetics. Mitochondrial inhibitors and uncouplers inhibit HIF-1 activation. During a controlled evaluation of chromatographic media in HIF-1-targeted natural product antitumor drug discovery, it was observed that Si gel has the highest potential to cause poor sample recovery, chemical alterations, and loss of bioactivity. HP20SS, a polystyrenic resin, can be used as an alternative to Si gel in the large scale pre-fractionation of plant or marine organism-derived extracts. However a final wash with an organic solvent, such as EtOAc, is required to completely elute the materials from the HP20SS columns. Highly lipophilic extracts also tend to lose bioactivity after elution through HP20SS columns.

A high rate of aerobic glycolysis in tumor cells is an attractive antitumor target. To discover natural product aerobic glycolysis inhibitors, a bioenergetics-based screening system was developed to evaluatea total of 10,648 10,000 extracts fom the NCI's Open Repository Program... Bioassay-guided isolation of the *Moronobea coccinea* extract resulted in isolation of a new compound named moronone (**1**). Moronone (**1**) is a protonophore that was active in the glycolysis inhibitor screening system. A prototypical protonophore (FCCP) was similarly active.

For successful identification of glycolysis inhibitors, the protonophoric compounds (nuisance compounds or false positives) should be rapidly dereplicated.

Even though mitochondrial inhibitors are useful as potential antitumor agents, long term exposure to mitochondrial inhibitors may result in adverse effects. The potential of mitochondrotoxic agents to cause idiosyncratic adverse effects was evident in the withdrawal of FDA-approved drugs from the market, due to their mitochondrial toxicity. Plant extracts used in botanical dietary supplement (BDS) products were evaluated for mitochondriotoxic activity. Among 46 active extracts, two extracts (blue cohosh and guggul) were subjected to further investigations. Three saponin-type compounds from blue cohosh [cauloside A (**3**), saponin PE (**4**), and cauloside C (**5**)] permeabilized the plasma and mitochondrial membranes, and produced cytotoxic effects in human breast tumor (T47D) and hepatocellular carcinoma (Hep3B) cell lines. Sesamin (**6**) and guggulsterol III (**7**) from guggul selectively inhibited complex I of the electron transport chain. Six compounds from guggul (including **6** and **7**) produced cytotoxic effects in a human breast tumor cell line (T47D). However, guggul extract was more potent than any of the individual compounds. Further investigation is required to identify the presence of other mitochondrial inhibitors in guggul extract. Purified compounds from blue cohosh andguggul, as well asthe extracts, need to be evaluated in primary cell lines or purified mitochondria, in order to assesstheir tumor selectivity profiles and potential in vivo toxicity. These results indicate a necessity for a large scale, systematic investigation of dietary supplements for the presence of the mitochondrial inhibitors.

BIBLIOGRAPHY

Abo-Khatwa, A. N.; al-Robai, A. A.; al-Jawhari, D. A. Lichen acids as uncouplers of oxidative phosphorylation of mouse-liver mitochondria. *Nat Toxins* **1996**, *4* (2), 96–102.

Acuna, U. M.; Jancovski, N.; Kennelly, E. J. Polyisoprenylated benzophenones from Clusiaceae: potential drugs and lead compounds. *Curr Top Med Chem* **2009**, *9* (16), 1560–1580.

Adams, J. The proteasome: a suitable antineoplastic target. *Nat Rev Cancer* **2004**, *4* (5), 349–360.

Agani, F. H.; Pichiule, P.; Chavez, J. C.; LaManna, J. C. The role of mitochondria in the regulation of hypoxia-inducible factor 1 expression during hypoxia. *J Biol Chem* **2000**, *275* (46), 35863–35867.

Alali, F. Q.; Liu, X. X.; McLaughlin, J. L. Annonaceous acetogenins: recent progress. *J Nat Prod* **1999**, *62* (3), 504–540.

Alberts, B.; Johnson, A.; Lewis, J.; Raff, M.; Roberts, K. Walter, P. *Molecular biology of the cell*. 4th ed.; Garland Science: New York, 2002; pp 771–772.

Almeida, A.; Bolanos, J. P.; Moncada, S. E3 ubiquitin ligase APC/C-Cdh1 accounts for the Warburg effect by linking glycolysis to cell proliferation. *Proc Natl Acad Sci U S A* **2010**, *107* (2), 738–741.

Ambekar, C. S.; Lee, J. S.; Cheung, B. M.; Chan, L. C.; Liang, R.; Kumana, C. R. Chloramphenicol succinate, a competitive substrate and inhibitor of succinate dehydrogenase: possible reason for its toxicity. *Toxicol In Vitro* **2004**, *18* (4), 441–447.

Arany, Z.; Huang, L. E.; Eckner, R.; Bhattacharya, S.; Jiang, C.; Goldberg, M. A.; Bunn, H. F.; Livingston, D. M. An essential role for p300/CBP in the cellular response to hypoxia. *Proc Natl Acad Sci U S A* **1996**, *93* (23), 12969–12973.

Arora, K. K.; Pedersen, P. L. Functional significance of mitochondrial bound hexokinase in tumor cell metabolism. Evidence for preferential phosphorylation of glucose by intramitochondrially generated ATP. *J Biol Chem* **1988**, *263* (33), 17422–17428.

Ashkenazi, A.; Dixit, V. M. Death receptors: signaling and modulation. *Science* **1998**, *281* (5381), 1305–1308.

Avula, B.; Wang, Y. -H.; Rumalla, C. S.; Ali, Z.; Smillie, T. J.; Khan, I. A. Analytical methods for determination of magnoflorine and saponins from roots of *Caulophyllum thalictroides* (L.) Michx. using UPLC, HPLC and HPTLC. *J Pharm Biomed Anal* **2011**, *56* (5), 895–903.

Bae, S. H.; Jeong, J. W.; Park, J. A.; Kim, S. H.; Bae, M. K.; Choi, S. J.; Kim, K. W. Sumoylation increases HIF-1α stability and its transcriptional activity. *Biochem Biophys Res Commun* **2004**, *324* (1), 394–400.

Baek, J. H.; Liu, Y. V.; McDonald, K. R.; Wesley, J. B.; Zhang, H.; Semenza, G. L. Spermidine/spermine N(1)-acetyltransferase-1 binds to hypoxia-inducible factor-1α (HIF-1α) and RACK1 and promotes ubiquitination and degradation of HIF-1α. *J Biol Chem* **2007**, *282* (46), 33358–33366.

Baggett, S.; Mazzola, E. P.; Kennelly, E. J. The benzophenones: Isolation, structural elucidation and biological activities; Atta-ur-Rahman, Ed.; Elsevier: Amsterdam, The Netherlands, 2005; Vol. 32, pp 721–771.

Ballot, C.; Kluza, J.; Lancel, S.; Martoriati, A.; Hassoun, S. M.; Mortier, L.; Vienne, J. C.; Briand, G.; Formstecher, P.; Bailly, C.; Neviere, R.; Marchetti, P. Inhibition of mitochondrial respiration mediates apoptosis induced by the anti-tumoral alkaloid lamellarin D. *Apoptosis* **2010**, *15* (7), 769–781.

Barger, J. F.; Plas, D. R. Balancing biosynthesis and bioenergetics: metabolic programs in oncogenesis. *Endocr Relat Cancer* **2010**, *17* (4), R287–R304.

Begriche, K.; Massart, J.; Robin, M. A.; Borgne-Sanchez, A.; Fromenty, B. Drug-induced toxicity on mitochondria and lipid metabolism: mechanistic diversity and deleterious consequences for the liver. *J Hepatol* **2011**, *54* (4), 773–794.

Bell, E. L.; Emerling, B. M.; Ricoult, S. J.; Guarente, L. SIRT3 suppresses hypoxia inducible factor-1α and tumor growth by inhibiting mitochondrial ROS production. *Oncogene* **2011**, *30* (26), 2986-96.

Bell, E. L.; Klimova, T. A.; Eisenbart, J.; Moraes, C. T.; Murphy, M. P.; Budinger, G. R.; Chandel, N. S. The Qo site of the mitochondrial complex III is required for the transduction of hypoxic signaling via reactive oxygen species production. *J Cell Biol* **2007**, *177* (6), 1029–1036.

Benson, J. D.; Chen, Y. N.; Cornell-Kennon, S. A.; Dorsch, M.; Kim, S.; Leszczyniecka, M.; Sellers, W. R.; Lengauer, C. Validating cancer drug targets. *Nature* **2006**, *441* (7092), 451–456.

Berra, E.; Benizri, E.; Ginouves, A.; Volmat, V.; Roux, D.; Pouyssegur, J. HIF prolyl-hydroxylase 2 is the key oxygen sensor setting low steady-state levels of HIF-1α in normoxia. *Embo J* **2003**, *22* (16), 4082–4090.

Bert, A. G.; Grepin, R.; Vadas, M. A.; Goodall, G. J. Assessing IRES activity in the HIF-1α and other cellular 5' UTRs. *RNA* **2006**, *12* (6), 1074–1083.

Betancur-Galvis, L.; Palomares, E.; Marco, J. A.; Estornell, E. Tigliane diterpenes from the latex of *Euphorbia obtusifolia* with inhibitory activity on the mammalian mitochondrial respiratory chain. *J Ethnopharmacol* **2003**, *85* (2-3), 279–282.

Bhattacharya, S.; Michels, C. L.; Leung, M. K.; Arany, Z. P.; Kung, A. L.; Livingston, D. M. Functional role of p35srj, a novel p300/CBP binding protein, during transactivation by HIF-1. *Genes Dev* **1999**, *13* (1), 64–75.

Bjornsti, M. A.; Houghton, P. J. The TOR pathway: a target for cancer therapy. *Nat Rev Cancer* **2004**, *4* (5), 335–348.

Bobkova, E. V.; Weber, M. J.; Xu, Z.; Zhang, Y. L.; Jung, J.; Blume-Jensen, P.; Northrup, A.; Kunapuli, P.; Andersen, J. N.; Kariv, I. Discovery of PDK1 kinase inhibitors with a novel mechanism of action by ultrahigh throughput screening. *J Biol Chem* **2010**, *285* (24), 18838–18846.

Bokesch, H. R.; Groweiss, A.; McKee, T. C.; Boyd, M. R. Laxifloranone, a new phloroglucinol derivative from *Marila laxiflora*. *J Nat Prod* **1999**, *62* (8), 1197–1199.

Boonlarppradab, C.; Faulkner, D. J. Eurysterols A and B, cytotoxic and antifungal steroidal sulfates from a marine sponge of the genus *Euryspongia*. *J Nat Prod* **2007**, *70* (5), 846–848.

Böttger, S.; Hofmann, K.; Melzig, M. F. Saponins can perturb biologic membranes and reduce the surface tension of aqueous solutions: A correlation? *Bioorg Med Chem* **2012**, *20* (9), 2822–2828.

Bramati, L.; Minoggio, M.; Gardana, C.; Simonetti, P.; Mauri, P.; Pietta, P. Quantitative characterization of flavonoid compounds in Rooibos tea (*Aspalathus linearis*) by LC-UV/DAD. *J Agric Food Chem* **2002**, *50* (20), 5513–5519.

Brand, K. A.; Hermfisse, U. Aerobic glycolysis by proliferating cells: a protective strategy against reactive oxygen species. *Faseb J* **1997**, *11* (5), 388–395.

Brand, M. D.; Nicholls, D. G. Assessing mitochondrial dysfunction in cells. *Biochem J* **2011**, *435* (2), 297–312.

Brandt, U.; Schagger, H.; von Jagow, G. Characterisation of binding of the methoxyacrylate inhibitors to mitochondrial cytochrome c reductase. *Eur J Biochem* **1988**, *173* (3), 499–506.

Bredel, M.; Jacoby, E. Chemogenomics: an emerging strategy for rapid target and drug discovery. *Nat Rev Genet* **2004**, *5* (4), 262–275.

Bronchud, M. H. *Principles of molecular oncology*. 3rd ed. ed.; Humana ; London : Springer [distributor]: Totowa, N.J., 2007.

Brown, G. C.; Lakin-Thomas, P. L.; Brand, M. D. Control of respiration and oxidative phosphorylation in isolated rat liver cells. *Eur J Biochem* **1990**, *192* (2), 355–362.

Broxterman, H. J.; Georgopapadakou, N. H. New cancer therapeutics: target-specific in, cytotoxics out? *Drug Resist Updat* **2004**, *7* (2), 79–87.

Bruick, R. K.; McKnight, S. L. A conserved family of prolyl-4-hydroxylases that modify HIF. *Science* **2001**, *294* (5545), 1337–1340.

Bugni, T. S.; Harper, M. K.; McCulloch, M. W.; Reppart, J.; Ireland, C. M. Fractionated marine invertebrate extract libraries for drug discovery. *Molecules* **2008a**, *13* (6), 1372–1383.

Bugni, T. S.; Richards, B.; Bhoite, L.; Cimbora, D.; Harper, M. K.; Ireland, C. M. Marine natural product libraries for high-throughput screening and rapid drug discovery. *J Nat Prod* **2008b**, *71* (6), 1095–1098.

Cadenas, E.; Han, D. Generation of reactive oxygen species by mitochondria In *Free Radicals and the Oxygen Paradox: Oxidative Stress in Biology, Aging and Disease*, Davies, K., Ed. The Biomedical & Life Sciences Collection, Henry Stewart Talks Ltd: London, 2007.

Cain, K.; Bratton, S. B.; Cohen, G. M. The Apaf-1 apoptosome: a large caspase-activating complex. *Biochimie* **2002**, *84* (2–3), 203–214.

Calgaro-Helena, A. F.; Devienne, K. F.; Rodrigues, T.; Dorta, D. J.; Raddi, M. S.; Vilegas, W.; Uyemura, S. A.; Santos, A. C.; Curti, C. Effects of isocoumarins isolated from *Paepalanthus bromelioides* on mitochondria: uncoupling, and induction/inhibition of mitochondrial permeability transition. *Chem Biol Interact* **2006**, *161* (2), 155–164.

Cao, S.; Schilling, J. K.; Miller, J. S.; Andriantsiferana, R.; Rasamison, V. E.; Kingston, D. G. Cytotoxic compounds from *Mundulea chapelieri* from the Madagascar Rainforest. *J Nat Prod* **2004**, *67* (3), 454–456.

Chan, S. Y.; Zhang, Y. Y.; Hemann, C.; Mahoney, C. E.; Zweier, J. L.; Loscalzo, J. MicroRNA-210 controls mitochondrial metabolism during hypoxia by repressing the iron-sulfur cluster assembly proteins ISCU1/2. *Cell Metab* **2009**, *10* (4), 273–284.

Chandel, N. S.; Maltepe, E.; Goldwasser, E.; Mathieu, C. E.; Simon, M. C.; Schumacker, P. T. Mitochondrial reactive oxygen species trigger hypoxia-induced transcription. *Proc Natl Acad Sci U S A* **1998**, *95* (20), 11715–11720.

Chandel, N. S.; Budinger, G. R.; Choe, S. H.; Schumacker, P. T. Cellular respiration during hypoxia. Role of cytochrome oxidase as the oxygen sensor in hepatocytes. *J Biol Chem* **1997**, *272* (30) 18808–18816,.

Chang, Q.; Qin, R.; Huang, T.; Gao, J.; Feng, Y. Effect of antisense hypoxia-inducible factor-1α on progression, metastasis, and chemosensitivity of pancreatic cancer. *Pancreas* **2006**, *32* (3), 297–305.

Cheng, G.; Zielonka, J.; Dranka, B. P.; McAllister, D.; Mackinnon, A. C., Jr.; Joseph, J.; Kalyanaraman, B. Mitochondria-targeted drugs synergize with 2-deoxyglucose to trigger breast cancer cell death. *Cancer Res* **2012**, *72* (10), 2634–2644.

Cheng, J.; Kang, X.; Zhang, S.; Yeh, E. T. SUMO-specific protease 1 is essential for stabilization of HIF1α during hypoxia. *Cell* **2007**, *131* (3), 584–595.

Chikamori, K.; Grozav, A. G.; Kozuki, T.; Grabowski, D.; Ganapathi, R.; Ganapathi, M. K. DNA topoisomerase II enzymes as molecular targets for cancer chemotherapy. *Curr Cancer Drug Targets* **2010**, *10* (7), 758–771.

Choi, H.; Chun, Y. -S.; Kim, S. -W.; Kim, M. -S.; Park, J. -W. Curcumin inhibits hypoxia-inducible factor-1 by degrading aryl hydrocarbon receptor nuclear translocator: a mechanism of tumor growth inhibition. *Mol Pharmacol* **2006**, *70* (5), 1664–1671.

Christofk, H. R.; Vander Heiden, M. G.; Harris, M. H.; Ramanathan, A.; Gerszten, R. E.; Wei, R.; Fleming, M. D.; Schreiber, S. L.; Cantley, L. C. The M2 splice isoform of pyruvate kinase is important for cancer metabolism and tumour growth. *Nature* **2008**, *452* (7184), 230–233.

Chudapongse, N.; Kamkhunthod, M.; Poompachee, K. Effects of *Phyllanthus urinaria* extract on HepG2 cell viability and oxidative phosphorylation by isolated rat liver mitochondria. *J Ethnopharmacol* **2010**, *130* (2), 315–319.

Chun, L. J.; Tong, M. J.; Busuttil, R. W.; Hiatt, J. R. Acetaminophen hepatotoxicity and acute liver failure. *J Clin Gastroenterol* **2009**, *43* (4), 342–349.

Ciardiello, F.; Tortora, G. EGFR antagonists in cancer treatment. *N Engl J Med* **2008**, *358* (11), 1160–1174.

Clark, E. P. A relation between rotenone, deguelin and Tephrosin. *Science* **1931**, *73* (1879), 17–18.

ClinicalTrials.gov A phase I/II trial of 2-deoxy-d-glucose (2DG) for the treatment of advanced cancer and hormone refractory prostate cancer.

http://clinicaltrials.gov/ct2/show/NCT00633087?term=2-DG&rank=3 (accessed July 3rd 2012).

ClinicalTrials.gov Dose escalation trial of 2-deoxy-D-glucose (2DG) in subjects with advanced solid tumors. http://clinicaltrials.gov/ct2/show/NCT00096707 (accessed April 3rd).

ClinicalTrials.gov http://clinicaltrials.gov/ct2/results?term=AT-101 (accessed July 6th 2012).

ClinicalTrials.gov Phase II study of CAP-232 in patients with refractory metastatic renal cell carcinoma. http://clinicaltrials.gov/ct2/show/NCT00422786 (accessed July 7th 2012).

Coley, A. F.; Dodson, H. C.; Morris, M. T.; Morris, J. C. Glycolysis in the african trypanosome: targeting enzymes and their subcellular compartments for therapeutic development. *Mol Biol Int* **2011**, *2011*, 123702.

Collins, I.; Workman, P. New approaches to molecular cancer therapeutics. *Nat Chem Biol* **2006**, *2* (12), 689–700.

Colombo, S. L.; Palacios-Callender, M.; Frakich, N.; De Leon, J.; Schmitt, C. A.; Boorn, L.; Davis, N.; Moncada, S. Anaphase-promoting complex/cyclosome-Cdh1 coordinates glycolysis and glutaminolysis with transition to S phase in human T lymphocytes. *Proc Natl Acad Sci U S A* **2010**, *107* (44), 18868–18873.

Coothankandaswamy, V.; Liu, Y.; Mao, S. C.; Morgan, J. B.; Mahdi, F.; Jekabsons, M. B.; Nagle, D. G.; Zhou, Y. -D. The alternative medicine pawpaw and its acetogenin constituents suppress tumor angiogenesis via the HIF-1/VEGF pathway. *J Nat Prod* **2010**, *73* (5), 956–961.

Cosse, J. P.; Michiels, C. Tumour hypoxia affects the responsiveness of cancer cells to chemotherapy and promotes cancer progression. *Anticancer Agents Med Chem* **2008**, *8* (7), 790–797.

Cotmore, J. M.; Burke, A.; Lee, N. H.; Shapiro, I. M. Respiratory inhibition of isolated rat liver mitochondria by eugenol. *Arch Oral Biol* **1979**, *24* (8), 565–568.

Cox, C. D.; Garbaccio, R. M. Discovery of allosteric inhibitors of kinesin spindle protein (KSP) for the treatment of taxane-refractory cancer: MK-0731 and analogs. *Anticancer Agents Med Chem* **2010**, *10* (9), 697–712.

Cragg, G. M.; Newman D. J. A tale of two tumor targets: Topoisomerase I and tubulin. The Wall and Wani contribution to cancer chemotherapy. *J Nat Prod* **2004**, *67* (2), 232–244.

Cuesta-Rubio, O.; Piccinelli, A. L.; Rastrelli, L. Chemistry and biological activity of polyisoprenylated benzophenone derivatives. 2005; Vol. 32 pp 671–720.

Czyzyk-Krzeska, M. F.; Meller, J. von Hippel-Lindau tumor suppressor: not only HIF's executioner. *Trends Mol Med* **2004**, *10* (4), 146–149.

Das, A. M. Regulation of mitochondrial ATP synthase activity in human myocardium. *Clin Sci (Lond)* **1998**, *94* (5), 499–504.

De Benedetti, A.; Graff, J. R. eIF-4E expression and its role in malignancies and metastases. *Oncogene* **2004**, *23* (18), 3189–3199.

Degli Esposti, M. Inhibitors of NADH-ubiquinone reductase: an overview. *Biochim Biophys Acta* **1998**, *1364* (2), 222–235.

Degli Esposti, M.; Ghelli, A.; Crimi, M.; Estornell, E.; Fato, R.; Lenaz, G. Complex I and complex III of mitochondria have common inhibitors acting as ubiquinone antagonists. *Biochem Biophys Res Commun* **1993**, *190* (3), 1090–1096.

Deng, Y.; Nicholson, R. A. Antifungal properties of surangin B, a coumarin from *Mammea longifolia*. *Planta Med* **2005**, *71* (4), 364–365.

DeYoung, M. P.; Horak, P.; Sofer, A.; Sgroi, D.; Ellisen, L. W. Hypoxia regulates TSC1/2-mTOR signaling and tumor suppression through REDD1-mediated 14-3-3 shuttling. *Genes Dev* **2008**, *22* (2), 239–251.

Di Cosimo, S.; Ferretti, G.; Papaldo, P.; Carlini, P.; Fabi, A.; Cognetti, F. Lonidamine: efficacy and safety in clinical trials for the treatment of solid tumors. *Drugs Today (Barc)* **2003**, *39* (3), 157–174.

Du, L.; Mahdi, F.; Jekabsons, M. B.; Nagle, D. G.; Zhou, Y. -D. Mammea E/BB, an isoprenylated dihydroxycoumarin protonophore that potently uncouples mitochondrial electron transport, disrupts hypoxic signaling in tumor cells. *J Nat Prod* **2010**, *73* (11), 1868–1872.

Du, L.; Mahdi, F.; Jekabsons, M. B.; Nagle, D. G.; Zhou, Y. -D. Natural and semisynthetic mammea-type isoprenylated dihydroxycoumarins uncouple cellular respiration. *J Nat Prod* **2011**, *74* (2), 240–248.

Duesberg, P. H.; Vogt, P. K. Differences between the ribonucleic acids of transforming and nontransforming avian tumor viruses. *Proc Natl Acad Sci U S A* **1970**, *67* (4), 1673–1680.

Dugoua, J. J.; Perri, D.; Seely, D.; Mills, E.; Koren, G. Safety and efficacy of blue cohosh (*Caulophyllum thalictroides*) during pregnancy and lactation. *Can J Clin Pharmacol* **2008**, *15* (1), e66–e73.

Dykens, J. A.; Will, Y. The significance of mitochondrial toxicity testing in drug development. *Drug Discov Today* **2007**, *12* (17-18), 777–785.

Eaton, S.; Bartlett, K.; Pourfarzam, M. Mammalian mitochondrial β-oxidation. *Biochem J* **1996**, *320* (Pt 2), 345–357.

Elingold, I.; Isollabella, M. P.; Casanova, M. B.; Celentano, A. M.; Perez, C.; Cabrera, J. L.; Diez, R. A.; Dubin, M. Mitochondrial toxicity and antioxidant activity of a prenylated flavonoid isolated from *Dalea elegans*. *Chem Biol Interact* **2008**, *171* (3), 294–305.

Elmore, S. Apoptosis: a review of programmed cell death. *Toxicol Pathol* **2007**, *35* (4), 495–516.

Fath, M. A.; Diers, A. R.; Aykin-Burns, N.; Simons, A. L.; Hua, L; Spitz, D. R. Mitochondrial electron transport chain blockers enhance 2-deoxy-D-glucose induced oxidative stress and cell killing in human colon carcinoma cells. *Cancer Biol Ther* **2009**, *8* (13), 1228–1236.

Ferrara, N. VEGF as a therapeutic target in cancer. *Oncology* **2005**, *69* (Suppl. 3), 11–16.

Finley, L. W.; Carracedo, A.; Lee, J.; Souza, A.; Egia, A.; Zhang, J.; Teruya-Feldstein, J.; Moreira, P. I.; Cardoso, S. M.; Clish, C. B.; Pandolfi, P. P.; Haigis, M. C. SIRT3 opposes reprogramming of cancer cell metabolism through HIF-1α destabilization. *Cancer Cell* **2011a**, *19* (3), 416-28.

Finley, L. W.; Haas, W.; Desquiret-Dumas, V.; Wallace, D. C.; Procaccio, V.; Gygi, S. P.; Haigis, M. C. Succinate dehydrogenase is a direct target of sirtuin 3 deacetylase activity. *PLoS One* **2011b**, *6* (8), e23295.

Flugel, D.; Gorlach, A.; Michiels, C.; Kietzmann, T. Glycogen synthase kinase 3 phosphorylates hypoxia-inducible factor-1α and mediates its destabilization in a VHL-independent manner. *Mol Cell Biol* **2007**, *27* (9), 3253–3265.

Fontenay, M.; Cathelin, S.; Amiot, M.; Gyan, E.; Solary, E. Mitochondria in hematopoiesis and hematological diseases. *Oncogene* **2006**, *25* (34), 4757–4767.

Francis, G.; Kerem, Z.; Makkar, H. P.; Becker, K. The biological action of saponins in animal systems: a review. *Br J Nutr* **2002**, *88* (6), 587–605.

Frazier, T. H.; Krueger, K. J. Hepatotoxic herbs: will injury mechanisms guide treatment strategies? *Curr Gastroenterol Rep* **2009**, *11* (4), 317–324.

Friedrich, T.; Ohnishi, T.; Forche, E.; Kunze, B.; Jansen, R.; Trowitzsch, W.; Hofle, G.; Reichenbach, H.; Weiss, H. Two binding sites for naturally occurring inhibitors in mitochondrial and bacterial NADH:ubiquinone oxidoreductase (complex I). *Biochem Soc Trans* **1994**, *22* (1), 226–230.

Fukuda, R.; Zhang, H.; Kim, J. W.; Shimoda, L.; Dang, C. V.; Semenza, G. L. HIF-1 regulates cytochrome oxidase subunits to optimize efficiency of respiration in hypoxic cells. *Cell* **2007**, *129* (1), 111–122.

Fuller, R. W.; Blunt, J. W.; Boswell, J. L.; Cardellina, J. H., II; Boyd, M. R. Guttiferone F, the first prenylated benzophenone from *Allanblackia stuhlmannii*. *J Nat Prod* **1999a**, *62* (1), 130–132.

Fuller, R. W.; Westergaard, C. K.; Collins, J. W.; Cardellina, J. H., 2nd; Boyd, M. R. Vismiaphenones D-G, new prenylated benzophenones from *Vismia cayennensis*. *J Nat Prod* **1999b**, *62* (1), 67–69.

Gabardi, S.; Munz, K.; Ulbricht, C. A review of dietary supplement-induced renal dysfunction. *Clin J Am Soc Nephrol* **2007**, *2* (4), 757–765.

Galban, S.; Kuwano, Y.; Pullmann, R., Jr.; Martindale, J. L.; Kim, H. H.; Lal, A.; Abdelmohsen, K.; Yang, X.; Dang, Y.; Liu, J. O.; Lewis, S. M.; Holcik, M.; Gorospe, M. RNA-binding proteins HuR and PTB promote the translation of hypoxia-inducible factor-1α. *Mol Cell Biol* **2008**, *28* (1), 93–107.

Gatenby, R. A.; Gillies, R. J. Why do cancers have high aerobic glycolysis? *Nat Rev Cancer* **2004**, *4* (11), 891–899.

Gauthier, C.; Legault, J.; Girard-Lalancette, K.; Mshvildadze, V.; Pichette, A. Haemolytic activity, cytotoxicity and membrane cell permeabilization of semi-synthetic and natural lupane- and oleanane-type saponins. *Bioorg Med Chem* **2009**, *17* (5), 2002–2008.

Gerald, D.; Berra, E.; Frapart, Y. M.; Chan, D. A.; Giaccia, A. J.; Mansuy, D.; Pouyssegur, J.; Yaniv, M.; Mechta-Grigoriou, F. JunD reduces tumor angiogenesis by protecting cells from oxidative stress. *Cell* **2004**, *118* (6), 781–794.

Gledhill, J. R.; Montgomery, M. G.; Leslie, A. G.; Walker, J. E. Mechanism of inhibition of bovine F_1-ATPase by resveratrol and related polyphenols. *Proc Natl Acad Sci U S A* **2007**, *104* (34), 13632–13637.

Gledhill, J. R.; Walker, J. E. Inhibitors of the catalytic domain of mitochondrial ATP synthase. *Biochem Soc Trans* **2006,** *34* (Pt 5), 989–992.

Goonewardene, T. I.; Sowter, H. M.; Harris, A. L. Hypoxia-induced pathways in breast cancer. *Microsc Res Tech* **2002**, *59* (1), 41–48.

Goyal, S. K.; Samsher; Goyal, R. K. Stevia (*Stevia rebaudiana*) a bio-sweetener: a review. *Int J Food Sci Nutr* **2010**, *61* (1), 1–10.

Granchi, C.; Roy, S.; Giacomelli, C.; Macchia, M.; Tuccinardi, T.; Martinelli, A.; Lanza, M.; Betti, L.; Giannaccini, G.; Lucacchini, A.; Funel, N.; Leon, L. G.; Giovannetti, E.; Peters, G. J.; Palchaudhuri, R.; Calvaresi, E. C.; Hergenrother, P. J.; Minutolo, F. Discovery of N-hydroxyindole-based inhibitors of human lactate dehydrogenase isoform A (LDH-A) as starvation agents against cancer cells. *J Med Chem* **2011–** *54* (6), 1599–1612.

Green, D. R.; Kroemer, G. The pathophysiology of mitochondrial cell death. *Science* **2004**, *305* (5684), 626–629.

Gregus, Z., Mechanisms of toxicity. In *Casarett and Doull's Toxicology: The basic science of poisons*, Klaassen, C. D., Ed. McGraw-Hill: New York 2008; pp 45-106.

Grieco, A.; Miele, L.; Pompili, M.; Biolato, M.; Vecchio, F. M.; Grattagliano, I.; Gasbarrini, G. Acute hepatitis caused by a natural lipid-lowering product: when "alternative" medicine is no "alternative" at all. *J Hepatol* **2009**, *50* (6), 1273–1277.

Gupta, P. B.; Onder, T. T.; Jiang, G.; Tao, K.; Kuperwasser, C.; Weinberg, R. A.; Lander, E. S. Identification of selective inhibitors of cancer stem cells by high-throughput screening. *Cell* **2009**, *138* (4), 645–659.

Gustafson, K. R. Natural product chemistry group, National Cancer Institute, Frederick, MD; and Nagle, D. G. Department of Pharmacognosy, The University of Mississippi, Oxford, MS. Personal communication 2008.

Gustafson, K. R.; Blunt, J. W.; Munro, M. G. H.; Fuller, R. W.; McKee, T. C.; Cardellina, J. H., II; McMahon, J. B.; Cragg, G. M.; Boyd, M. R. The guttiferones, HIV-inhibitory benzophenones from *Symphonia globulifera*, *Garcinia livingstonei*, *Garcinia ovalifolia* and *Clusia rosea*. *Tetrahedron* **1992**, *48* (46), 10093–101102.

Guzy, R. D.; Hoyos, B.; Robin, E.; Chen, H.; Liu, L.; Mansfield, K. D.; Simon, M. C.; Hammerling, U.; Schumacker, P. T. Mitochondrial complex III is required for hypoxia-induced ROS production and cellular oxygen sensing. *Cell Metab* **2005**, *1* (6), 401–408.

Guzy, R. D.; Sharma, B.; Bell, E.; Chandel, N. S.; Schumacker, P. T. Loss of the SdhB, but Not the SdhA, subunit of complex II triggers reactive oxygen species-dependent hypoxia-inducible factor activation and tumorigenesis. *Mol Cell Biol* **2008**, *28* (2), 718–731.

Hagen, T.; Taylor, C. T.; Lam, F.; Moncada, S. Redistribution of intracellular oxygen in hypoxia by nitric oxide: effect on HIF1α. *Science* **2003**, *302* (5652), 1975–1978.

Haller, C. A.; Benowitz, N. L. Adverse cardiovascular and central nervous system events associated with dietary supplements containing ephedra alkaloids. *N Engl J Med* **2000**, *343* (25), 1833–1838.

Hanahan, D.; Weinberg, R. A. Hallmarks of cancer: the next generation. *Cell* **2011**, *144* (5), 646–674.

Hanahan, D.; Weinberg, R. A. The hallmarks of cancer. *Cell* **2000**, *100* (1), 57–70.

Haridas, V.; Higuchi, M.; Jayatilake, G. S.; Bailey, D.; Mujoo, K.; Blake, M. E.; Arntzen, C. J.; Gutterman, J. U. Avicins: triterpenoid saponins from *Acacia victoriae* (Bentham) induce apoptosis by mitochondrial perturbation. *Proc Natl Acad Sci U S A* **2001**, *98* (10), 5821–5826.

Harvey, A. L. Natural products in drug discovery. *Drug Discov Today* **2008**, *13* (19-20), 894–901.

Hayes, A. W. Action of rubratoxin B on mouse liver mitochondria. *Toxicology* **1976**, *6* (2), 253–261.

Hellerstein, M. K. A critique of the molecular target-based drug discovery paradigm based on principles of metabolic control: Advantages of pathway-based discovery. *Metab Eng* **2008**, *10* (1), 1–9.

Herrero-Mendez, A.; Almeida, A.; Fernandez, E.; Maestre, C.; Moncada, S.; Bolanos, J. P. The bioenergetic and antioxidant status of neurons is controlled by continuous degradation of a key glycolytic enzyme by APC/C-Cdh1. *Nat Cell Biol* **2009**, *11* (6), 747–752.

Higashimura, Y.; Nakajima, Y.; Yamaji, R.; Harada, N.; Shibasaki, F.; Nakano, Y.; Inui, H. Up-regulation of glyceraldehyde-3-phosphate dehydrogenase gene expression by HIF-1 activity depending on Sp1 in hypoxic breast cancer cells. *Arch Biochem Biophys* **2011**, *509* (1), 1–8.

Hirota, K.; Semenza, G. L. Regulation of hypoxia-inducible factor-1 by prolyl and asparaginyl hydroxylases. *Biochem Biophys Res Commun* **2005**, *338* (1), 610–616.

Hockel, M.; Vaupel, P. Tumor hypoxia: definitions and current clinical, biologic, and molecular aspects. *J Natl Cancer Inst* **2001**, *93* (4), 266–276.

Hodges, T. W.; Hossain, C. F.; Kim, Y. -P.; Zhou, Y. -D.; Nagle, D. G. Molecular-targeted antitumor agents: The *Saururus cernuus* dineolignans manassantin B and 4-*O*-demethylmanassantin B are potent inhibitors of hypoxia-activated HIF-1. *J Nat Prod* **2004**, *67* (5), 767–771.

Hossain, C. F.; Kim, Y. -P.; Baerson, S. R.; Zhang, L.; Bruick, R. K.; Mohammed, K. A.; Agarwal, A. K.; Nagle, D. G.; Zhou, Y. -D. *Saururus cernuus* lignans - potent small molecule inhibitors of hypoxia-inducible factor-1. *Biochem Biophys Res Commun* **2005**, *333* (3), 1026–1033.

Hostettmann, K. M.; Marston, A. Triterpene saponins - pharmacological and biological properties. In *Chemistry and pharmacology of natural products: Saponins*, Chambridge University Press: New York, USA, 1995; p 284–286.

Huang, L. E.; Arany, Z.; Livingston, D. M.; Bunn, H. F. Activation of hypoxia-inducible transcription factor depends primarily upon redox-sensitive stabilization of its α subunit. *J Biol Chem* **1996**, *271* (50), 32253–32259.

Huang, L. E.; Gu, J.; Schau, M.; Bunn, H. F. Regulation of hypoxia-inducible factor-1α is mediated by an O_2-dependent degradation domain via the ubiquitin-proteasome pathway. *Proc Natl Acad Sci U S A* **1998**, *95* (14), 7987–7992.

Hussain, R. A.; Owegby, A. G.; Parimoo, P.; Waterman, P. G. Kolanone, a novel polyisoprenylated benzophenone with antimicrobial properties from the fruit of *Garcinia kola*. *Planta Med* **1982**, *44* (2), 78–81.

Inglese, J.; Auld, D. S.; Jadhav, A.; Johnson, R. L.; Simeonov, A.; Yasgar, A.; Zheng, W.; Austin, C. P. Quantitative high-throughput screening: a titration-based approach that efficiently identifies biological activities in large chemical libraries. *Proc Natl Acad Sci U S A* **2006**, *103* (31), 11473–11478.

Isaacs, J. S.; Jung, Y. J.; Mimnaugh, E. G.; Martinez, A.; Cuttitta, F.; Neckers, L. M. Hsp90 regulates a von Hippel Lindau-independent hypoxia-inducible factor-1α-degradative pathway. *J Biol Chem* **2002**, *277* (33), 29936–29944.

Isaacs, J. S.; Jung, Y. J.; Mole, D. R.; Lee, S.; Torres-Cabala, C.; Chung, Y. L.; Merino, M.; Trepel, J.; Zbar, B.; Toro, J.; Ratcliffe, P. J.; Linehan, W. M.; Neckers, L. HIF overexpression correlates with biallelic loss of fumarate hydratase in renal cancer: novel role of fumarate in regulation of HIF stability. *Cancer Cell* **2005**, *8* (2), 143–153.

Jain, M.; Arvanitis, C.; Chu, K.; Dewey, W.; Leonhardt, E.; Trinh, M.; Sundberg, C. D.; Bishop, J. M.; Felsher, D. W. Sustained loss of a neoplastic phenotype by brief inactivation of MYC. *Science* **2002**, *297* (5578), 102–104.

Jiang, B. H.; Zheng, J. Z.; Leung, S. W.; Roe, R.; Semenza, G. L. Transactivation and inhibitory domains of hypoxia-inducible factor-1α. Modulation of transcriptional activity by oxygen tension. *J Biol Chem* **1997**, *272* (31), 19253–19260.

Jiang, C.; Liu, S.; He, W.; Luo, X.; Zhang, S.; Xiao, Z.; Qiu, X.; Yin, H. A new prenylated flavanone from *Derris trifoliata* Lour. *Molecules* **2012**, *17* (1), 657–663.

Jin, Z.; El-Deiry, W. S. Overview of cell death signaling pathways. *Cancer Biol Ther* **2005**, *4* (2), 139–163.

Jones, D. P.; Lemasters, J. J.; Han, D.; Boelsterli, U. A.; Kaplowitz, N. Mechanisms of pathogenesis in drug hepatotoxicity putting the stress on mitochondria. *Mol Interv* **2010**, *10* (2), 98–111.

Jones, P.; Steinkühler, C. From natural products to small molecule ketone histone deacetylase inhibitors: development of new class specific agents. *Curr Pharm Des* **2008**, *14* (6), 545–561.

Juzyszyn, Z.; Czerny, B.; Mysliwiec, Z.; Pawlik, A.; Drozdzik, M. The effect of artichoke (*Cynara scolymus* L.) extract on respiratory chain system activity in rat liver mitochondria. *Phytother Res* **2010**, *24 Suppl 2*, S123–S128.

Kallio, P. J.; Okamoto, K.; O'Brien, S.; Carrero, P.; Makino, Y.; Tanaka, H.; Poellinger, L. Signal transduction in hypoxic cells: inducible nuclear translocation and recruitment of the CBP/p300 coactivator by the hypoxia-inducible factor-1α. *Embo J* **1998**, *17* (22), 6573–6586.

Kallio, P. J.; Wilson, W. J.; O'Brien, S.; Makino, Y.; Poellinger, L. Regulation of the hypoxia-inducible transcription factor-1α by the ubiquitin-proteasome pathway. *J Biol Chem* **1999**, *274* (10), 6519–6525.

Kaluz, S.; Kaluzova, M.; Stanbridge, E. J. Proteasomal inhibition attenuates transcriptional activity of hypoxia-inducible factor-1 (HIF-1) via specific effect on the HIF-1α C-terminal activation domain. *Mol Cell Biol* **2006**, *26* (15), 5895–5907.

Kamal, R.; Mathur, N. Rotenoids from *Lablab purpureus* L. and their bioefficacy against human disease vectors. *Parasitol Res* **2010**, *107* (6), 1481–1488.

Kamara, B. I.; Brandt, E. V.; Ferreira, D.; Joubert, E. Polyphenols from Honeybush tea (*Cyclopia intermedia*). *J Agric Food Chem* **2003**, *51* (13), 3874–3879.

Kamura, T.; Koepp, D. M.; Conrad, M. N.; Skowyra, D.; Moreland, R. J.; Iliopoulos, O.; Lane, W. S.; Kaelin, W. G., Jr.; Elledge, S. J.; Conaway, R. C.; Harper, J. W.; Conaway, J. W. Rbx1, a component of the VHL tumor suppressor complex and SCF ubiquitin ligase. *Science* **1999**, *284* (5414), 657–661.

Katschinski, D. M.; Le, L.; Schindler, S. G.; Thomas, T.; Voss, A. K.; Wenger, R. H. Interaction of the PAS B domain with Hsp90 accelerates hypoxia-inducible factor-1α stabilization. *Cell Physiol Biochem* **2004**, *14* (4-6), 351–360.

Ke, Q.; Costa, M., Hypoxia-inducible factor-1 (HIF-1). *Mol Pharmacol* **2006**, *70* (5), 1469–1480.

Kelmer Bracht, A.; Alvarez, M.; Bracht, A. Effects of *Stevia rebaudiana* natural products on rat liver mitochondria. *Biochem Pharmacol* **1985**, *34* (6), 873–882.

Kessler, R. J.; Vande Zande, H.; Tyson, C. A.; Blondin, G. A.; Fairfield, J.; Glasser, P.; Green, D. E., Uncouplers and the molecular mechanism of uncoupling in mitochondria. *Proc Natl Acad Sci U S A* **1977**, *74* (6), 2241–2245.

Khan, M. A.; Ali, M.; Alam, P. Phytochemical investigation of the fruit peels of *Citrus reticulata* Blanco. *Nat Prod Res* **2010**, *24* (7), 610–620.

Kim, J. Protective effects of Asian dietary items on cancers - soy and ginseng. *Asian Pac J Cancer Prev* **2008**, *9* (4), 543–548.

Kim, J. W.; Dang, C. V. Cancer's molecular sweet tooth and the Warburg effect. *Cancer Res* **2006**, *66* (18), 8927–8930.

Kim, J. W.; Tchernyshyov, I.; Semenza, G. L.; Dang, C. V. HIF-1-mediated expression of pyruvate dehydrogenase kinase: a metabolic switch required for cellular adaptation to hypoxia. *Cell Metab* **2006**, *3* (3), 177–185.

Kitagawa, M.; Misawa, M.; Ogawa, S.; Tashiro, E.; Imoto, M. A new, convenient cell-based screening method for small-molecule glycolytic inhibitors. *Biosci Biotechnol Biochem* **2011**, *75* (2), 367–369.

Klausmeyer, P.; McCloud, T. G.; Melillo, G.; Scudiero, D. A.; Cardellina, J. H., II; Shoemaker, R. H. Identification of a new natural camptothecin analogue in targeted screening for HIF-1α inhibitors. *Planta Med* **2007**, *73* (1), 49–52.

Klawitter, J.; Kominsky, D. J.; Brown, J. L.; Christians, U.; Leibfritz, D.; Melo, J. V.; Eckhardt, S. G.; Serkova, N. J. Metabolic characteristics of imatinib resistance in chronic myeloid leukaemia cells. *Br J Pharmacol* **2009**, *158* (2), 588–600.

Klimova, T.; Chandel, N. S. Mitochondrial complex III regulates hypoxic activation of HIF. *Cell Death Differ* **2008**, *15* (4), 660–666.

Ko, Y. H.; Pedersen, P. L.; Geschwind, J. F. Glucose catabolism in the rabbit VX2 tumor model for liver cancer: characterization and targeting hexokinase. *Cancer Lett* **2001**, *173* (1), 83–91.

Ko, Y. H.; Smith, B. L.; Wang, Y.; Pomper, M. G.; Rini, D. A.; Torbenson, M. S.; Hullihen, J.; Pedersen, P. L. Advanced cancers: eradication in all cases using 3-bromopyruvate therapy to deplete ATP. *Biochem Biophys Res Commun* **2004**, *324* (1), 269–275.

Koehn, F. E., High impact technologies for natural products screening. *Prog Drug Res* **2008**, *65*, 175–210.

Koumenis, C.; Naczki, C.; Koritzinsky, M.; Rastani, S.; Diehl, A.; Sonenberg, N.; Koromilas, A.; Wouters, B. G. Regulation of protein synthesis by hypoxia via activation of the

endoplasmic reticulum kinase PERK and phosphorylation of the translation initiation factor eIF2α. *Mol Cell Biol* **2002**, *22* (21), 7405–7416.

Kroemer, G.; Dallaporta, B.; Resche-Rigon, M. The mitochondrial death/life regulator in apoptosis and necrosis. *Annu Rev Physiol* **1998**, *60*, 619–642.

Kroemer, G.; Galluzzi, L.; Brenner, C. Mitochondrial membrane permeabilization in cell death. *Physiol Rev* **2007**, *87* (1), 99–163.

Kroemer, G.; Pouyssegur, J. Tumor cell metabolism: cancer's Achilles' heel. *Cancer Cell* **2008**, *13* (6), 472–482.

Kunze, B.; Sasse, F.; Wieczorek, H.; Huss, M. Cruentaren A, a highly cytotoxic benzolactone from Myxobacteria is a novel selective inhibitor of mitochondrial F_1-ATPases. *FEBS Lett* **2007**, *581* (18), 3523–3527.

Kurtoglu, M.; Gao, N.; Shang, J.; Maher, J. C.; Lehrman, M. A.; Wangpaichitr, M.; Savaraj, N.; Lane, A. N.; Lampidis, T. J. Under normoxia, 2-deoxy-D-glucose elicits cell death in select tumor types not by inhibition of glycolysis but by interfering with N-linked glycosylation. *Mol Cancer Ther* **2007**, *6* (11), 3049–3058.

Labbe, G.; Pessayre, D.; Fromenty, B. Drug-induced liver injury through mitochondrial dysfunction: mechanisms and detection during preclinical safety studies. *Fundam Clin Pharmacol* **2008**, *22* (4), 335–353.

Lagoa, R.; Graziani, I.; Lopez-Sanchez, C.; Garcia-Martinez, V.; Gutierrez-Merino, C. Complex I and cytochrome c are molecular targets of flavonoids that inhibit hydrogen peroxide production by mitochondria. *Biochim Biophys Acta* **2011**, *1807* (12), 1562–1572.

Lando, D.; Peet, D. J.; Whelan, D. A.; Gorman, J. J.; Whitelaw, M. L. Asparagine hydroxylation of the HIF transactivation domain a hypoxic switch. *Science* **2002**, *295* (5556), 858–861.

Lang, K. J.; Kappel, A.; Goodall, G. J. Hypoxia-inducible factor-1α mRNA contains an internal ribosome entry site that allows efficient translation during normoxia and hypoxia. *Mol Biol Cell* **2002**, *13* (5), 1792–1801.

Lehninger, A. L.; Nelson, D. L.; Cox, M. M. *Lehninger Principles of Biochemistry*. 4th ed. ed.; W.H. Freeman: New York, N.Y. ; Basingstoke, 2005.

Lemeshko, V. V.; Haridas, V.; Quijano Perez, J. C.; Gutterman, J. U. Avicins, natural anticancer saponins, permeabilize mitochondrial membranes. *Arch Biochem Biophys* **2006**, *454* (2), 114–122.

Lessene, G.; Czabotar, P. E.; Colman, P. M. BCL-2 family antagonists for cancer therapy. *Nat Rev Drug Discov* **2008**, *7* (12), 989–1000.

Li, J.; Mahdi, F.; Du, L.; Datta, S.; Nagle, D. G.; Zhou, Y. -D. Mitochondrial respiration inhibitors suppress protein translation and hypoxic signaling via the hyperphosphorylation and inactivation of translation initiation factor eIF2α and elongation factor eEF2. *J Nat Prod* **2011**, *74* (9), 1894–1901.

Li, X.; Wu, J. F. Recent developments in patent anti-cancer agents targeting the matrix metalloproteinases (MMPs). *Recent Pat Anticancer Drug Discov* **2010**, *5* (2), 109–141.

Li, Z.; Wang, D.; Messing, E. M.; Wu, G. VHL protein-interacting deubiquitinating enzyme 2 deubiquitinates and stabilizes HIF-1α. *EMBO Rep* **2005**, *6* (4), 373–378.

Liebler, D. C.; Guengerich, F. P. Elucidating mechanisms of drug-induced toxicity. *Nat Rev Drug Discov* **2005**, *4* (5), 410–420.

Lim, C. H. U., H.; Miyoshi, H.; Miyagawa, H.; Iwamura, H.; Ueno, T. Phytotoxic compounds cochlioquinones are inhibitors of mitochondrial NADH-ubiquinone reductase. *J. Pest. Sci.* **1996**, *21* (2), 213–215.

Lim, J. H.; Lee, Y. M.; Chun, Y. S.; Chen, J.; Kim, J. E.; Park, J. W. Sirtuin 1 modulates cellular responses to hypoxia by deacetylating hypoxia-inducible factor-1α. *Mol Cell* **2010**, *38* (6), 864–878.

Lin, X.; David, C. A.; Donnelly, J. B.; Michaelides, M.; Chandel, N. S.; Huang, X.; Warrior, U.; Weinberg, F.; Tormos, K. V.; Fesik, S. W.; Shen, Y. A chemical genomics screen highlights the essential role of mitochondria in HIF-1 regulation. *Proc Natl Acad Sci U S A* **2008**, *105* (1), 174–179.

Linington, R. G.; Gonzalez, J.; Urena, L. D.; Romero, L. I.; Ortega-Barria, E.; Gerwick, W. H. Venturamides A and B: antimalarial constituents of the panamanian marine Cyanobacterium *Oscillatoria* sp. *J Nat Prod* **2007**, *70* (3), 397–401.

Linnett, P. E.; Beechey, R. B. Inhibitors of the ATP synthethase system. *Methods Enzymol* **1979**, *55*, 472–518.

Liobikas, J.; Majiene, D.; Trumbeckaite, S.; Kursvietiene, L.; Masteikova, R.; Kopustinskiene, D. M.; Savickas, A.; Bernatoniene, J. Uncoupling and antioxidant effects of ursolic acid in isolated rat heart mitochondria. *J Nat Prod* **2011**, *74* (7), 1640–1644.

Liu, Y. V.; Baek, J. H.; Zhang, H.; Diez, R.; Cole, R. N.; Semenza, G. L. RACK1 competes with Hsp90 for binding to HIF-1α and is required for O_2-independent and Hsp90 inhibitor-induced degradation of HIF-1α. *Mol Cell* **2007**, *25* (2), 207–217.

Liu, Y. V.; Semenza, G. L. RACK1 vs. Hsp90: competition for HIF-1α degradation vs. stabilization. *Cell Cycle* **2007**, *6* (6), 656–659.

Liu, Y.; Liu, R.; Mao, S. C.; Morgan, J. B.; Jekabsons, M. B.; Zhou, Y. -D.; Nagle, D. G. Molecular-targeted antitumor agents. 19. Furospongolide from a marine *Lendenfeldia sp*. sponge inhibits hypoxia-inducible factor-1 activation in breast tumor cells. *J Nat Prod* **2008**, *71* (11), 1854–1860.

Liu, Y.; Morgan, J. B.; Coothankandaswamy, V.; Liu, R.; Jekabsons, M. B.; Mahdi, F.; Nagle, D. G.; Zhou, Y. -D. The Caulerpa pigment caulerpin inhibits HIF-1 activation and mitochondrial respiration. *J Nat Prod* **2009b**, *72* (12), 2104–2109.

Liu, Y.; Veena, C. K.; Morgan, J. B.; Mohammed, K. A.; Jekabsons, M. B.; Nagle, D. G.; Zhou, Y. -D. Methylalpinumisoflavone inhibits hypoxia-inducible factor-1 (HIF-1) activation by simultaneously targeting multiple pathways. *J Biol Chem* **2009a**, *284* (9), 5859–5868.

Lobell, R. B.; Omer, C. A.; Abrams, M. T.; Bhimnathwala, H. G.; Brucker, M. J.; Buser, C. A.; Davide, J. P.; deSolms, S. J.; Dinsmore, C. J.; Ellis-Hutchings, M. S.; Kral, A. M.; Liu, D.; Lumma, W. C.; Machotka, S. V.; Rands, E.; Williams, T. M.; Graham, S. L.; Hartman, G. D.; Oliff, A. I.; Heimbrook, D. C.; Kohl, N. E. Evaluation of farnesyl:protein transferase and geranylgeranyl:protein transferase inhibitor combinations in preclinical models. *Cancer Res* **2001**, *61* (24), 8758–8768.

Loscalzo, J. The cellular response to hypoxia: tuning the system with microRNAs. *J Clin Invest* **2010**, *120* (11), 3815–3817.

Luo, W.; Hu, H.; Chang, R.; Zhong, J.; Knabel, M.; O'Meally, R.; Cole, R. N.; Pandey, A.; Semenza, G. L. Pyruvate kinase M2 is a PHD3-stimulated coactivator for hypoxia-inducible factor 1. *Cell* **2011,** *145* (5), 732–744.

Luo, W.; Semenza, G. L. Pyruvate kinase M2 regulates glucose metabolism by functioning as a coactivator for hypoxia-inducible factor-1 in cancer cells. *Oncotarget* **2011**, *2* (7), 551–556.

Macheda, M. L.; Rogers, S.; Best J. D. Molecular and cellular regulation of glucose transporter (GLUT) proteins in cancer. *J Cell Physiol* **2005**, *202* (3) 654–662.

Macheda, M. L.; Rogers, S.; Best, J. D. Molecular and cellular regulation of glucose transporter (GLUT) proteins in cancer. *J Cell Physiol* **2005**, *202* (3), 654–662.

Mahdi, F.; Falkenberg, M.; Ioannou, E.; Roussis, V.; Zhou, Y. -D.; Nagle, D. G. Thyrsiferol inhibits mitochondrial respiration and HIF-1 activation. *Phytochem Lett* **2011**, *4* (2), 75–78.

Mahon, P. C.; Hirota, K.; Semenza, G. L. FIH-1: a novel protein that interacts with HIF-1α and VHL to mediate repression of HIF-1 transcriptional activity. *Genes Dev* **2001**, *15* (20), 2675–2686.

Mai, H. D.; Nguyen, T. T.; Pham, V. C.; Litaudon, M.; Guéritte, F.; Tran, D. T.; Nguyen, V. H. Cytotoxic prenylated isoflavone and bipterocarpan from *Millettia pachyloba*. *Planta Med* **2010**, *76* (15), 1739–1742.

Malumbres, M.; Barbacid, M. Cell cycle, CDKs and cancer: a changing paradigm. *Nat Rev Cancer* **2009**, *9* (3), 153–166.

Man, S.; Gao, W.; Zhang, Y.; Huang, L.; Liu, C. Chemical study and medical application of saponins as anti-cancer agents. *Fitoterapia* **2010**, *81* (7), 703–714.

Mao, S. C.; Liu, Y.; Morgan, J. B.; Jekabsons, M. B.; Zhou, Y. -D.; Nagle, D. G. Lipophilic 2,5-disubstituted pyrroles from the marine sponge *Mycale sp*. inhibit mitochondrial respiration and HIF-1 activation. *J Nat Prod* **2009**, *72* (11), 1927–1936.

Marcillat, O.; Zhang, Y.; Davies, K. J. Oxidative and non-oxidative mechanisms in the inactivation of cardiac mitochondrial electron transport chain components by doxorubicin. *Biochem J* **1989**, *259* (1), 181–189.

Marti, G.; Eparvier, V.; Moretti, C.; Susplugas, S.; Prado, S.; Grellier, P.; Retailleau, P.; Gueritte, F.; Litaudon, M. Antiplasmodial benzophenones from the trunk latex of *Moronobea coccinea* (Clusiaceae). *Phytochemistry* **2009**, *70* (1), 75–85.

Martinez-Abundis, E.; Garcia, N.; Correa, F.; Hernandez-Resendiz, S.; Pedraza-Chaverri, J.; Zazueta, C. Effects of α-mangostin on mitochondrial energetic metabolism. *Mitochondrion* **2010**, *10* (2), 151–157.

Mason, E. F.; Zhao, Y.; Goraksha-Hicks, P.; Coloff, J. L.; Gannon, H.; Jones, S. N.; Rathmell, J. C. Aerobic glycolysis suppresses p53 activity to provide selective protection from apoptosis upon loss of growth signals or inhibition of BCR-Abl. *Cancer Res* **2010**, *70* (20), 8066–8076.

Mathupala, S. P.; Ko, Y. H.; Pedersen, P. L. The pivotal roles of mitochondria in cancer: Warburg and beyond and encouraging prospects for effective therapies. *Biochim Biophys Acta* **2010**, *1797* (6-7), 1225–1230.

Matsuno-Yagi, A.; Hatefi, Y. Studies on the mechanism of oxidative phosphorylation. ATP synthesis by submitochondrial particles inhibited at F_0 by venturicidin and organotin compounds. *J Biol Chem* **1993**, *268* (9), 6168–6173.

Maxwell, P. H.; Wiesener, M. S.; Chang, G. W.; Clifford, S. C.; Vaux, E. C.; Cockman, M. E.; Wykoff, C. C.; Pugh, C. W.; Maher, E. R.; Ratcliffe, P. J. The tumour suppressor protein VHL targets hypoxia-inducible factors for oxygen-dependent proteolysis. *Nature* **1999**, *399* (6733), 271–275.

McChesney, J. D.; Venkataraman, S. K.; Henri, J. T. Plant natural products: back to the future or into extinction? *Phytochemistry* **2007**, *68* (14), 2015–2022.

McDonald, E.; Workman, P.; Jones, K. Inhibitors of the Hsp90 molecular chaperone: attacking the master regulator in cancer. *Curr Top Med Chem* **2006**, *6* (11), 1091–107.

McFarlin, B. L.; Gibson, M. H.; O'Rear, J.; Harman, P. A national survey of herbal preparation use by nurse-midwives for labor stimulation. Review of the literature and recommendations for practice. *J Nurse Midwifery* **1999**, *44* (3), 205–216.

McLaughlin, J. L. Paw paw and cancer: annonaceous acetogenins from discovery to commercial products. *J Nat Prod* **2008**, *71* (7), 1311–1321.

Melzig, M. F.; Bader, G.; Loose, R. Investigations of the mechanism of membrane activity of selected triterpenoid saponins. *Planta Med* **2001**, *67* (1), 43–48.

Minchenko, A.; Leshchinsky, I.; Opentanova, I.; Sang, N.; Srinivas, V.; Armstead, V.; Caro, J. Hypoxia-inducible factor-1-mediated expression of the 6-phosphofructo-2-kinase/fructose-2,6-bisphosphatase-3 (PFKFB3) gene. Its possible role in the Warburg effect. *J Biol Chem* **2002**, *277* (8), 6183–6187.

Mishra, K. P.; Ganju, L.; Sairam, M.; Banerjee, P. K.; Sawhney, R. C. A review of high throughput technology for the screening of natural products. *Biomed Pharmacother* **2008**, *62* (2), 94–98.

Moeller, B. J.; Dreher, M. R.; Rabbani, Z. N.; Schroeder, T.; Cao, Y.; Li, C. Y.; Dewhirst, M. W. Pleiotropic effects of HIF-1 blockade on tumor radiosensitivity. *Cancer Cell* **2005**, *8* (2), 99–110.

Mogi, T.; Kawakami, T.; Arai, H.; Igarashi, Y.; Matsushita, K.; Mori, M.; Shiomi, K.; Omura, S.; Harada, S.; Kita, K. Siccanin rediscovered as a species-selective succinate dehydrogenase inhibitor. *J Biochem* **2009**, *146* (3), 383–387.

Mohammed, K. A.; Hossain, C. F.; Zhang, L.; Bruick, R. K.; Zhou, Y. -D.; Nagle, D. G. Laurenditerpenol, a new diterpene from the tropical marine alga *Laurencia intricata* that

potently inhibits HIF-1 mediated hypoxic signaling in breast tumor cells. *J Nat Prod* **2004**, *67* (12), 2002–2007.

Montoya, M. Translation under hypoxia. *Nat Struct Mol Biol* **2012**, *19* (6), 602.

Monzote, L.; Stamberg, W.; Staniek, K.; Gille, L. Toxic effects of carvacrol, caryophyllene oxide, and ascaridole from essential oil of *Chenopodium ambrosioides* on mitochondria. *Toxicol Appl Pharmacol* **2009**, *240* (3), 337–347.

Moraes, R. M.; Bedir, E.; Barrett, H.; Burandt, C., Jr.; Canel, C.; Khan, I. A. Evaluation of *Podophyllum peltatum* accessions for podophyllotoxin production. *Planta Med* **2002**, *68* (4), 341–344.

Moreno-Sanchez, R.; Rodriguez-Enriquez, S.; Saavedra, E.; Marin-Hernandez, A.; Gallardo-Perez, J. C. The bioenergetics of cancer: is glycolysis the main ATP supplier in all tumor cells? *Biofactors* **2009**, *35* (2), 209–225.

Morgan, J. B.; Mahdi, F.; Liu, Y.; Coothankandaswamy, V.; Jekabsons, M. B.; Johnson, T. A.; Sashidhara, K. V.; Crews, P.; Nagle, D. G.; Zhou, Y. -D. The marine sponge metabolite mycothiazole: a novel prototype mitochondrial complex I inhibitor. *Bioorg Med Chem* **2010**, *18* (16), 5988–5994.

Mori, M.; Miura, S.; Morita, T.; Takiguchi, M.; Tatibana, M. Synthesis, intracellular transport and processing of mitochondrial urea cycle enzymes. *Adv Enzyme Regul* **1983**, *21*, 121–132.

Morikawa, N.; Nakagawa-Hattori, Y.; Mizuno, Y. Effect of dopamine, dimethoxyphenylethylamine, papaverine, and related compounds on mitochondrial respiration and complex I activity. *J Neurochem* **1996**, *66* (3), 1174–1181.

Mottram, J. C. A Factor of Importance in the Radio Sensitivity of Tumours. *British journal of radiology* **1936**, *9*, 606–614.

Munoz-Pinedo, C.; El Mjiyad, N.; Ricci, J. E. Cancer metabolism: current perspectives and future directions. *Cell Death Dis* **2012**, *3*, e248.

Mylonis, I.; Chachami, G.; Paraskeva, E.; Simos, G. Atypical CRM1-dependent nuclear export signal mediates regulation of hypoxia-inducible factor-1α by MAPK. *J Biol Chem* **2008**, *283* (41), 27620–27627.

Mylonis, I.; Chachami, G.; Samiotaki, M.; Panayotou, G.; Paraskeva, E.; Kalousi, A.; Georgatsou, E.; Bonanou, S.; Simos, G. Identification of MAPK phosphorylation sites and their role in the localization and activity of hypoxia-inducible factor-1α. *J Biol Chem* **2006**, *281* (44), 33095–33106.

Nadia, B. H.; Wided, K.; Kheira, B.; Hassiba, R.; Lamia, B.; Rhouati, S.; Alyane, M.; Zellagui, A.; Lahouel, M. Disruption of mitochondrial membrane potential by ferulenol and restoration by propolis extract: antiapoptotic role of propolis. *Acta Biol Hung* **2009**, *60* (4), 385–398.

Nagle, D. G.; Zhou, Y.-D. 2.20 - Natural products as probes of selected targets in tumor cell biology and hypoxic signaling. In: *Comprehensive natural products II*, Mander, L.; Liu, H. -W. Eds.; Elsevier: Oxford, United Kingdom, 2010; pp 651–683.

Nagle, D. G.; Zhou, Y.-D. Natural products as inhibitors of hypoxia-inducible factor-1. In *Bioactive compounds from natural sources, second edition: natural products as lead compounds in drug discovery*, Tringali, C. Ed. CRC press: 2011; pp 187–263.

Nakano, A.; Tsuji, D.; Miki, H.; Cui, Q.; El Sayed, S. M.; Ikegame, A.; Oda, A.; Amou, H.; Nakamura, S.; Harada, T.; Fujii, S.; Kagawa, K.; Takeuchi, K.; Sakai, A.; Ozaki, S.; Okano, K.; Nakamura, T.; Itoh, K.; Matsumoto, T.; Abe, M. Glycolysis inhibition inactivates ABC transporters to restore drug sensitivity in malignant cells. *PLoS One* **2011**, *6* (11), e27222.

Nakashima, R. A.; Mangan, P. S.; Colombini, M.; Pedersen, P. L. Hexokinase receptor complex in hepatoma mitochondria: evidence from N,N'-dicyclohexylcarbodiimide-labeling studies for the involvement of the pore-forming protein VDAC. *Biochemistry* **1986**, *25* (5), 1015–1021.

Napiwotzki, J.; Kadenbach, B. Extramitochondrial ATP/ADP-ratios regulate cytochrome *c* oxidase activity via binding to the cytosolic domain of subunit IV. *Biol Chem* **1998**, *379* (3), 335–339.

Narita, T.; Yin, S.; Gelin, C. F.; Moreno, C. S.; Yepes, M.; Nicolaou, K. C.; Van Meir, E. G. Identification of a novel small molecule HIF-1α translation inhibitor. *Clin Cancer Res* **2009**, *15* (19), 6128–6136.

National Institutes of Health Molecular libraries program: pathways to discovery. http://mli.nih.gov/mli/secondary-menu/nih-resources/ (accessed on March 11th 2012).

Neckers L. Using natural product inhibitors to validate Hsp90 as a molecular target in cancer. *Curr Top Med Chem* **2006**, *6* (11), 1163–1171.

Neto, C. C. Cranberry and its phytochemicals: a review of in vitro anticancer studies. *J Nutr* **2007**, *137* (1 Suppl), 186S–193S.

Newman, D. J. Natural Products Branch, National Cancer Institute, Frederick, MD; and Nagle, D. G. Department of Pharmacognosy, The University of Mississippi, Oxford, MS. Personal communication 2008.

Newman, D. J.; Cragg, G. M. Natural products as sources of new drugs over the 30 years from 1981 to 2010. *J Nat Prod* **2012**, *75* (3), 311–315.

Nicholls, D. G.; Ferguson, S. J. *Bioenergetics 3*. [3rd ed.] ed.; Amsterdam ; London ; Academic Press: 2002.

Nieminen, A. L.; Saylor, A. K.; Herman, B.; Lemasters, J. J. ATP depletion rather than mitochondrial depolarization mediates hepatocyte killing after metabolic inhibition. *Am J Physiol* **1994**, *267* (1 Pt 1), C67–C74.

Onnis, B.; Rapisarada, A.; Melillo, G. Development of HIF-1 inhibitors for cancer therapy. *J Cell Mol Med* **2009**, *13* (9A), 2780–2786.

Overall, C. M.; Klefield, O. Tumour microenvironment - opinion: validating matrix metalloproteinases as drug targets and anti-targets for cancer therapy. *Nat Rev Cancer* **2006**, *6* (3), 227–239.

Palmer, M. E.; Haller, C.; McKinney, P. E.; Klein-Schwartz, W.; Tschirgi, A.; Smolinske, S. C.; Woolf, A.; Sprague, B. M.; Ko, R.; Everson, G.; Nelson, L. S.; Dodd-Buter, T.; Bartlett, W. D.; Landzberg, B. R. Adverse events associated with dietary supplements: an observational study. *Lancet* **2003**, *361* (9352), 101–106.

Pan, Y.; Mansfield, K. D.; Bertozzi, C. C.; Rudenko, V.; Chan, D. A.; Giaccia, A. J.; Simon, M. C. Multiple factors affecting cellular redox status and energy metabolism modulate hypoxia-inducible factor prolyl hydroxylase activity in vivo and in vitro. *Mol Cell Biol* **2007**, *27* (3), 912–925.

Papandreou, I.; Cairns, R. A.; Fontana, L.; Lim, A. L.; Denko, N. C. HIF-1 mediates adaptation to hypoxia by actively downregulating mitochondrial oxygen consumption. *Cell Metab* **2006**, *3* (3), 187–197.

Papandreou, I.; Goliasova, T.; Denko, N. C. Anticancer drugs that target metabolism: Is dichloroacetate the new paradigm? *Int J Cancer* **2011**, *128* (5), 1001–1008.

Pardini, R. S.; Kim, C. H.; Biagini, R.; Morris, R. J.; Fletcher, D. C. Inhibition of mitochondrial electron-transport systems by nor-isoguaiacin. *Biochem Pharmacol* **1973**, *22* (15), 1921–1925.

Pardo-Andreu, G. L.; Nunez-Figueredo, Y.; Tudella, V. G.; Cuesta-Rubio, O.; Rodrigues, F. P.; Pestana, C. R.; Uyemura, S. A.; Leopoldino, A. M.; Alberici, L. C.; Curti, C. The anti-cancer agent nemorosone is a new potent protonophoric mitochondrial uncoupler. *Mitochondrion* **2011**, *11* (2), 255–263.

Pastorino, J. G.; Shulga, N.; Hoek, J. B. Mitochondrial binding of hexokinase II inhibits Bax-induced cytochrome c release and apoptosis. *J Biol Chem* **2002**, *277* (9), 7610–7618.

Patiar, S.; Harris, A. L. Role of hypoxia-inducible factor-1α as a cancer therapy target. *Endocr Relat Cancer* **2006**, *13 Suppl 1*, S61–S75.

Perry, W. L. III; Weitzman, A. The development of molecularly targeted anticancer therapies: an Eli Lilly and Company perspective. *Clin Adv Hematol Oncol* **2005**, *3* (3), 199–202.

Pitroda, S. P.; Wakim, B. T.; Sood, R. F.; Beveridge, M. G.; Beckett, M. A.; MacDermed, D. M.; Weichselbaum, R. R.; Khodarev, N. N. STAT1-dependent expression of energy metabolic pathways links tumour growth and radioresistance to the Warburg effect. *BMC Med* **2009**, *7*, 68.

Podolak, I.; Galanty, A.; Sobolewska, D. Saponins as cytotoxic agents: a review. *Phytochem Rev* **2010**, *9* (3), 425–474.

Pollard, P. J.; Briere, J. J.; Alam, N. A.; Barwell, J.; Barclay, E.; Wortham, N. C.; Hunt, T.; Mitchell, M.; Olpin, S.; Moat, S. J.; Hargreaves, I. P.; Heales, S. J.; Chung, Y. L.; Griffiths, J. R.; Dalgleish, A.; McGrath, J. A.; Gleeson, M. J.; Hodgson, S. V.; Poulsom, R.; Rustin, P.; Tomlinson, I. P. Accumulation of Krebs cycle intermediates and over-expression of HIF1α in

tumours which result from germline FH and SDH mutations. *Hum Mol Genet* **2005**, *14* (15), 2231–2239.

Radad, K.; Rausch, W. D.; Gille, G. Rotenone induces cell death in primary dopaminergic culture by increasing ROS production and inhibiting mitochondrial respiration. *Neurochem Int* **2006**, *49* (4), 379–386.

Rademakers, S. E.; Span, P. N.; Kaanders, J. H.; Sweep, F. C.; van der Kogel, A. J.; Bussink, J. Molecular aspects of tumour hypoxia. *Mol Oncol* **2008**, *2* (1), 41–53.

Raez, L. E. R., J.; Schlesselman, J.; Langmuir, V.; Tidmarsh, G.; Rocha-Lima, C.; Papadopoulos, K.; O'Connor, J.; Baldie, P.; Lampidis, T. Combining glycolytic inhibitors with chemotherapy: phase I trial of 2-deoxy-D-glucose and docetaxel in patients with solid tumors. *Journal of Clinical Oncology* **2005**, *23* (16S), 3190.

Rane, S.; He, M.; Sayed, D.; Vashistha, H.; Malhotra, A.; Sadoshima, J.; Vatner, D. E.; Vatner, S. F.; Abdellatif, M. Downregulation of miR-199a derepresses hypoxia-inducible factor-1α and Sirtuin 1 and recapitulates hypoxia preconditioning in cardiac myocytes. *Circ Res* **2009**, *104* (7), 879–886.

Rao, K. V.; Rao, N. S. Chemistry of *Saururus cernuus*, VI: Three new neolignans. *J Nat Prod* **1990**, *53* (1), 212–215.

Rasmussen, J. A. H., A. M.; Einhellig, F. A.; Thomas, J. A. Sorgoleone from root exudate inhibits mitochondrial functions. *J. Chem. Ecol.* **1992**, *18* (2), 197–207.

Reiling, J. H.; Sabatini, D. M. Stress and mTORture signaling. *Oncogene* **2006**, *25* (48), 6373–6383.

Robertson, J. D.; Orrenius, S. Role of mitochondria in toxic cell death. *Toxicology* **2002**, *181-182*, 491–496.

Robey, I. F.; Stephen, R. M.; Brown, K. S.; Baggett, B. K.; Gatenby, R. A.; Gillies, R. J. Regulation of the Warburg effect in early-passage breast cancer cells. *Neoplasia* **2008**, *10* (8), 745–756.

Rodriguez-Enriquez, S.; Marin-Hernandez, A.; Gallardo-Perez, J. C.; Carreno-Fuentes, L.; Moreno-Sanchez, R. Targeting of cancer energy metabolism. *Mol Nutr Food Res* **2009**, *53* (1), 29–48.

Rosenthal, P. J. Antimalarial drug discovery: old and new approaches. *J Exp Biol* **2003**, *206* (Pt 21), 3735–3744.

Roth, G. N.; Chandra, A.; Nair, M. G. Novel bioactivities of Curcuma longa constituents. *J Nat Prod* **1998**, *61* (4), 542–545.

Rous, P. A sarcoma of the fowl transmissible by an agent separable from the tumor cells. *J Exp Med* **1911**, *13* (4), 397–411.

Rowinsky, E. K. Lately, it occurs to me what a long, strange trip it's been for the farnesyltransferase inhibitors. *J Clin Oncol* **2006**, *24* (19), 2981–2984.

Roy, A.; Volgin, D. V.; Baby, S. M.; Mokashi, A.; Kubin, L.; Lahiri, S. Activation of HIF-1α mRNA by hypoxia and iron chelator in isolated rat carotid body. *Neurosci Lett* **2004**, *363* (3), 229–232.

Rukachaisirikul, V.; Pailee, P.; Hiranrat, A.; Tuchinda, P.; Yoosook, C.; Kasisit, J.; Taylor, W. C.; Reutrakul, V. Anti-HIV-1 protostane triterpenes and digeranylbenzophenone from trunk bark and stems of *Garcinia speciosa*. *Planta Med* **2003**, *69* (12), 1141–1146.

Runeberg, L. Uncoupling of oxidative phosphorylation in rat liver mitochondria with desaspidin and related phlorobutyrophenone derivative. *Biochem Pharmacol* **1962**, *11*, 237–242.

Ruvinsky, I.; Sharon, N.; Lerer, T.; Cohen, H.; Stolovich-Rain, M.; Nir, T.; Dor, Y.; Zisman, P.; Meyuhas, O. Ribosomal protein S6 phosphorylation is a determinant of cell size and glucose homeostasis. *Genes Dev* **2005**, *19* (18), 2199–2211.

Saito, K.; Kondo, E.; Matsushita, M. MicroRNA 130 family regulates the hypoxia response signal through the P-body protein DDX6. *Nucleic Acids Res* **2011**, *39* (14), 6086–6099.

Saling, S. C.; Comar, J. F.; Mito, M. S.; Peralta, R. M.; Bracht, A. Actions of juglone on energy metabolism in the rat liver. *Toxicol Appl Pharmacol* **2011**, *257* (3), 319–327.

Salomon, A. R.; Voehringer, D. W.; Herzenberg, L. A.; Khosla, C. Apoptolidin, a selective cytotoxic agent, is an inhibitor of F_0F_1-ATPase. *Chem Biol* **2001**, *8* (1), 71–80.

Salomon, A. R.; Voehringer, D. W.; Herzenberg, L. A.; Khosla, C. Understanding and exploiting the mechanistic basis for selectivity of polyketide inhibitors of F_0F_1-ATPase. *Proc Natl Acad Sci U S A* **2000**, *97* (26), 14766–14771.

Sams-Dodd, F. Target-based drug discovery: is something wrong? *Drug Discov Today* **2005**, *10* (2), 139–147.

Sanchez, W.; Maple, J. T.; Burquart, L. J.; Kamath, P. S. Severe hepatotoxicity associated with use of a dietary supplement containing usnic acid. *Mayo Clin Proc* **2006**, *81* (4), 541–544.

Sarafian, T. A.; Kouyoumjian, S.; Khoshaghideh, F.; Tashkin, D. P.; Roth, M. D. Δ9-tetrahydrocannabinol disrupts mitochondrial function and cell energetics. *Am J Physiol Lung Cell Mol Physiol* **2003**, *284* (2), L298–L306.

Scatena, R.; Bottoni, P.; Botta, G.; Martorana, G. E.; Giardina, B. The role of mitochondria in pharmacotoxicology: a reevaluation of an old, newly emerging topic. *Am J Physiol Cell Physiol* **2007**, *293* (1), C12–21.

Scatena, R.; Bottoni, P.; Pontoglio, A.; Mastrototaro, L.; Giardina, B. Glycolytic enzyme inhibitors in cancer treatment. *Expert Opin Investig Drugs* **2008**, *17* (10), 1533–1545.

Schepens, B.; Tinton, S. A.; Bruynooghe, Y.; Beyaert, R.; Cornelis, S. The polypyrimidine tract-binding protein stimulates HIF-1α IRES-mediated translation during hypoxia. *Nucleic Acids Res* **2005**, *33* (21), 6884–6894.

Schofield, C. J.; Ratcliffe, P. J. Oxygen sensing by HIF hydroxylases. *Nat Rev Mol Cell Biol* **2004**, *5* (5), 343–354.

Schwartz, D. L.; Powis, G.; Thitai-Kumar, A.; He, Y.; Bankson, J.; Williams, R.; Lemos, R.; Oh, J.; Volgin, A.; Soghomonyan, S.; Nishii, R.; Alauddin, M.; Mukhopadhay, U.; Peng, Z.; Bornmann, W.; Gelovani, J. The selective hypoxia inducible factor-1 inhibitor PX-478 provides in vivo radiosensitization through tumor stromal effects. *Mol Cander Ther* **2009**, *8* (4), 947–958.

Schwartz, J. D.; Rowinsky, E. K.; Youssoufian, H.; Pytowski, B.; Wu Y. Vascular endothelial growth factor receptor-1 in human cancer: concise review and rationale for development of IMC-18F1 (Human antibody targeting vascular endothelial growth factor receptor-1). *Cancer* **2010**, *116* (4 Suppl.) 1027–1032.

Seeram, N. P.; Schulman, R. N.; Heber, D. *Pomegranates : ancient roots to modern medicine*. CRC/Taylor & Francis: Boca Raton, 2006; p 244 p.

Seidel, V. Initial and Bulk Extraction. In *Natural products isolation*, 2nd ed.; Sarker, S. D.; Latif, Z.; Gray, A. I. Eds. Humana Press: Totowa, N.J., 2005; pp 27-46.

Selak, M. A.; Armour, S. M.; MacKenzie, E. D.; Boulahbel, H.; Watson, D. G.; Mansfield, K. D.; Pan, Y.; Simon, M. C.; Thompson, C. B.; Gottlieb, E. Succinate links TCA cycle

dysfunction to oncogenesis by inhibiting HIF-α prolyl hydroxylase. *Cancer Cell* **2005**, *7* (1), 77–85.

Semenza, G. L. Evaluation of HIF-1 inhibitors as anticancer agents. *Drug Discov Today* **2007**, *12* (19–20) 853–859.

Semenza, G. L. Hypoxia-inducible factor 1 and cancer pathogenesis. *IUBMB Life* **2008**, *60* (9), 591–597.

Semenza, G. L. Hypoxia-inducible factor 1: regulator of mitochondrial metabolism and mediator of ischemic preconditioning. *Biochim Biophys Acta* **2011,** *1813* (7), 1263–1268.

Semenza, G. L. Hypoxia-inducible factors: mediators of cancer progression and targets for cancer therapy. *Trends Pharmacol Sci* **2012**, *33* (4), 207–214.

Semenza, G. L. Regulation of cancer cell metabolism by hypoxia-inducible factor-1. *Semin Cancer Biol* **2009**, *19* (1), 12–16.

Semenza, G. L. Regulation of mammalian O_2 homeostasis by hypoxia-inducible factor-1. *Annu Rev Cell Dev Biol* **1999**, *15*, 551–578.

Semenza, G. L.; Agani, F.; Booth, G.; Forsythe, J.; Iyer, N.; Jiang, B. H.; Leung, S.; Roe, R.; Wiener, C.; Yu, A. Structural and functional analysis of hypoxia-inducible factor-1. *Kidney Int* **1997**, *51* (2), 553–555.

Semenza, G. L.; Jiang, B. H.; Leung, S. W.; Passantino, R.; Concordet, J. P.; Maire, P.; Giallongo, A. Hypoxia response elements in the aldolase A, enolase 1, and lactate dehydrogenase A gene promoters contain essential binding sites for hypoxia-inducible factor-1. *J Biol Chem* **1996**, *271* (51), 32529–32537.

Semenza, G. L.; Roth, P. H.; Fang, H. M.; Wang, G. L. Transcriptional regulation of genes encoding glycolytic enzymes by hypoxia-inducible factor 1. *J Biol Chem* **1994**, *269* (38), 23757–23763.

Semenza, G. L.; Wang, G. L. A nuclear factor induced by hypoxia via de novo protein synthesis binds to the human erythropoietin gene enhancer at a site required for transcriptional activation. *Mol Cell Biol* **1992**, *12* (12), 5447–5454.

Sharlow, E. R.; Lyda, T. A.; Dodson, H. C.; Mustata, G.; Morris, M. T.; Leimgruber, S. S.; Lee, K. H.; Kashiwada, Y.; Close, D.; Lazo, J. S.; Morris, J. C. A target-based high throughput screen yields Trypanosoma brucei hexokinase small molecule inhibitors with antiparasitic activity. *PLoS Negl Trop Dis* **2010**, *4* (4), e659.

Shawver, L. K.; Slamon, D.; Ullrich, A. Smart drugs: tyrosine kinase inhibitors in cancer therapy. *Cancer Cell* **2002**, *1* (2), 117–123.

Shimizu, Y. L., B. Purification of Water-Soluble Natural Products. In *Natural products isolation*, 2nd ed.; Sarker, S. D.; Latif, Z.; Gray, A. I. Eds. Humana Press: Totowa, N.J., 2005; pp 415–438.

Shin, D. H.; Li, S. H.; Chun, Y. S.; Huang, L. E.; Kim, M. S.; Park, J. W. CITED2 mediates the paradoxical responses of HIF-1α to proteasome inhibition. *Oncogene* **2008**, *27* (13), 1939–1944.

Shishodia, S.; Harikumar, K. B.; Dass, S.; Ramawat, K. G.; Aggarwal, B. B. The guggul for chronic diseases: ancient medicine, modern targets. *Anticancer Res* **2008**, *28* (6A), 3647–3664.

Shoshan, M. C. 3-Bromopyruvate: targets and outcomes. *J Bioenerg Biomembr* **2012**, *44* (1), 7–15.

Siems, W.; Sommerburg, O.; Schild, L.; Augustin, W.; Langhans, C. D.; Wiswedel, I. β-carotene cleavage products induce oxidative stress in vitro by impairing mitochondrial respiration. *Faseb J* **2002**, *16* (10), 1289–1291.

Skehan, P.; Storeng, R.; Scudiero, D.; Monks, A.; McMahon, J.; Vistica, D.; Warren, J. T.; Bokesch, H.; Kenney, S.; Boyd, M. R. New colorimetric cytotoxicity assay for anticancer-drug screening. *J Natl Cancer Inst* **1990**, *82* (13), 1107–1112.

Society of toxicology, http://www.toxicology.org/ai/pub/si05/SI05_Define.asp (accessed on May 4th 2012)

Soltoff, S. P. Rottlerin is a mitochondrial uncoupler that decreases cellular ATP levels and indirectly blocks protein kinase Cδ tyrosine phosphorylation. *J Biol Chem* **2001**, *276* (41), 37986–37992.

Song, X.; Liu, X.; Chi, W.; Liu, Y.; Wei, L.; Wang, X.; Yu, J. Hypoxia-induced resistance to cisplatin and doxorubicin in non-small cell lung cancer is inhibited by silencing of HIF-1α gene. *Cancer Chemother Pharmacol* **2006**, *58* (6), 776–784.

Sonveaux, P.; Vegran, F.; Schroeder, T.; Wergin, M. C.; Verrax, J.; Rabbani, Z. N.; De Saedeleer, C. J.; Kennedy, K. M.; Diepart, C.; Jordan, B. F.; Kelley, M. J.; Gallez, B.; Wahl, M. L.; Feron, O.; Dewhirst, M. W. Targeting lactate-fueled respiration selectively kills hypoxic tumor cells in mice. *J Clin Invest* **2008**, *118* (12), 3930–3942.

Spannuth, W. A.; Sood, A. K.; Coleman, R. L. Angiogenesis as a strategic target for ovarian cancer therapy. *Nat Clin Pract Oncol* **2008**, *5* (4), 194–204.

Sparg, S. G.; Light, M. E.; van Staden, J. Biological activities and distribution of plant saponins. *J Ethnopharmacol* **2004**, *94* (2-3), 219–243.

Staab, A.; Loffler, J.; Said, H. M.; Katzer, A.; Beyer, M.; Polat, B.; Einsele, H.; Flentje, M.; Vordermark, D. Modulation of glucose metabolism inhibits hypoxic accumulation of hypoxia-inducible factor-1α (HIF-1α). *Strahlenther Onkol* **2007**, *183* (7), 366–373.

Stickel, F.; Kessebohm, K.; Weimann, R.; Seitz, H. K. Review of liver injury associated with dietary supplements. *Liver Int* **2011**, *31* (5), 595–605.

Sturdik, E.; Cully, J.; Sturdikova, M.; Durcova, E. Stimulation of glycolysis in Ehrlich ascites carcinoma cells with phenylhydrazonopropanedinitrile and others uncouplers of oxidative phosphorylation. *Neoplasma* **1986**, *33* (5), 575–582.

Sturdy, M.; Krunic, A.; Cho, S.; Franzblau, S.; Orjala, J. Eucapsitrione, an anti-Mycobacterium tuberculosis anthraquinone derivative from the cultured freshwater cyanobacterium *Eucapsis* sp. *J Nat Prod* **2010**, *73* (8), 1441–1443.

Su, Y.; Yang, S.; Xiao, Z.; Wang, W.; Okunieff, P.; Zhang, L. Triptolide alters mitochondrial functions. *Adv Exp Med Biol* **2007**, *599*, 139–146.

Sudarshan, S.; Sourbier, C.; Kong, H. S.; Block, K.; Valera Romero, V. A.; Yang, Y.; Galindo, C.; Mollapour, M.; Scroggins, B.; Goode, N.; Lee, M. J.; Gourlay, C. W.; Trepel, J.; Linehan, W. M.; Neckers, L. Fumarate hydratase deficiency in renal cancer induces glycolytic addiction and hypoxia-inducible transcription factor-1α stabilization by glucose-dependent generation of reactive oxygen species. *Mol Cell Biol* **2009**, *29* (15), 4080–4090.

Sugden, M. C.; Holness, M. J. Recent advances in mechanisms regulating glucose oxidation at the level of the pyruvate dehydrogenase complex by PDKs. *Am J Physiol Endocrinol Metab* **2003**, *284* (5), E855–E862.

Sun, L.; Luo, C.; Long, J.; Wei, D.; Liu, J. Acrolein is a mitochondrial toxin: effects on respiratory function and enzyme activities in isolated rat liver mitochondria. *Mitochondrion* **2006**, *6* (3), 136–142.

Sun, Y. E3 Ubiquitin ligases as cancer targets and biomarkers. *Neoplasia* **2006**, *8* (8), 645–654.

Suski, J.; Lebiedzinska, M.; Machado, N. G.; Oliveira, P. J.; Pinton, P.; Duszynski, J.; Wieckowski, M. R. Mitochondrial tolerance to drugs and toxic agents in ageing and disease. *Curr Drug Targets* **2011**, *12* (6), 827–849.

Szakács, G.; Paterson, J. K.; Ludwig, J. A.; Booth-Genthe, C.; Gottesman, M. M. Targeting multidrug resistance in cancer. *Nat Rev Drug Discov* **2006**, *5* (3), 219–234.

Tamura, S. T., N.; Miyamoto, S.; Mori, R.; Suzuki, S.; Nagatsu, J. Isolation and physiological activities of piericidin A, a natural insecticide produced by *Streptomyces*. *Agr. Biol. Chem.* **1963**, *27*, 576–582.

Tatum, J. L.; Kelloff, G. J.; Gillies, R. J.; Arbeit, J. M.; Brown, J. M.; Chao, K. S.; Chapman, J. D.; Eckelman, W. C.; Fyles, A. W.; Giaccia, A. J.; Hill, R. P.; Koch, C. J.; Krishna, M. C.; Krohn, K. A.; Lewis, J. S.; Mason, R. P.; Melillo, G.; Padhani, A. R.; Powis, G.; Rajendran, J. G.; Reba, R.; Robinson, S. P.; Semenza, G. L.; Swartz, H. M.; Vaupel, P.; Yang, D.; Croft, B.; Hoffman, J.; Liu, G.; Stone, H.; Sullivan, D. Hypoxia: importance in tumor biology, noninvasive measurement by imaging, and value of its measurement in the management of cancer therapy. *Int J Radiat Biol* **2006**, *82* (10), 699–757.

Taylor, C. T. Mitochondria and cellular oxygen sensing in the HIF pathway. *Biochem J* **2008,** *409* (1), 19–26.

Teicher, B. A.; Holden, S. A.; al-Achi, A.; Herman, T. S. Classification of antineoplastic treatments by their differential toxicity toward putative oxygenated and hypoxic tumor

subpopulations in vivo in the FSaIIC murine fibrosarcoma. *Cancer Res* **1990**, *50* (11), 3339–3344.

Tello, D.; Balsa, E.; Acosta-Iborra, B.; Fuertes-Yebra, E.; Elorza, A.; Ordonez, A.; Corral-Escariz, M.; Soro, I.; Lopez-Bernardo, E.; Perales-Clemente, E.; Martinez-Ruiz, A.; Enriquez, J. A.; Aragones, J.; Cadenas, S.; Landazuri, M. O. Induction of the mitochondrial NDUFA4L2 protein by HIF-1α decreases oxygen consumption by inhibiting Complex I activity. *Cell Metab* **2011**, *14* (6), 768–779.

Thierbach, G.; Reichenbach, H. Myxothiazol, a new inhibitor of the cytochrome *b*-c_1 segment of th respiratory chain. *Biochim Biophys Acta* **1981**, *638* (2), 282–289.

Tormos, K. V.; Chandel, N. S. Inter-connection between mitochondria and HIFs. *J Cell Mol Med* **2010**, *14* (4), 795–804.

Tredan, O.; Galmarini, C. M.; Patel, K.; Tannock, I. F. Drug resistance and the solid tumor microenvironment. *J Natl Cancer Inst* **2007**, *99* (19), 1441–1454.

Trumpower, B. L. The protonmotive Q cycle. Energy transduction by coupling of proton translocation to electron transfer by the cytochrome bc_1 complex. *J Biol Chem* **1990**, *265* (20), 11409–11412.

Turner, N.; Li, J. Y.; Gosby, A.; To, S. W.; Cheng, Z.; Miyoshi, H.; Taketo, M. M.; Cooney, G. J.; Kraegen, E. W.; James, D. E.; Hu, L. H.; Li, J.; Ye, J. M. Berberine and its more biologically available derivative, dihydroberberine, inhibit mitochondrial respiratory complex I: a mechanism for the action of berberine to activate AMP-activated protein kinase and improve insulin action. *Diabetes* **2008**, *57* (5), 1414–1418.

Ullah, M. S.; Davies, A. J.; Halestrap, A. P. The plasma membrane lactate transporter MCT4, but not MCT1, is up-regulated by hypoxia through a HIF-1α-dependent mechanism. *J Biol Chem* **2006**, *281* (14), 9030–9037.

Uniacke, J.; Holterman, C. E.; Lachance, G.; Franovic, A.; Jacob, M. D.; Fabian, M. R.; Payette, J.; Holcik, M.; Pause, A.; Lee, S. An oxygen-regulated switch in the protein synthesis machinery. *Nature* **2012**, *486* (7401), 126–129.

Usta, J.; Kreydiyyeh, S.; Bajakian, K.; Nakkash-Chmaisse, H. In vitro effect of eugenol and cinnamaldehyde on membrane potential and respiratory chain complexes in isolated rat liver mitochondria. *Food Chem Toxicol* **2002**, *40* (7), 935–940.

Vander Heiden, M. G.; Cantley, L. C.; Thompson, C. B. Understanding the Warburg effect: the metabolic requirements of cell proliferation. *Science* **2009**, *324* (5930), 1029–1033.

Vander Heiden, M. G.; Christofk, H. R.; Schuman, E.; Subtelny, A. O.; Sharfi, H.; Harlow, E. E.; Xian, J.; Cantley, L. C., Identification of small molecule inhibitors of pyruvate kinase M2. *Biochem Pharmacol* **2010**, *79* (8), 1118–1124.

Varmus, H. The new era in cancer research. *Science* **2006**, *312* (5777), 1162–1165.

Varmus, H.; Pao, W.; Politi, K.; Podsypanina, K.; Du, Y. C. Oncogenes come of age. *Cold Spring Harb Symp Quant Biol* **2005**, *70*, 1–9.

Vaupel, P.; Harrison, L. Tumor hypoxia: causative factors, compensatory mechanisms, and cellular response. *Oncologist* **2004**, *9 Suppl 5*, 4–9.

Vaupel, P.; Kelleher, D. K.; Hockel, M. Oxygen status of malignant tumors: pathogenesis of hypoxia and significance for tumor therapy. *Semin Oncol* **2001**, *28* (2 Suppl 8), 29–35.

Von Jagow, G.; Gribble, G. W.; Trumpower, B. L. Mucidin and strobilurin A are identical and inhibit electron transfer in the cytochrome bc_1 complex of the mitochondrial respiratory chain at the same site as myxothiazol. *Biochemistry* **1986**, *25* (4), 775–780.

Von Jagow, G.; Link, T. A. Use of specific inhibitors on the mitochondrial bc_1 complex. *Methods Enzymol* **1986**, *126*, 253–271.

Wallace, K. B. Mitochondrial off targets of drug therapy. *Trends Pharmacol Sci* **2008**, *29* (7), 361–366.

Wang, G. L.; Jiang, B. H.; Rue, E. A.; Semenza, G. L. Hypoxia-inducible factor-1 is a basic-helix-loop-helix-PAS heterodimer regulated by cellular O_2 tension. *Proc Natl Acad Sci U S A* **1995**, *92* (12), 5510–5514.

Wang, T.; Marquardt, C.; Foker, J. Aerobic glycolysis during lymphocyte proliferation. *Nature* **1976**, *261* (5562), 702–705.

Wang, Y.; Zhang, Y.; Yu, B., The cytotoxicity of saponins correlates with their cellular internalization. *ChemMedChem* **2007b,** *2* (3), 288-91.

Wang, Y.; Zhang, Y.; Zhu, Z.; Zhu, S.; Li, Y.; Li, M.; Yu, B. Exploration of the correlation between the structure, hemolytic activity, and cytotoxicity of steroid saponins. *Bioorg Med Chem* **2007a**, *15* (7), 2528–2532.

Warburg, O. On the origin of cancer cells. *Science* **1956**, *123* (3191), 309–314.

Ward, R. A.; Brassington, C.; Breeze, A. L.; Caputo, A.; Critchlow, S.; Davies, G.; Goodwin, L.; Hassall, G.; Greenwood, R.; Holdgate, G. A.; Mrosek, M.; Norman, R. A.; Pearson, S.; Tart, J.; Tucker, J. A.; Vogtherr, M.; Whittaker, D.; Wingfield, J.; Winter, J.; Hudson, K. Design and synthesis of novel lactate dehydrogenase a inhibitors by fragment-based lead generation. *J Med Chem* **2012**, *55* (7), 3285–3306.

Wassler, M.; Jonasson, I.; Persson, R.; Fries, E. Differential permeabilization of membranes by saponin treatment of isolated rat hepatocytes. *Biochem J* **1987**, *247* (2), 407–415.

Weeks, A. J.; Paul, R. L.; Marsden, P. K.; Blower, P. J.; Lloyd, D. R. Radiobiological effects of hypoxia-dependent uptake of 64Cu-ATSM: enhanced DNA damage and cytotoxicity in hypoxic cells. *Eur J Nucl Med Mol Imaging* **2010**, *37* (2), 330–338.

Wei, Y. H.; Lu, C. Y.; Lin, T. N.; Wei, R. D. Effect of ochratoxin A on rat liver mitochondrial respiration and oxidative phosphorylation. *Toxicology* **1985**, *36* (2-3), 119–130.

Weinstein, I. B. Cancer. Addiction to oncogenes--the Achilles heal of cancer. *Science* **2002**, *297* (5578), 63–64.

Wellcome trust Sanger Institute, http://www.sanger.ac.uk/genetics/CGP/Census/ (accessed on July 7th 2012).

Wesche, H.; Xiao, S. H.; Young, S. W. High throughput screening for protein kinase inhibitors. *Comb Chem High Throughput Screen* **2005**, *8* (2), 181–195.

Wolf, A.; Agnihotri, S.; Micallef, J.; Mukherjee, J.; Sabha, N.; Cairns, R.; Hawkins, C.; Guha, A. Hexokinase 2 is a key mediator of aerobic glycolysis and promotes tumor growth in human glioblastoma multiforme. *J Exp Med* **2011**, *208* (2), 313–326.

Wolvetang, E. J.; Johnson, K. L.; Krauer, K.; Ralph, S. J.; Linnane, A. W. Mitochondrial respiratory chain inhibitors induce apoptosis. *FEBS Lett* **1994**, *339* (1-2), 40–44.

Xu, D.; Yao, Y.; Lu, L.; Costa, M.; Dai, W. Plk3 functions as an essential component of the hypoxia regulatory pathway by direct phosphorylation of HIF-1α. *J Biol Chem* **2010**, *285* (50), 38944–38950.

Xu, Z.; Nagashima, K.; Sun, D.; Rush, T.; Northrup, A.; Andersen, J. N.; Kariv, I.; Bobkova, E. V. Development of high-throughput TR-FRET and AlphaScreen assays for identification of potent inhibitors of PDK1. *J Biomol Screen* **2009**, *14* (10), 1257–1262.

Yee Koh, M.; Spivak-Kroizman, T. R.; Powis, G. HIF-1 regulation: not so easy come, easy go. *Trends Biochem Sci* **2008**, *33* (11), 526–534.

Yeh, G. Y.; Eisenberg, D. M. Kaptchuk, T. J.; Phillips, R. S. Systematic review of herbs and dietary supplements for glycemic control in diabetes. *Diabetes Care* **2003**, *26* (4), 1277–1294.

Yellapu, R. K.; Mittal, V.; Grewal, P.; Fiel, M.; Schiano, T. Acute liver failure caused by 'fat burners' and dietary supplements: a case report and literature review. *Can J Gastroenterol* **2011**, *25* (3), 157–160.

Yeung, S. J.; Pan, J.; Lee, M. H. Roles of p53, MYC and HIF-1 in regulating glycolysis - the seventh hallmark of cancer. *Cell Mol Life Sci* **2008**, *65* (24), 3981–3999.

Yoo, C. B.; Jones, P. A. Epigenetic therapy of cancer: past, present and future. *Nat Rev Drug Discov* **2006**, *5* (1), 37–50.

Young, R. M.; Wang, S. J.; Gordan, J. D.; Ji, X.; Liebhaber, S. A.; Simon, M. C. Hypoxia-mediated selective mRNA translation by an internal ribosome entry site-independent mechanism. *J Biol Chem* **2008**, *283* (24), 16309–16319.

Zafra-Polo, M. C.; Gonzalez, M. C.; Tormo, J. R.; Estornell, E.; Cortes, D. Polyalthidin: new prenylated benzopyran inhibitor of the mammalian mitochondrial respiratory chain. *J Nat Prod* **1996**, *59* (10), 913–916.

Zhang, H.; Bosch-Marce, M.; Shimoda, L. A.; Tan, Y. S.; Baek, J. H.; Wesley, J. B.; Gonzalez, F. J.; Semenza, G. L. Mitochondrial autophagy is an HIF-1-dependent adaptive metabolic response to hypoxia. *J Biol Chem* **2008**, *283* (16), 10892–10903.

Zhang, H.; Gao, P.; Fukuda, R.; Kumar, G.; Krishnamachary, B.; Zeller, K. I.; Dang, C. V.; Semenza, G. L. HIF-1 inhibits mitochondrial biogenesis and cellular respiration in VHL-deficient renal cell carcinoma by repression of C-MYC activity. *Cancer Cell* **2007**, *11* (5), 407–420.

Zhao, F.; Mancuso, A.; Bui, T. V.; Tong, X.; Gruber, J. J.; Swider, C. R.; Sanchez, P. V.; Lum, J. J.; Sayed, N.; Melo, J. V.; Perl, A. E.; Carroll, M.; Tuttle, S. W.; Thompson, C. B. Imatinib resistance associated with BCR-ABL upregulation is dependent on HIF-1α-induced metabolic reprograming. *Oncogene* **2010**, *29* (20), 2962–2972.

Zhong, L.; D'Urso, A.; Toiber, D.; Sebastian, C.; Henry, R. E.; Vadysirisack, D. D.; Guimaraes, A.; Marinelli, B.; Wikstrom, J. D.; Nir, T.; Clish, C. B.; Vaitheesvaran, B.; Iliopoulos, O.; Kurland, I.; Dor, Y.; Weissleder, R.; Shirihai, O. S.; Ellisen, L. W.; Espinosa, J. M.; Mostoslavsky, R. The histone deacetylase Sirt6 regulates glucose homeostasis via HIF-1α. *Cell* **2010**, *140* (2), 280–293.

Zhou, J.; Callapina, M.; Goodall, G. J.; Brune, B. Functional integrity of nuclear factor kappaB, phosphatidylinositol 3'-kinase, and mitogen-activated protein kinase signaling allows tumor necrosis factor α-evoked Bcl-2 expression to provoke internal ribosome entry site-dependent translation of hypoxia-inducible factor-1α. *Cancer Res* **2004**, *64* (24), 9041–9048.

Zhou, J.; Hara, K.; Inoue, M.; Hamada, S.; Yasuda, H.; Moriyama, H.; Endo, H.; Hirota, K.; Yonezawa, K.; Nagata, M.; Yokono, K. Regulation of hypoxia-inducible factor-1 by glucose availability under hypoxic conditions. *Kobe J Med Sci* **2007**, *53* (6), 283–296.

Zhou, M.; Zhao, Y.; Ding, Y.; Liu, H.; Liu, Z.; Fodstad, O.; Riker, A. I.; Kamarajugadda, S.; Lu, J.; Owen, L. B.; Ledoux, S. P.; Tan, M. Warburg effect in chemosensitivity: targeting lactate dehydrogenase-A re-sensitizes taxol-resistant cancer cells to taxol. *Mol Cancer* **2010**, *9*, 33.

Zhou, Y.; Garcia-Prieto, C.; Carney, D. A.; Xu, R. H.; Pelicano, H.; Kang, Y.; Yu, W.; Lou, C.; Kondo, S.; Liu, J.; Harris, D. M.; Estrov, Z.; Keating, M. J.; Jin, Z.; Huang, P. OSW-1: a natural compound with potent anticancer activity and a novel mechanism of action. *J Natl Cancer Inst* **2005**, *97* (23), 1781–1785.

Zhu, H.; Chen, X. P.; Luo, S. F.; Guan, J.; Zhang, W. G.; Zhang, B. X. Involvement of hypoxia-inducible factor-1α in multidrug resistance induced by hypoxia in HepG2 cells. *J Exp Clin Cancer Res* **2005**, *24* (4), 565–574.

Zu, X. L.; Guppy, M. Cancer metabolism: facts, fantasy, and fiction. *Biochem Biophys Res Commun* **2004**, *313* (3), 459–465.

APPENDIX

NATURE PUBLISHING GROUP LICENSE

TERMS AND CONDITIONS

Jul 25, 2012

This is a License Agreement between Sandipan Datta ("You") and Nature Publishing Group ("Nature Publishing Group") provided by Copyright Clearance Center ("CCC"). The license consists of your order details, the terms and conditions provided by Nature Publishing Group, and the payment terms and conditions.

All payments must be made in full to CCC. For payment instructions, please see information listed at the bottom of this form.

License Number	2915450131484
License date	May 24, 2012
Licensed content publisher	Nature Publishing Group
Licensed content publication	Nature Chemical Biology
Licensed content title	New approaches to molecular cancer therapeutics
Licensed content author	Ian Collins and Paul Workman
Licensed content date	Dec 1, 2006
Volume number	2
Issue number	12

Type of Use	reuse in a thesis/dissertation
Requestor type	academic/educational
Format	print and electronic
Portion	figures/tables/illustrations
Number of figures/tables/illustrations	5
High-res required	no
Figures	figure 1 figure 2 figure 5
Author of this NPG article	no
Your reference number	
Title of your thesis / dissertation	Discovery of small-molecule natural products that target cellular bioenergetics
Expected completion date	Jul 2012
Estimated size (number of pages)	150
Total	0.00 USD

Terms and Conditions

Terms and Conditions for Permissions

Nature Publishing Group hereby grants you a non-exclusive license to reproduce this material for this purpose, and for no other use, subject to the conditions below:

1. NPG warrants that it has, to the best of its knowledge, the rights to license reuse of this material. However, you should ensure that the material you are requesting is original to Nature Publishing Group and does not carry the copyright of another

entity (as credited in the published version). If the credit line on any part of the material you have requested indicates that it was reprinted or adapted by NPG with permission from another source, then you should also seek permission from that source to reuse the material.

2. Permission granted free of charge for material in print is also usually granted for any electronic version of that work, provided that the material is incidental to the work as a whole and that the electronic version is essentially equivalent to, or substitutes for, the print version. Where print permission has been granted for a fee, separate permission must be obtained for any additional, electronic re-use (unless, as in the case of a full paper, this has already been accounted for during your initial request in the calculation of a print run). NB: In all cases, web-based use of full-text articles must be authorized separately through the 'Use on a Web Site' option when requesting permission.

3. Permission granted for a first edition does not apply to second and subsequent editions and for editions in other languages (except for signatories to the STM Permissions Guidelines, or where the first edition permission was granted for free).

4. Nature Publishing Group's permission must be acknowledged next to the figure, table or abstract in print. In electronic form, this acknowledgement must be visible at the same time as the figure/table/abstract, and must be hyperlinked to the journal's homepage.

5. The credit line should read:

   Reprinted by permission from Macmillan Publishers Ltd: [JOURNAL NAME] (reference citation), copyright (year of publication)

   For AOP papers, the credit line should read:

   Reprinted by permission from Macmillan Publishers Ltd: [JOURNAL NAME], advance online publication, day month year (doi: 10.1038/sj.[JOURNAL ACRONYM].XXXXX)

   Note: For republication from the *British Journal of Cancer*, the following credit lines apply.

   Reprinted by permission from Macmillan Publishers Ltd on behalf of Cancer Research UK: [JOURNAL NAME] (reference citation), copyright (year of publication) For AOP papers, the credit line should read:

   Reprinted by permission from Macmillan Publishers Ltd on behalf of Cancer Research UK: [JOURNAL NAME], advance online publication, day month year (doi: 10.1038/sj.[JOURNAL ACRONYM].XXXXX)

6. Adaptations of single figures do not require NPG approval. However, the adaptation should be credited as follows:

   Adapted by permission from Macmillan Publishers Ltd: [JOURNAL NAME] (reference citation), copyright (year of publication)

   Note: For adaptation from the *British Journal of Cancer*, the following credit line applies.

   Adapted by permission from Macmillan Publishers Ltd on behalf of Cancer Research UK: [JOURNAL NAME] (reference citation), copyright (year of

publication)

7. Translations of 401 words up to a whole article require NPG approval. Please visit http://www.macmillanmedicalcommunications.com for more information.

   Translations of up to a 400 words do not require NPG approval. The translation should be credited as follows:

   Translated by permission from Macmillan Publishers Ltd: [JOURNAL NAME] (reference citation), copyright (year of publication).

   Note: For translation from the *British Journal of Cancer*, the following credit line applies.

   Translated by permission from Macmillan Publishers Ltd on behalf of Cancer Research UK: [JOURNAL NAME] (reference citation), copyright (year of publication)

We are certain that all parties will benefit from this agreement and wish you the best in the use of this material. Thank you.

Special Terms:

v1.1

If you would like to pay for this license now, please remit this license along with your payment made payable to "COPYRIGHT CLEARANCE CENTER" otherwise you will be invoiced within 48 hours of the license date. Payment should be in the form of a check or money order referencing your account number and this invoice number RLNK500786204.

Once you receive your invoice for this order, you may pay your invoice by credit card. Please follow instructions provided at that time.

Make Payment To:

Copyright Clearance Center

Dept 001

P.O. Box 843006

Boston, MA 02284-3006

For suggestions or comments regarding this order, contact RightsLink Customer Support: customercare@copyright.com or +1-877-622-5543 (toll free in the US) or +1-978-646-2777.

Gratis licenses (referencing $0 in the Total field) are free. Please retain this printable license for your reference. No payment is required.

NATURE PUBLISHING GROUP LICENSE

TERMS AND CONDITIONS

Jul 25, 2012

This is a License Agreement between Sandipan Datta ("You") and Nature Publishing Group ("Nature Publishing Group") provided by Copyright Clearance Center ("CCC"). The license consists of your order details, the terms and conditions provided by Nature Publishing Group, and the payment terms and conditions.

All payments must be made in full to CCC. For payment instructions, please see information listed at the bottom of this form.

License Number	2926250631558
License date	Jun 11, 2012
Licensed content publisher	Nature Publishing Group
Licensed content publication	Cell Death and Differentiation
Licensed content title	Mitochondrial complex III regulates hypoxic activation of HIF
Licensed content author	T Klimova, N S Chandel
Licensed content date	Jan 25, 2008
Volume number	15
Issue number	4

Type of Use	reuse in a thesis/dissertation
Requestor type	academic/educational
Format	print and electronic
Portion	figures/tables/illustrations
Number of figures/tables/illustrations	3
High-res required	no
Figures	3,4,5
Author of this NPG article	no
Your reference number	
Title of your thesis / dissertation	Discovery of small-molecule natural products that target cellular bioenergetics
Expected completion date	Jul 2012
Estimated size (number of pages)	150
Total	0.00 USD

Terms and Conditions

Terms and Conditions for Permissions

Nature Publishing Group hereby grants you a non-exclusive license to reproduce this material for this purpose, and for no other use, subject to the conditions below:

1. NPG warrants that it has, to the best of its knowledge, the rights to license reuse of this material. However, you should ensure that the material you are requesting is original to Nature Publishing Group and does not carry the copyright of another

entity (as credited in the published version). If the credit line on any part of the material you have requested indicates that it was reprinted or adapted by NPG with permission from another source, then you should also seek permission from that source to reuse the material.

2. Permission granted free of charge for material in print is also usually granted for any electronic version of that work, provided that the material is incidental to the work as a whole and that the electronic version is essentially equivalent to, or substitutes for, the print version. Where print permission has been granted for a fee, separate permission must be obtained for any additional, electronic re-use (unless, as in the case of a full paper, this has already been accounted for during your initial request in the calculation of a print run). NB: In all cases, web-based use of full-text articles must be authorized separately through the 'Use on a Web Site' option when requesting permission.
3. Permission granted for a first edition does not apply to second and subsequent editions and for editions in other languages (except for signatories to the STM Permissions Guidelines, or where the first edition permission was granted for free).
4. Nature Publishing Group's permission must be acknowledged next to the figure, table or abstract in print. In electronic form, this acknowledgement must be visible at the same time as the figure/table/abstract, and must be hyperlinked to the journal's homepage.
5. The credit line should read:

   Reprinted by permission from Macmillan Publishers Ltd: [JOURNAL NAME] (reference citation), copyright (year of publication)

For AOP papers, the credit line should read:

Reprinted by permission from Macmillan Publishers Ltd: [JOURNAL NAME], advance online publication, day month year (doi: 10.1038/sj.[JOURNAL ACRONYM].XXXXX)

Note: For republication from the *British Journal of Cancer*, the following credit lines apply.

Reprinted by permission from Macmillan Publishers Ltd on behalf of Cancer Research UK: [JOURNAL NAME] (reference citation), copyright (year of publication) For AOP papers, the credit line should read:

Reprinted by permission from Macmillan Publishers Ltd on behalf of Cancer Research UK: [JOURNAL NAME], advance online publication, day month year (doi: 10.1038/sj.[JOURNAL ACRONYM].XXXXX)

6. Adaptations of single figures do not require NPG approval. However, the adaptation should be credited as follows:

   Adapted by permission from Macmillan Publishers Ltd: [JOURNAL NAME] (reference citation), copyright (year of publication)

   Note: For adaptation from the *British Journal of Cancer*, the following credit line applies.

   Adapted by permission from Macmillan Publishers Ltd on behalf of Cancer Research UK: [JOURNAL NAME] (reference citation), copyright (year of publication)

7. Translations of 401 words up to a whole article require NPG approval. Please visit http://www.macmillanmedicalcommunications.com for more information.

Translations of up to a 400 words do not require NPG approval. The translation should be credited as follows:

Translated by permission from Macmillan Publishers Ltd: [JOURNAL NAME] (reference citation), copyright (year of publication).

Note: For translation from the *British Journal of Cancer*, the following credit line applies.

Translated by permission from Macmillan Publishers Ltd on behalf of Cancer Research UK: [JOURNAL NAME] (reference citation), copyright (year of publication)

We are certain that all parties will benefit from this agreement and wish you the best in the use of this material. Thank you.

Special Terms: v1.1

If you would like to pay for this license now, please remit this license along with your payment made payable to "COPYRIGHT CLEARANCE CENTER" otherwise you will be invoiced within 48 hours of the license date. Payment should be in the form of a check or money order referencing your account number and this invoice number RLNK500797024.

Once you receive your invoice for this order, you may pay your invoice by credit card. Please follow instructions provided at that time.

Make Payment To:

Copyright Clearance Center

Dept 001

P.O. Box 843006

Boston, MA 02284-3006

For suggestions or comments regarding this order, contact RightsLink Customer Support: customercare@copyright.com or +1-877-622-5543 (toll free in the US) or +1-978-646-2777.

Gratis licenses (referencing $0 in the Total field) are free. Please retain this printable license for your reference. No payment is required.

VITA

Sandipan Datta, son of Swapan Kumar Datta and Anuradha Datta was born in Howrah, West Bengal, India on October 6, 1980. After completing his schooling from Vivekananda Institution, Howrah, he obtained the Bachelor of Pharmacy degree from Sree Siddaganga College of Pharmacy, Rajiv Gandhi University of Health Sciences, Tumkur, Karnataka, India. Subsequently, he was awarded Govt. of India scholarship and obtained the degree of Master of Pharmacy (Pharmacognosy) at Bharati Vidyapeeth Deemed University's Poona College of Pharmacy, Pune, Maharashtra, India. He joined the Department of Pharmacognosy, The University of Mississippi under the supervision of Dr. Dale G. Nagle and Yu-Dong Zhou in 2007. He was awarded Natural Products and Neuroscience Predoctoral Fellowship from the NIH in 2009 and 2010. He was elected as the president of the Graduate Student Council in 2010 and was inducted in the 2010-2011 class of Who's Who Among Students in American Universities and Colleges. He received the Department of Pharmacognosy, The University of Mississippi service award in 2011. Following are the publications/potential publications from his research:

Li, J.; Mahdi, F.; Du, L.; **Datta, S**.; Nagle, D. G.; Zhou, Y. -D. Mitochondrial Respiration Inhibitors Suppress Protein Translation and Hypoxic Signaling via the Hyperphosphorylation and Inactivation of Translation Initiation Factor eIF2α and Elongation Factor eEF2 *J Nat Prod*. **2011**, *74(9)*, 1894-1901.

Du, L.; Mahdi, F.; **Datta, S**.; Jekabsons, M. B.; Zhou, Y. -D.; Nagle, D. G. "Structures and Mechanisms of Antitumor Agents – Xestoquinones Uncouple Cellular Respiration and Disrupt HIF Signaling in Human Breast Tumor Cells" (in press)

Datta, S.; Li, J.; Zhou, Y. -D.; Nagle, D. G. "Identification of Small-molecule Glycolysis Inhibitors Through a Bioenergetics-based Screening" (in preparation).

Datta, S.; Li, J.; Zhou, Y. -D.; Nagle, D. G. "Comparative Evaluation of Chromatographic Media in Molecular-targeted Antitumor Drug Discovery" (in preparation).

Datta, S.; Mahdi, F.; Li, J.; Du, L.; Smillie, T. J.; Khan, I. A.; Jekabsons, M. B.; Zhou, Y. -D.; Nagle, D. G. "Assessing the potential mitochondrial-mediated toxicity of herbal dietary supplements" (planned manuscript).